CHEMICAL REVIEWS

Review

Cite This: *Chem. Rev.* XXXX, XXX, XXX−XXX

pubs.acs.org/CR

Rationally Engineered Nucleic Acid Architectures for Biosensing Applications

Mingshu Xiao,[†] Wei Lai,[†] Tiantian Man,[†] Binbin Chang,[†] Li Li,[†] Arun Richard Chandrasekaran,*[,‡] and Hao Pei*[,†]

[†]Shanghai Key Laboratory of Green Chemistry and Chemical Processes, School of Chemistry and Molecular Engineering, East China Normal University, 500 Dongchuan Road, Shanghai 200241, P. R. China

[‡]The RNA Institute, University at Albany, State University of New York, Albany, New York 12222, United States

ABSTRACT: Development of biosensing platforms plays a key role in research settings for identification of biomarkers and in clinical applications for diagnostics. Biosensors based on nucleic acids have taken many forms, from simple duplex-based constructs to stimuli-responsive nucleic acid nanostructures. In this review, we look at various nucleic acid-based biosensors, the different read-out strategies employed, and their use in chemical and biological sensing. We also look at current developments in DNA nanotechnology-based biosensors and how rational design of such constructs leads to more efficient biosensing platforms.

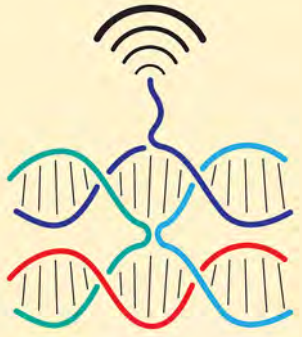

CONTENTS

1. INTRODUCTION

From being an icon of modern biology, DNA is now used for the assembly of interfacial structures and the bottom-up construction of nanoscale architectures.[1−3] The inherent molecular recognition properties of DNA and the resulting programmable self-assembly make DNA versatile for the fabrication of such nanoscale materials. The four canonical nucleotides and their Watson−Crick base pairings (A:T and C:G) provide predictable self-assembly, while the structural features of DNA (diameter of ∼2 nm, helical pitch of ∼3.4−3.6 nm, and persistence length of ∼50 nm) make it suitable for robust construction. Hierarchical assembly from smaller units can be achieved by single-stranded overhangs called sticky ends that connect duplexes from different motifs or nanostructures. Over the past two decades, DNA nanotechnology has moved from proof-of-concept structural demonstrations to applications in many different fields.[4−12] Perhaps one of the most widely developed fields that

Received: February 20, 2019

DOI: 10.1021/acs.chemrev.9b00121
Chem. Rev. XXXX, XXX, XXX−XXX

utilizes the properties of nucleic acids is biosensing, where DNA nanomaterials or DNA structures in combination with other materials are designed to detect biological or chemical moieties.

In this review, we provide a comprehensive overview of DNA-based biosensing approaches and specifically discuss DNA nanostructures and their use in biological and chemical sensing. In Section 2, we discuss strategies utilized in creating DNA nanostructures in structural as well as dynamic DNA nanotechnology. Design principles obtained from a multitude of studies that involve construction of DNA nanostructures now provide a toolset to customize these nanostructures for biosensing purposes. In Section 3, we discuss how different biosensing strategies are read out and how these techniques compare to each other. Some of the most commonly used readout techniques we discuss in this article include optical methods (fluorescence, FRET, and nanoparticle-based), electrochemical, gel-based, atomic force microscopy (AFM), and surface enhanced Raman spectroscopy (SERS). We then discuss in Section 4 DNA nanostructures that are used in sensing of nucleic acids, pH, enzyme activity, biomacromolecules, and metal ions. For each case, we provide examples of nanostructures and their features including the limit of detection, and whether the strategies have been used for clinically relevant samples or tested in biological fluids. In Section 5, we briefly discuss *in situ* sensing and provide our outlook and perspective of the field in Section 6.

2. FRAMEWORK NUCLEIC ACIDS

Ned Seeman first proposed the idea of using DNA to build structures in the early 1980s.[13] The DNA double helix is inherently linear, and thus, branched DNA junctions are required for multidimensional assembly. For this purpose, similar to the biologically occurring Holliday junctions,[14] scientists created synthetic branched DNA junctions with 4, 5, 6, 8, or 12 arms around the junction.[15−20] Such branched junctions form the basis of multicrossover DNA tiles and motifs that comprise framework-like DNA nanostructures dubbed framework nucleic acid (FNA) architectures. Some of the early developments using FNAs include the creation of DNA-based objects such as a cube (Figure 1A)[21] and a truncated octahedron (Figure 1B).[22] Different DNA strands are designed to bind to their complementary regions in other strands and assemble into the desired structure, that is, creating a designed framework. In subsequent studies, an octahedron was built from a 1.7 kilobase DNA strand that was folded by five short strands (Figure 1C).[23] This structure was a precursor to the now well-known DNA origami strategy and used paranemic-crossover to connect the struts of the octahedron.[24] In other examples, DNA icosahedra have been constructed using a modular approach where multiple 5-arm DNA junctions are first assembled into two halves of an icosahedron, and the two halves are then assembled into a full octahedron through sticky end cohesion (Figure 1D).[25] A DNA tetrahedron composed of four strands was assembled by a single step annealing (Figure 1E,F),[26] while 3D DNA prisms (triangular, square, pentagonal, and hexagonal prisms) have been constructed using a stepwise strategy (Figure 1G).[27] One of the most common DNA motifs, the DNA three-point-star,[28−31] has been used in the hierarchical assembly of cubes, tetrahedra, dodecahedra, and buckyballs (Figure 1H,I).[32,33] Similarly, a DNA icosahedron can be hierarchically assembled from five-point-star DNA motifs (Figure 1J).[34] In addition to the many DNA objects constructed,[30,35] such polyhedra are also assembled using a combination of DNA and RNA strands.[36,37]

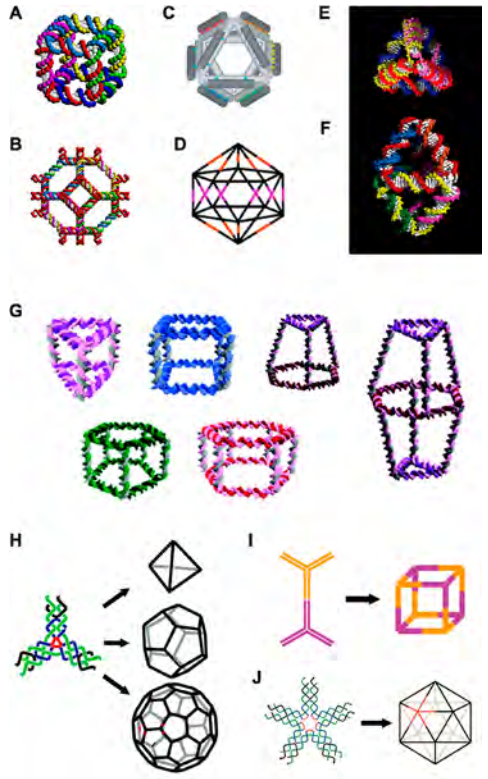

Figure 1. Nanoscale DNA objects. (A) DNA cube. Reprinted with permission from ref 21. Copyright 1991 Springer Nature. (B) Truncated octahedron. Reprinted with permission from ref 22. Copyright 1994 American Chemical Society. (C) Octahedron. Reprinted with permission from ref 23. Copyright 2004 Springer Nature. (D) Icosahedron. Reprinted with permission from ref 25. Copyright 2009 Wiley-VCH. (E) Tetrahedron. (F) Double tetrahedron. Reprinted with permission from ref 26. Copyright 2005 AAAS. (G) DNA prisms. Reprinted with permission from ref 27. Copyright 2007 American Chemical Society. (H) Tetrahedron, octahedron, and buckyball assembled from a three-point-star motif. Reprinted with permission from ref 32. Copyright 2008 Springer Nature. (I) Cube assembled from three-point-star motif. Reprinted with permission from ref 33. Copyright 2009 American Chemical Society. (J) Icosahedron assembled from a five-point-star motif. Reprinted with permission from ref 34. Copyright 2008 National Academy of Sciences.

In addition, FNAs also include RNA as a building block[38−40] to create pristine RNA nanostructures and objects such as prisms and polyhedra.[41−46]

Ned Seeman's original proposal was to use DNA to build a three-dimensional scaffold to solve the macromolecular crystallization problem.[47] The idea was to build a periodic 3D DNA lattice (i.e., a crystal) and host external guests so as to solve the crystal structures of guests that are usually hard to crystallize on their own (membrane proteins, for example). Early steps toward this goal involved the development of a variety of DNA motifs (Figure 2).[28,48−52] Some well-established DNA motifs are the double-crossover (DX)[53] and the triple-crossover (TX) motifs[54] that are used in creating periodic 2D lattices. The paranemic-crossover (PX) DNA[55] is another motif that has been used in creating covalently linked 1D[56,57] and 2D DNA arrays.[58,59] Many other DNA motifs have been developed for the construction of FNAs,[60] and these structures are used as breadboards for programmable organization of nanoparticles and biomolecules.[61−64] Moving a step closer to achieving the original vision of DNA nanotechnology, the tensegrity triangle

DOI: 10.1021/acs.chemrev.9b00121
Chem. Rev. XXXX, XXX, XXX−XXX

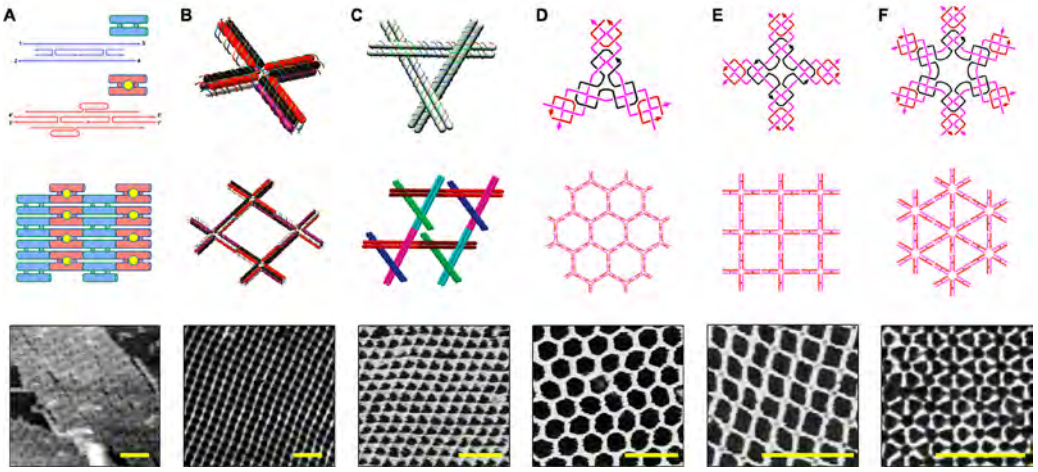

Figure 2. Two-dimensional DNA arrays. (A) Double-crossover (DX)-based alternating 2D array. Reprinted with permission from ref 48. Copyright 1998 Springer Nature. (B) Cross-shaped double-decker tile. Reprinted with permission from ref 49. Copyright 2011 American Chemical Society. (C) Tensegrity triangle with double-crossover edges. Reprinted with permission from ref 50. Copyright 2006 American Chemical Society. (D) Three-point-star motif. Reprinted with permission from ref 28. Copyright 2005 American Chemical Society. (E) Four-point-star (cross) motif. Reprinted with permission from ref 51. Copyright 2010 Wiley-VCH. (F) Six-point-star motif. Reprinted with permission from ref 52. Copyright 2006 American Chemical Society. AFM images for each type of 2D array are shown in the bottom panel. Scale bars: 100 nm.

motif[65] was used to create the first rationally designed 3D DNA crystal (Figure 3).[66] The three duplex edges of the motif are connected at the vertices by strand crossovers.[65] The triangles connect to each other infinitely in three directions through sticky end cohesion, resulting in the formation of a 3D FNA system (i.e., a designed crystal). The edge length of this motif can be modified to yield crystals with varying cavity sizes,[66,67] and the crystal can be designed to contain two different asymmetric units by controlling the sequences of the component units.[68] The cavities in these designed crystals can be used to attach and hold other macromolecules and for use in crystallographic analysis. This application requires high resolution crystal structures, and scientists have improved the stability of this system through biological production of component strands,[69] modification of sticky end length and sequence,[70] reinforcement of sticky ends via triplex interactions[71] and light-induced cross-linking of the component motifs guided by triplex formation.[72] The crystallization process can also be modulated by designed "agents" that alter the kinetics of crystal formation.[73] The sequence effect and role of heterogeneity in the crystals have also been analyzed.[74] Moving toward the goal of hosting external guests, these designer DNA crystals have been modified to bind triplex-forming oligonucleotides (TFOs),[75] an electronic component (polyaniline),[76] a DNA displacement device,[77] and to study stressed DNA molecules.[78]

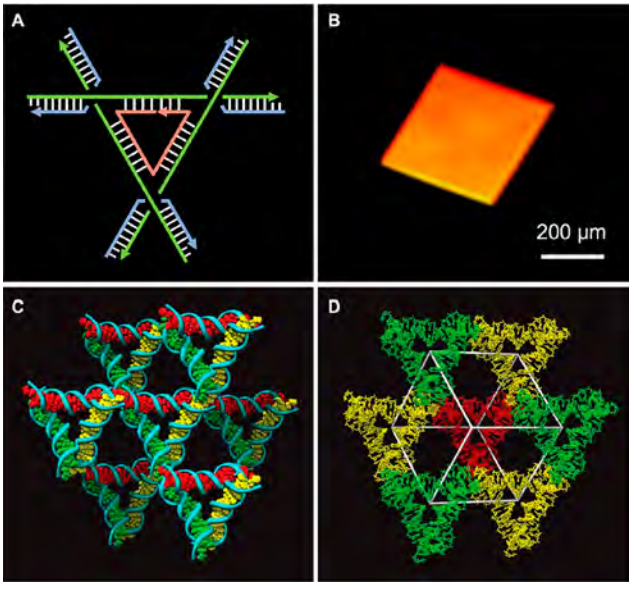

Figure 3. 3D DNA crystals. (A) Schematic of a two-turn tensegrity triangle motif showing strand crossovers at the three vertices and sticky ends at the ends of each edge. (B) Representative crystal formed from the tensegrity triangle motif. Note that the starting unit (the motif) is ~7 nm across and yields crystals that are a few hundred micrometers in dimensions. (C) Triangle connects to six others via sticky end cohesion; the three different directions are shown in three colors. (D) Crystal structure showing the rhombohedral cavity formed within eight triangle motifs. Reprinted with permission from ref 66. Copyright 2009 Springer Nature.

Another strategy to build DNA nanostructures is DNA origami, where a long single stranded scaffold DNA is folded into defined shapes by hundreds of short complementary staple strands (Figure 4A).[7,79,80] FNAs based on DNA origami include twisted bundles,[81] solid/hollow[82] 3D structures, and wireframe and mesh-like architectures (Figure 4B–G).[83,79,81,84–86] The strategy was later extended to 2D arrays and larger objects by addition of sticky ends to origami tiles (Figure 4H).[87,88] Other recent strategies in DNA-based construction are the molecular canvas strategy[89] and assembly using DNA bricks,[90] both of which are based on single stranded DNA tiles.[91]

For researchers to create FNAs, a variety of designing platforms and simulated techniques have been developed. For the creation of small FNAs such as tiles and motifs, programs like Sequin[92] and Uniquimer[93] are used for sequence symmetry minimization of component DNA strands. Scientists have also developed modeling software such as Gideon,[94] Tiamat,[95] and Uniquimer 3D[96] for designing and visualizing DNA motifs. For DNA origami, caDNAno is used to design hexagonal and square lattice DNA origami structures,[97] while Daedalus is used to create 3D structures based on wireframe DNA origami.[98] In

DOI: 10.1021/acs.chemrev.9b00121
Chem. Rev. XXXX, XXX, XXX−XXX

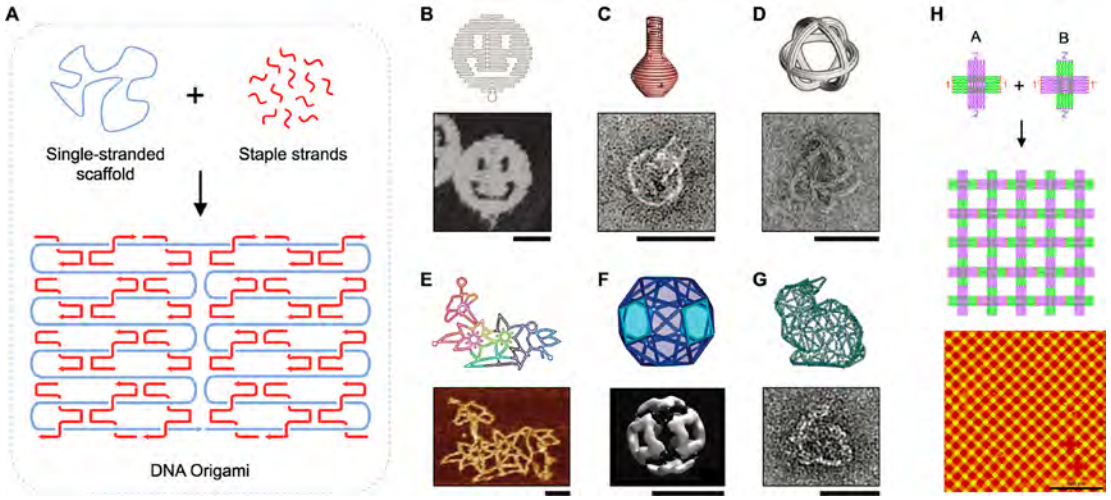

Figure 4. DNA origami structures. (A) In DNA origami, a long scaffold strand is folded into the desired shape by short complementary staple strands. Reprinted with permission from ref 7. Copyright 2018 Elsevier. (B) Smiley face made using DNA origami. Reprinted with permission from ref 79. Copyright 2006 Springer Nature. (C) Hollow flask. Reprinted with permission from ref 84. Copyright 2011 AAAS. (D) Wireframe DNA object. Reprinted with permission from ref 81. Copyright 2009 AAAS. (E) 2D pattern of flowers-and-bird. (F) Snub cube. Reprinted with permission from ref 85. Copyright 2015 Springer Nature. (G) Nanoscale bunny. Reprinted with permission from ref 86. Copyright 2015 Springer Nature. (H) 2D DNA array formed using a DNA origami cross. Reprinted with permission from ref 87. Copyright 2010 Wiley-VCH.

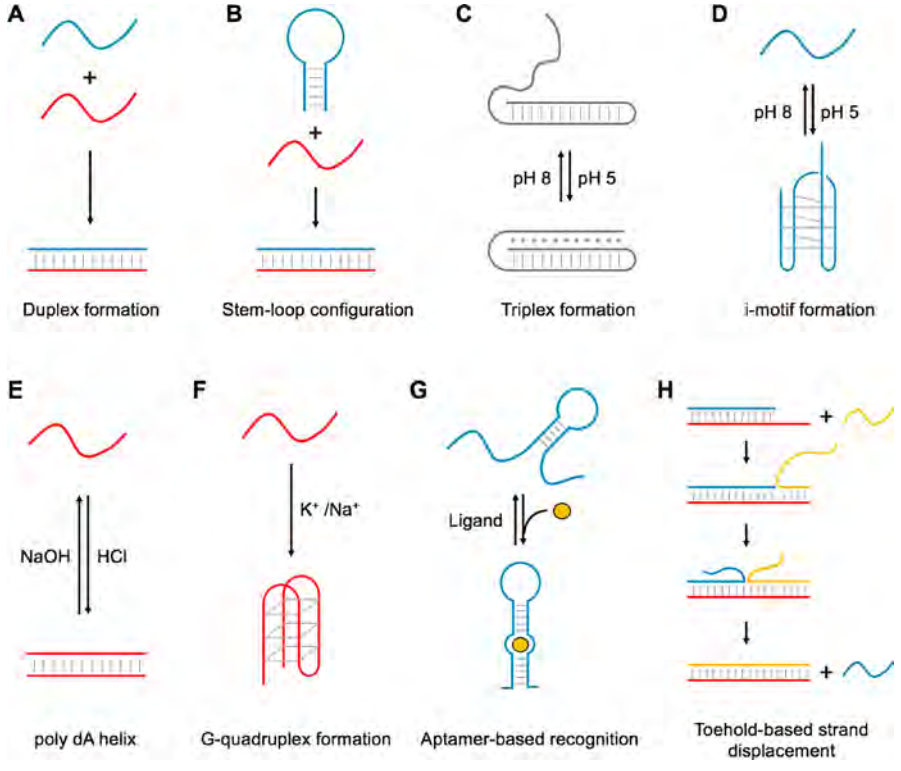

Figure 5. Concepts used in biosensing platforms. (A, B) Sequence-specific DNA hybridization in a duplex and stem-loop configuration, (C) triplex formation under acidic conditions, (D) i-motif formation under acidic conditions by C-rich DNA strands, (E) poly dA helix formation under acidic conditions by poly-A strands, (F) G-quadruplex formation in the presence of K^+ or Na^+, (G) aptamer reconfiguration in the presence of specific ligands, and (H) toehold-based strand displacement.

addition, the program CanDo can be used to predict the solution shape of DNA nanostructures along with their mechanical flexibility.[99] Recently, scientists developed an algorithmic approach called PERDIX (Programmed Eulerian Routing for DNA Design using X-overs) that enables anyone to create wireframe 2D origami objects of any desired shape and size.[100]

Apart from structural aspects and development, the field of DNA nanotechnology has also given rise to dynamic DNA machines[101−103] and DNA devices[104−106] that respond to chemical or environmental stimuli. This concept is extended to DNA-based biosensors that rely on specific recognition events between a substrate and the target analyte (e.g., nucleic acid and protein detection) or programmed conformational changes

DOI: 10.1021/acs.chemrev.9b00121
Chem. Rev. XXXX, XXX, XXX−XXX

(e.g., pH sensing).[107] DNA nanostructures have some advantages for being used in biosensing.[108,109] (1) The intermolecular recognition of rationally designed DNA sequences allows highly precise design and construction of DNA nanostructures. (2) The nanoscale dimensions of these structures provide large surface-to-volume ratios, thus resulting in large signal changes on target binding. (3) DNA sequences can now be synthesized in large quantities in a cost-effective manner and can be chemically modified to enhance their functionality.

A majority of nucleic acid-based biosensors involve hybridization of a DNA or RNA strand to its complement (Figure 5A) or a complementary region in a stem-loop (Figure 5B). Such stem-loop configurations can also be used to monitor global changes such as changes in temperature by using a fluorophore-quencher pair on the ends of the strands. In some sensing devices, small molecule-DNA conjugates are used instead of DNA strands for construction of biosensors,[105,110−118] in which the small molecules often act as signal tags. Biosensors for other stimuli such as pH changes are based on structures that involve triplexes (Figure 5C),[119] i-motif formation (Figure 5D),[120] or poly dA helix formation (Figure 5E),[121] all of which are sequence specific and occur under acidic conditions. G-Quadruplex formation is another sequence specific conformational change that occurs under specific ionic conditions such as the presence of K^+ or Na^+ (Figure 5F).[122] In addition, aptamer-based recognition has also been widely used in biosensors (Figure 5G). These are single stranded oligonucleotides that can bind with high affinity to ions (e.g., K^+, Hg^{2+}, Pb^{2+}), small organic molecules (e.g., ATP, amino acids, vitamins), peptides, proteins (e.g., thrombin and growth factors), and even whole cells or microorganisms (e.g., bacteria),[123,124] resulting in a secondary structure formation. Toehold-based strand displacement (Figure 5H) has also been used for target readouts and signal amplification in many DNA-based biosensing platforms.[125,126]

3. READOUT STRATEGIES FOR BIOSENSING

To effectively analyze clinical samples, some of the main requisites for biomolecular detection systems are high sensitivity (i.e., low limit of detection, LOD), high specificity ensuring accurate discrimination, and short test-to-answer time enabling routine use of diagnostic test results.[127] Moreover, these metrics should also be validated in complex biofluids such as saliva, urine, and blood. Currently, the enzyme-linked immunosorbent assay (ELISA) and polymerase chain reaction (PCR) are two traditional techniques for biosensing.[128,129] ELISA is an antibody sandwich assay that achieves clinically relevant levels of specificity and sensitivity for protein biomarkers but is still limited by its moderate sensitivity (picomolar) and the slow diffusion of biomolecules.[130,131] PCR is the current gold standard for nucleic acid analysis and provides detection of low copy numbers with single-nucleotide specificity. However, PCR assays are time-consuming and require skilled lab personnel making it difficult to be used in point-of-care settings. Therefore, advanced platforms with improved sensitivity and specificity along with ease-of-use are desirable in bioanalysis. To circumvent these issues, direct readout strategies represent effective solutions. Detection systems coupled to an appropriate readout device can convert recognition or binding events into optical, electronic, or electrochemical readout and so on via a signal transducer, thus accelerating analysis time and reducing the analytical cost.[132] In addition, such devices integrated with DNA nanotechnology can further improve their sensitivity and specificity.[133] As such, the integrated readout strategies for biosensing are fast, highly sensitive, and specific and hold great potential for clinical applications. In this section, we discuss fluorescence-based, FRET-based, nanoparticle-based, electrochemical-based, gel electrophoresis-based, AFM-based, and SERS-based readout strategies for biosensing.

3.1. Fluorescence-Based Readout Strategy

Fluorescence detection methods are predominantly employed for biological assays due to the commercial availability of a wide spectrum of fluorophores, the ease of fluorescent labeling, an immediate response, and the inherent capability for real-time detection. In addition, fluorescence detection has high sensitivity with a limit detection down to 1 nM using common benchtop fluorometers.[134,135] Natural nucleic acids are non-fluorescent or negligibly fluorescent,[136] and all fluorescent DNA-based sensors employ external fluorophores. A fluorophore is characterized by numerous properties including extinction coefficient, quantum yield (emission intensity), excitation/emission wavelengths, fluorescence lifetime, and fluorescence anisotropy. DNA-based sensors allow fine-tuning of these properties. For example, fluorophores can be functionalized to nucleic acids by a variety of interactions such as covalent or noncovalent attachments, intercalation, and electrostatic or hydrophobic interactions and at defined positions on a DNA or RNA strand.

The development of nucleic acid probes has benefited from advances in molecular biology techniques and chemical synthesis of nucleic acids since the early 1960s.[137,138] In the postgenomic era, various kinds of highly sensitive and selective DNA probes have been developed through various molecular design strategies. Molecular beacons (MBs), first reported in 1996 by Tyagi and Kramer, are prime examples of such DNA probes.[139] In the absence of a target, MBs with a stem-loop structure bring the quencher and fluorophore at opposite ends of the MBs into close proximity, resulting in fluorescence quenching. Upon addition of a target molecule, the strong intermolecular hybridization between the target and the loop sequence of the MB opens the stem duplex, moving the fluorophore and quencher away from each other, thus restoring fluorescence.[139−142] Other features such as the thermodynamic stability of the hairpin structure, switchable response, and the option to use different fluorophore combinations all contribute to MBs being exceptional DNA probes with excellent selectivity and sensitivity as well as detection in real-time.[143] With these features, MBs have been used extensively in the field of biosensing.[144−146]

The Ye group reported a label-free fluorescent MB based on DNA-templated silver nanoclusters (NCs) for detection of adenosine and adenosine deaminase.[147] In this work, the fluorescent MB probes are composed of three regions: (i) the nanocluster region with the cytosine-rich sequence for synthesis of AgNCs, (ii) the aptamer region for ATP assembly, and (iii) the 15-nt overhang region with a guanine-rich sequence as a fluorescence enhancer when placed in proximity to the as-prepared AgNCs.[148] As a result of the target-induced allosteric effect, the presence of ATP reconfigures the probe into a hairpin structure, resulting in enhanced fluorescence. This method enables detection of ATP and adenosine deaminase at 1 mM and 5 U, respectively. Working toward multi-input analysis, Lee et al. constructed a novel MB-based sensor for recognition of dual targets (Figure 6A).[149] They used a DNA four-way junction to

DOI: 10.1021/acs.chemrev.9b00121
Chem. Rev. XXXX, XXX, XXX−XXX

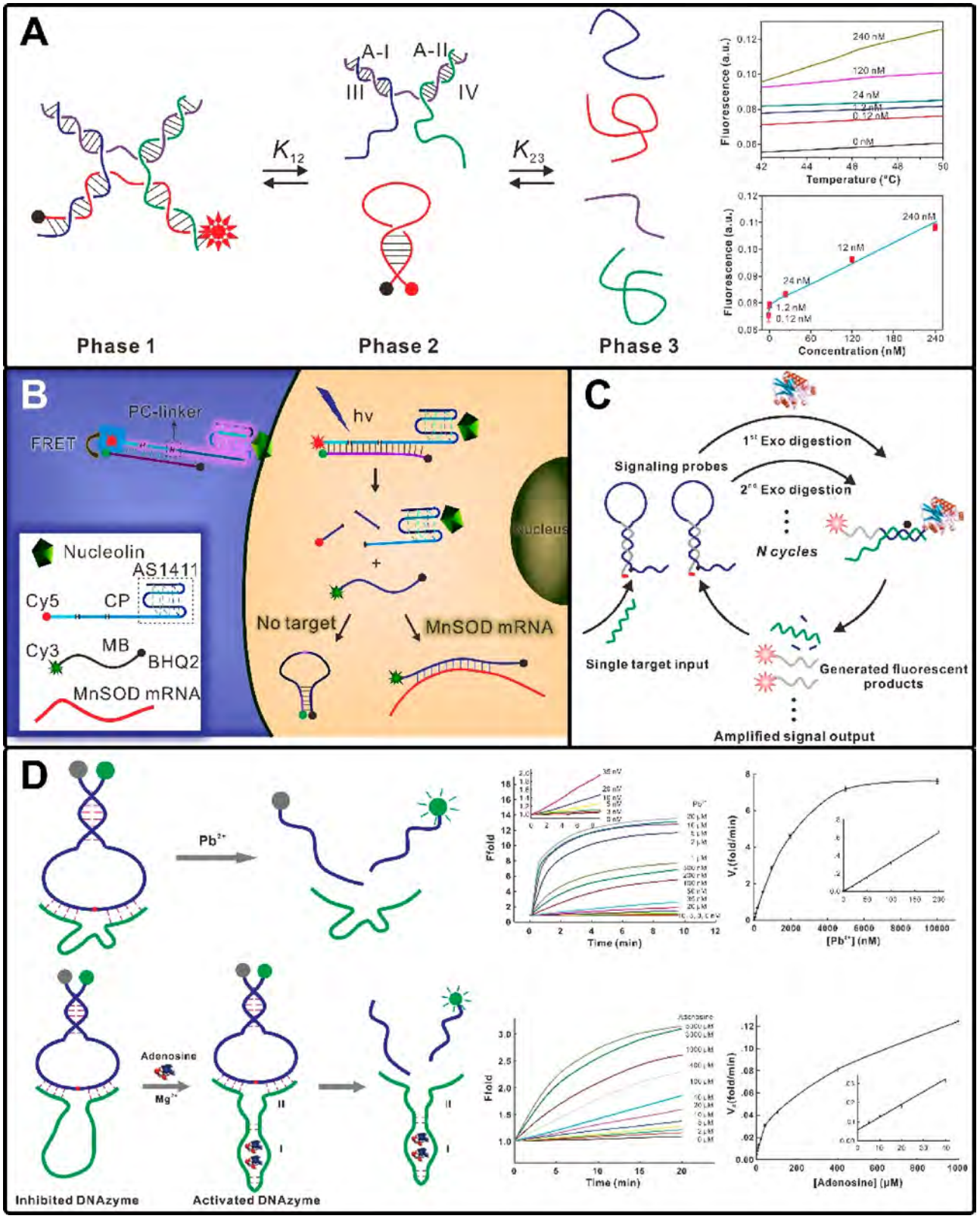

Figure 6. (A) MB-based sensor recognizing dual targets for subtyping of influenza A virus. Adapted with permission from ref 149. Copyright 2015 American Chemical Society. (B) Targeted, self-delivered, and photocontrolled MB for mRNA detection in living cells. Reproduced with permission from ref 153. Copyright 2013 American Chemical Society. (C) Exonuclease III-aided target recycling for amplified DNA detection. Reproduced with permission from ref 155. Copyright 2010 American Chemical Society. (D) Catalytic MBs for amplified detection of metal ions and organic molecules. Adapted with permission from ref 159. Copyright 2010 American Chemical Society.

analyze genuine genetic sequences of hemagglutinin and neuraminidase in an influenza A H5N2 isolate. This MB-based sensor yielded a linear calibration range from 1.2 to 240 nM with a detection limit of 120 pM. In addition, chemical and structural

DOI: 10.1021/acs.chemrev.9b00121
Chem. Rev. XXXX, XXX, XXX−XXX

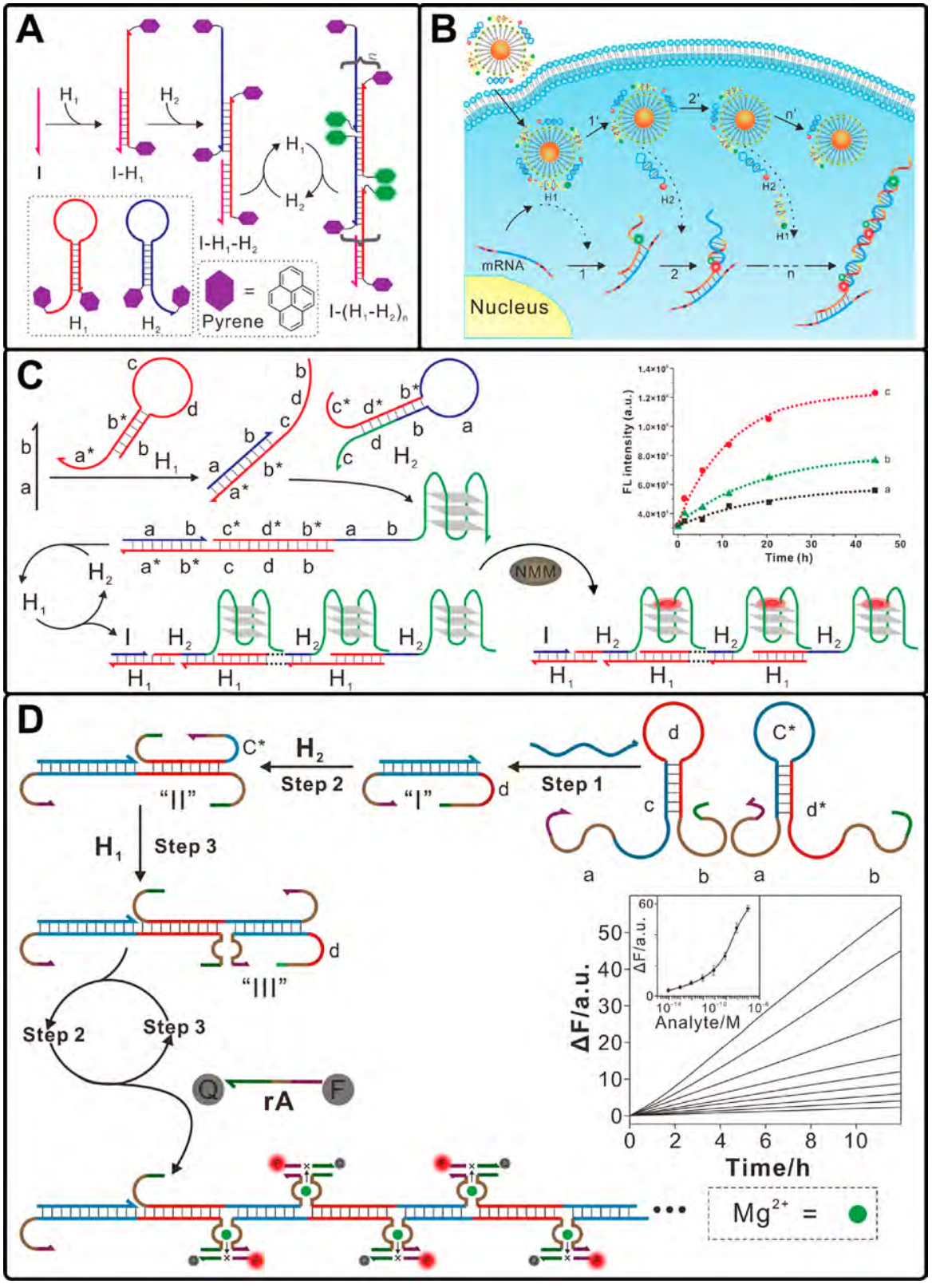

Figure 7. (A) Pyrene-excimer probes based on the HCR for DNA detection. Adapted with permission from ref 160. Copyright 2011 Wiley-VCH. (B) Electrostatic nucleic acid nanoassembly for intracellular mRNA imaging via HCR. Reproduced with permission from ref 162. Copyright 2015 American Chemical Society. (C) G-Quadruplex nanowires for label-free and enzyme-free DNA detection. Adapted with permission from ref 163. Copyright 2011 Royal Society of Chemistry. (D) Autonomous assembly of polymers consisting of DNAzyme wires for amplified detection of DNA. Adapted with permission from ref 164. Copyright 2011 American Chemical Society.

modifications (e.g., 2′OMe RNA) are often used to improve the intracellular performance of probes.[150−152] For example, the Tan group developed an aptamer-based MB for intracellular mRNA analysis, with added features such as photocontrol and

DOI: 10.1021/acs.chemrev.9b00121
Chem. Rev. XXXX, XXX, XXX−XXX

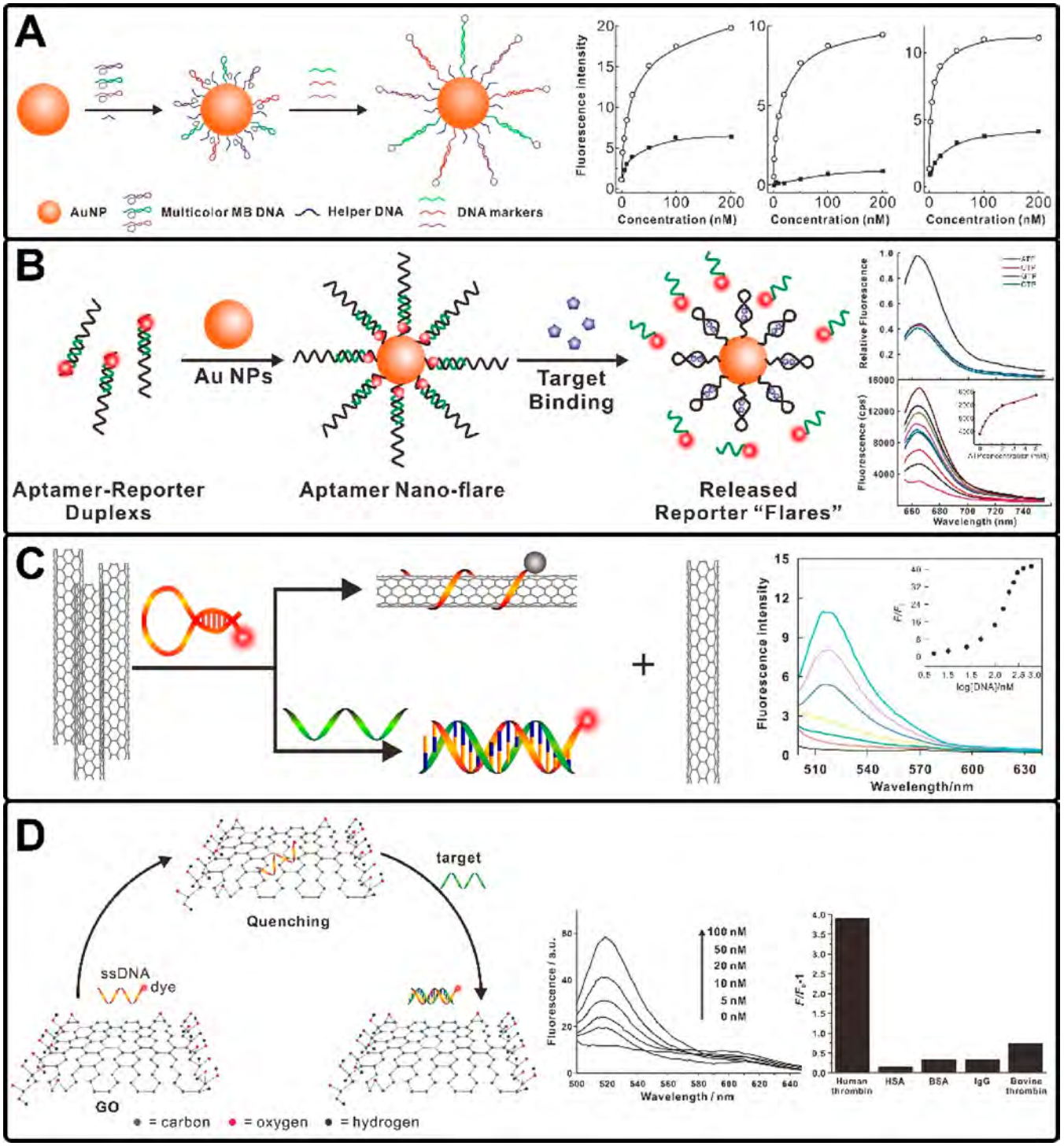

Figure 8. (A) Sequence-specific DNA analysis using AuNP-conjugated multicolor beacons. Adapted with permission from ref 166. Copyright 2009 Wiley-VCH. (B) AuNP-based aptamer nanoflares for molecular detection in living cells. Adapted with permission from ref 167. Copyright 2009 American Chemical Society. (C) SWCNT-based fluorescent sensor for DNA. Adapted with permission from ref 171. Copyright 2008 American Chemical Society. (D) Graphene platform for DNA/protein detection. Adapted with permission from ref 174. Copyright 2009 Wiley-VCH.

targeted delivery (Figure 6B).[153] An internalizing aptamer was designed as a carrier probe for delivery of the MB to specific cells. In addition, the carrier probe sequence contained two photolabile groups to signal target mRNA and to control the intracellular function of the MB. The probe reaches the target cell by aptamer-mediated recognition (AS1411) of nucleolin on the cell membrane, followed by release of the MB by light illumination for mRNA monitoring. The MB allows live-cell mRNA imaging, while the carrier probe allows tracking of the MB before photoinitiation and as a reference signal for ratiometric detection of mRNAs.

The traditional MB-based fluorescence methods are restricted by their sensitivity because of the 1:1 hybridization event between the probe and the target. Therefore, these methods are often combined with amplification strategies (e.g., enzyme-assisted signal amplification) to improve their detection

DOI: 10.1021/acs.chemrev.9b00121
Chem. Rev. XXXX, XXX, XXX−XXX

performance.[154] In one study, Zuo et al. generated a nuclease-amplified DNA detection system (Figure 6C)[155] in which recycling of target molecules by exonuclease III increased the sensitivity of the assay. This exonuclease-amplified strategy can detect target DNA at concentrations as low as 10 pM, showing an enhanced sensitivity compared to the MB alone. Kong et al. conducted a similar work in which they used MB-based junction probes for efficient detection of nucleic acids, and used target-triggered enzymatic recycling for signal amplification,[156] achieving a detection limit of 50 pM. Duan et al. used a hairpin-mediated enzymatic amplification strategy for detection of miR-21 with a LOD of 10 fM at 37 °C and 1 aM at 4 °C.[157] Yang and co-workers used backbone-modified MBs and duplex-specific nuclease-based signal amplification for highly sensitive and selective detection of miRNAs.[158] The results showed a good linear range from 0.5 pM to 500 pM with a LOD of 0.4 pM. Combining the advantages of MBs for highly efficient quenching with a catalytic beacon for amplified sensing, and the Lu group reported a catalytic and molecular beacon (CAMB) technique for Pb^{2+} detection with a LOD of 600 pM (Figure 6D).[159] In addition, the aptamer sequence introduced into DNAzyme for modifying CAMB enables amplified sensing of ATP with a LOD of 500 nM. Thus, CAMB methods can be used for sensitive detection of a wide range of targets.

Hybridization chair reaction (HCR) is an important technique that is used in many biosensing platforms. Two main parameters for efficient HCR are the fluorescence readout of the target-activated HCR process and the optical transduction of the HCR mechanism via fluorescent or catalytic labels. Using HCR, the Tan group designed pyrene-excimer probes for the detection of nucleic acids in complex biological fluids (Figure 7A).[160] In this design, the pyrene monomer transitioned into the pyrene excimer once the HCR process was initiated by the target DNA. The two "initiator" hairpins were modified with pyrene residues at both ends and exhibited strong monomer emissions due to spatial separation of the pyrene units. The target DNA-triggered HCR process brings the two pyrene units in close proximity, thereby depleting the monomer emission and enhancing excimer emission. This method allows detection of target DNA with a LOD of 256 fM. The Li group reported a Hg^{2+}-initiated HCR process through T-Hg^{2+}-T coordination chemistry for Hg^{2+} detection, yielding a LOD of 0.3 nM.[161] To achieve sensitive detection of intracellular miRNA, the Jiang group developed an electrostatically assembled nucleic acid nanostructure, demonstrating HCR in living cells (Figure 7B).[162] In the presence of a target, DNA probes are released from the nanostructure via HCR. The intracellular HCR strategy provides signal amplification and allows ultrasensitive imaging of mRNA expression with a LOD of 0.5 pM, close to a single molecule per cell.

Ren et al. used one-dimensional DNA nanostructures that contained precisely positioned G-quadruplexes for label-free and enzyme-free detection of nucleic acids (Figure 7C).[163] The presence of target DNA initiated the HCR process by opening of two hairpins (H1 and H2). The stem region of hairpin H2 contains the caged sequence of the G-quadruplex. HCR results in the formation of G-quadruplex nanowires that then bind to the G-quadruplex-specific fluorescent label N-methyl mesoporphyrin IX (NMM) providing a readout signal (LOD = 25 nM). Catalytic units (e.g., DNAzymes) coupled to HCR products can be used for amplification of nucleic acid detection. The Willner group developed autonomously assembled polymers composed of DNAzyme wires for amplification of DNA detection (Figure 7D).[164] The presence of DNA target activates the HCR process for generation of catalytically active, Mg^{2+}-dependent, DNAzyme unit-decorated polymeric DNA nanowires. A substrate labeled with a fluorophore/quencher pair was cleaved by the DNAzyme units in the DNA nanowires, producing enhanced fluorescence. The LOD of this system for detection of BRCA1 oncogene was 10 fM.

While fluorescence-based detection is usually highly sensitive, the detection sensitivity is often limited by its high background emission. Organic quenchers have proven their utility in fluorescence-based sensors, but they suffer from relatively low quenching efficiency. Gold nanoparticles (AuNPs) have shown ultrahigh quenching efficiency for background suppression in biosensors and have been considered as superior quenchers to organic ones.[165] As a proof-of-concept, Song et al. implemented AuNPs (15 nm) for constructing multicolor nanobeacons (Figure 8A).[166] Three DNA probes designed for three tumor-suppressor genes, each carrying a unique fluorophore, were immobilized on the AuNP surface. The increased surface area of AuNPs exhibited enhanced quenching efficiency. The nanobeacons showed rapid hybridization kinetics (minutes) and produced a specific response to the different gene targets. This nanobeacon design can be extended to detect non-nucleic acid targets by using aptamers. The Mirkin group developed aptamer nanoflares for detecting ATP in living cells (0.1−3.0 mM) (Figure 8B).[167] The same group then used Au-based nanoflares for mRNA detection in live cells[168,169] and the detection of live tumor cells from human blood.[170]

Several other nanomaterials (e.g., graphene, graphene oxide (GO), carbon nanotubes (CNTs)) have been shown to interact differently with ssDNA and dsDNA, providing another approach for biomolecular recognition. Using the fluorescence quenching efficiency of single-walled carbon nanotubes (SWCNTs), Yang et al. developed a SWCNT-based sensor for DNA (Figure 8C).[171] They verified that fluorophore-labeled DNA probes are efficiently quenched in the presence of SWNTs, while the probes would be released from SWCNTs upon hybridization with target DNA, resulting in fluorescence recovery (LOD = 4 nM). In another study, Zhang et al. detected mercury ions using a CNT-DNA hybrid fluorescent sensor with a LOD of 14.5 nM.[172]

Graphene also possesses ultrahigh quenching ability due to its long-range nanoscale resonance energy transfer. Molecular dynamics studies show that ssDNA adsorbs strongly to GO sheets while dsDNA does not.[173] Similar to the SWCNT-based sensors, Yang and colleagues constructed a graphene platform employing GO to adsorb and quench dye-labeled DNA probes (Figure 8D).[174] Upon hybridization with the target, DNA probes are released from GO, restoring fluorescence. By using dye-labeled aptamers instead of ssDNA probes, this platform can detect human thrombin with a LOD of 2 nM. The Fan group reported a GO-based fluorescence quenching assay for the detection of DNA phosphorylation, enabling detection of polynucleotide kinase down to 0.001 units per mL.[175] Lu et al. used a graphene-peptide complex to monitor peptide−protein interactions.[176] Zhang et al. combined the features of isothermal strand-displacement polymerase reaction and fluorescence quenching ability of GO to detect different miRNA targets.[177] The Ye group designed a graphene-based "on/off" fluorescence switch for multiplexed detection of DNA, thrombin, Ag^{+}, Hg^{2+}, and cysteine,[178] with corresponding LODs of 1 nM, 5 nM, 20 nM, 5.7 nM, and 60 nM.

DOI: 10.1021/acs.chemrev.9b00121
Chem. Rev. XXXX, XXX, XXX−XXX

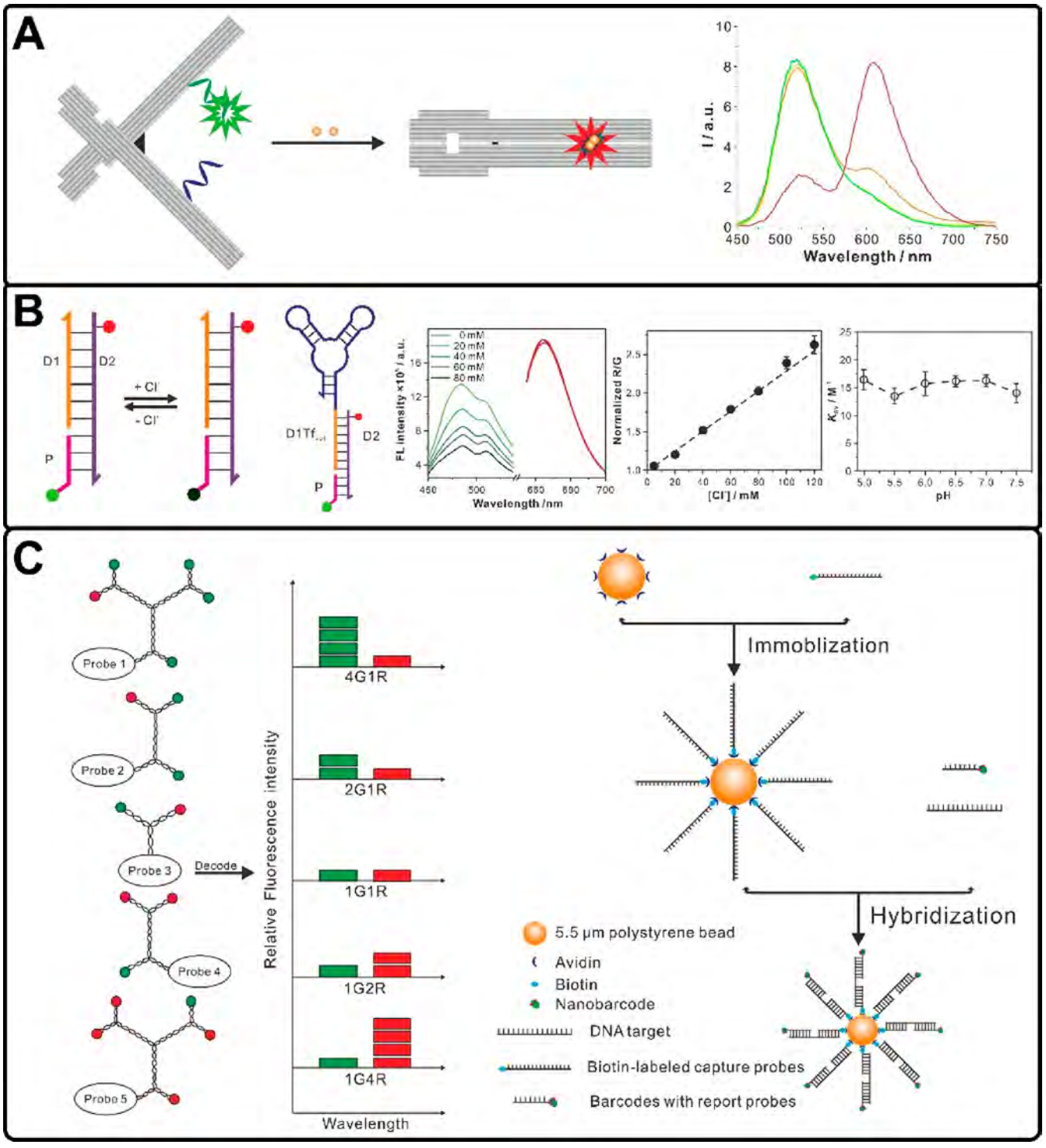

Figure 9. (A) DNA origami traffic lights with a split aptamer sensor for a bicolor fluorescence readout. Adapted with permission from ref 185. Copyright 2017 American Chemical Society. (B) pH-independent DNA nanodevice for quantifying chloride transport in living cells. Reproduced with permission from ref 186. Copyright 2015 Springer Nature. (C) DNA-based fluorescence nanobarcodes for multiplexed detection of pathogen DNA. Reproduced with permission from ref 187. Copyright 2005 Springer Nature.

Apart from the examples discussed so far, other nanomaterials have also been applied in this field. Spherical graphite nanoparticles (GN) can be employed as a fluorescence quencher. Piao et al. developed MB-containing GN-based probes for mRNA detection, obtaining a LOD of 0.3 nM.[179] Using poly(3,4-ethylene dioxythiophene) NPs with high quenching capability, Zhang et al. achieved a detection limit of 30 pM for nucleic acid detection.[180] The Wang group reported photoinduced electron transfer (PET) between DNA/AgNCs and G-quadruplex-hemin complexes for the first time.[181] The nanocluster-based MB probes exhibit extremely low background signal since the fluorescence is quenched in the DNA/AgNC complex. As a result, this PET system provides specific detection of target biomolecules such as DNA and ATP with LODs of 0.6

DOI: 10.1021/acs.chemrev.9b00121
Chem. Rev. XXXX, XXX, XXX−XXX

nM and 8.0 nM, respectively. Another type of material used in biosensing are transition metal dichalcogenide nanosheets that also possess high quenching ability.[182,183] For example, Zhang and co-workers used MoS_2, TiS_2, and TaS_2 nanosheets for the detection of DNA sequences.[184]

DNA nanostructures and nanodevices show many advantages for construction of fluorescence-based biosensors specifically in rationally programming the properties of fluorophores. In one study, Walter et al. built an aptamer-based DNA origami "traffic light" sensor with dual-color fluorescence readout (Figure 9A).[185] In this work, a split aptamer for ATP was incorporated into two levers of a DNA origami. The addition of ATP triggers shape transition of the DNA origami, bringing the dyes closer together, resulting in green to red fluorescence color change. The topological change of the DNA origami was further confirmed by AFM. This system provides an avenue for chemical−biological and bioanalytical research on the single-molecule level. The Krishnan group developed a pH-independent DNA nanodevice (called Clensor) for quantifying chloride transport in organelles of living cells (Figure 9B).[186] The Clensor consists of sensing, normalizing, and targeting modules, and it allows ratiometric sensing of chloride ions across the entire physiological regime. In addition, Clensor has been successfully applied for monitoring the resting chloride concentration in the lumen of acidic organelles in *Drosophila melanogaster*. For rapid, multiplexed, sensitive, and specific molecular detection, Luo and co-workers developed dendrimer-like DNA-based, fluorescence-intensity-coded nanobarcodes (Figure 9C).[187] The nanobarcodes contain predesigned codes and capture probes that allow multiplexed detection of several pathogenic DNA strands with a sensitivity of 0.6 fM.

3.2. FRET-Based Readout Strategy

In the past decades, Forster or fluorescence resonance energy transfer (FRET) has been used extensively as a readout strategy in biosensing.[188−192] FRET is a nonradiative fluorescence quenching phenomenon with energy transferred from an excited donor to an acceptor fluorophore within close proximity as a result of long-range dipole−dipole interaction.[193,194] FRET occurs only when the distance between donors and acceptors (FRET pair) is typically less than 10 nm.[195,196] Fortunately, many reactions in biology such as DNA hybridization, antibody-based immunological recognition, enzyme-catalyzed hydrolysis, or transformation occur within such distances. Because of this high consistency, the FRET technique shows huge advantages over other techniques in analyzing molecular interactions, and conformational and dynamic changes in biomolecules. In addition, FRET also possesses improved sensitivity, short observation time scale in nanoseconds, the working range of distances over which most of the biomolecular processes occur, and the relative simplicity of the experiment. Given their predominant advantages, FRET-based biosensors are particularly effective in the study and detection of such biological events.[197−199] Especially, single-molecule FRET has become a sensitive and powerful tool for determining conformational changes and molecular interactions.[200−202] For instance, the Hildebrandt group used single-FRET-pair distance-tuning to study multiplexed nucleic acid hybridization.[203]

FRET pairs have a crucial influence on the performance of FRET assays, such as distance between donor and acceptor, overlap of donor emission spectrum and acceptor absorption spectrum, dipole−dipole interaction, quantum yield, and fluorescence lifetime of the dyes, etc. Excitation transfer from a donor to an acceptor is through such dipole−dipole interaction, resulting in quenching of the donor dye and excitation of the acceptor. Thus, the FRET process decreases the intensity of the donor fluorescence, quantum efficiency, and overall lifetime, making these parameters vital when choosing a FRET pair. Numerous studies have shown that fluorescent donor or acceptor molecules with remarkable optical properties can substantially improve the efficiency of energy transfer, resulting in superior sensitivity of FRET-based biosensors.[204,205] Typically, fluorescent donor molecules are divided into two groups: traditional fluorophores such as organic fluorescent dyes[206,207] and fluorescent proteins,[208−210] and emerging nanoparticle-based materials[211] such as semiconductor quantum dots (QDs),[212] upconversion nanoparticles (UCNPs),[213−215] and graphene-based derivatives.[216,217] In the following text, we introduce advances in FRET-based biosensors that utilize the aforementioned materials as fluorescent donor in combination with DNA nanotechnology for bioanalysis.

3.2.1. Traditional Fluorophores. Traditional fluorophores including organic fluorescent dyes and fluorescent proteins are widely used in FRET-based biological applications. A class of fluorophores with the representative examples FAM, FITC, Cy3/Cy5, Texasred, and organic fluorescent dyes can emit from the UV to near-infrared region.[206] Moreover, organic fluorescent dyes show instinctive traits, such as small size, solubility, high quantum yields, and the ease of modifications or bioconjugation, which make them important for dye-to-dye FRET systems. These traits make FRET an effective tool for nucleic acid analysis. By monitoring the fluorescence signal change, the FRET strategy allows observation of the interaction between the fluorophore-labeled DNA probe and target.[218−220] For example, You et al. designed a DNA probe that transduces transient membrane encounter events into readable cumulative fluorescence signals by means of FRET.[221] Jin et al. established a multiplexed miRNA FRET assay that integrates biophotonic aspects with RNA base pairing and ligation steps,[222] achieving multiplexed quantification of three miRNAs at detection limits ranging from 0.2 to 0.9 nM. However, some disadvantages such as pH sensitivity, low chemical stability, easy photobleaching, and relatively short fluorescent lifetime restrict them in FRET-based applications. Another representative of traditional fluorophores are fluorescent proteins, which are commonly used as biolabels for monitoring dynamic intracellular interactions. Although fluorescent proteins with high quantum yield and outstanding photostability can be used for long-term detection in living cells,[223] the wide range of excitation/emission spectra of fluorescent proteins induce cross-talk effect, and the detection efficiency is also limited by their large size.[224]

The DNA-fueled tweezers developed for FRET-based biosensors address the aforementioned limitations to a certain extent.[125] This device consists of two nucleic acid arms connected by a flexible hinge. Each end of the hinge strand can be modified to contain a donor or an acceptor to enable readout of the tweezers' operation through FRET. When the device is "open", the two dyes are spatially separated, yielding an inefficient FRET process. A 'fuel' strand binds to the single-stranded overhang of the tweezer's arms and "closes" the tweezer, bringing the dyes within close proximity, thus achieving efficient FRET. An 'antifuel' strand that can hybridize with the full sequence of the 'fuel' strand can then displace the 'fuel' strand from the tweezer, thereby opening the tweezer again. Inspired by this, Han et al. reported a pair of DNA tweezers that can capture, hold, and release a target accompanying its "close"

DOI: 10.1021/acs.chemrev.9b00121
Chem. Rev. XXXX, XXX, XXX−XXX

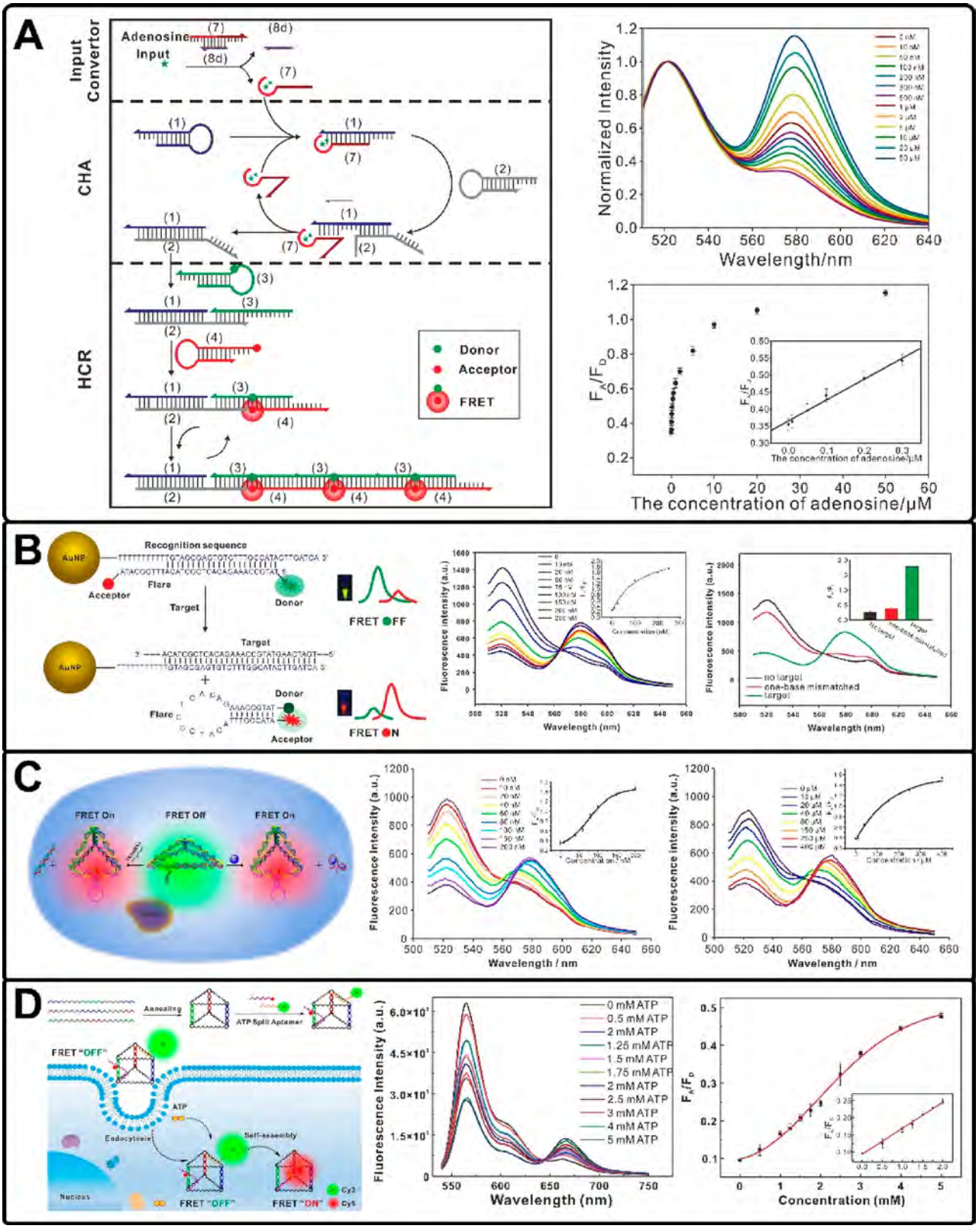

Figure 10. (A) FRET-based bilayer nonenzymatic nucleic acid circuits and their amplification cascades for adenosine detection. Adapted with permission from ref 227. Copyright 2016 American Chemical Society. (B) FRET nanoflares for intracellular mRNA detection. Adapted with permission from ref 230. Copyright 2015 American Chemical Society. (C) FRET-switching DNA tetrahedron MB for detection of DNA and ATP. Adapted with permission from ref 231. Copyright 2016 American Chemical Society. (D) FRET-based DNA nanoprism with a split aptamer for ATP sensing in living cells. Adapted with permission from ref 232. Copyright 2017 American Chemical Society.

and "open" actions.[225] The Simmel group constructed a DNA molecular machine based on a DNA aptamer, where FRET was to monitor the dynamic process of the molecular machine while binding or releasing thrombin.[226] Wang and co-workers

DOI: 10.1021/acs.chemrev.9b00121
Chem. Rev. XXXX, XXX, XXX−XXX

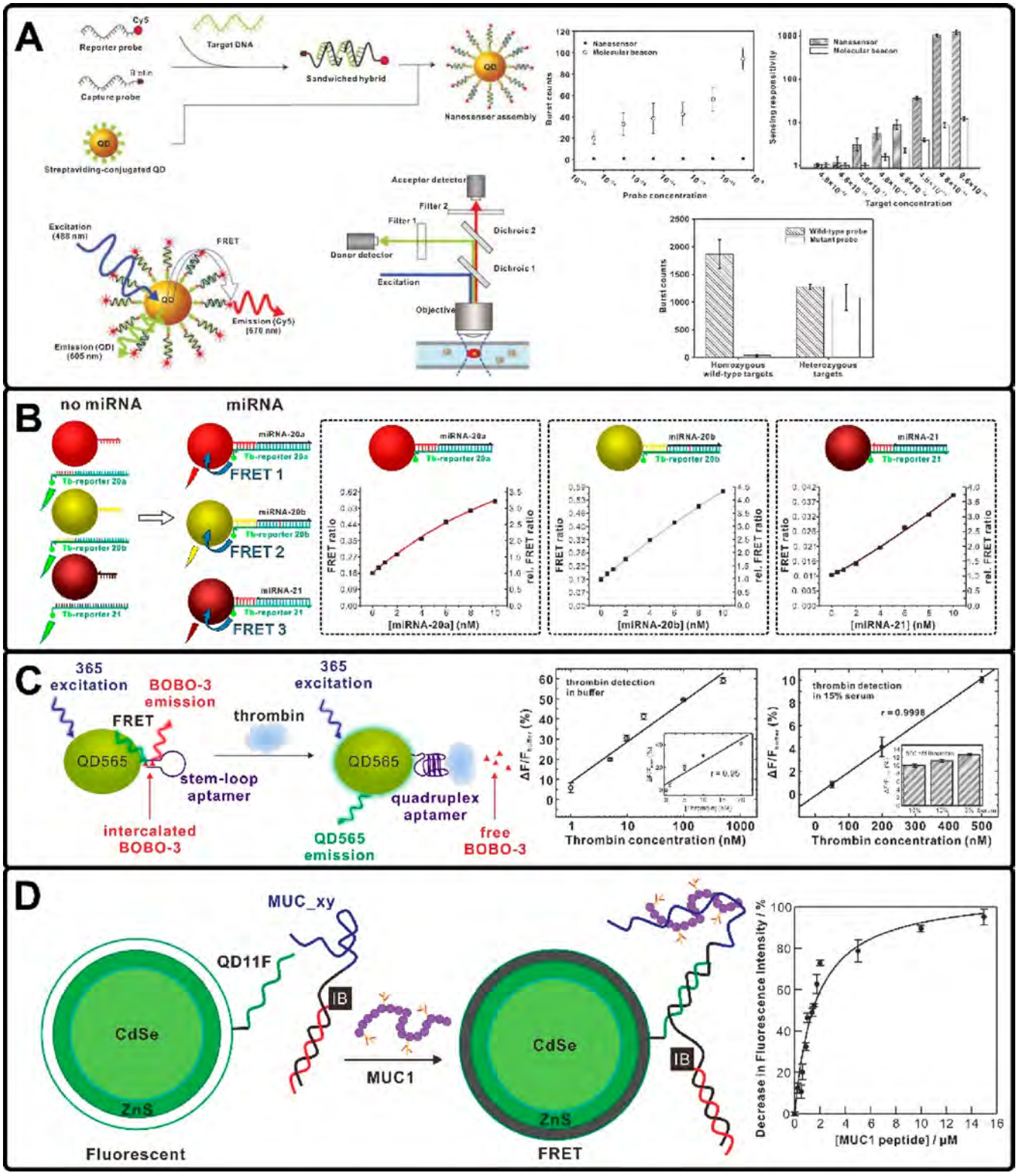

Figure 11. (A) Single-QD-based DNA nanosensors. Reproduced with permission from ref 253. Copyright 2005 Springer Nature. (B) Multiplexed miRNA diagnostic assay using QD-based FRET. Adapted with permission from ref 259. Copyright 2015 American Chemical Society. (C) QD-aptamer beacon with a intercalated dye for label-free thrombin detection. Adapted with permission from ref 260. Copyright 2011 Elsevier. (D) QD-based FRET readout for aptamer-based detection of epithelial tumor marker mucin 1. Adapted with permission from ref 262. Copyright 2009 American Chemical Society.

engineered robust nonenzymatic nucleic acid circuits (Figure 10A),[227] in which a catalyzed hairpin assembly (CHA) activates a HCR circuit to yield a FRET-based readout. This self-assembly process was monitored in real time using FRET signals. The powerful amplification cascades empower this DNA device to sensitively detect adenosine in buffer or human serum down to 200 pM. In the same way, Wang et al. constructed an enzyme-

DOI: 10.1021/acs.chemrev.9b00121
Chem. Rev. XXXX, XXX, XXX−XXX

free concatenated DNA circuit for the detection of miR-21 with a detection limit of 2 pM.[228]

Another effective strategy to construct FRET-based sensors is by using NPs as carriers for fluorophore-labeled DNA.[229] In one example, the Wang group developed FRET nanoflares for sensing mRNA in living cells (Figure 10B).[230] The nanoflares consist of an AuNP, recognition sequences, and flares. In the absence of a target, the recognition sequence-modified AuNP hybridizes to flares labeled with donors and acceptors at two ends, thus separating them to reduce the FRET efficiency. Target addition results in the gradual substitution of flares from the AuNPs. The released flares form hairpin structures, bringing the donor and acceptor into close proximity, resulting in high FRET efficiency. The FRET nanoflares allow dynamic detection of mRNA between 0 and 250 nM. In contrast to the conventional single-dye nanoflares, such upgraded FRET nanoflares eliminate false positive signals by chemical interferences (e.g., nuclease, glutathione) and thermodynamic fluctuations. In a follow-up study, they designed a competition-mediated FRET-switching DNA tetrahedron molecular beacon (CF-DTMB) (Figure 10C).[231] The target analyte binds to recognition strands that are part of the tetrahedron and releases them, changing from a FRET "off" to a FRET "on" state. This design enables detection of DNA from 0 to 200 nM with a LOD of 7.6 nM and detection of ATP from 0 to 400 μM with a LOD of 10.4 μM. Additionally, Zheng et al. reported a DNA triangular prism (TP) encapsulating a split aptamer for ATP sensing in living cells (Figure 10D).[232] They demonstrated that the DNA-TP nanoprobe is a stable, sensitive, and selective biosensor and can quantitatively detect ATP in the range of 0.03 to 5 mM with a LOD of 30 μM. Moreover, the DNA-TP nanoprobe can serve as an *in situ* FRET off-to-on biosensor for specific, high-contrast imaging of target molecules.

With the advent of advanced nanoscience and nanotechnology, multiple promising NPs with special optical properties have been used either as donors or acceptors in FRET assays, enhancing the use of FRET in medical and biological applications. For instance, NPs including QDs,[188] UCNPs,[233] and graphene QDs,[234] have been found to have photoluminescence (PL) because of quantum confinement effect. These photoluminescent NPs are highly photostable with high quantum yield, enhanced brightness, and long fluorescent lifetime, which make them good candidates as donors in FRET. In addition, some NPs with unique electronic properties are responsible for super quenching. For example, AuNPs,[235] graphene and its derivatives,[236,237] and graphene-like 2D nanomaterials[238,239] can be used as efficient fluorescence quenchers in FRET assays. To avoid repetition from Section 3.1, biosensing assays involving NPs as donors for FRET are discussed in the following text.

3.2.2. Quantum Dots as FRET Donors. QDs consisting of the elements from groups II and VI or groups III and V in the periodic table are highly luminescent semiconductors. They are known for their small size (1−20 nm) and size-dependent optical and electronic properties caused by quantum confinement. The most common QDs such as CdTe, CdSe, InP, and InGaP have been used as fluorescent labels in various biological applications. Compared to traditional organic dyes, QDs offer many advantages as FRET donors such as narrow and tunable emission spectra, better photostability, resistance to photobleaching or chemical degradation, and higher quantum yield (40% to 90%) as well as a long fluorescence lifetime (20−50 ns).[206,207,240−244] Moreover, their photoluminescent properties allow maximum spectral overlap by tuning the size and minimizing the crosstalk between FRET pairs, thus preventing interfering background signal and increasing the FRET efficiency.[245,246] Furthermore, QDs with broad excitation spectra and narrow defined emission peaks, higher molar extinction coefficient, and large Stokes shift allow the use of multicolor QDs for multiplexing purposes and enable imaging or tracking of multiple molecular targets at the same time.[247−250]

Numerous QD-FRET-based sensors have been reported for analysis of nucleic acids.[188,251,252] The Wang group constructed a FRET-based sandwich sensor for DNA detection utilizing streptavidin-modified CdSe-ZnS QD as a donor and Cy5 dye as an acceptor (Figure 11A).[253] In this system, the capture strands are conjugated with biotin, while the report strands are labeled with Cy5. Hybridization of target DNA with capture strands and reporter strands results in the formation of a sandwich structure. Thereafter, binding of streptavidin to biotin brings the Cy5-labeled sandwich hybrids and QDs into close proximity, resulting in the efficient FRET effect. This QD-based FRET biosensor had a LOD of 4.8 fM. In addition, cationic polymers serving as a bridge to bring the dye-labeled DNA and QD together have been used for DNA hybridization detection.[254,255] Krull and co-workers fabricated a series of optical fiber-based QD-FRET platforms for nucleic acid detection,[256−258] in which QDs conjugated to optical fibers and containing dye acceptors bound to target oligonucleotides provide a FRET effect. The LOD of this DNA detection platform ranged from 1 nM to 10 nM. Qiu et al. designed a multiplexed FRET involving three different semiconductor QDs and a luminescent terbium complex to detect three different miRNAs with a LOD of ∼1 nM (Figure 11B).[259] In the assay, three different QDs were conjugated with short DNA strands that are partly complementary to three different reporter DNAs conjugated with terbium. The terbium-reporter DNAs also contain another region that is complementary to one of the three miRNAs (miRNA-20a, miRNA-20b, miRNA-21). Terbium-reporters bind to their respective miRNAs forming an RNA/DNA hybrid. The short overhang on the terbium side hybridizes to the complementary QD-DNA, resulting in the formation of three miRNA-specific RNA/DNA duplexes that can be identified by the specific terbium-to-QD FRET pairs for photoluminescence-based detection. This QD-based FRET strategy provided rapid and multiplexed miRNA detection.

QD-based FRET immunoassays have been applied in biomedical applications. For protein analysis, aptamers are often conjugated to QDs to generate QD-aptamer FRET assays so that the target proteins can be conjugated to QDs to induce the FRET process. Chi et al. detected thrombin using a QD-aptamer FRET assay (Figure 11C).[260] A single-stranded antithrombin aptamer probe was covalently conjugated to a QD, and the BOBO-3 dye intercalated into a double helix exhibited an efficient FRET before thrombin binding. When thrombin binds to the aptamer, the induced conformational change from a stem-loop to a quadruplex dissociates BOBO-3 from the QD-aptamer, resulting in decreased FRET, allowing detection of thrombin with a LOD of 1 nM. Besides protein analysis, QD-based FRET immunoassays have also been used for the detection of cancer biomarkers.[261] Cheng et al. detected epithelial tumor marker Mucin 1 (MUC1) based on the QD-based FRET readout (Figure 11D).[262] The increased proximity of the quencher and QDs results in increased FRET, allowing MUC1 detection in the nanomolar level.

DOI: 10.1021/acs.chemrev.9b00121
Chem. Rev. XXXX, XXX, XXX−XXX

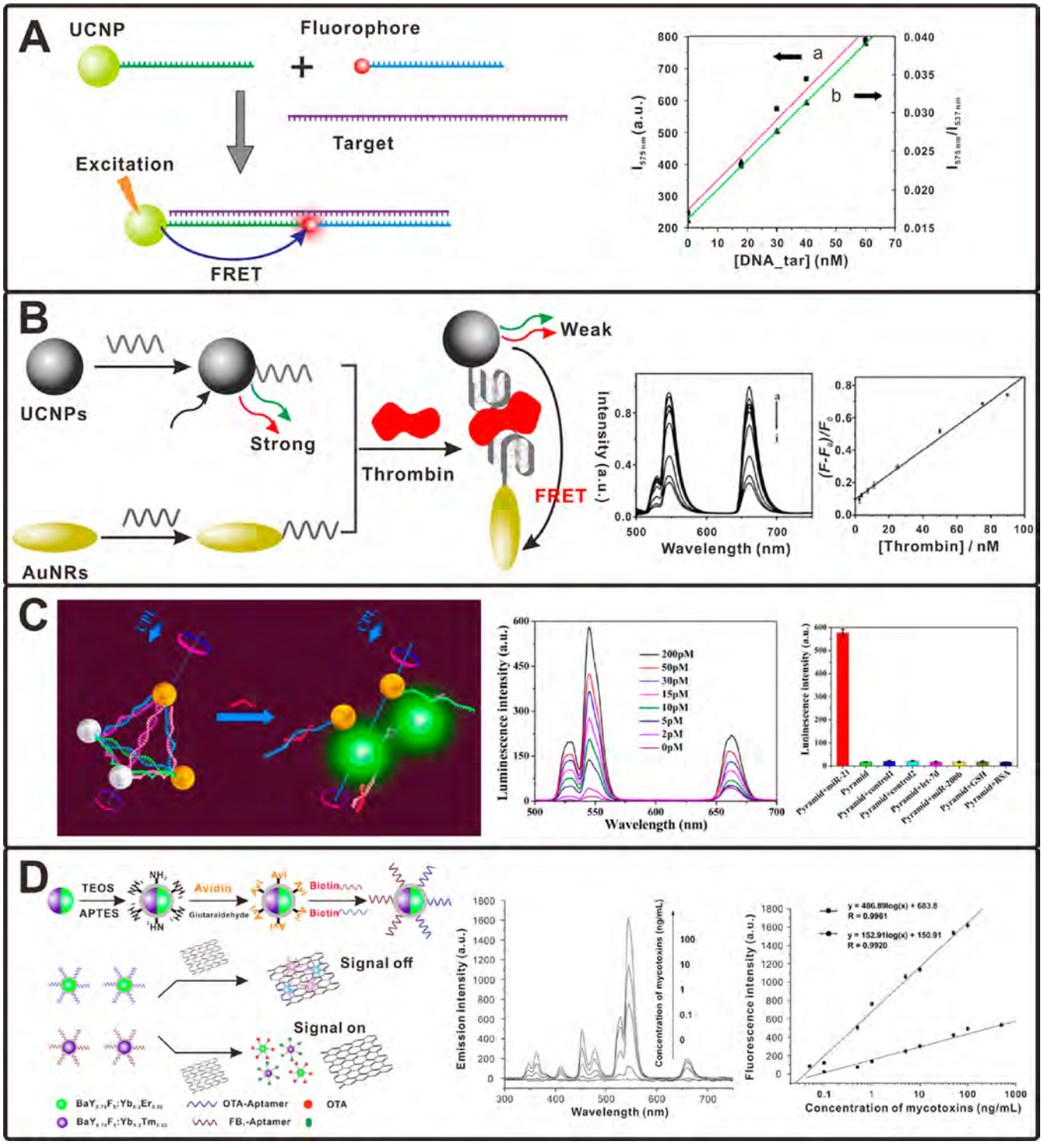

Figure 12. (A) Photon UCNP-based sensor for sensitive and specific detection of nucleic acids. Adapted with permission from ref 271. Copyright 2006 American Chemical Society. (B) Aptamer-based sensing for thrombin via FRET between UCNPs and AuNRs. Adapted with permission from ref 275. Copyright 2013 Elsevier. (C) Chiroplasmonic nanopyramids self-assembled from AuNPs and UCNPs for dual-mode quantification of miRNA in living cells. Reproduced with permission from ref 278. Copyright 2016 American Chemical Society. (D) Multiplexed FRET aptasensor between UCNPs and GO for the simultaneous determination of mycotoxins. Adapted with permission from ref 279. Copyright 2012 American Chemical Society.

Despite its advantages, the limitations of the QD-based FRET strategy cannot be ignored. QDs suffer from luminescence intermittency known as blinking, which can cause problems in applications. This problem can be alleviated by shell engineering or decreasing the excitation intensity.[263] The diameter of the QDs and surface coating need to be taken into consideration because FRET efficiency depends on the distance between FRET pairs. In addition, the large size of QDs may impair the energy transfer efficiency of QD-based FRET assays, which makes their efficiency lower than those with organic dyes.[264,265]

DOI: 10.1021/acs.chemrev.9b00121
Chem. Rev. XXXX, XXX, XXX−XXX

Furthermore, the synthesis procedures of conventional semiconductor QDs always involve toxic components, which hinder their further biological application.[266,267]

3.2.3. Upconversion Nanoparticles as FRET Donors. Lanthanide-doped UCNPs are a new generation of fluorophores that have aroused interest because of their unique advantages such as a narrow emission peak, large Stoke shifts, a high quantum yield, good chemical stability, and low toxicity.[268] These prominent features make UCNPs promising alternatives to traditional fluorophores applied in FRET-based biological detection. Compared to QDs, UCNPs converting near-infrared radiation (NIR) into visible light via nonlinear optical processes cause less harm to biological samples.[269] In general, UCNPs as donors need to be coupled with a down-converting acceptor molecule in FRET assays wherein the fluorophore should be chosen for the excitation spectra of the down-converting fluorophores and the spectral overlap between the emission spectra of the UCNPs. Given that NIR excitation light is far away from the excitation spectra of most acceptor molecules, UCNPs have thus been regarded as excellent donor candidates.[270]

The FRET strategies exploiting UCNP-organic dye as FRET pairs have been extensively used for various biological applications. For instance, Zhang et al. used Er^{3+}-doped $NaYF_4$ particles as donor and TAMRA as acceptor for constructing a nucleotide sensor (Figure 12A).[271] Using target DNA for cohybridization with short oligonucleotide-modified UCNPs and another TAMRA-labeled oligonucleotide, this sandwich assay can determine target DNA with a LOD of 1.3 nM. Thereafter, Chen et al. also developed a similar sandwich DNA sensor.[272] In this work, the presence of free carboxylic acid groups confers $NaYF_4$:Yb,Er NPs high solubility in water and allows conjugation with streptavidin. Hwang et al. used UCNP-based FRET to detect a specific sequence (*IS6110*) of *Mycobacterium tuberculosis* complex in saliva, with a LOD of 100 copies/μL.[273] Wu et al. constructed a NIR-responsive DNA probe composed of ssDNA attached to positively charged UCNPs.[274] This DNA probe enables detection of DNA targets using the nucleic acid stain SYBR Green I with a LOD of complementary ssDNA at 3.2 nM and three-base mismatched ssDNA at 7.6 nM.

UCNP-AuNP (or AuNR) pairs have been used for construction of FRET-based biosensors. Chen et al. used an aptamer-based FRET system to detect thrombin (Figure 12B),[275] in which $NaYF_4$:Yb,Er UCNPs and AuNRs serve as donor and acceptor, respectively. The thrombin acts as a bridge to connect UCNPs and AuNRs, both containing thrombin aptamers. Therefore, the fluorescence quenching efficiency of UCNPs increases with an increase in thrombin concentration, showing a good linear relationship between 2.5 nM and 90 nM with a LOD of 1.5 nM. The Yang group developed a strategy based on $BaGdF_5$:Yb/Er UCNPs and AuNPs for detecting short genes of the H7 subtypes with a LOD of 7 pM.[276] The same group then used a similar method for detection of Ebola virus oligonucleotide with LOD down to the femtomolar level.[277] To detect intracellular miRNA, the Kuang group fabricated DNA-driven Au-UCNP pyramids (Figure 12C),[278] in which the miRNA recognition sequences were incorporated into each edge of the DNA frame. Hybridization of target miRNA to this binding sequence results in dissociation of the DNA frame, separating the AuNPs and UCNPs and restoring the luminescence of the UCNPs. The luminescence intensity of this assay ranges from 0.16 to 43.65 fM with a LOD of 0.12 fM.

Another strategy often used in biosensing is UCNP-GO FRET. Wu et al. developed a strategy to detect ochratoxin A (OTA) and fumonisin B1 (FB1) at the same time using multicolor UCNPs and GO as the FRET pair (Figure 12D).[279] In the initial state of the platform, two aptamer-modified UCNPs exhibit high upconversion fluorescence. As a result of the strong $\pi-\pi$ stacking effect between the aptamers and GO, the proximity of the aptamers-UCNPs and GO was close upon the addition of GO, thus quenching the UCNP fluorescence. In the presence of OTA and FB1, the conformation changes of aptamers led to the restoration of UCNP fluorescence. This platform enables detection of OTA in the range from 0.05 ng mL^{-1} to 0.1 μg mL^{-1} with a LOD of 0.02 ng mL^{-1} and detection of FB1 in the range from 0.1 ng mL^{-1} to 0.5 μg mL^{-1} with a LOD of 0.1 ng mL^{-1}. Similarily, Liu et al. developed a FRET assay to detect ATP, where the donor was UCNPs and the acceptor was GO.[280] The linear detection range for this assay was 0.5 to 100 μM, and the detection limit for ATP was 80 nM. The Kanaras group reported a UCNP/GO-based DNA sensor that could detect DNA down to 5 pM.[281] In addition to GO, graphene can be used as acceptor in FRET assays. For example, Liu and co-workers developed a FRET aptasensor for kanamycin detection where UCNPs were the donor and graphene the acceptor. This assay had a detection limit of 9 pM.[282]

FRET assays require the emission of UCNPs to be in the visible light range for excitation of acceptor. Therefore, more research studies have focused on the design of UCNPs for precise control over their properties (e.g., the size, crystal phase, dopant concentration, and local homogeneity),[283,284] thereby obtaining the tunable bandwidth and color for spectral alignment. Despite their distinctive properties, the dissolubility in aqueous solutions, lack of target biorecognition, and bioanalytical functions hamper their further applications.[285] To address this issue, numerous studies have reported surface functionalization of UCNPs such as poly(acrylic acid) coating, silica coating, and attachment of biomolecules (e.g., nucleic acids, antibody, peptides).[286,287] In addition, it is still challenging to synthesize sub 10 nm particles with high luminescence efficiency for intracellular applications.[285] Tremendous effort has been devoted to developing various advanced synthetic procedures to prepare small size UCNPs with sufficient luminescent intensity.[288,289]

3.2.4. Graphene Derivatives as Donors. Graphene has attracted tremendous attention since its discovery in 2004[290] because of its excellent thermal, mechanical, and electronic properties.[291,292] Pristine graphene is a one-atom-thick planar sheet structure with sp^2 carbon atoms in a honeycomb lattice. However, due to a zero band gap, no photoluminescence is observed under any wavelength excitation.[293] Fortunately, graphene derivatives such as graphene quantum dots (GQDs) and graphene oxide (GO) can fill these gaps through specific physical and chemical processes. In this section, the optical properties of graphene derivatives in FRET assays are discussed.

3.2.4.1. Fluorescent GO as Donors. Unlike pristine graphene, GO exhibits various photoluminescent properties in visible and NIR regions, which results from sp^2/sp^3 carbons and oxygen functional groups on the surface or at edges.[294] Many studies have disclosed that the recombination of electron−hole pairs in the disrupted π networks containing both sp^2 and sp^3 carbon atoms is the essential reason for the visible and NIR emissions.[295,296] Hence, the wavelength and intensity of emission of GO are determined by the amount and state of sp^3 carbon linking groups, and its emission can be altered by

DOI: 10.1021/acs.chemrev.9b00121
Chem. Rev. XXXX, XXX, XXX−XXX

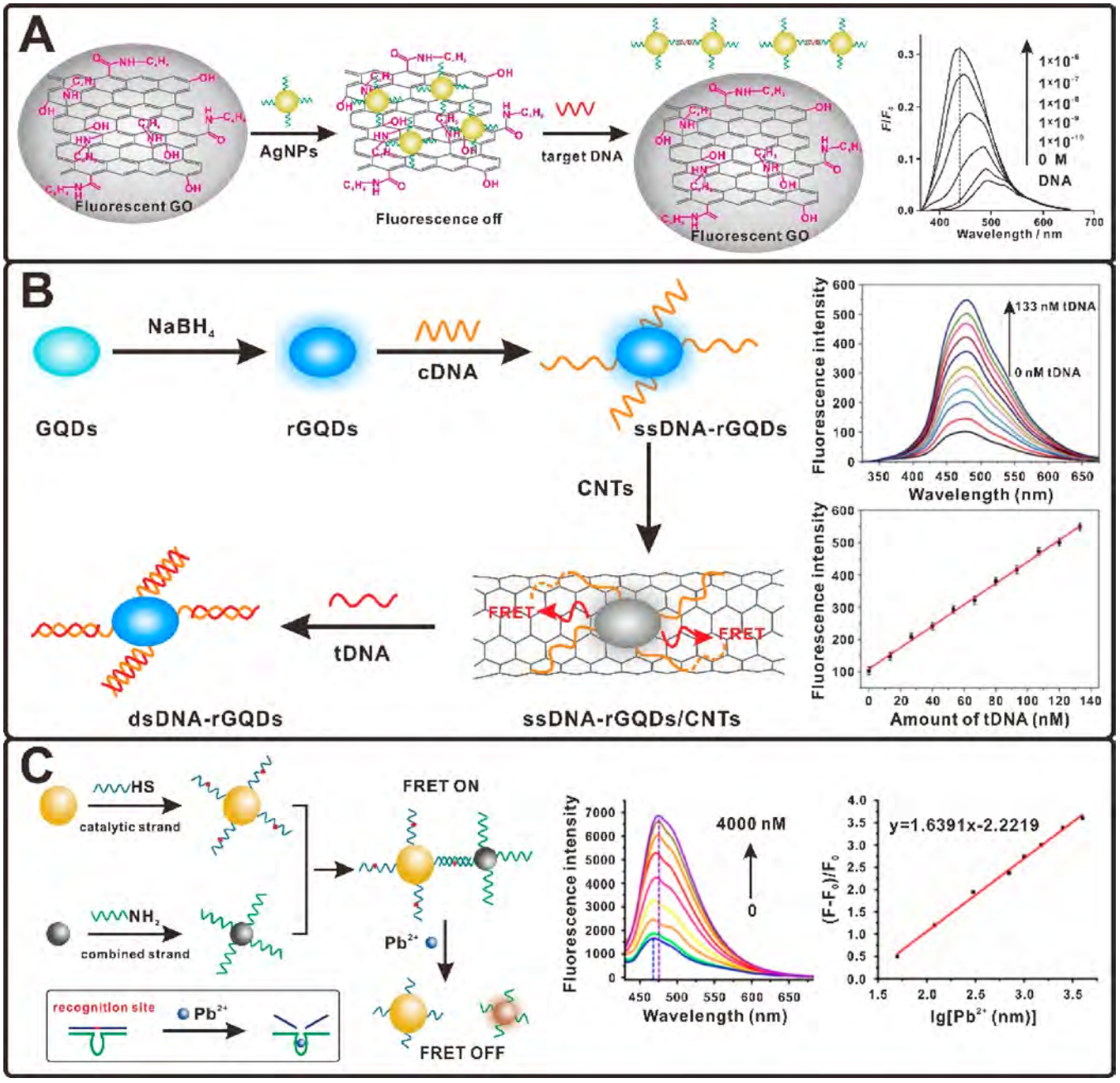

Figure 13. (A) Fluorescence "off-to-on" mechanism of GO-NHBu nanosheets for DNA detection. Adapted with permission from ref 301. Copyright 2012 Wiley-VCH. (B) DNA nanosensor based on GQDs and CNTs. Adapted with permission from ref 314. Copyright 2014 Elsevier. (C) "Turn-on" fluorescence sensor for Pb^{2+} detection based on GQDs and AuNPs. Adapted with permission from ref 318. Copyright 2018 Elsevier.

simple manipulations such as controlling surface chemistry, solid or liquid state of GO sheets, and pH value of the solvent. Moreover, compared to traditional organic fluorophores, the photoluminescence of fluorescent GO is quite stable against chemical and photonic bleaching.[296−298]

Photoluminescent GO-based FRET assays are also used for biological analysis. For example, Liu et al. used probe-modified photoluminescent GO as a donor and target DNA-modified AuNP as an acceptor for DNA hybridization detection.[299] The hybridization between ssDNA-GO and ssDNA-AuNP leads to the close distance between GO and AuNPs, concomitantly fluorescence quenching. Measuring the fluorescence intensity allows detection of target DNA down to 200 nM. The Seo group reported a fluorescent GO-based immuno-FRET system for pathogen detection.[300] In this system, the antibodies are first immobilized on a GO array surface via covalent binding. AuNP-DNA-antibody can be coupled with GO-antibody to form a sandwich structure upon capture of the target pathogen, thus quenching the fluorescence of GO. This method enables pathogen detection down to 10^5 pfu mL^{-1}. Additionally, Mei et al. constructed a portable platform based on fluorescent GO for DNA detection (Figure 13A).[301] After GO treated with *N*-butylamine (NHBu), the resulting GO-NHBu composites emit a bright blue fluorescence at 440 nm. Through nonspecific surface interactions, AgNPs as acceptors can adsorb onto the surface of GO-NHBu, thus strongly quenching the fluorescence of GO-NHBu. Addition of target DNA results in disassociation of AgNPs from the GO-NHBu nanosheets, restoring the

DOI: 10.1021/acs.chemrev.9b00121
Chem. Rev. XXXX, XXX, XXX−XXX

fluorescence. The recovered fluorescence provides rapid identification and quantification of DNA, with a LOD of 10 pM.

3.2.4.2. GQDs as Donors. GQDs are small fragments of GO with a diameter under 20 nm in single or few layers of thickness.[302] Similar to GO, GQDs contain sp^2 carbon domains and are surrounded with functional groups such as epoxy and carboxyl groups. Because of the quantum confinement effect and edge effect, more defects of oxygen and other functional groups on the GQD surface bestow GQDs with excellent photoluminescent properties.[302,303] Two main approaches (i.e., top-down methods, bottom-up methods) have been developed for GQD synthesis.[304−306] Previous research studies have demonstrated that the synthesized GQDs exhibit various traits, such as tunable optical properties, high brightness, excellent photostability, long fluorescence lifetime, nontoxicity, and exceptional biocompatibility,[302,307−309] making them excellent candidates as FRET donors. Moreover, GQDs have high surface-to-volume ratios and provide higher molecular adsorption via $\pi-\pi$ stacking interactions due to the larger sensing area, thus enhancing the FRET efficiency. The quantum confinement effect and surface effect are considered as the two dominant parameters for photoluminescence of GQDs.[294,307,310] Besides, it is shown that the photoluminescent properties of GQDs can be also altered via various surface modifications.[307,310] Other parameters including excitation wavelength,[303] pH value,[311] and solvent types[312] can have an influence on the emission spectra and quantum yield. For example, the protonation of the free zigzag sites of the GQDs in acidic solution can induce the destruction of emissive triple carbine state, whereas these free zigzag sites can be maintained in alkaline condition and emit photoluminescence.[313]

GQDs have been used as energy donors in FRET assays. For example, the Feng group conducted a series of studies for DNA detection.[314−316] In one study, Feng and co-workers constructed a nanosensor based on FRET between GQDs and carbon nanotubes (CNTs) (Figure 13B).[314] To obtain a brighter fluorescence, GQDs were reduced with $NaBH_4$ to prepare rGQDs. The fluorescence of ssDNA−rGQDs probe is quenched by adsorption of the ssDNA−rGQDs on the surface of CNTs through electrostatic attraction and $\pi-\pi$ stacking interactions. When the target DNA hybridizes with ssDNA-rGQDs to form dsDNA-rGQDs, it induces detachment of dsDNA−rGQDs from CNTs, resulting in fluorescence recovery. This assay has a linear range of up to 133 nM with a LOD of 0.4 nM. The same group achieved simultaneous detection of multiple DNA targets by using a FRET assay combining dual-color GQD nanoprobes and CNTs.[315] In another study, the Feng group used GQDs as donors and GO as acceptors for DNA detection, with a linear range of 6.7−46 nM and a LOD of 75 pM.[316] Shi et al. reported a FRET sensor with GQDs as donors and AuNPs as acceptors for detection of the food-borne pathogen *Staphylococcus aureus* specific gene sequence with a LOD of 1 nM.[235] Besides DNA analysis, GQDs have been used as energy donors for protein and ion detection. For instance, He et al. combined a fluorescent probe composed of ssDNA-binding protein and GQDs with Apt-BHQ1 for kanamycin detection based on the FRET principle.[317] This method shows a linear range from 0.01 to 90 ng/mL with a detection limit of 6 pg/mL. Recently, Niu et al. used GQDs and AuNPs to construct a "turn-on" fluorescence sensor for Pb^{2+} detection (Figure 13C).[318] Initially, both GQDs and AuNPs were modified with DNA, and they could be connected via DNA hybridization. Their close proximity led to fluorescence quenching of GQDs. However, in the presence of Pb^{2+}, the DNAzyme cleaves the "rA" site, thus releasing GQDs from AuNPs and recovering the fluorescence. This sensor has a detection range from 50 nM to 4 μM, with a LOD of 16.7 nM.

Although great progress has been made in graphene derivative-based biosensors,[319] there are certain issues that need to be addressed for practical applications. Apart from fabrication methods, more efforts should be paid to precise control over the dimension and surface chemistry of graphene derivatives.[211] By modulating the size and surface, the emission spectra can be tuned, but the excitation-dependent effect of photoluminescence is still a problem.[320] Moreover, exploring their optical properties, developing new biofunctionalization strategies, improving dispersity in water, and decreasing toxicity in living cells would further expand their biomedical applications.[216]

3.3. Nanoparticle-Based Readout Strategy

With the advent of nanotechnology, many different nanoscale materials have been developed for biosensing purposes such as transducers for transforming and amplifying the signal.[321] Nanomaterials hold unique physicochemical properties such as significant surface-to-volume ratios, strong signal intensities, and finely tunable surface chemistries, providing desirable and unmatched characteristics for construction of sensors.[322,323] For instance, nanomaterials with large surface areas can be capable of loading various signal labels (e.g., DNAs, enzymes, organic dyes), enabling sensitive analysis.[324] It is well-established that DNA can be assembled on given nanomaterials via some simple yet effective methods such as $\pi-\pi$ stacking, electrostatic adsorption, and covalent binding. In general, the nanoarchitecture of this complex includes a nanomaterial core and a monolayer of DNA. Such DNA-nanomaterial complexes combine the molecular recognition properties of DNA with optical and electronic properties of nanomaterials.[325] Moreover, these complexes possess other new features including high affinity between the DNA-nanomaterial complex and target, strong degradation resistance, and high cellular uptake.[326] These properties make DNA-nanomaterial hybrid systems promising for the development of new sensing platforms. In this section, nanoparticle-based readout strategies, including gold nanomaterials, carbon nanomaterials, two-dimensional nanomaterials, and quantum dots (QDs), are discussed.

3.3.1. Gold Nanomaterials. AuNPs are the most common and stable metallic nanomaterials and have elicited considerable interest recently because of their many features and properties such as facile synthesis, tunable size and shape, easy surface modification, high DNA-loading efficiency, sized-related electronic and optical properties, good biocompatibility, and high intracellular stability.[327,328] Notably, the strong interaction between thiol and AuNP offers an easy-to-handle and low-cost approach for AuNP modification.

On the basis of their special electronic properties, AuNPs exhibit a "superquenching" ability for fluorescence via long-range resonance energy transfer.[329,330] The Mirkin group reported that DNA-AuNP complexes termed nanoflares enable detection of ATP and mRNA in living cells.[167,168,331] Bai et al. conducted an AuNP assay for selecting quadruplex-binding ligands.[327] Initially, AuNPs carrying fluorescein-tagged DNA probes show weak fluorescence. Once the target ligand binds to the DNA probes, the linear probes change conformation to G-quadruplexes, increasing the distance between DNA probes and AuNPs, leading to enhanced fluorescence. Lu and co-workers

DOI: 10.1021/acs.chemrev.9b00121
Chem. Rev. XXXX, XXX, XXX−XXX

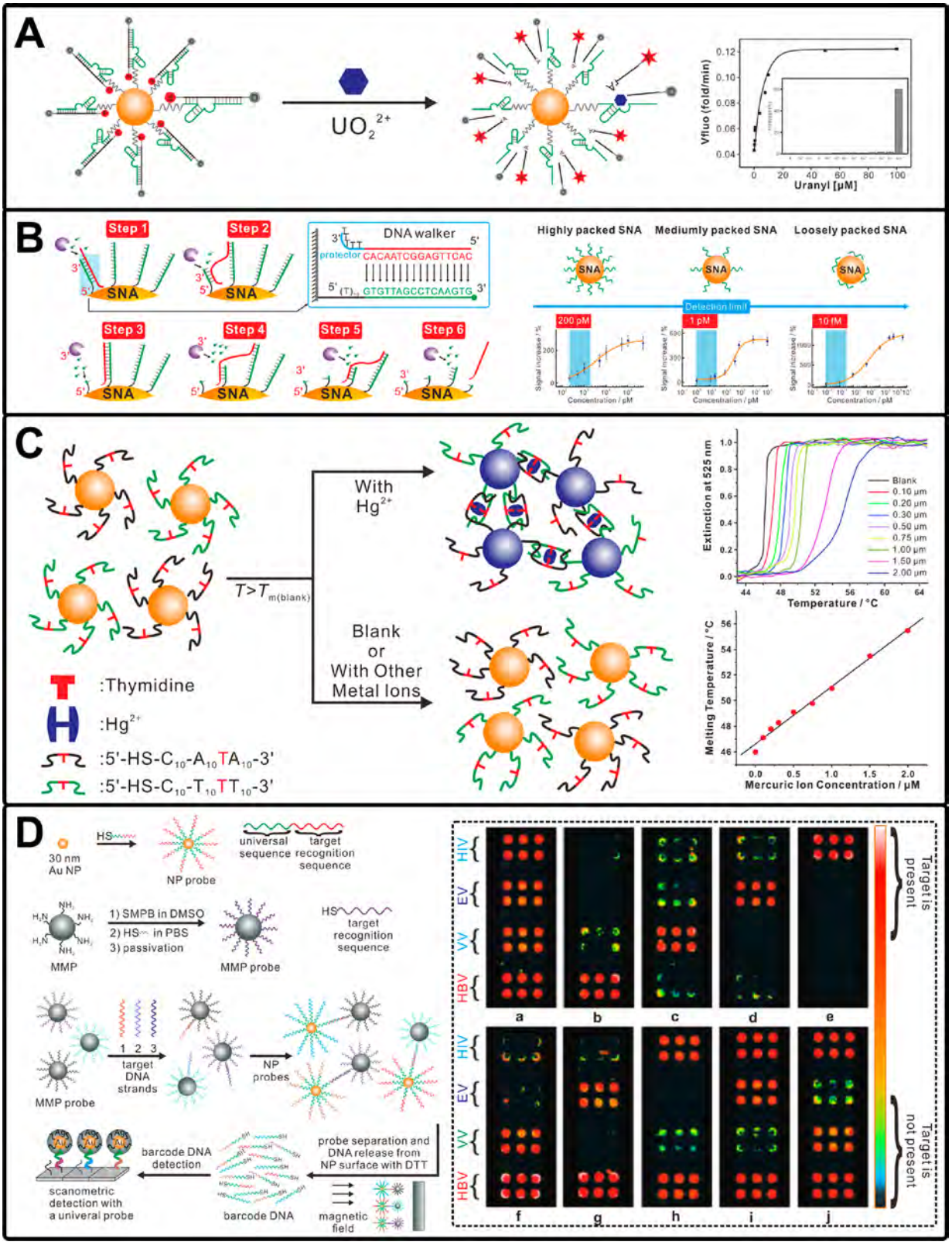

Figure 14. (A) DNAzyme-AuNP probe for UO_2^{2+} in living cells. Adapted with permission from ref 332. Copyright 2013 American Chemical Society. (B) Exo III-powered, on-particle stochastic DNA walker for DNA detection. Adapted with permission from ref 333. Copyright 2017 Wiley-VCH. (C) DNA-functionalized-AuNPs for colorimetric detection of Hg^{2+}. Reproduced with permission from ref 335. Copyright 2007 Wiley-VCH. (D) Biobarcoded NP probes for multiplexed DNA detection. Reproduced with permission from ref 340. Copyright 2006 Wiley-VCH.

constructed a DNAzyme-AuNP probe to detect uranyl ion (UO_2^{2+}) in living cells (Figure 14A).[332] Addition of UO_2^{2+} causes the fluorophore-labeled substrate strand to be cleaved by DNAzyme, releasing the shorter strand from AuNPs and thus recovering the fluorescence. This DNAzyme-based probe showed exceptional selectivity and sensitivity for UO_2^{2+}

DOI: 10.1021/acs.chemrev.9b00121
Chem. Rev. XXXX, XXX, XXX−XXX

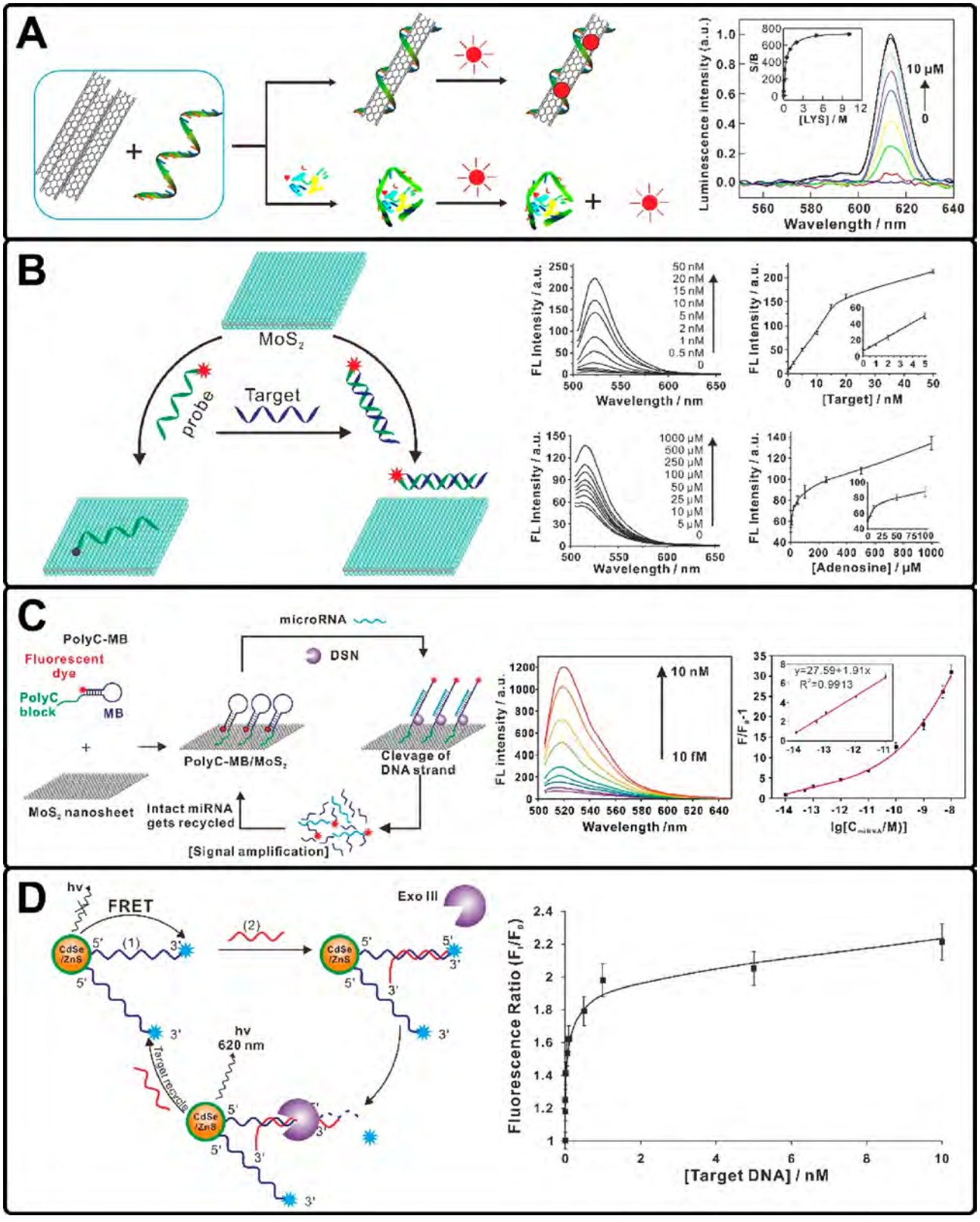

Figure 15. (A) Conjugate Eu^{3+} complex and aptamer-wrapped CNTs for protein detection. Adapted with permission from ref 342. Copyright 2011 American Chemical Society. (B) Single-layer MoS_2-based nanoprobes for homogeneous detection of biomolecules. Adapted with permission from ref 353. Copyright 2013 American Chemical Society. (C) Affinity-modulated MB on MoS_2 nanosheets for miRNA detection. Adapted with permission from ref 358. Copyright 2018 American Chemical Society. (D) Functionalized semiconductor QDs for Exo III-aided amplified multiplexed analysis of DNA. Adapted with permission from ref 363. Copyright 2011 American Chemical Society.

detection. Moreover, it demonstrated that this DNAzyme-AuNP probe can be used *in vivo* as a metal ion sensor. Recently, the Pei group reported an Exo III-powered stochastic DNA walker (Figure 14B).[333] The DNA walker autonomously moves

DOI: 10.1021/acs.chemrev.9b00121
Chem. Rev. XXXX, XXX, XXX−XXX

on a spherical nucleic acid (SNA)-based 3D track, producing cascade signal amplification. The performance of the DNA walker was dependent on the density of DNA and conformation of the walking track. Thereafter, they constructed three kinds of SNA-based stochastic DNA walkers (highly packed SNA, moderately packed SNA, and loosely packed SNA) for DNA detection, achieving LODs of 200 pM, 1 pM, and 10 fM, respectively.

AuNPs can also be used as colorimetric reporters due to their remarkable optical properties.[334] Using the AuNP aggregation-induced color changes, DNA-functionalized AuNPs have been applied for construction of biosensors for metal ions, nucleic acids, small molecules, proteins, and cancer cells. For instance, Lee et al. used DNA-AuNPs in aqueous media for colorimetric detection of Hg^{2+} (Figure 14C).[335] The DNA-AuNP aggregation is eliminated at a given temperature, resulting in a color change-based detection for ~100 nM (= 20 ppb) Hg^{2+}. The high solubility of the DNA-AuNPs allows this assay to be conducted in aqueous media without the need for organic cosolvents. In another study, the Liu group conducted a similar work, utilizing DNA-AuNP conjugates for colorimetric detection of Hg^{2+} with a LOD of sub-10 nM.[336] On the basis of ATP-induced duplex-to-aptamer structural switching, Wang et al. constructed a AuNP-aptamer system for ATP detection with a LOD of 0.6 μM.[337] The Tan group developed a colorimetric approach based on aptamer-conjugated AuNPs for detection of cancer cells.[338] Using the concept of cholera toxin-induced aggregation of lactose-stabilized AuNPs, Schofield et al. developed a simple and rapid method for identifying cholera toxin, yielding a LOD of 54 nM.[339] By designing discernible barcode DNA sequences, the Mirkin group developed biobarcode NP probes for detection of multiple DNA targets (Figure 14D).[340] In this work, oligonucleotide sequences of 30–33 bases from (a) hepatitis B virus surface-antigen gene (HBV), (b) variola virus (small pox, VV), (c) Ebola virus (EV), and (d) human immunodeficiency virus (HIV) were chosen as model systems. The barcode for each target is the sequence-specific nucleotide probe, while the remainder of the sequence is universal for scanometric detection and readout. They showed that these four DNA targets can be detected with high selectivity at midfemtomolar concentrations.

3.3.2. Carbon Nanomaterials. SWCNTs and GO have powerful quenching capability for organic dyes because of long-range resonance energy transfer. Additionally, previous work has demonstrated that ssDNA is adsorbed noncovalently onto the surface of SWCNTs and GO through $\pi-\pi$ stacking. In 2008, Yang et al. reported that self-assembled SWCNT/fluorophore-labeled DNA complexes can act as a MB with little background interference,[171] and such complexes were verified to have the ability to recognize and detect specific DNA sequences. In a follow-up study, they exploited ssDNA-SWCNT complexes for detection of both DNA and proteins.[341] Ouyang et al. used antilysozyme aptamer and europium (III) (Eu^{3+}) complex along with CNTs for lysozyme (LYS) detection (Figure 15A).[342] Initially, a mixture of chlorosulfonylated tetradentate β-diketone-Eu^{3+} and the antilysozyme aptamer was adsorbed on CNTs, displaying weak luminescence. The presence of target LYS triggered the release of aptamer and luminescent Eu^{3+} complex from CNTs resulting in enhanced luminescence. This method can detect LYS with a LOD of 0.9 nM.

Only a few articles report pristine graphene for sensing because of its high hydrophobicity in spite of its excellent fluorescence quenching ability.[343] GO is a derivative of graphene, where the carboxylate groups contribute to its high water solubility. In addition, GO holds traits of easy synthesis and facile surface modification.[344] These properties make GO attract more attention in the study of DNA-based sensors. Most sensing systems based on DNA-GO complexes are built on the fact that ssDNA with different lengths and conformations can exhibit different affinity for GO. Up to now, GO has been applied in DNA sensors detecting metal ions, proteins, DNA mutations, and other compounds.[345] By rational design, fluorescent assays based on DNA-GO complexes can be made to exhibit very low background fluorescence. For example, the Li group designed an aptamer/GO nanocomplex for intracellular ATP probing.[236] Liu and co-workers established a GO/DNA system for investigating mechanisms of DNA sensing on GO.[346] By virtue of a simple ion-exchange process, the Loh group synthesized a GO-organic dye ionic complex as an optical sensor for DNA, obtaining a LOD of 1 nM.[347] In another example, the Wang group used a GO/aptamer strategy for multiplexed detection while also enabling logic operations.[348] They used FAM-labeled aptamers for ATP and thrombin, both of which were adsorbed onto GO to form a GO/aptamer complex. This adsorption quenches the fluorescence of FAM. Through logic-gated operation, the sensor can detect ATP or thrombin, releasing the FAM-labeled aptamers from the GO surface, thus increasing the fluorescence signal. This system has a dynamic range of 500 nM to 50 μM for ATP and 0.04–10 nM for thrombin, with a LOD of 500 nM and 0.04 nM for ATP and thrombin, respectively.

3.3.3. Two-Dimensional Nanomaterials. Two-dimensional (2D) nanomaterials including transition metal dichalcogenides (e.g., MoS_2, WS_2, TiS_2, TaS_2) have received extensive attention because of their 2D structure being analogous to graphene.[349−351] Such layered 2D nanomaterials have high fluorescence quenching efficiency, high water dispersibility, facile surface modification, and different affinities toward ssDNA and dsDNA.[182,352] On the basis of these properties, Zhu et al. used single-layer MoS_2-based fluorogenic sensor for DNA and small molecules (Figure 15B).[353] The dye-labeled ssDNA probe is first adsorbed on MoS_2, thus quenching the fluorescence. Once the ssDNA probes hybridize with the complementary target DNA, the resulting duplex is only weakly adsorbed on to MoS_2, thus moving the dye-labeled probes away from the surface and recovering the fluorescence signal. They used this strategy for the detection of DNA and adenosine with a LOD of 0.5 nM and 5 μM, respectively. Liu and his co-workers explored few kinds of 2D nanomaterial including MoS_2, WS_2, and GO for adsorption and sensing.[354] Their results showed that DNA is adsorbed by GO through hydrogen bonding and $\pi-\pi$ stacking, while MoS_2 and WS_2 mainly use van der Waals force for adsorption. Fluorescent DNA probes adsorbed on these 2D materials for DNA detection exhibited a similar detection limit (~20 nM). The Jiang group developed a miRNA detection platform using the fluorescence quenching ability of WS_2 nanosheet and duplex-specific nuclease assisted signal amplification, showing high sensitivity with a LOD of 300 fM.[183] Recently, Xiao et al. constructed a MoS_2-based nanoprobe for miRNA quantification, obtaining a LOD of 10 fM.[355]

The Liu group conducted a study revealing that poly cytosine (poly-C) DNA is a high affinity ligand for transition metal dichalcogenides (e.g., MoS_2, WS_2).[356] Therefore, a dye-labeled diblock DNA probe containing a poly-C block attached to the surface of transition metal dichalcogenides provides minimal background fluorescence. This work provides a simple yet

DOI: 10.1021/acs.chemrev.9b00121
Chem. Rev. XXXX, XXX, XXX−XXX

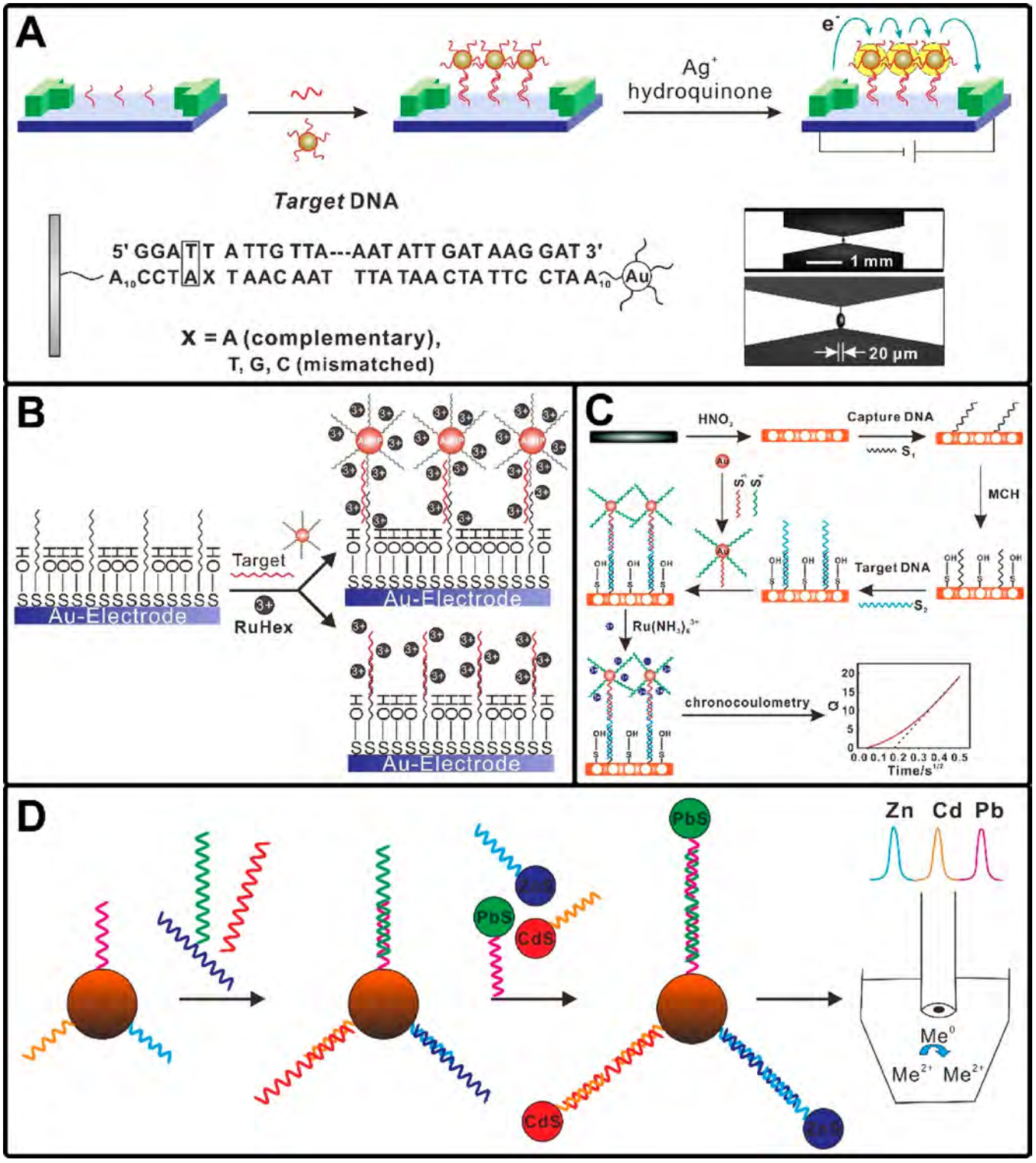

Figure 16. (A) Array-based electrical detection of DNA with nanoparticle probes. Adapted with permission from ref 387. Copyright 2002 AAAS. (B) Nanoparticle-mediated amplification and nanoscale control of DNA assembly at electrodes for DNA detection. Adapted with permission from ref 390. Copyright 2006 American Chemical Society. (C) Nanoporous gold electrode and multifunctional DNA-Au biobarcodes for DNA detection. Adapted with permission from ref 392. Copyright 2008 American Chemical Society. (D) Electrochemical coding technology for simultaneous detection of multiple DNA targets. Adapted with permission from ref 395. Copyright 2003 American Chemical Society.

effective method for constructing DNA-based sensors.[357] As a proof of concept, Xiao et al. designed diblock MBs with poly-C tails anchored on MoS_2 nanosheets as probes for miRNA detection (Figure 15C).[358] In the design, the poly-C block is attached to MoS_2, while the MB block is available for hybridization to the target, and a duplex-specific nuclease enables signal amplification by target recycling. By changing the length of poly-C, they regulated the density of probes on MoS_2 for achieving higher quenching efficiency. Moreover, the poly-C block can effectively inhibit the adsorption of enzyme-cleaved

DOI: 10.1021/acs.chemrev.9b00121
Chem. Rev. XXXX, XXX, XXX−XXX

oligonucleotides on MoS_2, yielding enhanced signal. Consequently, both lower background signal and higher amplified signal contribute to the nanoprobe having ultrahigh sensitivity (limit of detection ~3.4 fM), specificity to detect a single nucleotide mismatch, and selectivity to detect target miRNA from serum samples. This method shows promise for quantitative analysis of miRNAs in clinical diagnosis and biomedical research.

3.3.4. Quantum Dots. Semiconductor QDs have been applied for optical and photoelectrochemical sensing and biosensing due to their excellent photophysical properties such as high luminescence quantum yields, size-controlled luminescence properties, narrow luminescence bands, and large Stokes shifts, and stability toward photobleaching.[359,360] The Willner group modified semiconductor QDs with hemin/G-quadruplex horseradish-peroxidase-mimicking DNAzyme for biosensing purpose.[361] They discovered that the oxidation of luminol by H_2O_2 catalyzed by hemin/G-quadruplex yields chemiluminescence with a luminescence spectrum overlapping the absorbance bands of differently sized CdSe/ZnS QDs. Thus, the chemiluminescence resonance energy transfer (CRET) between hemin/G-quadruplex-QDs conjugates can be used for bioanalysis. CRET-based platforms using hemin/G-quadruplex-modified CdSe/ZnS QDs enable the analysis of Hg^{2+}, ATP, DNA, and thrombin with LODs of 10 nM, 100 nM, 10 nM, and 1.4 nM, respectively.[361,362] QDs are not only used as optical labels but also as nanoscale carrier of probes for amplified detection of DNA. For instance, Freeman et al. used exonuclease III-catalyzed recycling of the target DNA and analyzed using semiconductor QDs (Figure 15D),[363] in which quencher-modified QDs are used as optical trace. Binding of target DNA to QDs induces the exonuclease-triggered recycling of the target DNA, resulting in enhanced luminescence of the QDs. This method has a LOD of 1 pM. Additionally, the QDs integrated with enzyme-mediated signal amplification can be used to detect vesicular epithelial growth factor (a detection limit of 875 pM).[364]

Nucleic acid-stabilized metal nanoclusters (NCs) provide an additional means for developing DNA sensors and aptasensors.[365] Specific nucleic acid sequences stabilize metal NCs (e.g., AgNCs) displaying a luminescent property, and this property depends on the sizes of the metal aggregates and the sequences of the stabilizing capping oligonucleotides. Using this principle, Liu et al. built a hybrid system composed of nucleic-acid-functionalized AgNCs and GO for construction of DNA sensors and aptasensors.[366] In this work, two types of DNA-stabilized AgNCs, the red-emitting AgNCs (616 nm) and near-infrared-emitting AgNCs (775 nm), were used. DNA-stabilized AgNCs can be increasingly adsorbed on GO through the interaction of ssDNA to the GO surface, resulting in the fluorescence quenching of AgNCs. In the presence of the target, the ssDNA probes are converted to duplexes, and single stranded aptamer probes are converted to aptamer-substrate complexes, thus causing desorption of the DNA-stabilized AgNCs from GO, and recovering the fluorescence. This system was used for the detection of the hepatitis B virus gene, immunodeficiency virus gene, ATP, and thrombin with a detection limit of 0.5 nM, 1 nM, 2.5 μM, and 0.5 nM, respectively.

3.4. Electrochemical-Based Readout Strategy

Electrochemical readout of analytes represents another effective approach to the rapid molecular analysis.[127,367] An electrochemical readout uses the flow of current at the surface of a sensor to monitor the presence or absence of an analyte, reported by the binding of redox-active groups to specific analytes. At present, several different electrochemical-based methods such as sandwich electrochemical assays,[368,369] structural switching-based electrochemical detection,[370−372] nanostructured microelectrode-based electrochemical detection,[373,374] amplified strategy for electrochemical detection (e.g., enzymatic amplification-based detection approach, enzyme-free amplification-based detection approach),[375−378] and DNA nanostructure-based electrochemical detection[379,380] have been developed in pursuit of high levels of sensitivity and stringent specificity.

The sandwich electrochemical assay format is similar to ELISA. Electrochemical assays can be designed by replacing the detection antibody with redox active labels (e.g., methylene blue) or nanoparticles that can generate electrochemical signals.[381,382] In one example, an anti-TNT aptamer reports the presence of the target 2,4,6 trinitrotoluene (TNT), which binds to a primary amine immobilized on gold electrodes via acid−base pairing.[383] The presence of TNT and aptamer increases the potential barrier to redox molecules, thereby hindering the exchange of electrons with the Au electrode. Using the transfer resistance, the detection of 10 fM TNT was accomplished. Xia et al. developed a supersandwich structure containing multiple labels for sensitive and selective DNA detection with a detection limit of 100 fM, a thousand-fold increase from the traditional assay.[384] Fapyane et al. reported an electrochemical enzyme-linked sandwich assay for nucleic acid analysis.[385] Recently, Yang et al. constructed a sandwich electrochemical biosensor for the detection of MCF-7 human breast cancer cells.[386] Mirkin and colleagues reported a three-component sandwich approach for detection of DNA (Figure 16A),[387] in which hybridized target DNA is used to bind oligonucleotides functionalized with AuNPs. Silver deposition facilitated by these AuNPs can bridge the connection between the two flanking microelectrodes, resulting in readily measurable conductivity changes that are related to analyte-probe binding events. Using this technology, a sensitivity of 500 fM in target DNA and a point mutation selectivity was achieved.

AuNPs are also used in signaling hybridization events in a sandwich-based assay.[388,389] In one study, the target DNA is captured by capture probe DNA immobilized on gold electrodes, followed by hybridization with AuNP-tagged reporter probe DNA (Figure 16B).[390] Electrochemical signals of $[Ru(NH_3)_6]^{3+}$ bound to capture probes via electrostatic interactions were measured by chronocoulometry. The sensor performance including sensitivity and specificity was improved because of the incorporation of AuNPs for signal transduction.[391] This strategy could detect 10 fM DNA targets with single nucleotide specificity. Hu et al. used a similar strategy for DNA detection, with dynamic range of 8.0×10^{-17}−1.6×10^{-12} M, LOD of 28 aM, and single-nucleotide specificity (Figure 16C).[392] Apart from AuNPs, other particles (e.g., platinum NPs, AgNPs) have been exploited for signal transduction to improve the detection performance of biosensors.[393,394] Employing NP labels with different redox potentials, Wang et al. created a multiplexed detection strategy for DNA targets (Figure 16D).[395] Magnetic beads containing ssDNA probes hybridize with target DNA, and subsequently hybridize with the NP-labeled reporter DNA, wherein three encoding NPs (ZnS, CdS, and PbS) can differentiate the signals of three DNA targets. Unhybridized DNA can be removed magnetically,

DOI: 10.1021/acs.chemrev.9b00121
Chem. Rev. XXXX, XXX, XXX−XXX

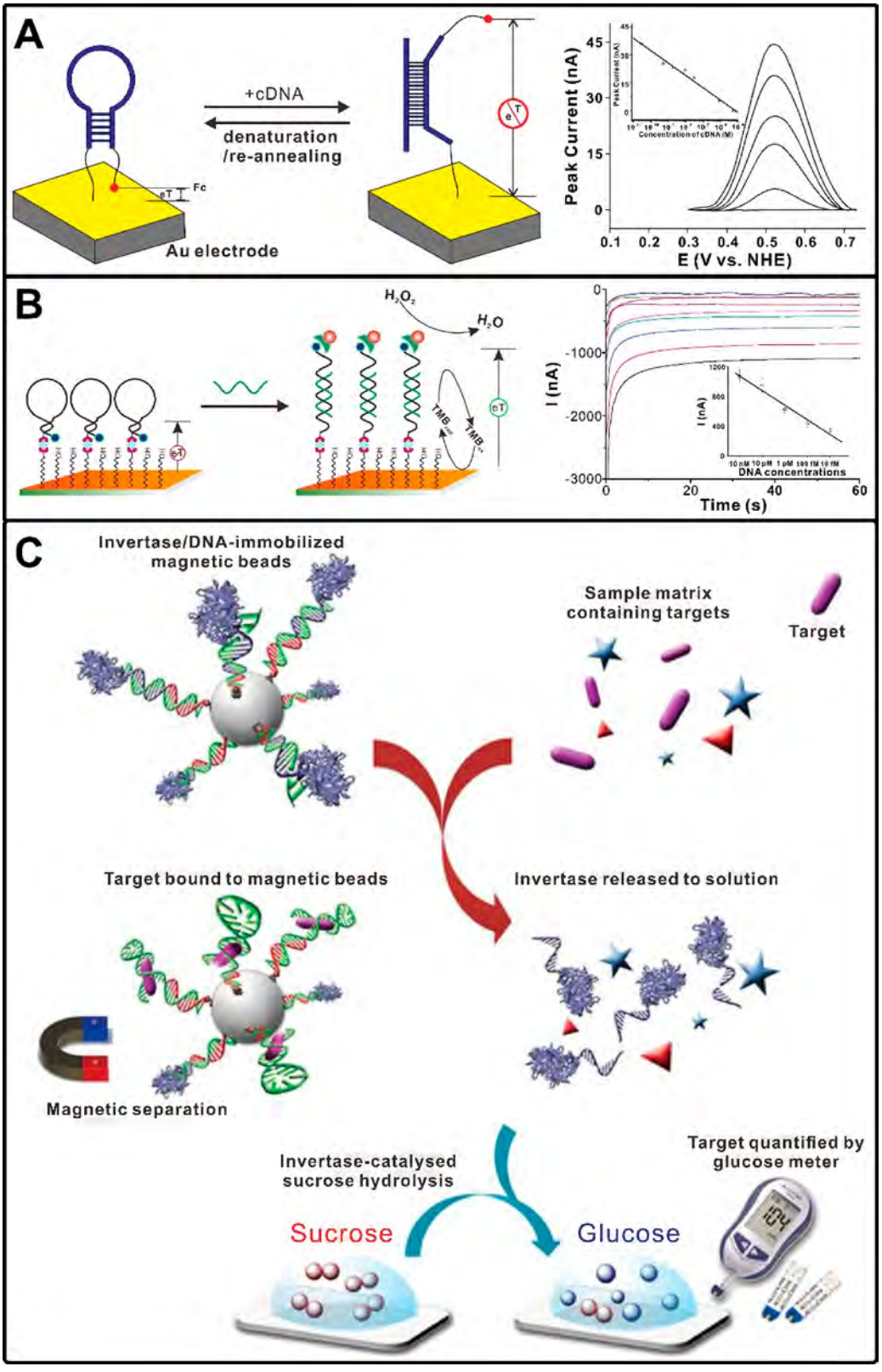

Figure 17. (A) Electrochemical interrogation of conformational changes as a reagentless method for sequence-specific detection of DNA. Adapted with permission from ref 397. Copyright 2003 National Academy of Sciences. (B) Enzyme-based E-DNA sensor for sequence-specific detection of DNA targets. Adapted with permission from ref 401. Copyright 2006 American Chemical Society. (C) Functional DNA sensors integrated with personal glucose meters for quantification of a variety of analytical targets. Adapted with permission from ref 402. Copyright 2011 Springer Nature.

enabling sensitive and selective stripping-voltammetric measurements of three different DNA targets.

Structural switching-based electrochemical sensors generate predictable signals via controllable structure changes such as reconfiguration of biomolecules.[396] Signal transduction is

DOI: 10.1021/acs.chemrev.9b00121
Chem. Rev. XXXX, XXX, XXX−XXX

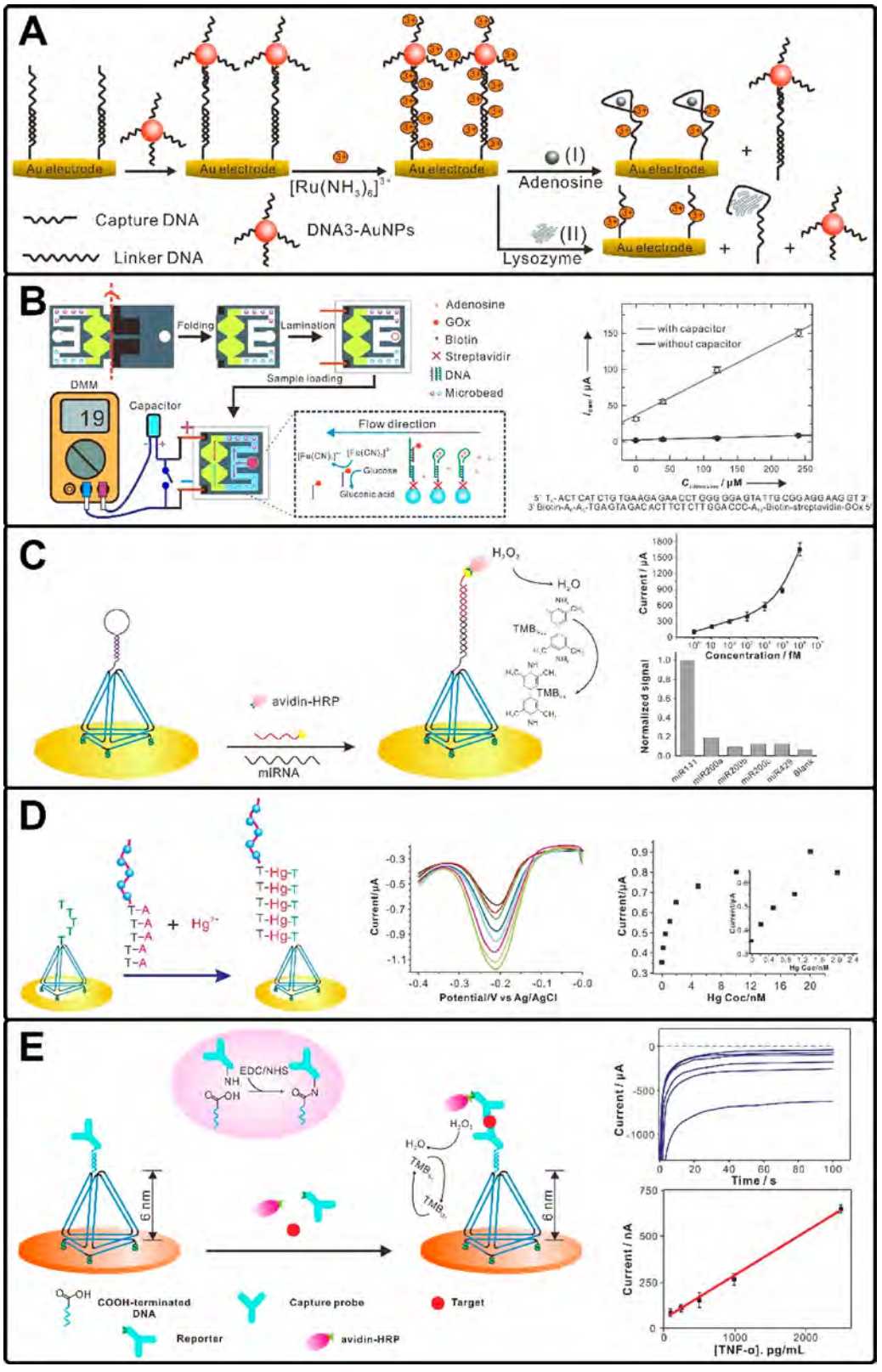

Figure 18. (A) Lysozyme or adenosine detection with DNA-AuNPs amplification. Adapted with permission from ref 404. Copyright 2009 American Chemical Society. (B) Aptamer-based origami paper analytical device for electrochemical detection of adenosine. Adapted with permission from ref 406. Copyright 2012 Wiley-VCH. (C) DNA nanostructure-based E-DNA sensor for microRNA analysis. Adapted with permission from ref 413. Copyright 2014 American Chemical Society. (D) Electrochemical tetrahedron-structured DNA-based biosensor for Hg^{2+} detection. Adapted with permission from ref 414. Copyright 2011 Royal Society of Chemistry. (E) DNA nanostructure-decorated gold surfaces for regenerable electrochemical immunological sensing of TNF-α. Adapted with permission from ref 418. Copyright 2011 Royal Society of Chemistry.

DOI: 10.1021/acs.chemrev.9b00121
Chem. Rev. XXXX, XXX, XXX−XXX

provided by target-responsive variations of probe structures with many attractive features (e.g., no target labeling, high sensitivity, exceptionally selectivity).[397] Therefore, integrating such variations with advanced electronic transducers is of great utility in designing simple and potentially generalizable biosensors.[398]

Fan et al. designed an electrochemical DNA sensor based on the reconfiguration of a DNA hairpin (Figure 17A).[397] A stem-loop attached to AuNP on one end holds a ferrocene on the other end. In the stem configuration, the ferrocene is held close to the Au surface, causing a high electrochemical signal. When target DNA binds to the hairpin, it opens the stem, moving the ferrocene away from the surface and thus reducing the signal. This process can be monitored using the distance-dependent electron transfer (ET) property of the coupled ferrocene. This signal-off sensor has a LOD of 10 pM. Using a similar signal-off concept, Kim and colleagues used a hairpin containing a thrombin aptamer sequence that was conjugated to a gold electrode.[399] Methylene blue intercalates into the stem region of the hairpin and acts as redox-active reporter. Addition of thrombin reconfigures the hairpin into a G-quadruplex and binds to it, releasing the intercalated methylene blue and causing a reduction in the electrochemical signal. The linear range for this method was 0 to 50.8 nM with a LOD of 11 nM.

To develop an electrochemical DNA sensor with improved sensitivity, Zuo et al. used a target-responsive electrochemical aptamer switch (TREAS).[400] In this strategy, an aptamer sequence was conjugated to gold electrode and contained a ferrocene group on the other end. This strand is hybridized to a complementary DNA so that the ferrocene group is away from the electrode. The presence of ATP leads the electroactive ferrocene moiety to move from the distant position to the proximal position, resulting in increased electrochemical signal. The signal-on, reagentless sensor with generalizability and simplicity can selectively detect ATP. Liu et al. reported an enzyme-based electrochemical DNA sensor with femtomolar sensitivity (Figure 17B).[401] A DNA probe with stem-loop structure was modified with biotin on one end so that it can be immobilized on an avidin-modified gold electrode surface. The other end of the probe contained a digoxygenin (DIG) molecule. As a result of steric effects, DIG is shielded from interacting with a bulky horseradish peroxidase-linked-anti-DIG antibody (anti-DIG-HRP). Then a significant structural change induced by hybridization of probes with the DNA targets facilitates accessibility of DIG to the anti-DIG-HRP. This binding event is read out as an electrochemical current signal with a LOD of 10 fM and has the ability to distinguish single nucleotide mismatches. The Lu group proposed a method for utilizing a pocket-sized personal glucose meter to quantify nonglucose targets (Figure 17C).[402] In this method, a functional DNA−invertase conjugate releases invertase on binding to a target, and this invertase is converted to glucose and read out using the meter. This system was used to detect cocaine (LOD 3.4 mM), adenosine (LOD 18 mM), interferon-gamma (LOD 2.6 nM), and uranium (LOD 9.1 nM).

DNA-functionalized metal nanoparticles have been used to improve the sensitivity of sensors.[370,403] Deng et al. developed an aptamer-based electrochemical biosensor for small molecules and proteins (Figure 18A).[404] With an elaborate design for introducing adenosine and lysozyme aptamers into DNA/DNA duplex, the switching of aptamers from DNA/DNA duplex to DNA/target complex allows the detection of adenosine or lysozyme. The binding event is monitored by the electrochemical response of surface-bound $[Ru(NH_3)_6]^{3+}$. In addition, DNA-functionalized AuNPs that can host more $[Ru(NH_3)_6]^{3+}$ cations can enhance the sensitivity of the aptasensor to achieve a LOD of 20 pM for adenosine and 0.01 μg/mL for lysozyme. In another study, Su et al. built an electrochemical biosensor based on conformational changes of DNA on MoS_2 nanosheets modified with AuNPs, enabling simultaneous determination of ATP and thrombin (LOD of 0.74 nM and 1.2 pM, respectively).[405]

Crooks and co-workers fabricated a self-powered origami paper analytical device (oPAD) for electrochemical detection of adenosine with a LOD of 11.8 μM (Figure 18B).[406] Within the sensor, the presence of the target analyte causes reconfiguration of an adenosine aptamer, leading to the release of GOx-labeled DNA strands. The released GOx catalyzes the oxidation of glucose, resulting in conversion of $[Fe(CN)_6]^{3+}$ to $[Fe(CN)_6]^{4+}$. The change in current during this process can be monitored using a digital multimeter. The sensor can also be equipped with dual channels for a control lane (lacking the adenosine aptamer) and a test lane (with the aptamer).

DNA-based nanostructures represent an effective approach to increase the sensitivity of electrochemical detection.[407−409] One of the main parameters in this regard is control over density of probes on the surface, made possible using tetrahedral nanostructures made of DNA. Such control allows orientation of the probes in an upright configuration and thus increases accessibility to target binding.[410−412] In one study, Lin et al. employed tetrahedra structured probes (TSP) to construct an electrochemical DNA sensor for miRNA detection (Figure 18C).[413] In this design, a DNA tetrahedron is used to ensure the controlled density and improved reactivity of a stem-loop structure. This design also increases the specificity of the assay. Sensitivity can be further enhanced using enzyme catalytic amplification. The sensitivity of this method is as low as 1 fM and has specificity to differentiate highly similar miRNA analogs.

By introducing a DNA probe containing a T-rich sequence at the top vertex of a DNA tetrahedron, Yin and co-workers developed a DNA-based sensor for the detection of Hg^{2+} ions (Figure 18D).[414] A functional oligonucleotide (FO) with the sequence of T_5-G_5 is used to integrate with an electrochemically active molecule (methylene blue) and to identify Hg^{2+} ions. After incubation with Hg^{2+} ions and FO, the TSPs produce enhanced electrochemical signal via the formation of thymine-Hg^{2+}-thymine complex (T-Hg^{2+}-T). This "turn-on" biosensor has a dynamic range of 100 pM to 20 nM with a detection limit of 100 pM, 100-fold lower than that obtained with the ssDNA-based sensor. In addition, selectivity is at least 10 000-fold higher for Hg^{2+} ion than competing metal ions.

In TSP-based platforms, the top vertex can be designed to contain a a split aptamer for cocaine.[415] This sensor has a detection limit of 33 nM and has the ability to work in sera or other adulterated samples. In addition, Ge et al. reported an electrochemical sensor for the genotyping of SNPs based on branched TSPs.[416] Similarily, Bu et al. designed an ATP sensor using anti-ATP aptamers.[417] This platform also allows anchoring antibodies with defined orientations and thus aid in improving the performance of immunological sensing (Figure 18E).[418] For example, the tumor-necrosis-factor alpha (TNF-α) antibody can be tagged on a DNA tetrahedron. Pei et al. found that the constructed electrochemical immunosensors based on TSPs showed superior sensitivity and selectivity in comparison with the conventional immunosensor.[418]

Material properties in the nanoscale play a major role in designing electrode-based sensors.[127] Rationally designed

DOI: 10.1021/acs.chemrev.9b00121
Chem. Rev. XXXX, XXX, XXX−XXX

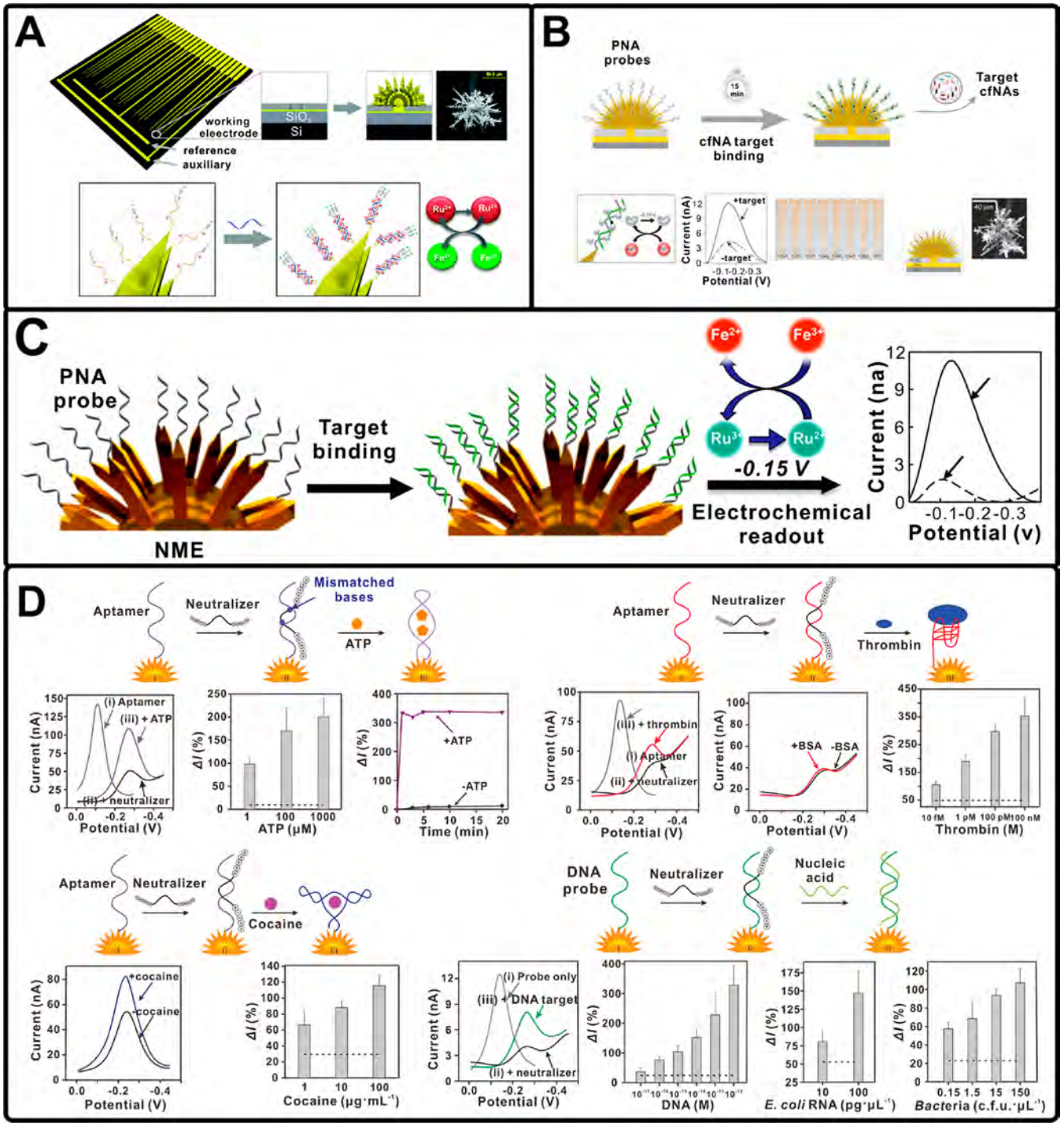

Figure 19. (A) NME platform for bacterial detection. Adapted with permission from ref 425. Copyright 2012 American Chemical Society. (B) Clamp chip for the electrochemical analysis of mutated cfNAs. Adapted with permission from ref 426. Copyright 2015 Springer Nature. (C) DNA clutch probes for circulating tumor DNA analysis. Adapted with permission from ref 429. Copyright 2016 American Chemical Society. (D) Universal detector based on neutralizer displacement. Adapted with permission from ref 430. Copyright 2012 Springer Nature.

electrochemical sensing elements aid in improving both the sensitivity and rapid detection of nucleic acids.[419,420] Previous works have demonstrated that DNA probes anchored on nanostructured microelectrode (NME) surfaces restrict steric interactions between probes and increase the hybridization efficiency.[421−424] On the basis of these details, the Kelley group reported a detection platform combining an electrochemical reporter system with NMEs (Figure 19A).[425] They created patterned microelectrodes on the surface of silicon chips that promote collisions with slow-moving analytes in solution, thus addressing the diffusional limitations.[422] Moreover, the nanoscale roughness of NMEs facilitates binding of probes to target nucleic acids. NMEs coupled with an electrocatalytic reporter strategy allow this integrated platform to specifically detect bacteria with a detection limit of 1 CFU/μL within 30 min (in microbiology, a colony-forming unit (CFU) is a unit used to estimate the number of viable bacteria or fungal cells in a sample).

DOI: 10.1021/acs.chemrev.9b00121
Chem. Rev. XXXX, XXX, XXX−XXX

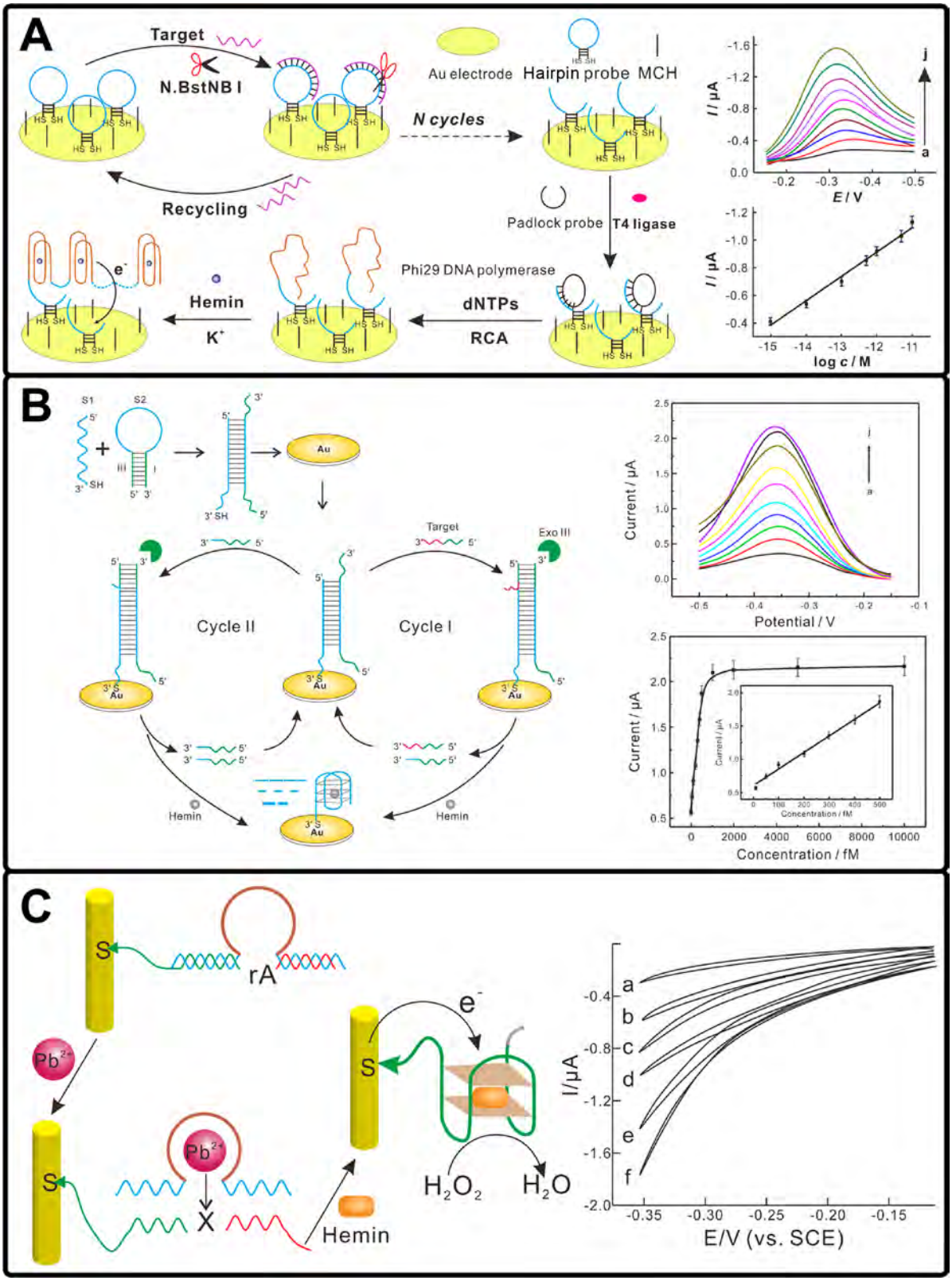

Figure 20. (A) Dual amplified electrochemical detection of mutant DNA biomarkers based on nuclease-assisted target recycling and rolling circle amplifications. Adapted with permission from ref 450. Copyright 2014 Elsevier. (B) Electrochemical detection of nucleic acids based on autocatalytic and exonuclease III-assisted target recycling strategy. Adapted with permission from ref 459. Copyright 2013 American Chemical Society. (C) Amplified surface plasmon resonance and electrochemical detection of Pb^{2+} ions using the Pb^{2+}-dependent DNAzyme and hemin/G-quadruplex as a label. Adapted with permission from ref 478. Copyright 2012 American Chemical Society.

In a follow-up study, the Kelley group devised an electrochemical clamp assay for the detection of circulating nucleic acids in serum (Figure 19B).[426] Via the electrodeposition of dendritic gold nanostructures, the White group constructed

DOI: 10.1021/acs.chemrev.9b00121
Chem. Rev. XXXX, XXX, XXX−XXX

electrochemical, aptamer-based sensors on NMEs for detection of ATP and tobramycin, and sensor performance in terms of signal-to-noise and stability was greatly improved due to its nanostructured surface.[427] In the same way, Liu et al. developed a sensing strategy with LOD in the fM range.[428] To further increase the sensitivity of the clamp, a thin layer of Pd is used for coating Au structures to form finely structured NMEs. The micron-size scale of the NMEs improves its roughness for the interaction with analyte molecules, thereby maximizing the sensitivity.[35] To boost the accuracy of this approach, peptide nucleic acid (PNA) probes have also been used to functionalize the NMEs. Once the bound target is washed, target presence can be read out using an electrocatalytic reporter pair composed of $Ru(NH_3)_6^{3+}$ and $Fe(CN)_6^{3-}$. The electrochemical clamp assay achieves a limit of detection of 1 fg/μL, and statistically significant signals are obtained within five minutes.

Das et al. introduced DNA clutch probes (DCPs) to detect mutated sequences using PNA probe-functionalized NMEs (Figure 19C).[429] The hybridization events can be reflected by the electrochemical signal. As a result, the assay exhibits excellent sensitivity and specificity in the detection of mutated circulating tumor DNA, detecting 1 fg/μL of a target mutation in the presence of 100 pg/μL of wild-type DNA. Kelley and co-workers developed a neutralizer displacement assay to detect analytes irrespective of their charges (Figure 19D).[430] In this assay, a neutralizer bound to an aptamer probe-modified NMEs can be displaced when analyte binding occurs, leading to a significant change in the surface charge. They used this system for the detection of different biomarkers including DNA, RNA, ATP, cocaine, thrombin, and *E. coli* bacteria, with the detection limit of ~100 aM, 10 pg μL^{-1}, 1 $\mu g\ mL^{-1}$, 1 mM, 10 fM, and 0.15 cfu/μL, respectively. NME-based electrochemical detection has also been used to detect analytes such as mRNA,[431] miRNA,[432] pathogen,[433] even bacteria,[434] and circulating tumor cells.[435]

To realize the ultrasensitive electrochemical detection of analytes, several enzyme-based amplification strategies such as PCR, rolling circle amplification (RCA), and nicking endonuclease-based signal amplification have been employed to measure biorecognition events.[436−441] For instance, Yeung et al. reported the first electrochemistry-based real-time PCR technique for sequence-specific nucleic acid detection.[442] Since nicking endonucleases digest only one strand of dsDNA at specific sequences,[443] any amplification strategies are based on nicking endonucleases.[444,445] Liu et al. detected miRNAs using an electrochemical sensor in which enzyme-assisted p-aminophenol redox cycling causes an increase in the anodic current.[446] This miRNA sensor showed a linear range of 10 fM-5 pM with a LOD of 3 fM. RCA is an isothermal enzymatic process to generate long ssDNA or RNA using a short DNA or RNA strand as a primer and circular DNA as a template in the presence of DNA polymerases (e.g., Φ29 polymerase).[447,448] This facilitated the production of a high number of tandemly linked copies of a covalently closed circle in only a few minutes.[449] The Xiang group created a biosensor for the mutant human p53 gene based on G-quadruplex/hemin complexes, with amplification provided by nicking endonuclease-assisted target recycling (Figure 20A).[450] In this work, a hairpin probe recognizes and binds to the target mutant DNA, which is then cleaved by an endonuclease. The released target DNA hybridizes with the intact HPs and initiates the DNA recycling process by the endonuclease. The signal can also be amplified using RCA where long DNA sequences with massive tandem-repeat G-quadruplex sequences can be formed, and in association with hemin, amplify the electrochemical signal. As a result, this dual amplified biosensor has a detection limit of 0.25 fM with single nucleotide specificity.

The enzyme-based target recycling strategy is attractive for trace-level detection of target analytes owing to its specific recognition of sequences.[451,452] For example, the Ju group utilized nicking endonuclease-initiated recycling hybridization process in combination with RCA for detecting nucleic acids.[453] Unlike nicking endonucleases, exonuclease III (Exo III) is a sequence-independent enzyme without need of a specific recognition site as it only cleaves the mononucleotides from 3′ terminus of dsDNA in the case of substrate with a blunt or recessed 3′-terminus.[454,455] Exo III thus allows flexibility in amplification of certain biosensing signals.[456] In one study, Wu et al. constructed a label-free electrochemical DNA sensor based on Exo III-aided target recycling strategy.[457] Similar strategies have been developed for ATP detection.[458] Tang and co-workers developed a DNA biosensor that also utilized Exo III-assisted target recycling (Figure 20B).[459] In this strategy, a G-quadruplex-forming sequence was hybridized with a MB and anchored on an electrode. Binding of target DNA to this MB forms a duplex and releases the G-quadruplex-forming sequence. The formed duplex is digested by Exo III, resulting in target recycling, while the quadruplex-forming oligomers fold into G-quadruplex-hemin complexes on the electrode surface, producing an electrochemical response, providing a LOD of 10 fM.

Various non-natural DNAzymes such as metal-ion-dependent DNAzymes, cofactor-dependent DNAzymes, and hemin/G-quadruplex HRP-mimicking DNAzymes have been developed in the past decade.[460−464] As these DNAzymes can serve as amplifying labels, various DNAzyme-based electrochemical sensing platforms have been constructed for analysis of nucleic acids, proteins, and metal ions.[465−469] Dong et al. fabricated DNAzyme/Pt NPs/CNTs bioconjugate on gold electrodes for amplified electrochemical DNA analysis,[470] with a LOD of 0.6 fM and single nucleotide specificity. By taking advantage of structure-switching DNAzymes, Liang et al. built an efficient signal-on electrochemical sensor for L-histidine with a LOD of 0.1 pM.[471] Yuan et al. utilized hemin/G-quadruplex combined with NADH oxidase and HRP-mimicking DNAzyme for fabricating a pseudobienzyme-amplifying system for thrombin detection, with a dynamic range of 0.5 pM to 20 nM and a LOD of 0.15 pM.[472] Lu et al. developed an electrochemical biosensor for ATP using cofactor-dependent enzymatic ligation and self-cleaving DNAzyme-amplified target recycling.[473] In another study, electrochemical detection of lead (Pb) in the parts-per-billion range was done on the basis of conformation states of an electrode-bound DNAzyme assembly.[474]

Metal ion-dependent DNAzyme-based electrochemical readout signals can also be used for amplified detection of various metal ions.[475−477] In one study, the concentration of lead ion in the target sample activates hemin/G-quadruplex DNAzymes that in turn provided output signals for electrochemical analysis of Pb^{2+} ions (Figure 20C).[478] This method enables the detection of Pb^{2+} with a detection limit of 100 pM.

Although enzyme-based amplification strategies can be used for detection of low-abundance analytes, these methods might involve multiple assay steps and require special reaction conditions. Recently, enzyme-free signal amplification techniques with negligible background (e.g., HCR, CHA reactions) have been engineered to initiate hundred-fold catalytic amplification reactions, achieving great improvements in convenience and sensitivity.[479−482] Moreover, these enzyme-

DOI: 10.1021/acs.chemrev.9b00121
Chem. Rev. XXXX, XXX, XXX−XXX

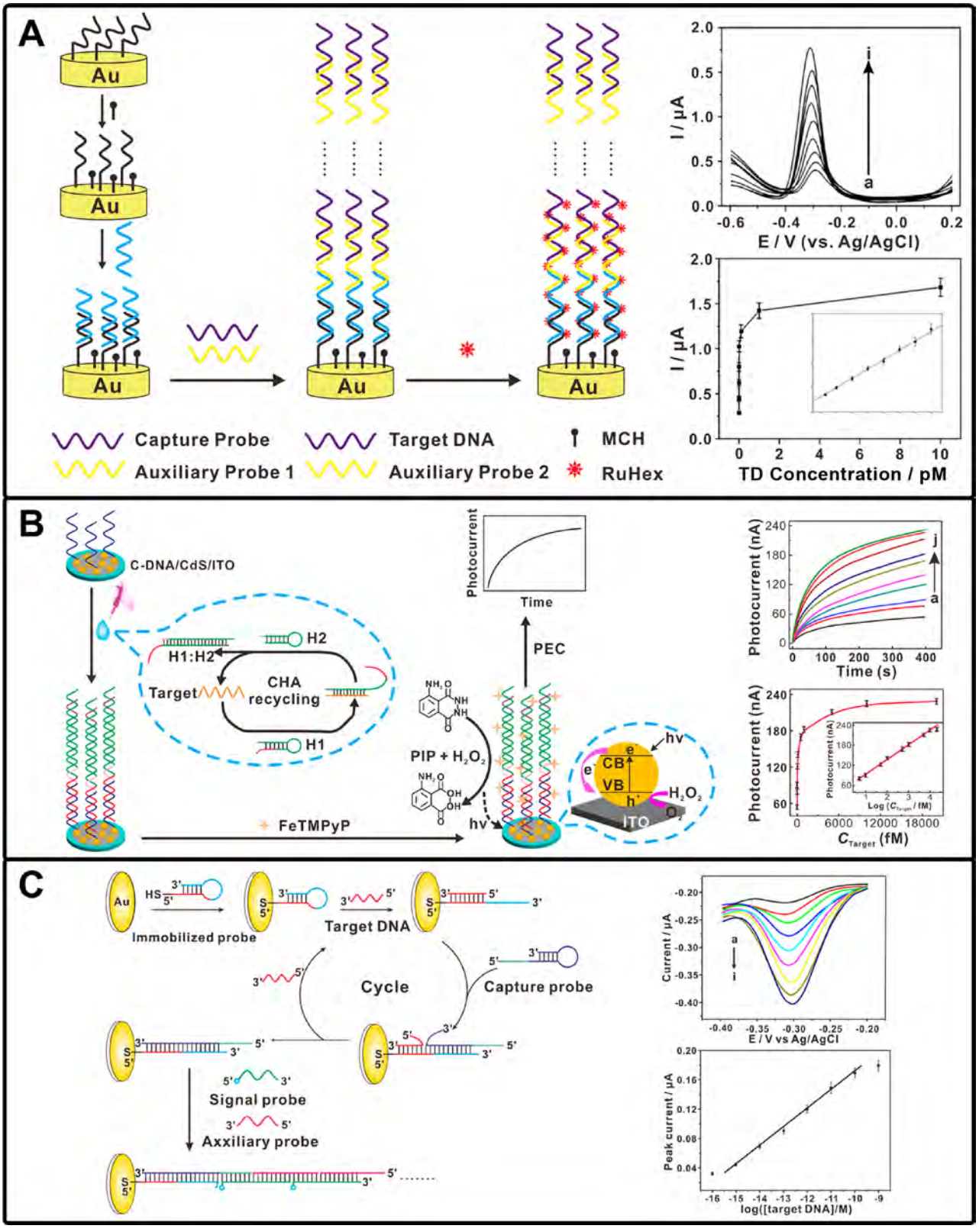

Figure 21. (A) Enzyme-free and label-free ultrasensitive electrochemical detection of HIV DNA based on long-range self-assembled DNA nanostructures. Adapted with permission from ref 485. Copyright 2012 American Chemical Society. (B) CHA-programmed porphyrin−DNA complex as photoelectrochemical initiator for DNA biosensing. Adapted with permission from ref 490. Copyright 2015 American Chemical Society. (C) Enzyme-free and ultrasensitive electrochemical detection of nucleic acids by target CHA and HCR. Adapted with permission from ref 484. Copyright 2013 Elsevier.

DOI: 10.1021/acs.chemrev.9b00121
Chem. Rev. XXXX, XXX, XXX−XXX

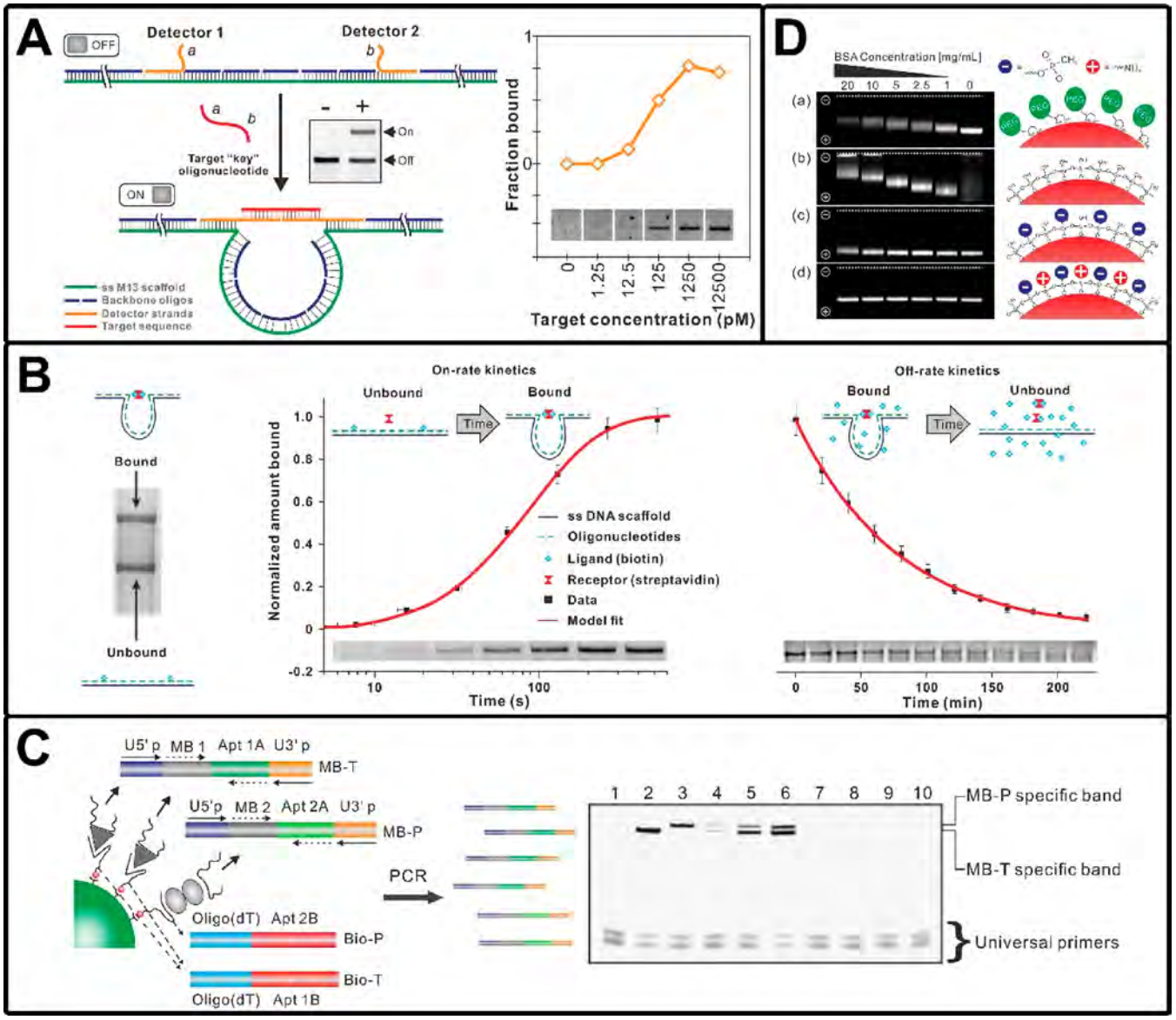

Figure 22. (A) Programmable DNA nanoswitches for detection of nucleic acid sequences. Adapted with permission from ref 499. Copyright 2016 American Chemical Society. (B) DNA nanoswitches for gel-based biomolecular interaction analysis. Adapted with permission from ref 505. Copyright 2015 Springer Nature. (C) Dual-aptamer-based multiplex protein biosensor. Adapted with permission from ref 514. Copyright 2010 Elsevier. (D) Gel-based reaction tuning for discovery of protein- and DNA-imperceptible nanoparticle hard coating. Adapted with permission from ref 515. Copyright 2015 American Chemical Society.

free signal amplification methods capable of specific signal transduction have been integrated with electrochemical techniques for ultrasensitive DNA analysis.[384,483,484]

Isothermal HCR activated in the presence of a target analyte results in the formation of DNA polymeric nanowires, with signal amplification provided by the redox-active species coupled to the HCR products. For instance, Chen et al. described an *in situ* HCR signal-based method for detection of specific DNA sequences at the femtomolar level (15 fM) (Figure 21A).[485] In another study, two auxiliary probe-induced cascade hybridization events produced long-range self-assembled DNA nanostructures, where each target DNA connects a DNA nanostructure to a capture probe on the electrode surface.[486] $[Ru(NH_3)_6]^{3+}$, a redox indicator bound to the DNA nanostructures provides the electrochemical signals for detecting DNA sequences as low as 5 aM even in cell lysates or human serum.

A free-energy-driven isothermal autonomous CHA process is another approach to realize enzyme-free signal amplification. In this process, an initiator strand activates a DNA hairpin to produce complex nanostructures, thus yielding stable duplex DNA nanoscale assemblies.[487,488] This strategy can be modified for electrochemical detection of DNA.[489] On the basis of target-CHA and porphyrin-mediated chemiluminescence, Zang et al. constructed an enzyme-free photoelectrochemical strategy for ultrasensitive detection of DNA (Figure 21B).[490] They used target-assisted CHA reaction to form dsDNA that can be anchored on an electrode containing capture DNA and CdS QDs. Porphyrin (FeTMPyP) is assembled on a dsDNA scaffold via the groove interaction. This assembly catalyzes luminol oxidation to generate a chemiluminescent signal. The linear range of detection for this assay is 5 to 10 000 fM with a LOD of 2.2 fM. Liu et al. combined CHA and HCR for two-step signal amplification to achieve a detection limit of 0.1 fM for DNA

DOI: 10.1021/acs.chemrev.9b00121
Chem. Rev. XXXX, XXX, XXX−XXX

detection, with a high selectivity to differentiate mismatched DNA (Figure 21C).[484]

3.5. Gel Electrophoresis-Based Readout Strategy

Gel electrophoresis has been a workhorse of biological research for over 60 years, providing a simple method for separation and analysis of biomolecules (i.e., DNA, RNA, and proteins) and their fragments based on their size and charge.[491−493] Compared to other separation techniques such as centrifugation, capillary electrophoresis, filtration, etc., gel electrophoresis allows multiple runs in parallel on the same gel. By coating nanoparticles with a charged polymer, gel electrophoresis can be used for nanoparticle separation.[494−496] In addition to analyte separation, gel electrophoresis enables semiquantitative analysis based on the band intensity. For instance, Wang et al. reported a simple, inexpensive, high-throughput strategy that exploits nondenaturing polyacrylamide gel electrophoresis (PAGE) for detection of amplification products from microsatellite DNA markers.[497]

Gel electrophoresis can be used for analysis of nucleic acids because the phosphate backbone of nucleic acids is negatively charged in buffer. For example, Gibson et al. proposed an isothermal, single-reaction method for enzymatic assembly of DNA molecules up to several hundred kilobases, in which the assembled DNA molecules and cloned products were demonstrated with agarose gels.[498] The Halvorsen group designed a programmable DNA nanoswitch for detection of DNA sequences (Figure 22A).[499,500] In the presence of the target sequence, the DNA nanoswitch undergoes a predefined conformational change, switching from a linear "off" configuration to a looped "on" configuration. The on and off states can be identified on an agarose gel, and the strategy achieved a detection range of ∼1 pM to ∼10 nM with picomolar level sensitivity. The same group then extended the technique for detecting miRNAs from unprocessed cellular total RNA.[501] This method was amplification-free, did not require any labels, and had a LOD of 0.2 aM. Further, the nanoswitches can also be multiplexed to identify different targets simultaneously.[502,503] The Halvorsen group used this to demonstrate multiplexed detection of five miRNAs from differentiating skeletal myoblasts in a single lane. Hansen et al. used this DNA nanoswitch to detect prostate-specific antigen (PSA) and showed a dynamic range from ∼60 fM to ∼60 pM and a LOD of 44 fM in 20% serum.[504] Koussa et al. used these DNA nanoswitches to measure kinetic and equilibrium parameters for different molecular interactions (Figure 22B).[505] According to induced topological changes, these nanoswitches are capable of reporting molecular interactions. In addition, the different interaction states can be easily resolved as distinct bands on a gel. These features endow this nanoswitch with the ability to monitor and control reactions. Moreover, DNA acts as an amplifying transducer for biosensing applications. In one study, Dirks et al. used an aptamer construct exposing an initiator strand upon binding ATP for HCR amplification of ATP detection.[506] The detection of ATP and specificity in differentiating ATP from GTP were proved by gel electrophoresis.

Gel electrophoresis can also be applied for detection of single nucleotide differences. Noll and Collins utilized denaturing gradient gel electrophoresis (DGGE) to identify DNA polymorphisms and to discriminate between two DNA molecules that differed by a single-base substitution.[507] However, this method could only detect ∼50% of all possible single-base changes for DNA fragment sizes of 50 to 1000 base pairs. Sheffield et al. improved this method by using PCR to attach a 40-bp GC-rich sequence (GC-clamp) to genomic DNA fragments, achieving improved detection of single-base changes.[508] Using the GC-clamp strategy and DGGE to analyze these fragments, Weinstein et al. found heterozygous mutations in the Gs (guanine nucleotide-binding protein) alpha-subunit gene in two kindreds.[509] Another study detected single base changes in human genomic DNA using the same method.[510] Orita et al. developed mobility shift analysis of single-stranded DNAs on neutral polyacrylamide gel electrophoresis to detect DNA polymorphisms and distinguished two alleles at chromosomal loci.[511]

Gel electrophoresis technology is extended to protein analysis as well. Two-dimensional gel electrophoresis followed by mass spectroscopy has been a valuable tool for discovery-oriented protein measurements over 40 years,[512] but with this technology, it is difficult to detect a single and focused sets of proteins.[513] Affinity-based techniques have been reported to provide unique advantages in terms of sensitivity and flexibility for single-proteins analysis. Xie et al. established an aptamer-based method for parallel protein analysis (Figure 22C).[514] The method depends on recognition of the target protein by two unique aptamers targeting different epitopes on the protein. After addition of target proteins, binding, and washing, sensing aptamers were eluted and amplified by multiplex PCR, and the resulting PCR products were separated by GE and visualized. Gel electrophoresis results confirmed that this dual-aptamer-based multiplex protein biosensor enables simultaneous and quantitative detection of thrombin and platelet-derived growth factor-BB (PDGF-BB) with LODs of 333 pM and 3.3 nM, respectively. Given that agarose gel electrophoresis is an ideal tool to evaluate the protein corona, Welsher et al. proposed a simple yet sensitive assay based on gel electrophoresis to evaluate protein binding to NPs with different surface chemistry (Figure 22D).[515] Using gel banding and retardation as a readout for protein adsorption, the surface chemistry was optimized to yield a mixed charge surface, displaying specific binding resistance to a wide range of serum proteins and nucleic acids.

3.6. AFM-Based Readout Strategy

Use of an atomic force microscope (AFM) is another important technique in biomolecular analysis.[516,517] Through decades of development, this technique not only enables analysis of surface characteristics at the nanometer scale but also allows observation and manipulation of surfaces under physiological conditions.[518−521] Accordingly, these traits make the AFM an ideal tool for conducting research at the single-molecule level.[522] In certain cases, the AFM can provide 3D views of samples,[523] while also able to measure piconewton (10^{-12} N) forces associated with single molecules,[524,525] and topological analysis of nanostructure or cell surfaces.[526−529] Consequently, the AFM shows great advantages as a single molecule tool for sensing molecular recognition interactions on biosurfaces.[530]

AFM-based force spectroscopy is a useful tool to study structural changes in DNA. Using AFM to measure the interaction forces between single strands of DNA, Lee et al. observed the unfolding of nucleic acids.[527] Because of its structural variations and biological functions, G-quadruplexes have sparked a growing interest in the field of structural and molecular biology.[531] To this end, the Sugiyama group used real-time AFM to detect the formation and disruption of a G-quadruplex structure within a DNA origami scaffold (Figure 23A).[532] During scanning of the sample in the presence of K^+,

DOI: 10.1021/acs.chemrev.9b00121
Chem. Rev. XXXX, XXX, XXX−XXX

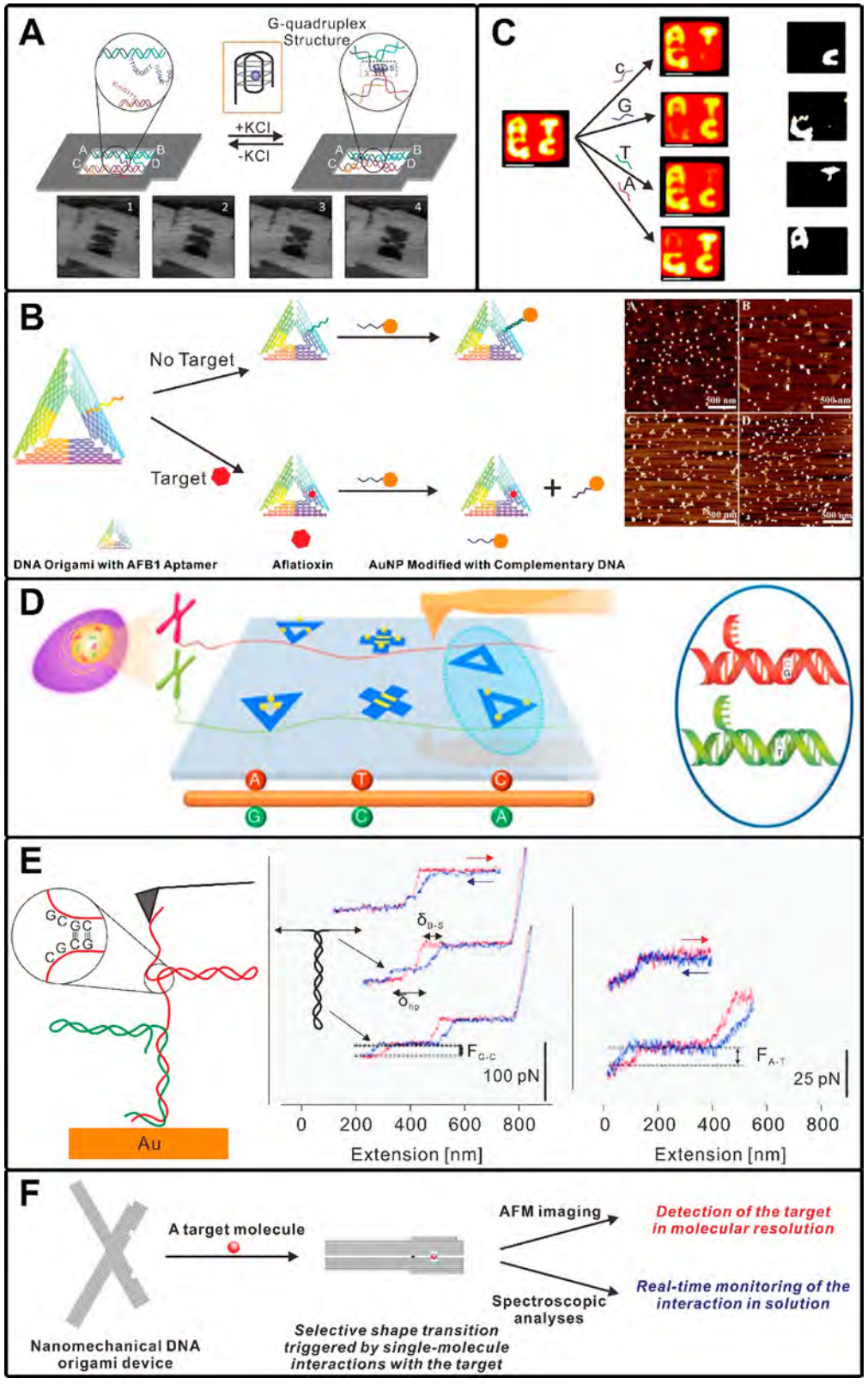

Figure 23. (A) Visualization of dynamic conformational switching of the G-quadruplex in a DNA nanostructure with an AFM. Adapted with permission from ref 532. Copyright 2010 American Chemical Society. (B) Aptamer-tagged DNA origami for spatially addressable detection of aflatoxin B1. Adapted with permission from ref 537. Copyright 2017 Royal Society of Chemistry. (C) Label-free detection and symbolic display of SNP on DNA origami. Adapted with permission from ref 539. Copyright 2011 American Chemical Society. (D) AFM-based single-molecule nanomechanical haplotyping with DNA origami shape IDs. Reprinted with permission from ref 540. Copyright 2017 Springer Nature. (E) Direct measurement of base-pairing forces using an AFM. Adapted with permission from ref 541. Copyright 1999 Springer Nature. (F) Detection of various targets using DNA origami devices. Adapted with permission from ref 543. Copyright 2011 Springer Nature.

DOI: 10.1021/acs.chemrev.9b00121
Chem. Rev. XXXX, XXX, XXX−XXX

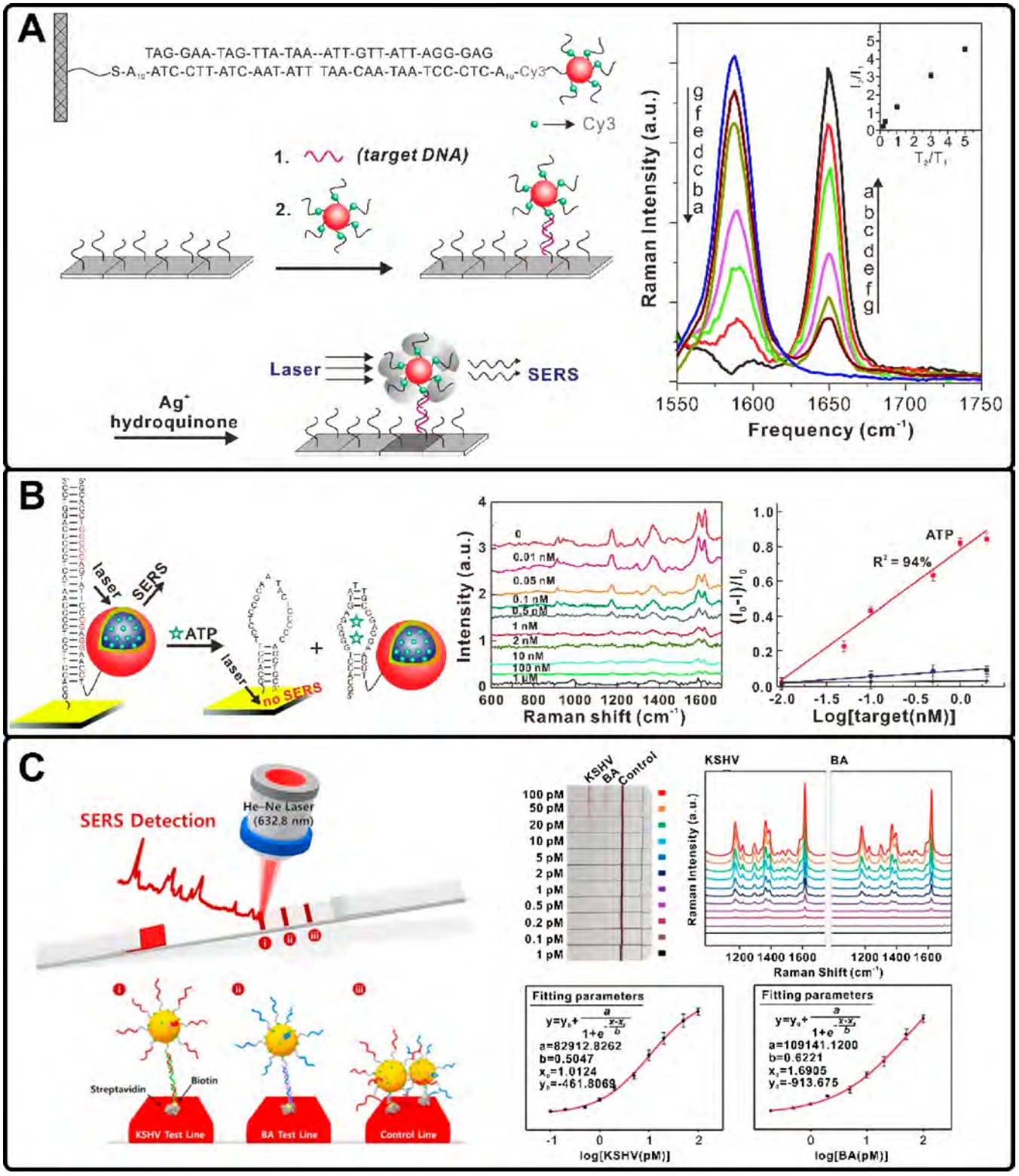

Figure 24. (A) AgNPs with Raman spectroscopic fingerprints for DNA and RNA detection. Reproduced with permission from ref 558. Copyright 2002 AAAS. (B) Aptamer biosensor based on SERS for ATP detection. Adapted with permission from ref 561. Copyright 2012 American Chemical Society. (C) SERS-based lateral flow assay biosensor for simultaneous detection of dual nucleic acids. Reproduced with permission from ref 569. Copyright 2017 American Chemical Society.

the two dsDNA chains with G-tracks formed the X-shaped structure from an initially separated state; the preformed G-quadruplex was disrupted in the absence of K^+ and reverted to the separated state. As such, monitoring the global structural changes of the two incorporated dsDNA chains in the DNA frame using AFM allows the single-molecule observation of the dynamic formation and disruption of a G-quadruplex.

DOI: 10.1021/acs.chemrev.9b00121
Chem. Rev. XXXX, XXX, XXX−XXX

Single-molecule level understanding of DNA conformations facilitates construction of reproducible, robust, and ultrasensitive sensors.[533,534] The Ye group observed the nanoscale conformations of individual DNA molecules on a gold surface passivated with a hydroxyl-terminated alkanethiol self-assembled monolayer (SAM) with *in situ* electrochemical AFM.[535] In a follow-up study, the Ye group reported that single DNA hybridization events were visualized on a novel surface with an unprecedented resolution using an AFM.[536] Initially, the tethered probes covalently anchored to a carboxyl-terminated SAM were lifted away from the surface under a saline tris-acetate-EDTA buffer because of the electrostatic repulsion, which facilitated hybridization between probes and targets with minimal nonspecific adsorption. On the addition of divalent nickel cations, the hybridized dsDNA adsorbs onto the surface. As a result, the use of AFM for high-resolution imaging of single DNA hybridization events was achieved by switching the DNA−surface interaction between a strong state and a weak state. In addition, Lu et al. used the AFM to visually detect aflatoxin B1 (AFB1) by using a combination of aptamer-tagged DNA origami with ssDNA-functionalized AuNPs (Figure 23B).[537] In the absence of AFB1 molecules, the AuNPs are linked to DNA origami at the predetermined location via DNA hybridization. Upon addition of AFB1 molecules, the aptamer probes recognize and bind to the target molecules, resulting in folded structures. Thus, the attachment of AuNPs on the designed sites of DNA origami can reflect the amount of AFB1 in the detection system.

AFM has been also applied for enhanced recognition of single nucleotide polymorphisms (SNPs). Han et al. designed locked nucleic acid coupled into a hairpin DNA oligonucleotide probe to detect SNP.[538] On target binding, the difference in stiffness on the surface was analyzed using AFM nanolithography technique. Consequently, this strategy can discriminate between perfectly complementary and singly mismatched targets. By combining the effectiveness of branch migration process and AFM imaging, Seeman and co-workers established a reliable method to visualize the target nucleotide symbol in a SNP assay (Figure 23C).[539] The DNA origami contained graphical representations of the four possible nucleotide alphabetic characters (i.e., A, T, G, and C), and on binding a specific DNA sequence, the character matching the SNP nucleotide disappears on the origami surface. AFM images provide a direct symbolic readout identifying the nucleotide carried by the target. Recently, the Fan group developed DNA origami structures as shape IDs for nanomechanical imaging of SNPs (Figure 23D).[540]

An AFM can be also used to analyze mechanochemistry at the single-molecule level. Rief et al. employed single-molecule force spectroscopy based on AFM technology to show that the mechanics of DNA overstretching is sequence dependent (Figure 23E). They used this technique to directly measure the base pair-unbinding forces for G-C to be 20 ± 3 pN and for A-T to be 9 ± 3 pN.[541] Leitner et al. used force distance cycles to record individual molecular recognition events between streptavidin-modified AFM tip-tethered proteins and the DNA structures,[542] verifying that the interaction between streptavidin and biotinylated DNA nanostructure is specific. Kuzuya et al. created functional nanomechanical DNA origami devices as versatile and visible 'single-molecule beacons' (Figure 23F).[543] Using 'DNA origami pliers' and 'DNA origami forceps' composed of two levers of ∼170 nm in length connected at a fulcrum, they detected conformational changes on addition of various targets such as metal ions and proteins using an AFM.

3.7. SERS-Based Readout Strategy

Surface-enhanced Raman scattering (SERS) has been explored for its potential in biosensing in the last several decades.[544−547] In contrast to conventional Raman, SERS has strong signal intensity (factors up to $\sim 10^{14}$) due to the hot spot in metallic nanostructured spaces. In addition, SERS possesses other attractive merits, such as narrow Raman band, and high resistance to interferences of environmental factors such as oxygen, humidity, and foreign species.[548] These features make SERS a promising tool for ultrasensitive biosensing with the target of attaining single-molecule level detection.[549−551] Further development in the design and fabrication of novel SERS-active nanostructures has been enriched by the ability to create complex structures using DNA.[552−554] By integrating SERS with DNA nanotechnology, various kinds of SERS biosensor have been established, broadening its analytical applications.[555−557]

Metal NPs (e.g., AuNPs, AgNPs)-based SERS biosensors have been extensively studied for sensitive and specific detection of biomolecules. In 2002, the Mirkin group used DNA-coated AuNPs coupled with Raman-active dyes for detection of nucleic acids with a LOD of 20 fM (Figure 24A).[558] Using the target ssDNA to assemble AgNPs-based probes on Ag film, Braun et al. detected ssDNA with SERS.[559] This study revealed that a few AgNPs are sufficient to produce intense and reliable SERS signals, indicating that highly reproducible signals can be generated at the near-single nanoparticle level. In addition to nucleic acid detection, metal NP-based SERS methods have been extended to the analysis of small molecules and biomarkers (e.g., proteins, telomerase), even cells, bacteria, and viruses.[560] In one study, Li et al. constructed a SERS probe composed of gold nanostar@Raman label@SiO_2 core−shell NPs for quantitative detection of ATP (Figure 24B).[561] Addition of ATP removes the SERS probe from the duplex DNA on the gold film, resulting in the reduced Raman signal. This SERS-based on−off sensor enables detection of ATP with a limit of detection of 12.4 pM. Cottat et al. used aptamer-tagged optical nanoantennas for SERS-based detection of the manganese super oxide dismutase down to the nM level.[562]

Excellent multiplexing ability is another advantage of the SERS technique.[563−565] The sharp bands of Raman spectra make SERS an ideal candidate for multiplexed detection. For example, Sun et al. developed a SERS-based nonfluorescent probe for multiplexed DNA detection.[566] Song and co-workers proposed an efficient multiplexed assay strategy to detect specific DNA in a controlled and reproducible manner using SERS.[567] They designed mixed DNA-functionalized NP probes for improving the multiplexing capacity. Once the target DNA is added, different single-component DNA-functionalized NPs can be hybridized simultaneously with single mixed DNA-functionalized NP probe, thus achieving multiplexed DNA detection. Wang et al. constructed SERS-based inverse molecular sentinel (iMS) nanoprobes.[568] Once binding the target, the iMS nanoprobes undergo a conformational change, resulting in the "OFF-to-ON" signal switch, and this iMS technique enables multiplexed detection of miR-21 and miR-34a. Recently, the Choo group built a SERS-based lateral flow assay (LFA) biosensor for the simultaneous detection of two DNA markers (Kaposi's sarcoma-associated herpesvirus (KSHV) and bacillary angiomatosis (BA)) (Figure 24 C).[569] The LFA strip was

DOI: 10.1021/acs.chemrev.9b00121
Chem. Rev. XXXX, XXX, XXX−XXX

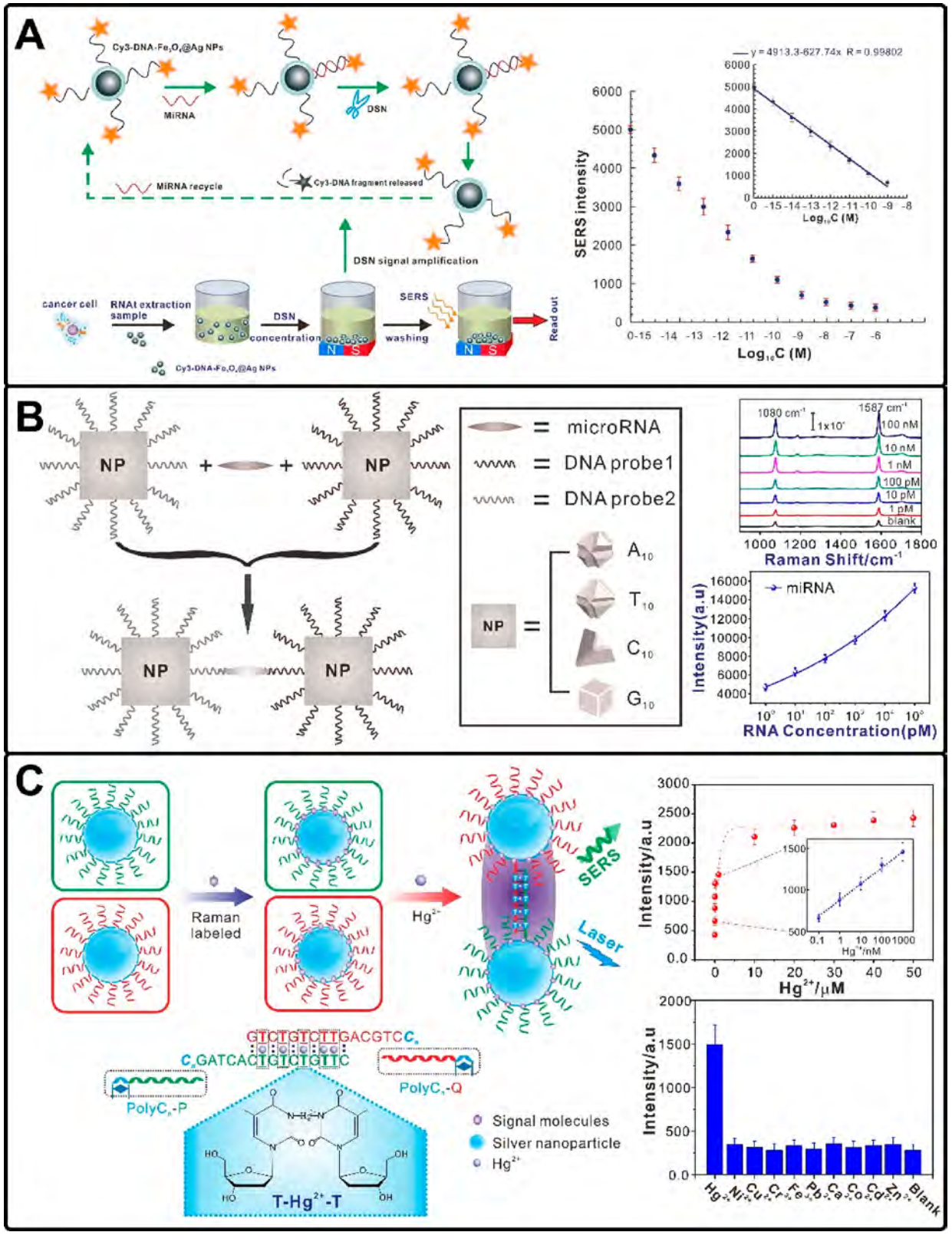

Figure 25. (A) Fe_3O_4@Ag magnetic NPs as a signal amplification platform for SERS detection of miRNA. Adapted with permission from ref 576. Copyright 2016 Elsevier. (B) DNA-encoded Raman-active anisotropic NPs for miRNA detection. Adapted with permission from ref 577. Copyright 2017 American Chemical Society. (C) Poly cytosine-mediated nanotags for SERS detection of Hg^{2+}. Adapted with permission from ref 578. Copyright 2017 Royal Society of Chemistry.

composed of two test lines and one control line, and a 1:1 molar mixture of detection DNA-immobilized SERS nanotags was stored in the conjugate pad. KSHV and BA detection DNAs attached to Au NPs can be captured by corresponding probe DNAs on the first and second test lines, and excess Au NPs would be captured by control DNAs on the third control line

DOI: 10.1021/acs.chemrev.9b00121
Chem. Rev. XXXX, XXX, XXX−XXX

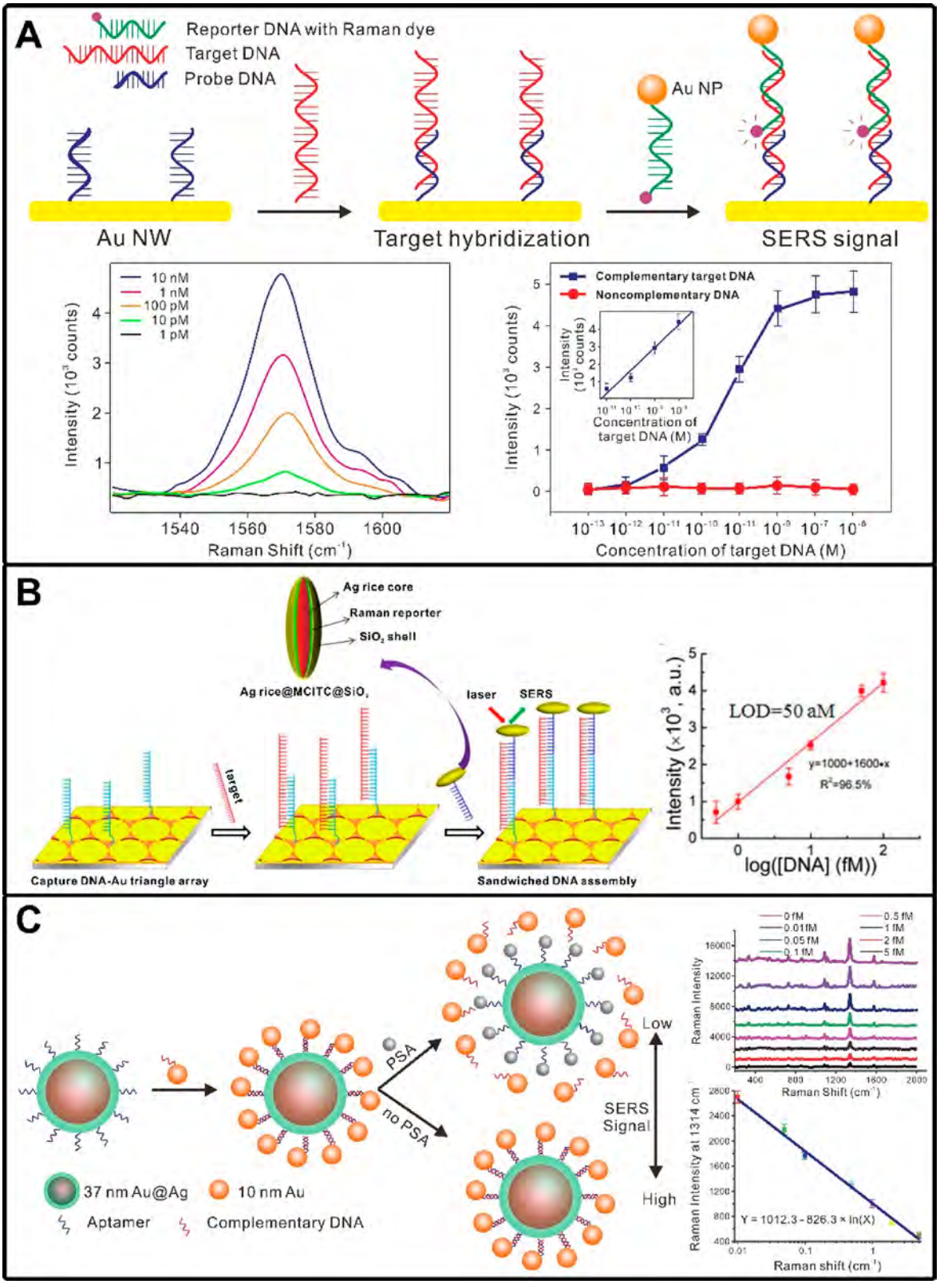

Figure 26. (A) AuNP-on-wire SERS sensor for patterned multiplex pathogen DNA detection. Adapted with permission from ref 581. Copyright 2010 American Chemical Society. (B) Plasmonic nanorice antenna on triangle nanoarray for SERS detection of Hepatitis B virus DNA. Reproduced with permission from ref 582. Copyright 2013 American Chemical Society. (C) Aptamer-based SERS detection of PSAs by heterogeneous satellite nanoassemblies. Adapted with permission from ref 585. Copyright 2014 Royal Society of Chemistry.

through DNA hybridization. As such, the SERS-based LFA sensing platform could simultaneously detect KSHV and BA with LODs of 0.043 and 0.074 pM, respectively.

Since single-NPs have insufficient Raman signal-enhancing capability, single-NPs-based SERS biosensors have been coupled with other signal amplification strategies to improve

DOI: 10.1021/acs.chemrev.9b00121
Chem. Rev. XXXX, XXX, XXX−XXX

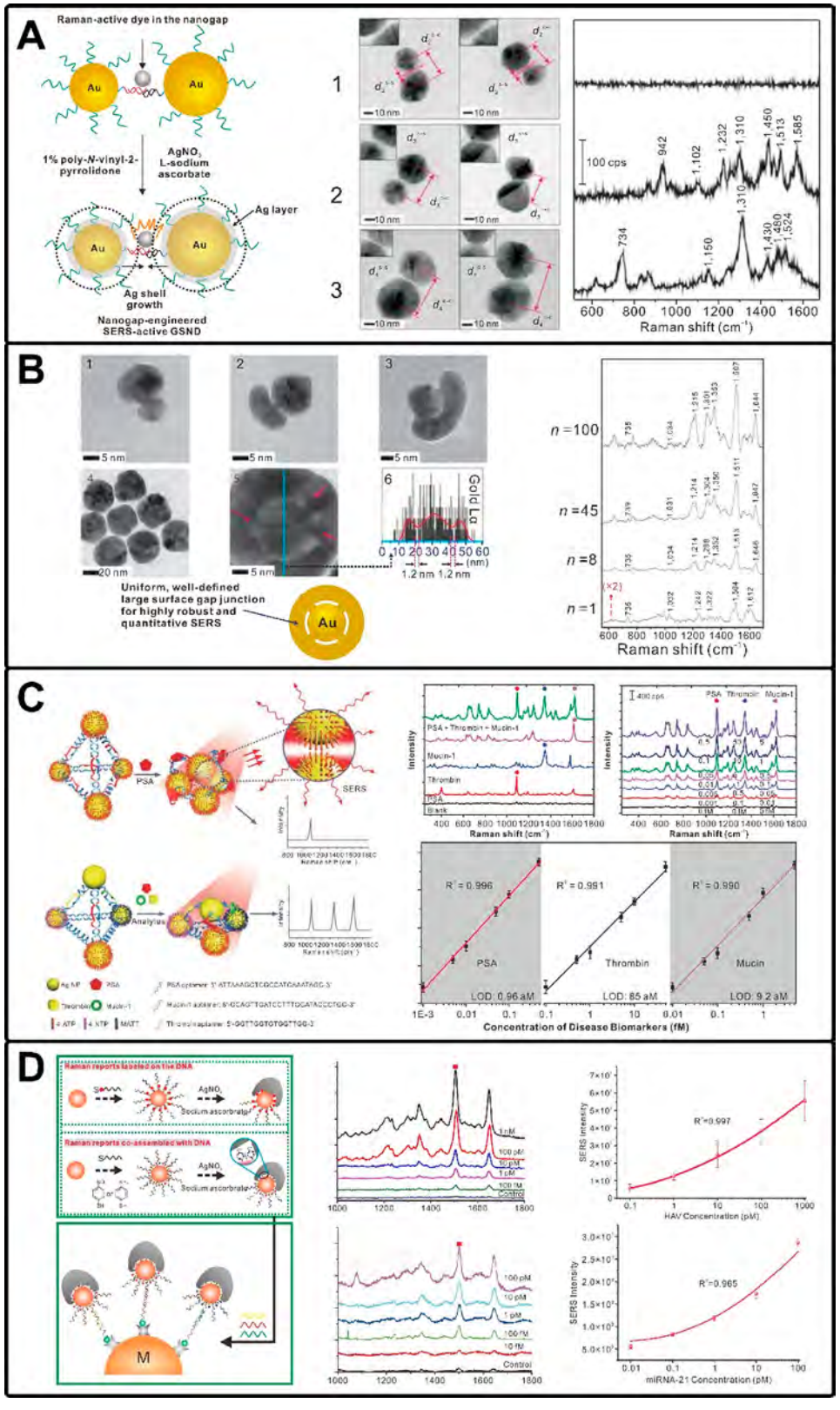

Figure 27. (A) Nanogap-engineerable Raman-active nanodumbbells for single-molecule detection. Reproduced with permission from ref 587. Copyright 2010 Springer Nature. (B) DNA-tailorable gold nanobridged nanogap particles (Au-NNP) with a highly stable and reproducible SERS signal. Reproduced with permission from ref 552. Copyright 2011 Springer Nature. (C) SERS encoded silver pyramids for multiplexed detection of disease biomarkers. Reproduced with permission from ref 589. Copyright 2015 Wiley-VCH. (D) Multicolor gold−silver nanomushrooms as SERS Probes for multiplex DNA/miRNA detection. Reproduced with permission from ref 592. Copyright 2017 American Chemical Society.

their sensitivity.[570−572] In 2012, Ye et al. developed a SERS detection system with an autonomous DNA machine for multiple isothermal amplification to detect specific nucleic acid sequences with a LOD of 0.2 fM.[573] Thereafter, based on a smart

DOI: 10.1021/acs.chemrev.9b00121
Chem. Rev. XXXX, XXX, XXX−XXX

multifunctional probe for dual cyclical nucleic acid strand-displacement polymerization, Zhang et al. developed a technique for miRNA with a LOD of 6.3 fM.[574] In addition, magnetic enrichment is another approach for signal amplification.[575] Pang et al. designed Raman tags-DNA probes modified Fe_3O_4@AgNPs that act both as SERS and duplex-specific nuclease signal amplification (DSNSA) platform (Figure 25A).[576] Upon hybridization of target miRNA with DNA on Fe_3O_4@Ag NPs, DSN cleaves the DNA in the DNA/RNA hybrid duplex and releases the RNA to rehybridize with another DNA probe, triggering the signal-amplification via target recycling. Subsequently, target miRNA let-7b can be captured, concentrated, and directly quantified within a PE tube because of the superparamagnetic Fe_3O_4@AgNPs. As a result of DNA-assisted signal-amplification and Fe_3O_4@AgNP-mediated magnetic enrichment, this biosensor can detect miRNA down to 0.3 fM and discriminate single-nucleotide differences in let-7 family of miRNAs.

Using analytes to control the aggregation of NPs is an effective approach to produce a larger SERS effect. In 2008, Graham and co-workers reported the interaction of DNA for controlling the aggregation of dye-coded, DNA-functionalized AgNPs for the first time.[553] This target-dependent, sequence-specific DNA hybridization assembly can selectively turn on a significantly enhanced SERS effect, opening a new opportunity to design SERS-based sensors. According to this principle, Qi et al. developed DNA-encoded Raman-active anisotropic NPs for miRNA detection (Figure 25B).[577] They used 10-mer oligo-A, -T, -C, and -G to mediate the growth of Ag cubic seeds into different Raman-active anisotropic NPs. The resulting AgNPs were further encoded with DNA probes to serve as effective SERS probes. Target miRNA causes aggregation of these SERS probes, further amplifying the Raman signals. This method allows detection sensitivity down to 1 pM. This strategy can also be applied for ion detection. The Li group developed poly cytosine (polyC)-mediated SERS nanotags as a sensor system for Hg^{2+} detection (Figure 25C).[578] The Hg^{2+} can be captured by the SERS nanotags via mismatched T−T base pairs to form T−Hg^{2+}−T bridges, thereby inducing the aggregation of nanotags and yielding drastically amplified SERS signals. In addition to the anchoring function (inducing formation of intrinsic silver-cytosine coordination), polyC can also aid in engineering the Raman-activity of SERS nanotags by mediating its length. Consequently, these polyC-mediated SERS nanotags can detect Hg^{2+} in the concentration range from 0.1 to 1000 nM and good selectivity over other metal ions. Similarly, Xu et al. utilized T−Hg^{2+}−T base pairs to assembly Au nanochains for ultrasensitive SERS detection of mercury with a low LOD of 0.45 pg mL^{-1}.[579]

Single sophisticated nanostructures containing multiple hot spots have been used for developing SERS-active probes for sensitive biological detection. Compared to the silver or gold NPs with relatively low enhancement factors (EF) (10^4−10^5), such nanostructures possess much higher EF up to 10^7−10^9 because of their efficient SERS hot spots.[580] Kang et al. constructed a Au particle-on-wire system as a new SERS-active substrate for multiplexed DNA detection (Figure 26A).[581] Li et al. developed silver "nanorice" antennae on a patterned gold triangle nanoarray, making these antennae serve as periodically aligned plasmonic hot spots (Figure 26B).[582] This strategy has a LOD of 50 aM for hepatitis B virus DNA and can discriminate mutant DNA with a single nucleotide differences. The core−satellite structures assembled by AuNPs or AgNPs with a remarkable SERS effect can improve the sensitivity of detection.[583,584] For example, Xu and co-workers constructed satellite nanoassemblies consisting of Au@Ag NP as a core NP and AuNPs as satellite NPs for use as SERS probes (Figure 26C),[585] in which the aptamer specific to prostate-specific antigen (PSA) and its partial complementary DNA are used to assemble core−satellite nanostructures. Presence of PSA causes release of satellite NPs from the core NP, reducing the signal. This technique method can detect PSA with a LOD of 4.8 aM. In a follow-up study, they used the same strategy to detect Mucin-1 with LOD of 4.3 aM.[586]

Designing reproducible nanometer gap junctions to fabricate single nanostructures with high SERS signals facilitates the improved sensitivity of biosensors. Nam and co-workers developed SERS-active gold-silver core−shell nanodumbbells (Figure 27A) that allow the nanoscale gap between two NPs to be precisely engineered by nucleic acids.[587] These single-DNA-tethered nanodumbbells create Raman signals for reproducible single-molecule detection. In follow-up studies, they found that the EF values of Au-Ag core−shell nanodumbbells with < 1nm interparticle gaps are narrowly distributed between 1.9×10^{12} and 5.9×10^{13}.[588] Besides the design of such exterior nanogaps, they synthesized well-defined gold core−shell nanostructures with interior nanogaps (Figure 27B), which can be capable of generating highly stable and reproducible SERS signals.[552] The gold nanostructures with narrowly distributed EF 1.0×10^8 and 5.0×10^9 were demonstrated to show high sensitivity toward single-molecule detection.

Using a similar principle, the Kuang group constructed DNA-frame driven Ag-pyramids bearing multiple aptamers and triple Raman reporters as a versatile platform for detecting multiple disease biomarkers (Figure 27C).[589] The target biomarker binds to the specific aptamer and reconfigures the pyramidal nanostructures, leading to enhanced Raman signal. As a result, this platform enables simultaneous, multiplexed, and quantitative determination of disease biomarkers with a LOD of 0.96 aM, 85 aM, and 9.2 aM and a detection range of 1−500 aM, 0.1−50 fM, and 0.01−5 fM for PSA, thrombin, and mucin 1, respectively. The effective SERS encoded Ag-pyramids with multivariate recognition provide accurate and distinct identification of disease biomarkers in clinical science. Thereafter, they used DNA-frame driven Au-pyramids for intracellular telomerase activity sensing with a limit of detection of 6.2×10^{-15} IU.[590] The Fan group prepared a DNA-mediated gold-silver nanomushroom, where they tuned the interior nanogaps between the gold and silver by adjusting the surface density of 6-carboxy-X-rhodamine-labeled ssDNA on the AuNPs.[591] Moreover, they found that the SERS intensity of the designed structures is dependent on the area of the nanogap, and the SERS signal EF is $\sim 1.0 \times 10^9$. In another study, they used this gold−silver nanomushroom for multiplexed and simultaneous SERS detection of various DNA and RNA targets (Figure 27D).[592] Notably, the DNA involved in the nanostructures can act not only as gap DNA but also probe DNA, and DNA's involvement thus bestows the nanostructures with the inherent ability to recognize DNA and RNA targets. Consequently, this method can detect DNA and miRNA down to 100 fM and 10 fM, respectively.

DNA origami technology has been demonstrated as a powerful means to create high-yield SERS-active NP assemblies.[593,594] As a result of its addressability and programmability, DNA origami enables excellent positioning control of individual NPs on its surface.[595−598] In this way, the interparticle gaps

DOI: 10.1021/acs.chemrev.9b00121
Chem. Rev. XXXX, XXX, XXX−XXX

Table 1. Summary of Readout Strategies for Biosensing

type of readout strategies	types of structures of nucleic acid	analytes	LOD	ref
fluorescence-based readout strategy	G-quadruplexes	DNA	25 nM	163
	fluorescence-labeled DNA probes	DNA	4 nM	171
	molecular beacon-based junction probes	DNA	50 pM	156
	DNA hairpin	DNA	10 pM	155
	DNA nanowires	BRCA1 oncogene	10 fM	164
	molecular beacon	miRNA	0.4 pM	158
	DNA hairpin	miRNA	10 fM at 37 °C	157
			1 aM at 4 °C	
	dye-labeled DNA probe	Human thrombin	2 nM	174
	aptamer	ATP	0.1 mM	167
	split aptamer	ATP	single-molecule level	185
	dsDNA	Cl^{1-}	5 mM	186
	T-rich DNA	Hg^{2+}	0.3 nM	161
	molecular beacon	ATP	50 nM	159
		Pb^{2+}	600 pM	
	fluorescence-labeled DNA probes	DNA	1 nM	178
		thrombin	5 nM	
		Ag^{+}	20 nM	
		Hg^{2+}	5.7 nM	
		cysteine	60 nM	
	G-quadruplex	DNA	0.6 nM	181
		ATP	8.0 nM	
FRET-based readout strategy	ssDNA	DNA	1.3 nM	271
	ssDNA	DNA	75 pM	316
	Cy5-labeled ssDNA	DNA	4.8 fM	253
	dsDNA	mRNA	10 nM	230
	Tb-labeled ssDNA	miRNA	1 nM	259
	DNA tetrahedron	miRNA	0.12 fM	278
	Apt-BHQ1	kanamycin	6 pg/mL	317
	aptamer	thrombin	1.5 nM	275
	ssDNA aptamer	thrombin	1 nM	260
	DNA nanoprism	ATP	30 μM	232
	aptamer	ATP	80 nM	280
	two-layer nonenzymatic nucleic acid circuits	adenosine	200 pM	227
	ssDNA	Pb^{2+}	16.7 nM	317.
	DNA tetrahedron	DNA	7.6 nM	231.
		ATP	10.4 μM	
	ssDNA probe	miRNA-20	0.2 nM	221
		miRNA-21	0.9 nM	
nanoparticle-based readout strategy	dsDNA	DNA	1 pM	363
	spherical nucleic acid	DNA	500 fM	340
	spherical nucleic acid	DNA	10 fM	333
	ssDNA	miRNA	3.4 fM	358
	antilysozyme aptamer	lysozyme	0.9 nM	342
	DNAzyme	uranyl ion	45 pM	332
	T-rich DNA	Hg^{2+}	100 nM	335.
electrochemical-based readout strategy	ssDNA	DNA	2.7 pM	392
	stem-loop structure	DNA	10 fM	401
	DNA tetrahedron	miRNA	1 fM	413
	spherical nucleic acid	cell-free nucleic acids	1 pg μL^{-1}	429
	spherical nucleic acid	cell-free nucleic acids	1 fg μL^{-1}	426
	dsDNA	adenosine	11.08 μM	406.
	DNA tetrahedron	Hg^{2+}	0.1 nM	414
	aptamer	lysozyme	0.01 μg mL^{-1}	404
		adenosine	0.02 nM	
	aptamer	cocaine	3.4 μM	402
		adenosine	18 μM	
		interferon-gamma of tuberculosis	2.6 nM	
		uranium	9.1 nM	
	dsDNA	cocaine	1 mg mL^{-1}	430
		DNA	100 nM	

DOI: 10.1021/acs.chemrev.9b00121
Chem. Rev. XXXX, XXX, XXX−XXX

Table 1. continued

type of readout strategies	types of structures of nucleic acid	analytes	LOD	ref
		staphylococcus	10 pg μL^{-1}	
		saprophyticus	0.15 c.f.u. mL^{-1}	
		thrombin	10 fM	
gel electrophoresis-based readout strategy	dsDNA	DNA	~1 pM	499
	DNA scaffold	prostate-specific antigen	44 fM	504
	aptamer	thrombin	333 pM	514
		platelet-derived growth factor-BB	3.3 nM	
AFM-based readout strategy	DNA origami	observation of G quadruplex formation		531
	single-stranded DNA probes	visualization of single DNA hybridization events		536
	aptamer-tagged DNA origami	aflatoxin B1	0.8 ng mL^{-1}	537
	locked nucleic acid-integrated hairpin DNA probes	single-base mismatch	discrimination ratio of 2 to 3	538
	DNA origami	SNP		539
	DNA origami	miRNA	200 nM	543
		Ag^{+}	10 μM	
SERS-based readout strategy	ssDNA	HIV-1 DNA	~0.24 pg/mL	557
	ssDNA	DNA	10 pM	581
	ssDNA	hepatitis B virus DNA	50 aM	582
	ssDNA	miRNA	1 pM	577
	cyclical nucleic acid	miRNA	6.3 fM.	574
	ssDNA	miRNA	0.3 fM	576
	DNA-based pyramids	telomerase activity	6.2×10^{-15} IU	590
	ssDNA	PSA	4.8 aM	585.
	aptamer	ATP	12.4 pM	561
	ssDNA	Hg^{2+}	0.45 pg mL^{-1}	578
	ssDNA	Kaposi's sarcoma-associated herpesvirus	0.043 pM	569
		bacillary angiomatosis	0.074 pM	
	DNA-based pyramids	PSA	0.96 aM	589
		thrombin	85 aM	
		mucin 1	9.2 aM	

between assembled plasmonic NP dimers on DNA origami can be precisely tuned, producing dramatic SERS effect.[594] Therefore, such DNA origami-mediated nanoassemblies show great promise for single-molecule detection.[599] In one study, Au nanostar dimers interparticle gaps of 7 and 13 nm were assembled on DNA origami.[600] The produced SERS enhancements with EF of 2×10^{10} and 8×10^{9} are strong enough for single analyte detection. Such SERS substrates with controlled interparticle separation distance and stoichiometry provide a reproducible and potential platform for single-molecule sensing. In a similar method, the Ding group controlled the geometrical configuration of bowtie nanoantennae with an ~5 nm gap to observe single-molecule SERS of individual nanostructures.[601] The Keyser group constructed DNA origami-based assembly of AuNP (40 nm) dimers with gaps of 3.3 ± 1 nm that allowed detection of dye molecules and ssDNA .[602] Thereafter, the gap sizes between particles ranging from 1 to 2 nm were also achieved.[603] To sum up, utilization of DNA origami for fabrication of addressable plasmonic nanosensors speeds up the process for future sensing applications with single-molecule resolution.[600,601]

The versatility of DNA-based structures has allowed the creation of structures with different types of read outs. Small DNA-based devices predominantly depend on a fluorescence or a FRET-based readout. While this strategy requires fluorophore-conjugated DNA strands, the readout can be observed using instruments that are already available in most research laboratories. Specifically, optical methods based on nanoparticles provide a colorimetric approach where detection of a specific biomarker can be seen by the naked eye as a color change. This approach is especially useful and geared toward a point-of-care system where one can detect disease biomarkers on the field without the need for an expensive instrument or a proper lab setup. The minimal background signal in these strategies could still be minimized so that the limit of detection falls within clinical levels. Many other complex nanostructures have been built using DNA, especially using the origami method. These strategies are interesting demonstrations of the programmable nature of DNA nanostructures; however, as a readout method, the AFM is least suitable for a routine detection platform. Moreover, it is an expensive instrument (an AFM) and requires skilled personnel to analyze the samples, and the LOD in this case depends on a manual (or an automated) count of the number of reconfigured nanostructures on the microscope field. Gel-based techniques, especially those involving the DNA nanoswitches, are aligned more with the existing workflow of most laboratories.[501] Moreover, the ease of use and familiarity with the workflow enables use in research laboratories, while there could still be improvements made for it to be adaptable in clinical settings. Electrochemical sensors are the most studied, even within the field of DNA nanotechnology-based biosensing. Development of disposable electrodes and quicker readouts are primary advantages. This readout is also poised to be suitable for point-of-care and development of portable readers will be suitable to make that possible. Recently, SERS-based approaches are also studied more and this readout could be more appealing if the required instruments and workflow are simplified for the end user (see Table 1).

DOI: 10.1021/acs.chemrev.9b00121
Chem. Rev. XXXX, XXX, XXX−XXX

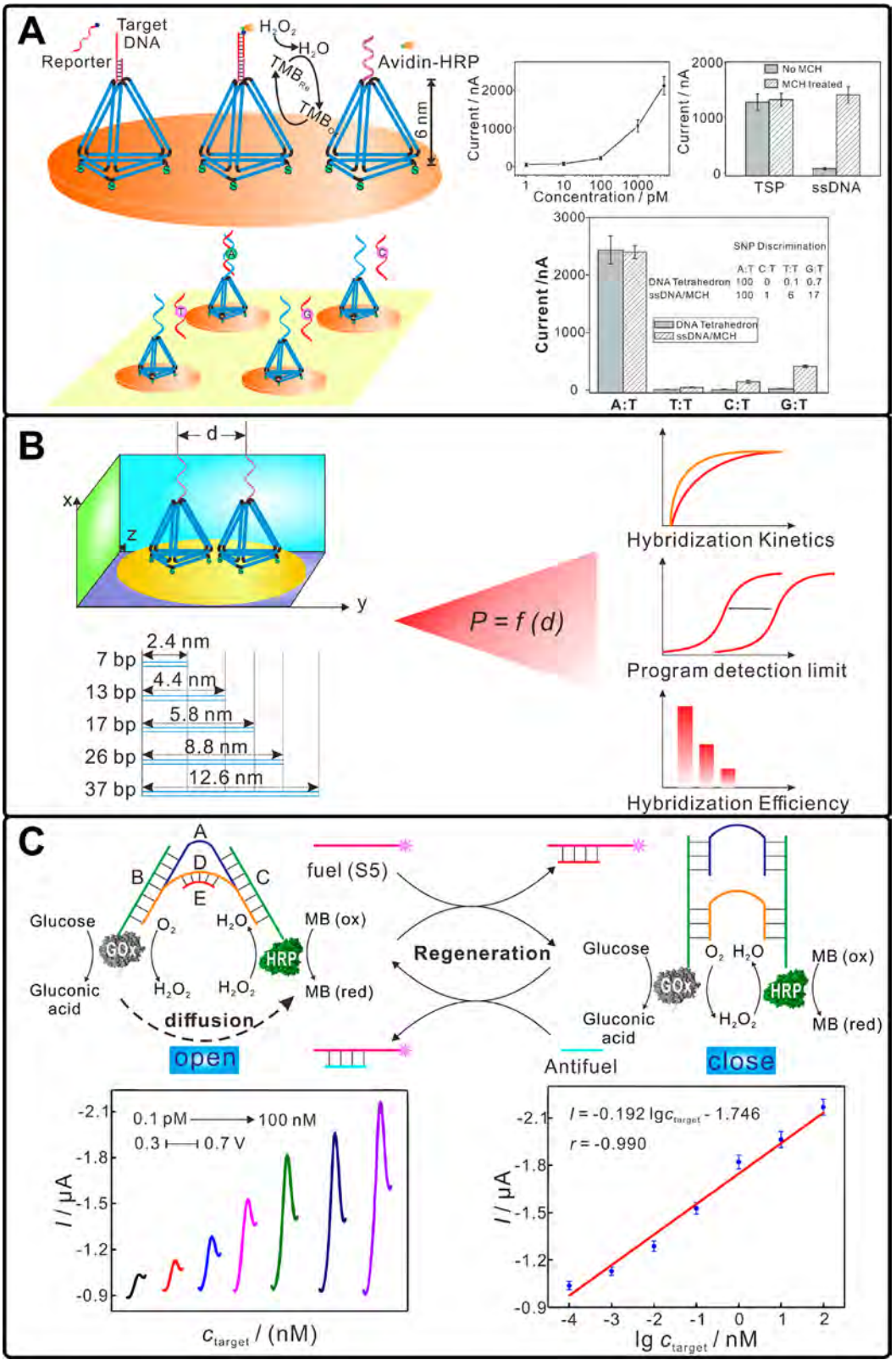

Figure 28. (A) DNA nanostructure-based biomolecular probe carrier platform for electrochemical biosensing. Adapted with permission from ref 638. Copyright 2010 Wiley-VCH. (B) Programmable engineering of a biosensing interface with tetrahedral DNA nanostructures for DNA detection. Reproduced with permission from ref 643. Copyright 2015 Wiley-VCH. (C) Regenerated DNA nanotweezer dynamically regulating enzyme cascade amplification for DNA detection. Adapted with permission from ref 652. Copyright 2018 American Chemical Society.

DOI: 10.1021/acs.chemrev.9b00121
Chem. Rev. XXXX, XXX, XXX−XXX

4. DNA NANOSTRUCTURES FOR BIOSENSING

The exploitation of DNA as a material building block to create DNA nanostructures with controlled geometries and spatial configurations has elicited tremendous interest since Seeman's proposal in the early 1980s.[13,66,604] The precise self-recognition capability of nucleic acids contributes to assembly of a variety of DNA motifs and complexes ranging from a few nanometers to micrometers.[408,605] Moreover, engineering complex DNA nanostructures with twists and curves can be achieved by targeted insertions and deletions of bases to control their flexibility and stress.[81] More importantly, the DNA origami technology provides an unprecedented approach to construct all arbitrarily shaped nanoscale molecular structures.[3,606,607] The ability to construct robust nanostructures that can also respond to cues is one of the main advantages of DNA nanostructures for biosensing.[608,609] Compared to ssDNA probes or duplex probes, the DNA nanostructure-based probes show powerful capability of engineering sensing interfaces such as an ordered and upright orientation and spatial segregation of neighboring probes.[610] These traits contribute to the improved target accessibility.[611] Additionally, the hanging DNA strands on DNA nanostructures can serve as excellent recognition elements,[612] and DNA nanostructures are facile to be functionalized with small molecules, antibodies as well as nanoparticles,[613] and thus endowed with nanometer-scale addressability.[614] Moreover, DNA nanostructures resistance to enzyme degradation is favorable for intracellular sensing. Accordingly, researchers have devoted extensive efforts to the development of DNA nanostructures for biosensing.[475,615−623] For example, highly rigid and well-defined TDNs can be engineered with high precision and with multiple functionalities, making them robust biosensing platforms for both *in vitro* and *in vivo* detection.[418,624−631] In the following text, we discuss DNA nanostructure-based biosensing of nucleic acids, pH, enzyme activity, protein biomarkers, and metal ions.

4.1. Nucleic Acid Detection

Nucleic acid analysis plays an important part in lab-based research and clinical diagnosis.[174,632,633] In view of their broad applications, many different strategies have been developed for sensitive and cheap detection of DNA or RNA molecules. In these strategies, oligonucleotides often serve as the molecular recognition elements, with Watson−Crick base pairing rules making the sensing event highly predictable and tunable by rational design of the probe sequence.[605,607] For example, Yang and co-workers generated a long-range self-assembled nanostructure-based DNA biosensor,[486] in which a cascade of hybridization events achieves significantly amplified electrochemical signals with a LOD of 5 aM human immunodeficiency virus (HIV) DNA. In another study, Ochmann et al. developed DNA origami-based optical antennas for fluorescence enhancement in the detection of Zika virus nucleic acids.[634]

Sequence recognition at solid surfaces is essential for DNA sensors,[419,635] but confinement of DNA probes on surface reduces the accessibility of target molecules to probes for DNA hybridization in homogeneous solutions.[636,637] To address this critical challenge, Pei et al. designed tetrahedron-structured probes (TSPs) to achieve improved probe−target recognition properties (Figure 28A).[638] This 3D nanostructure was anchored at Au surfaces via their thiol groups and contained with a single stranded probe at the top that allows both spatial positioning on the electrode surface as well as better accessibility for target binding.[397] They demonstrated that the TSPs with mechanical rigidity and structural stability exhibited good capability for anchoring DNA on surfaces and were able to detect DNA down to 1 pM with excellent sequence specificity. In addition, some groups used DNA origami nanostructures for improving the binding kinetics to the target thus enhancing detection performance of biosensors such as sensitivity and detection time.[639,640]

Apart from desirable speed and sensitivity, the kinetics and thermodynamics of biomolecular recognition on biosensing interfaces should be taken into consideration when designing biosensors.[641,642] To this end, the Fan group proposed a programmable "soft lithography" strategy for engineering the interface of electrochemical DNA sensors (Figure 28B).[643] By mediating the size of TDNs (TDN-7, TDN-13, TDN-17, TDN-26, and TDN-37, with edge length 2.4, 4.4, 5.8, 8.8, and 12.6 nm, respectively) anchored on millimeter-sized gold electrodes, the lateral spacing and interactions of DNA probes on each TDN could be finely tuned, which profoundly affected both the kinetics and thermodynamics of DNA hybridization. They discovered that a more densely packed monolayer without using TDN exhibited a slow reaction rate (0.01 min^{-1}) and TDN-37 presented a 20-fold increase in the reaction rate (0.20 min^{-1}); the hybridization efficiency was low at 15.9% with a distance of 1.8 nm and saturates at 82% with a lateral distance of 6 nm; a slow hybridization process (about 90 min) was observed for a distance of 1.8 nm and improved hybridization kinetics (saturation within 10 min) for TDN-37; the limit of detection was lowered from 10 pM (TDN-7) to 1 fM (TDN-26) with increasing sizes of TDNs. Overall, this novel method effectively improved the performance of DNA biosensors. To tackle slow reaction kinetics and complicated encoding/decoding procedures in current multiplexed analysis methods,[644−646] Zhu and co-workers reported the positional encoding/decoding with self-assembled DNA nanostructures (PED-SADNA) method for multiplexed DNA detection.[647] This PED-SADNA-based system with fast reaction kinetics has been proven to enable routine application in PCR-free settings.

Enzyme cascade amplification is an effective strategy to develop DNA biosensors with high sensitivity,[648,649] in which designing a reliable scaffold to regulate interenzyme distance remains challenging.[650,651] To address these issues, Kou et al. generated a DNA tweezer to dynamically regulate the interenzyme spacing for DNA detection (Figure 28C).[652] The presence of target switched this DNA tweezer from opened state with a relatively high interenzyme distance (19−24 nm) to the closed state with short distance (5−10 nm). Interenzyme distance transformation led to enhanced catalytic efficiency, achieving sensitive detection of target DNA with a low detection limit of 30 fM. Moreover, dynamically controllable enzyme cascade catalysis could be further realized by regulating interenzyme distance in an "open-close-open" way.

The identity and health of a cell are inferred by its RNA repertoire. Despite various methods for RNA detection, for example, the Liedl group developed an RNA nanosensor with a LOD of 100 pM based on switchable plasmonic chirality;[653] the detection of specific cellular nucleic acids yet remains a great challenge.[617] As most mature mRNA or miRNA are located in the cytoplasm, the nanodevices are required to access the cytoplasm. In addition, signal amplification strategies are necessary to achieve sensitive detection of many RNA species due to their low copy number. Moreover, the accessibility of certain sequences is reduced by the secondary structure or RNA-

DOI: 10.1021/acs.chemrev.9b00121
Chem. Rev. XXXX, XXX, XXX−XXX

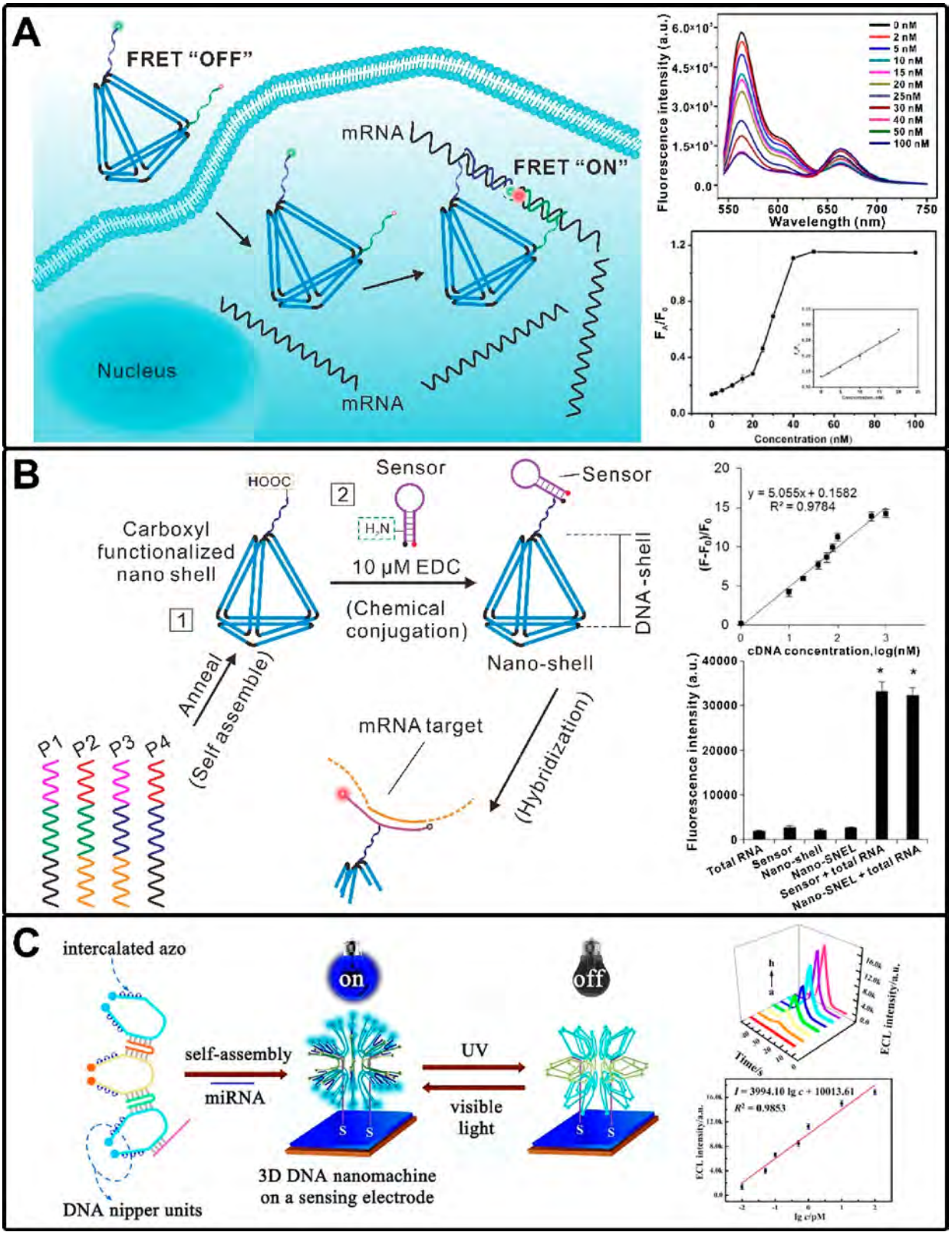

Figure 29. (A) FRET-based DNA tetrahedron nanotweezer for highly reliable detection of mRNA in living cells. Adapted with permission from ref 658. Copyright 2017 American Chemical Society. (B) Nature-inspired DNA nanosensor for real-time *in situ* detection of mRNA in living cells. Adapted with permission from ref 659. Copyright 2015 American Chemical Society. (C) Highly ordered and field-free 3D DNA nanostructure for RNA sensing. Adapted with permission from ref 664. Copyright 2018 American Chemical Society.

binding proteins, making ultrasensitive detection of cellular nucleic acids more important.

As tumor-related mRNA is closely associated with tumor progression,[654] accurate detection of endogenous tumor-related mRNA is vital to early diagnosis of cancer. Using conventional

DOI: 10.1021/acs.chemrev.9b00121
Chem. Rev. XXXX, XXX, XXX−XXX

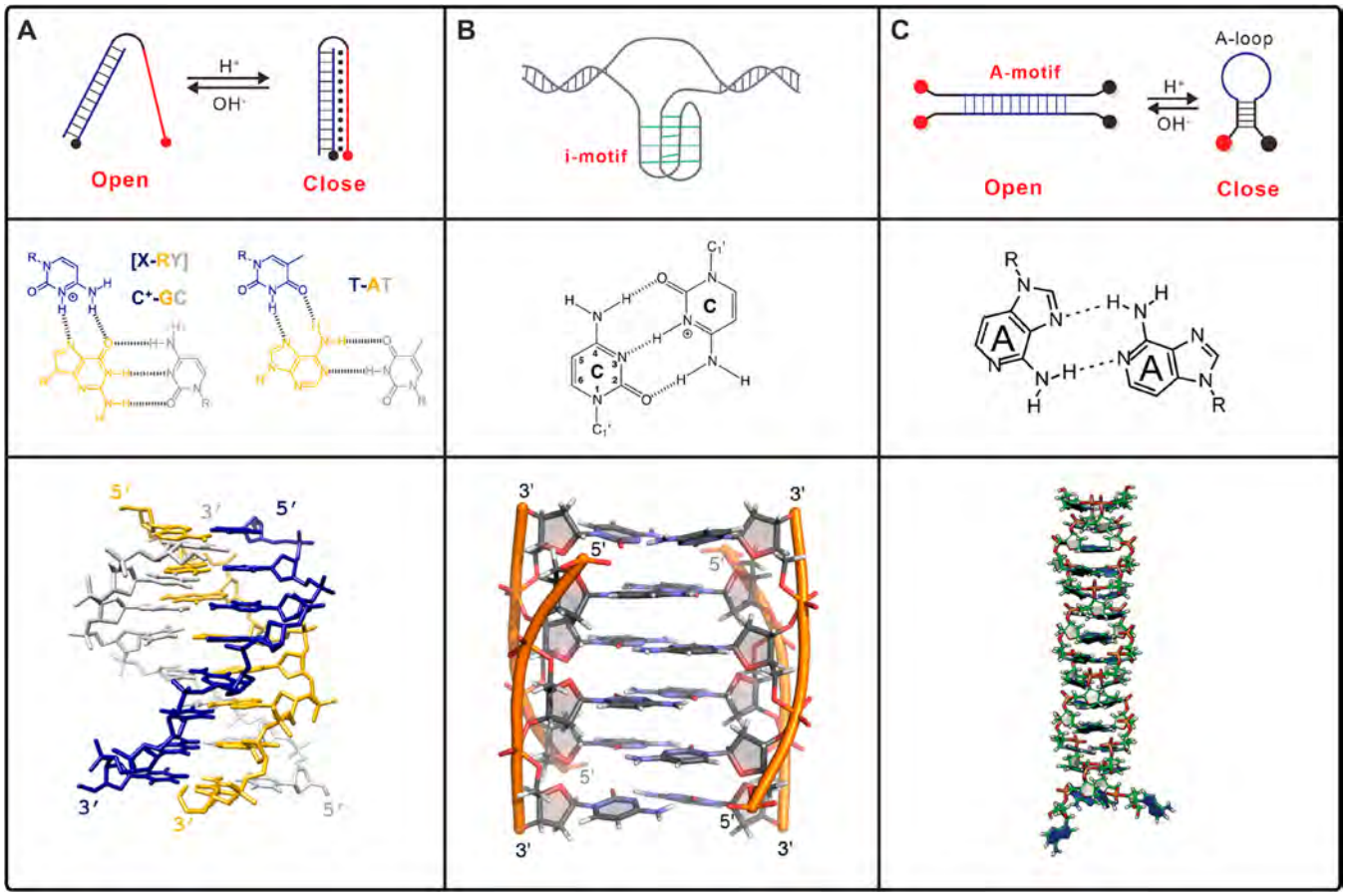

Figure 30. pH-dependent structures encompassing (A) DNA triplexes, (B) i-motif, (C) polyA-motif. Middle row shows chemical structure and bottom row shows crystal structure of DNA triplex,[684] crystal structure of i-motif,[685] and molecular dynamic simulated model of poly-A helix.[121]

methods such as Northern blots,[655] microarray analysis,[656] and reverse transcription polymerase chain reaction (RT-PCR),[657] it is difficult to monitor tumor-related mRNA at the cellular level, not to mention transient spatiotemporal variations of RNA. Most fluorescence probes currently used are compromised by intrinsic interferences (e.g., nuclease digestion, protein binding, thermodynamic fluctuations) in complex biological matrices,[230] thereby leading to false-positive signals. To address these challenges, the Tan group developed a DNA tetrahedron nanotweezer (DTNT) as an intracellular DNA nanoprobe for detecting tumor-related mRNA in living cells (Figure 29A).[658] If target mRNA is not present, this DTNT shows low FRET efficiency (FRET "OFF") due to long distance between labeled donor and acceptor fluorophores. DTNT achieves high FRET efficiency (FRET "ON") once the target mRNA brings the dual fluorophores in close proximity. This prevents false-positive signals and reduces any the signal variations related to system fluctuations.[207] In contrast to other traditional nanomaterials, the DTNT exhibited higher cellular permeability, faster response, and much higher biostability. Moreover, DTNT enables differentiation of transient spatiotemporal variations of mRNA in living cells, showing a good linear correlation from 0 to 20 nM with a LOD of 0.33 nM.

Similarly, Leong and co-workers constructed a nanosnail-inspired nucleic acid locator (nano-SNEL) for detection of mRNA in living cells (Figure 29B).[659] The nano-SNEL consisted of a sensory glyceraldehyde 3-phosphate dehydrogenase-specific molecular beacon that detects target mRNA, while a DNA nanoshell component protects the molecular beacon from degradation. They demonstrated nano-SNEL to be non-cytotoxic with an innate transfection ability and high biostability, thus avoiding false positive signals. As a result, robust *in situ* hybridized MB signals were obtained when target mRNA was present, achieving accurate and sensitive detection of mRNA, with a LOD of 0.94 nM.

MicroRNAs are another kind of clinically important biomarkers for early cancer diagnostics and prognostics.[660,661] The Huang group designed an electrochemical DNA sensor[662] in which controlled density of MB probes was achieved using DNA tetrahedron. Regulating the thermodynamic stability of MB probes improves their reactivity and decreases the background signal as well. Because of the enzyme-mediated signal amplification and recognition capability of MBs, this E-DNA sensor is sensitive to 1 fM and is specific to particular microRNA sequences. Ge et al. reported a 3D tetrahedral DNA nanostructure as an ultrasensitive detection platform for nucleic acid analysis and used HCR-based signal amplification.[663] This strategy was used to detect DNA and microRNA, with detection limits of 100 aM and 10 aM, respectively.

Recently, the Yuan group developed a highly ordered 3D DNA nanomachine assembled from azobenzene-functionalized DNA nippers that reversibly isomerize under irradiation by UV and visible light (Figure 29C).[664] The initial state of the nanomachine is a "closed" configuration in which the electrochemiluminescence (ECL) emitters $Ru(bpy)_2^{2+}$ and the quencher Alexa Fluor (AF) are separated, showing a "signal off" ECL response. Upon miRNA interaction with the nanomachine, the nippers "open" to hybridize with the

DOI: 10.1021/acs.chemrev.9b00121
Chem. Rev. XXXX, XXX, XXX−XXX

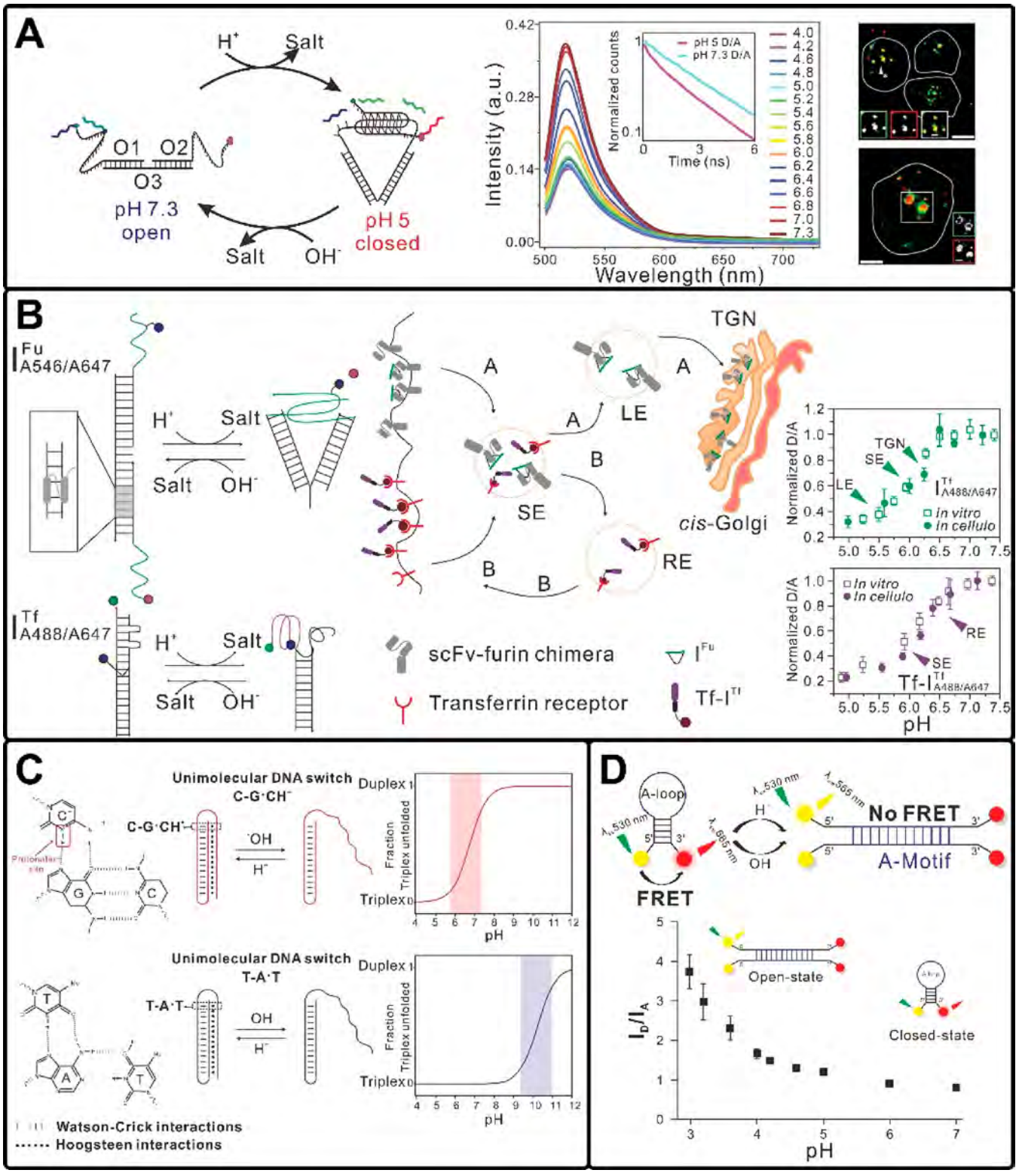

Figure 31. (A) DNA nanomachine mapping spatial and temporal pH changes inside living cells. Adapted with permission from ref 120. Copyright 2009 Springer Nature. (B) Two DNA nanomachines mapping pH changes along intersecting endocytic pathways. Adapted with permission from ref 698. Copyright 2013 Springer Nature. (C) Triplex DNA structure-based pH nanosensors for monitoring pH variations. Reproduced with permission from ref 119. Copyright 2004 American Chemical Society. (D) Molecular beacon-based DNA switch for reversible pH sensing. Adapted with permission from ref 688. Copyright 2016 Royal Society of Chemistry.

miRNA, and the close proximity between $Ru(bpy)_2^{2+}$ and AF results in an enhancement of the ECL signal. Moreover, irradiation-induced trans-to-cis conversion for azobenzene leads to dehybridization/hybridization of the nipper,[665,666] releasing miRNA from the machine. In this way, they achieved reversibility of the DNA nanomachine and generated the miRNA sensing system. In contrast to traditional Au-based 3D nanomachines, this 3D DNA nanomachine with organized and

DOI: 10.1021/acs.chemrev.9b00121
Chem. Rev. XXXX, XXX, XXX−XXX

high local concentration of nippers exhibited an improved efficiency, resulting in sensitive detection of miRNA-21 (LOD: 6.6 fM).

4.2. pH Sensors

Regulation of various biological processes in nature such as enzyme catalysis, membrane function, protein folding, and apoptosis require specific pH levels.[667−670] Synthetic probes and switches that respond to specific pH changes have potential use in *in vivo* imaging, clinical diagnostics, and drug delivery.[671−674] Because of the programmability and biocompatibility of DNA chemistry,[101,675−678] DNA-based probes or nanomachines that can change their state under pH stimuli have been developed,[679−682] and such devices typically take advantage of DNA secondary structures with specific protonation site. With the advent of DNA nanotechnology, these pH-dependent structures encompassing triplex DNA, i-motifs, and A-motifs have been used as building modules for constructing pH sensors (Figure 30).[683−685]

Yurke et al. developed a DNA tweezer assembled from three strands of DNA.[125] The addition of an auxiliary DNA strand controls the opening and closing of this machine. On the basis of this, the Willner group constructed DNA tweezers using C-rich arms and a nucleic acid cross-linker.[686] In low pH (pH = 5.2), the C-rich strand forms a quadruplex structure, thus releasing the cross-linking nucleic acid and opening the tweezer. At neutral conditions (pH = 7.2), the C-quadruplex structure unfolds and captures the cross-linking nucleic acid, thus closing the tweezer. The opening and closing of the tweezer can be monitored by FRET for pH detection.[687,688]

The i-motif is formed from cytosine-rich sequences where the strands fold into two parallel-stranded C−H.C$^+$ base paired duplexes in an antiparallel orientation, and their stabilization requires slightly acidic conditions.[617,689,690] The protonation/deprotonation of cytosine leads to switching of the i-motif between an open and closed state.[691−694] Because of its pH responsiveness, the i-motif structure is used to construct pH sensors for probing changes in pH. On the basis of this i-motif, Nesterova reported a highly responsive pH sensor[695] in which rational design of an i-motif structure and incorporation of allosteric control elements allows for tuning both response sensitivity and transition. Kuzuya et al. introduced short DNA fragments with 12-mer sequences (5′-AACCCCAACCCC-3′) into nanomechanical DNA origami pliers.[696] Once cytosine is protonated to form the i-motif under acidic conditions, the DNA origami pliers are transformed into a closed parallel form from the open cross form. This sophisticated detection platform shows potential application as single-molecular pH sensors.

With regard to research on i-motif structure as a pH indicator, the Krishnan group has conducted a systematic study.[120,697−699] In 2009, they developed a DNA device called the i-switch for imaging spatiotemporal pH changes (Figure 31A).[120] The switch consisted of two duplex domains connected by a hinge. On the outside ends of the helices, each duplex contained a C-rich single stranded extension. At pH 5, the C-rich extensions form an i-motif, "closing" the switch, thus causing a FRET signal. Nanomachine is composed of two double helices connected with a flexible hinge, in which an incorporated i-motif structure serves as a pH-dependent switch to open/close the tweezers. On the basis of FRET, the i-switch as a pH sensor can efficiently report pH from pH 5.5 to 6.8 and also be used to detect spatiotemporal pH changes related to endosomal maturation in living cells. Additionally, this work mapped the pH of a specific receptor-mediated endocytic pathway by coupling the pH sensor to the protein transferrin. The same group also used a DNA nanodevice *in vivo* to detect pH changes in the nematode *Caenorhabditis elegans*.[697]

It remains challenging to achieve simultaneous functionality of multiple DNA nanomachines within the same cell though previous work demonstrated that DNA nanodevices can map spatiotemporal pH inside endosomes *in cellulo* as well as *in vivo*. To address this challenge, Krishnan and co-workers deployed two differently programmed DNA nanomachines along different cellular endocytic pathways and mapped pH changes along both pathways simultaneously (Figure 31B).[698] This work confirmed that DNA-based nanostructures can be used to monitor different pathways in the same cell, providing possibilities of multiplexing DNA nanodevices in living systems.

Another type of pH-sensitive switches can be created using triplex DNA structures formed by parallel Hoogsteen interactions.[700,701] Therefore, such DNA nanoswitches based on the DNA duplex−triplex transition show great promise for developing pH sensors.[702] Moreover, DNA triplex nanodevices, compared to i-motif-based nanomachines, display faster response speed, which is beneficial for detecting pH changes related to instantaneous biological processes on shorter time scales.[703] The Tan group developed a novel DNA nanomachine on the basis of the DNA triplex structure containing C$^+$.GC triplets and pH-dependent FRET.[703] Because of its pH-dependent duplex−triplex transition, this DNA nanomachine is demonstrated to be an efficient reporter of pH from 5.3 to 6.0 with a fast response of a few seconds. By complexing with PEI to facilitate the endocytosis process and avoid enzymatic degradation,[704,705] the dynamic responding range of the nanoswitch can be extended to 4.6−7.8. More importantly, this pH-dependent DNA nanomachine allowed monitoring of spatiotemporal pH changes associated with endocytosis, providing the possibility of using self-assembled DNA nanomachines for imaging, targeted therapies, and controllable drug delivery. Our group also designed a triplex DNA device that can respond to changes in pH.[706] By incorporating pH independent dyes on the device, we coupled it with MoS_2 nanosheets so that the signal comes from the interaction of the device with the nanosheets. In the duplex state (pH = 8), the triplex-forming oligonucleotide can interact with the MoS_2 (by adsorption) and thus has reduced fluorescence. At pH 5, the third strand forms a triple with the duplex region and thus moves away from the nanosheet and restores fluorescence. This change in fluorescence acts as an indicator of pH change.

By exploiting pH-sensitive parallel Hoogsteen interactions in triplex DNA, Idili et al. designed and programed a pH-triggered DNA-based nanoswitch (Figure 31C).[119] The switch consisted of an intramolecular hairpin where the stem was held by Watson−Crick base pairing, and the hairpin strand binds to the stem via parallel Hoogsteen interactions. The C$^+$.GC triplets require the protonation of the N3 of cytosine at slightly acidic condition ($pK_a \approx 6.5$),[707] while TAT triplets are destabilized at alkaline environment ($pK_a \approx 10$).[708] Using this idea, they finely tuned the pH dependence of this DNA triplex nanoswitch over more than 5 pH units by regulating the relative content of T.AT/C$^+$.GC triplets.

Adenine (A)-rich polydeoxyadenylic acid (poly-$(dA)_n$) and polyadenylic acid (poly-$(rA)_n$) with a single helical structure are found to form a parallel-stranded double helix (termed A-motif) at acidic pH.[121,709] Adenine nucleobases undergoing protonation at the N^1 (AH^+) position lead to the formation of A-motif

DOI: 10.1021/acs.chemrev.9b00121
Chem. Rev. XXXX, XXX, XXX−XXX

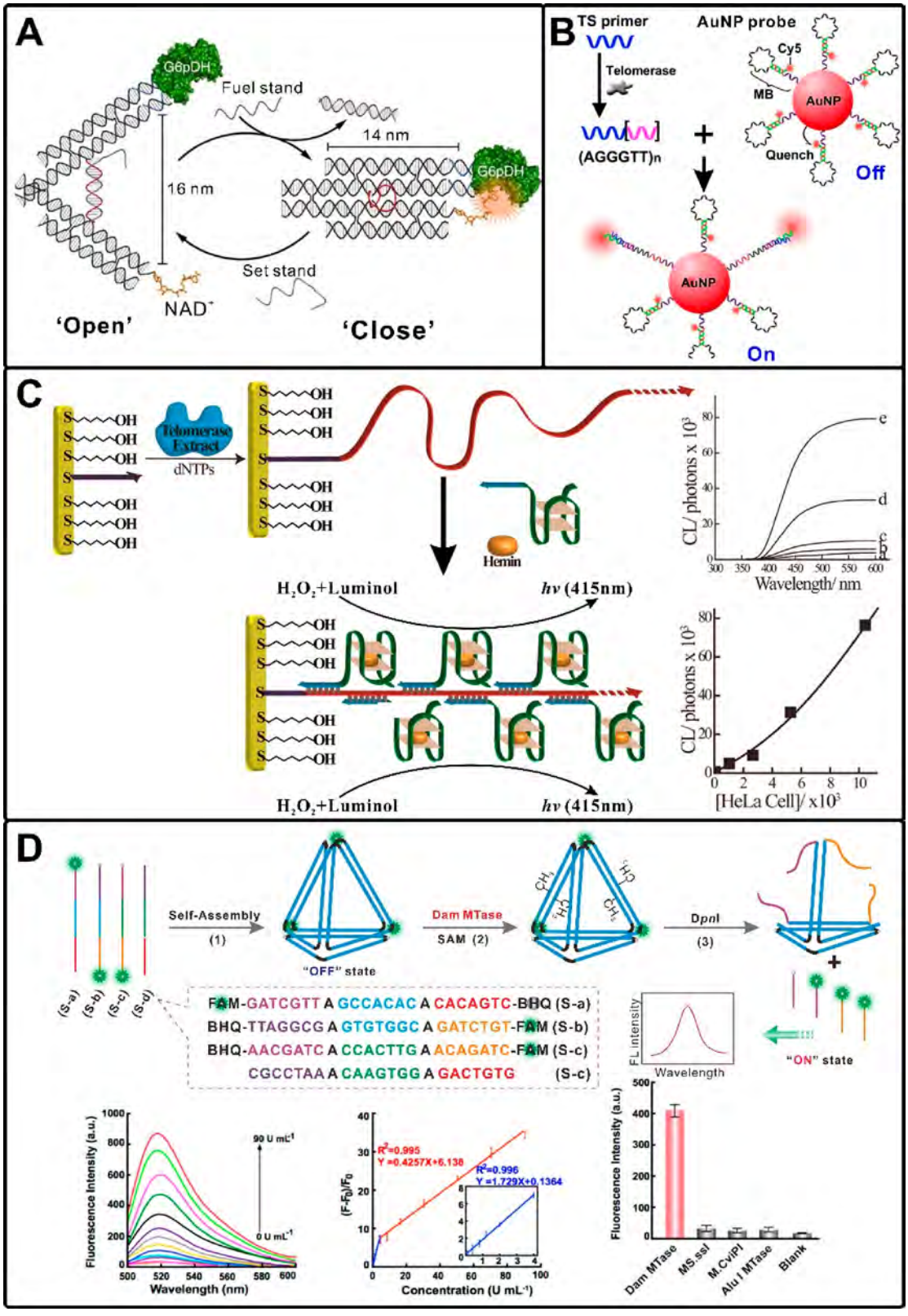

Figure 32. (A) DNA tweezer-regulated enzyme nanoreactor. Reproduced with permission from ref 738. Copyright 2013 Springer Nature. (B) Telomerase-responsive probe for *in situ* monitoring of intracellular telomerase activity. Adapted with permission from ref 752. Copyright 2014 American Chemical Society. (C) Amplified chemiluminescence surface detection of telomerase activity using catalytic nucleic acid labels. Adapted with permission from ref 755. Copyright 2004 American Chemical Society. (D) Collapse of DNA tetrahedron nanostructure for "off−on" fluorescence detection of DNA methyltransferase activity. Adapted with permission from ref 769. Copyright 2017 American Chemical Society.

via reverse Hoogsteen [AH^+−H^+A] hydrogen bonding interactions, further stabilized by electrostatic interactions between the AH^+ and the phosphate backbone. Chakraborty et al. demonstrated that changes in the pH can trigger reconfiguration

DOI: 10.1021/acs.chemrev.9b00121
Chem. Rev. XXXX, XXX, XXX−XXX

between two different helical forms of dA_{15}.[121] This pH-trigger transition is in the construction molecular pH sensors.[710−712]

Given that the most existing DNA-based colorimetric sensors are applied in sensing at high pH 5.5−7.6, Saha et al. developed a colorimetric pH sensor for high solution acidity based on A-motifs.[713] They tuned the pH response range of the sensor (pH 2−5.5) by mediating the length and the sequence of the poly dA tracts. In contrast with other DNA-based pH sensors that require a critical amount of salts for their functionality,[687,714] this pH sensor is capable of functioning in salt-free or extremely low salt conditions. Therefore, this A-motif-based pH sensor is particularly suitable for pH sensing at lower ranges such as environmental pollution, and industrial toxification. Narayanaswamy et al. designed an exquisite DNA device composed of an A-rich molecular beacon (MB) that reversibly switches between MB and A-motif efficiently in the pH range of 5 to 3 (Figure 31D).[688] After encapsulation in synthetic vesicles, this DNA switch allows for monitoring intracellular pH in live cells. On the basis of the MB to A-motif transition, this pH-dependent DNA switch inspires the development of DNA nanodevices for drug delivery applications as well. Besides, the Bald group developed DNA origami-based FRET nanoarrays as ratiometric pH sensors in which coumarin 343 served as a pH-inert FRET donor and FAM as a pH-responsive acceptor.[715] This sensor has been proven to show sensitive response for the pH range of 5−8.

4.3. Enzyme Activity Measurements

Many important reactions related to biological processes and diseases are catalyzed by enzymes.[716] Control over these enzyme activities using molecular cues or stimuli has a crucial impact on many metabolic functions.[717,718] Indeed, tremendous work has showed that the activity of certain enzymes can serve as an indicator of disease states such as cancer, stroke, and neurodegeneracy.[719−722] There is therefore a need for rapid assays for characterizing enzyme activities.[723−725] Emerging synthetic mimics of enzyme regulation circuitry outside of the cell facilitate our understanding of cellular metabolism.[726−728]

DNA nanostructures can be utilized as powerful tools to organize molecules on the nanoscale as a result of their site-specific functionalization and nanomechanical control capabilities.[607,676,729,730] Structures such as autonomous walkers,[731,732] nanotweezers[733,734] and nanorobots[735,736] enable controlled encapsulation and release of payloads. Moreover, protein−DNA conjugation chemistry can precisely position proteins on DNA scaffolds,[737] providing an effective approach for enzyme activity sensing. For example, the Yan group reported a DNA tweezer nanostructure, which can actuate the activity of a glucose-6-phosphate dehydrogenase (G6pDH)/NAD^+ enzyme/cofactor pair (Figure 32A).[738] Initially, the spatially separated G6pDH/cofactor pair positioned on different arms of the DNA tweezers presented inhibited enzyme activity. Specific oligonucleotides can be used as triggers to change the conformation of the DNA tweezer from its open to the closed state, thereby activating enzymatic function due to close proximity of the enzyme/cofactor pair. In another study, the Andersen group developed a reconfigurable DNA nanovault for precisely regulating enzyme activity by rational design of nanovaults in response to specific DNA signals.[739] As such, exploitation of DNA nanostructures for controlling the enzyme activity holds great potential in diagnostic applications.[740]

Telomeres are special functional complexes consisting of short tandem repeated DNA sequences (TTAGGG) at the ends of the chromosomes, protecting them against degradation or fusion.[741,742] In healthy cells, telomeres undergo progressive shortening during cell proliferation, which results in cell senescence and finally induces cell apoptosis.[743,744] Nevertheless, telomerases maintain the length of telomeres in cancer cells.[745] Telomerase is a ribonucleoprotein complex capable of adding TTAGGG hexamer repeats to the end of telomers, thereby causing immortal or malignant cells.[746−748] Extensive studies have demonstrated that over 85% of different cancer cells are associated with elevated amounts of telomerase, making them useful biomarkers in cancer diagnosis.[749,590,750,751] The Ju group used a smart vesicle kit for *in situ* quantification and dynamic monitoring of intracellular telomerase activity (Figure 32B).[752] The vesicle kit consisted of a telomerase primer and a Cy5-tagged MB-functionalized AuNP probe. Because of surface energy transfer, the Cy5 fluorophore tagged on MB is quenched by AuNPs.[753] By coencapsulating the probe and telomerase primer in liposome, the vesicle kit can be transfected into cytoplasm. Subsequently, the 3′ end of telomerase primer is extended by telomerase to produce telomere repeat sequences, which is complementary to the loop of the MB. As a result, the hairpin changes to the "on" state, increasing the fluorescence, allowing *in situ* imaging and quantitative detection of cytoplasmic telomerase activity. Using this method, the cytoplasmic telomerase activity was estimated to be 3.2×10^{-11}, 2.4×10^{-11}, and 8.6×10^{-13} IU in HeLa, BEL tumor, and QSG normal cell, respectively. This strategy accelerates the understanding of telomerase-involved biological processes and provides a favorable analytical tool for cancer diagnosis, therapy, and telomerase-related drug screening.

Another strategy to detect telomerase is by coupling them to DNAzymes.[475,754] The Willner group exploited the hemin/G-quadruplex HRP-mimicking DNAzyme as a catalytic reporting unit for chemiluminescent detection of telomerase (Figure 32C).[755] The primer DNA strand (purple) is attached to Au surfaces via Au-S chemistry. After recognition by telomerase, the primer DNA units are elongated with the tandem telomer repeat units, which are complementary to a functional nucleic acid stand (blue) containing a G-quadruplex sequence. Their hybridization leads to the formation of a hybrid DNA nanostructure with the repeated telomer/G-quadruplex HRP-mimicking DNAzyme. The G-quadruplex/hemin DNAzyme structure in combination with hemin catalyzes the oxidation of luminol by H_2O_2 thus generating chemiluminescence. This chemiluminescence intensity depends on the content of telomerase. This method was used to detect telomerase extracted from 1000 HeLa cells.

DNA methylation plays a pivotal role in various biological processes such as cell growth and proliferation, gene expression, and chromatin organization.[756−758] The DNA methylation process has been proven to be catalyzed by DNA methyltransferases (MTases). During this process, a methyl group from S-adenosyl methionine is transferred to target adenine or cytosine residues in the recognition sequences (5′-GATC-3′).[759] Recent studies revealed that aberrant DNA methylation is a hallmark of many diseases.[760−762] DNA MTases are essential for bacterial virulence and viability because it can protect bacterial DN against cleavage via modification of cytosine at C5 or N4 and adenine at N6.[763] Moreover, DNA MTase is also a potential drug target for certain types of cancer.[764] Therefore, highly precise and sensitive methods are required for detecting MTase activity and screening of its inhibitors in both clinical diagnostics and therapeutics.[765,766] For example, using DNA-modified AuNPs coupled with enzyme linkage reactions, Liu et

DOI: 10.1021/acs.chemrev.9b00121
Chem. Rev. XXXX, XXX, XXX−XXX

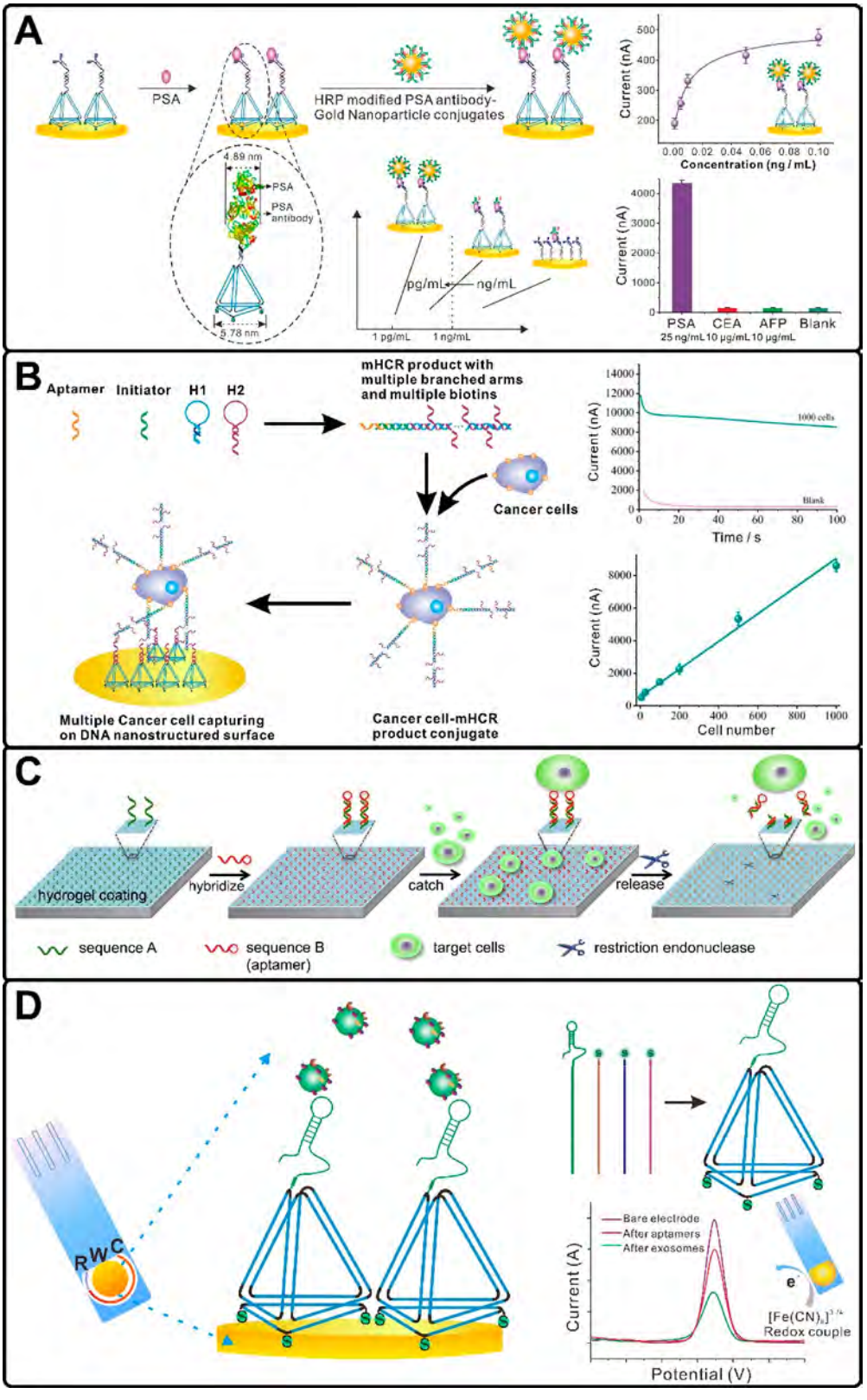

Figure 33. (A) Electrochemical detection of PSA with antibodies anchored on a DNA nanostructural scaffold. Adapted with permission from ref 792. Copyright 2014 American Chemical Society. (B) DNA nanostructured biosensors for multivalent capture and detection of cancer cells based on multibranched HCR amplification. Adapted with permission from ref 796. Copyright 2014 American Chemical Society. (C) Endonuclease-responsive aptamer-functionalized hydrogel coating for sequential catch and release of cancer cells. Reproduced with permission from ref 797. Copyright 2013 Elsevier. (D) Aptasensor with expanded nucleotide based on DNA NTH for electrochemical detection of cancerous exosomes. Adapted with permission from ref 803. Copyright 2017 American Chemical Society.

DOI: 10.1021/acs.chemrev.9b00121
Chem. Rev. XXXX, XXX, XXX−XXX

al. combined DNA-modified AuNPs and enzyme linkage reactions to create a colorimetric assay for MTase activity, showing linearity between 1.0 to 10 U/mL (LOD of 0.3 U/mL).[767] Yuan and colleagues proposed an exonuclease III-mediated target recycling strategy for sensitive detection of DNA MTase activity, with a LOD of 0.01 U/mL.[768]

In view of its highly rigid and versatile functionality, Ju and colleagues developed a DNA tetrahedron nanostructure as an "off−on" fluorescent probe for detecting MTase (Figure 32D).[769] The DNA tetrahedron was assembled with three rationally designed strands dual-labeled with fluorophores and quenchers and starts in the "off" state. Two edges of the DNA tetrahedron contain recognition sites that can be methylated by MTase, and these methylated sites are further cleaved upon addition of the restriction endonuclease DpnI. This reaction disassembles the DNA tetrahedron, moving the fluororphores away from the quenchers, and turning it to the "on" state. The sensitivity of this strategy can be improved using nicking enzyme-assisted signal amplification, enabling detection of MTase with a LOD of 0.045 U mL^{-1}. As a result, this strategy based on DNA nanostructures is anticipated to be applied in clinical diagnostics.

4.4. Biomarker Detection

One of the main diseases affecting worldwide population is cancer.[770] To treat cancer, early diagnosis methods and a strategy to monitor biomarker levels after treatment are of prime importance.[771,772] Cancer-associated biomarkers are quantifiable indicators of specific cancer states, and their detection plays a critical role in identifying patients with different clinical stages and in developing adaptive therapeutic strategies.[773,774] Sensitive and specific detection of cancer biomarkers is challenging because of the structural characteristics of nucleic acids, tumor heterogeneity-induced specific protein signatures, and difficulty to achieve sample concentration.[775,776] Although various technologies have been developed for detecting cancer biomarkers, most existing methods involve complex steps, are expensive, and are not easily adaptable for use in point-of-care settings. In the last three decades, DNA nanomaterials have attracted attention for cancer detection because of their unique features: (1) the Watson−Crick base pairing rules bestows the DNA with precise predictability and reproducibility; (2) DNA nanostructures presents stronger nuclease resistance over ssDNA and dsDNA;[777] (3) DNA nanostructures are natural biopolymers and show prominent biocompatibility and biodegradability making them suitable for *in vivo* application;[778−781] and (4) DNA nanostructures are facile to be functionalized with fluorescent dyes,[593] quantum dots,[782,783] antibodies,[736] and cancer-targeting organic compounds.[784,785] These advantages make DNA nanostructures useful tools in constructing biosensors for the detection of tumor biomarkers.[615] In one such example, Zhao et al. created a multivalent DNA network from repeating aptamer domains. They used this structure to capture and isolate specific types of cancer cells.[786]

Proteins control the live of biological cells in metabolic and signaling pathways and in complexes, for example, the molecular machines that synthesize and use ATP, replicate and translate genes, or build up the cytoskeletal infrastructure.[787] Therefore, their abnormal expression is often related to certain diseases.[788] Disease-related protein biomarkers are also useful to monitor treatment response or identify recurrence or progression after treatment.[789−791] Currently, analysis of protein biomarkers with low abundance is compromised by several challenges (difficulty to amplify signal, sensitivity to ambient environment, high background of other proteins).[771] As a result, sensitivity, specificity, and accuracy are basic requirements to consider when biosensors are constructed. As the nanoscale-spacing of immobilized antibodies has a critical effect on the detection sensitivity, Zuo et al. developed a DNA tetrahedron structure to assemble antibody monolayers (Figure 33A).[792] By exploiting the enzyme-modified AuNPs as signal amplifier, they obtained a low detection limit of 1 pg/mL PSA, which is sensitive enough to monitor the prognosis of prostate cancer. The Yan group assembled signaling aptamers periodically on 2D DNA nanoarrays.[793] By incorporating a thrombin binding-aptamer sequence into DNA tiles, thrombin can be organized into periodical DNA nanoarrays because of its molecular recognition capability. Using fluorescence increase due to binding of thrombin to its aptamer, this system can be used to detect thrombin at subnanomolar concentrations. The Lammertyn group designed two distinct DNA origami structures to position thrombin-specific aptamers with different densities and distances from the fiber optic surface plasmon resonance surface, allowing for detection of thrombin with a wide linear range (1−248 nM).[794]

Direct detection of cancer cells is another route to diagnosing cancer and cancer metastasis early but is hindered by the low abundance of circulating tumor cells (CTCs) in peripheral blood.[773,775,776,795] Zuo et al. used multibranched HCR (mHCR) for cancer cell detection (Figure 33B).[796] Branched arms of the structure allow attachment to the gold electrode surface, while multiple avidin-HRP molecules provide signal amplification. This strategy enables detection of as few as four MCF-7 cells. Nanostructures decorated with aptamers also serve in catch and release of specific cell types. Wang et al. used aptamer-functionalized hydrogels with restriction endonucleases to catch and release the target cancer cell (Figure 33C).[797] This hydrogel "caught" target cancer cells with a densities of ∼1000 cells per mm^2 but nonspecific cells with densities of ∼5−15 cells/mm^2. The endonucleases used in this method specifically cleave the aptamer sequences, releasing 99% of the bound cells and 98% of the released cells maintaining viability.

Exosomes are nanoscale extracellular membrane-bound phospholipid vesicles (50−100 nm in diameter) actively secreted by mammalian cells.[798,799] Exosomes are considered as biomarkers in various diseases including cancer because they carry abundant macromolecules from parental cells such as transmembrane and cytosolic proteins, mRNA, DNA, and miRNA.[800,801] The evaluation of cell-secreted exosomes and collection of clinical information without biopsy could be useful clinical and research tools.[802] The Tan group developed a portable electrochemical aptasensor for rapid and direct detection of hepatocellular exosomes (Figure 33D).[803] The aptasensor consists of a DNA nanotetrahedron (NTH) with an expanded nucleotide-containing aptamer. The individual aptamer distributed at defined nanoscale distances decreases the hindrance effect and maintains spatial orientation, thereby improving biomolecular recognition. The improved accessibility results in this NTH-assisted aptasensor shows 100-fold improved sensitivity in detecting exosomes (2.09×10^4/mL) when compared to single-stranded aptamer-functionalized aptasensor (3.96×10^5/mL).

DOI: 10.1021/acs.chemrev.9b00121
Chem. Rev. XXXX, XXX, XXX−XXX

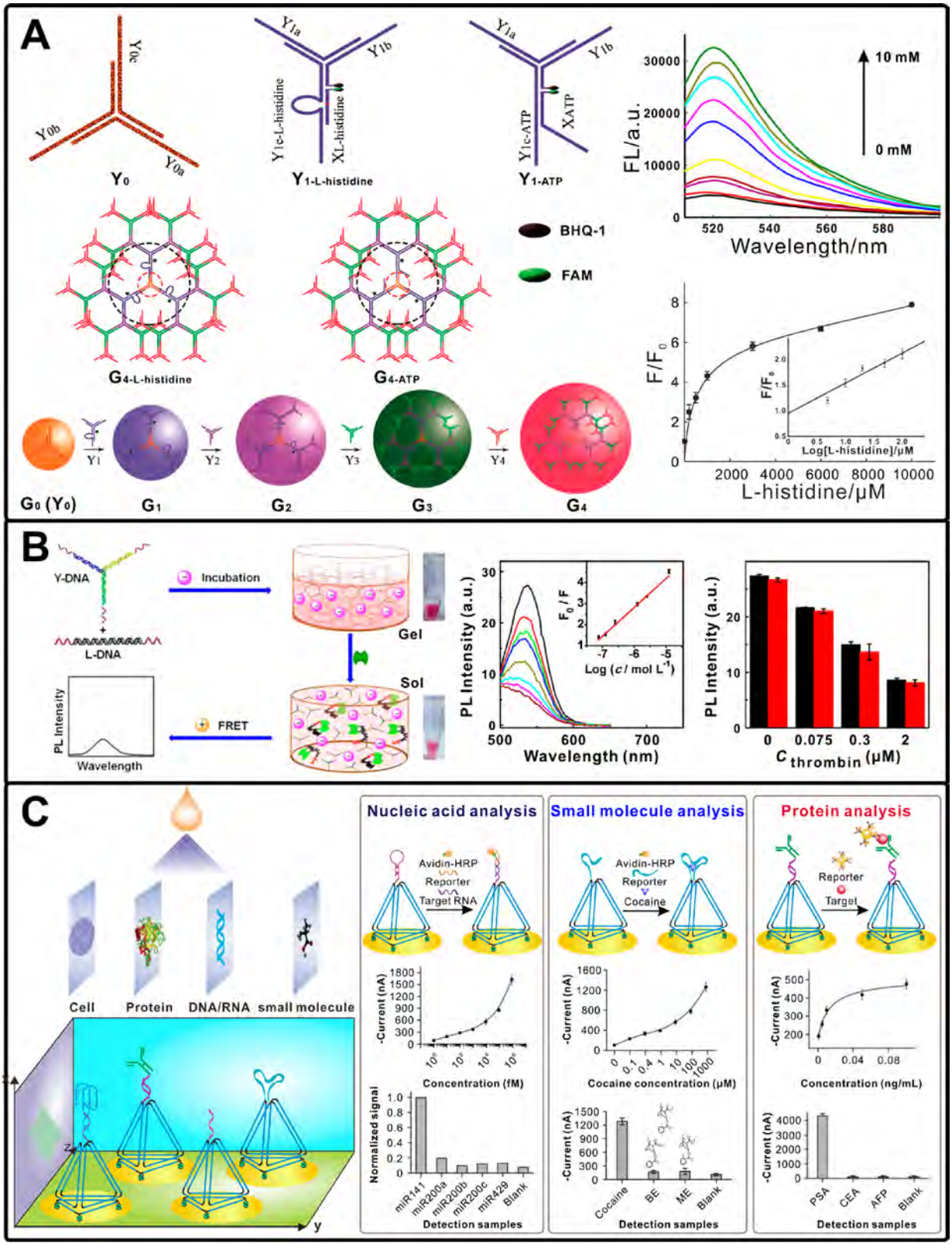

Figure 34. (A) Efficient nanocarrier of functional nucleic acids for intracellular molecular sensing. Adapted with permission from ref 825. Copyright 2014 American Chemical Society. (B) Self-assembled DNA hydrogel as switchable material for aptamer-based fluorescent detection of thrombin. Adapted with permission from ref 826. Copyright 2013 American Chemical Society. (C) DNA-nanostructure-based universal biosensing platform for electrochemical detection of nucleic acids, proteins, small molecules, and cells. Adapted with permission from ref 625. Copyright 2016 Springer Nature.

DOI: 10.1021/acs.chemrev.9b00121
Chem. Rev. XXXX, XXX, XXX−XXX

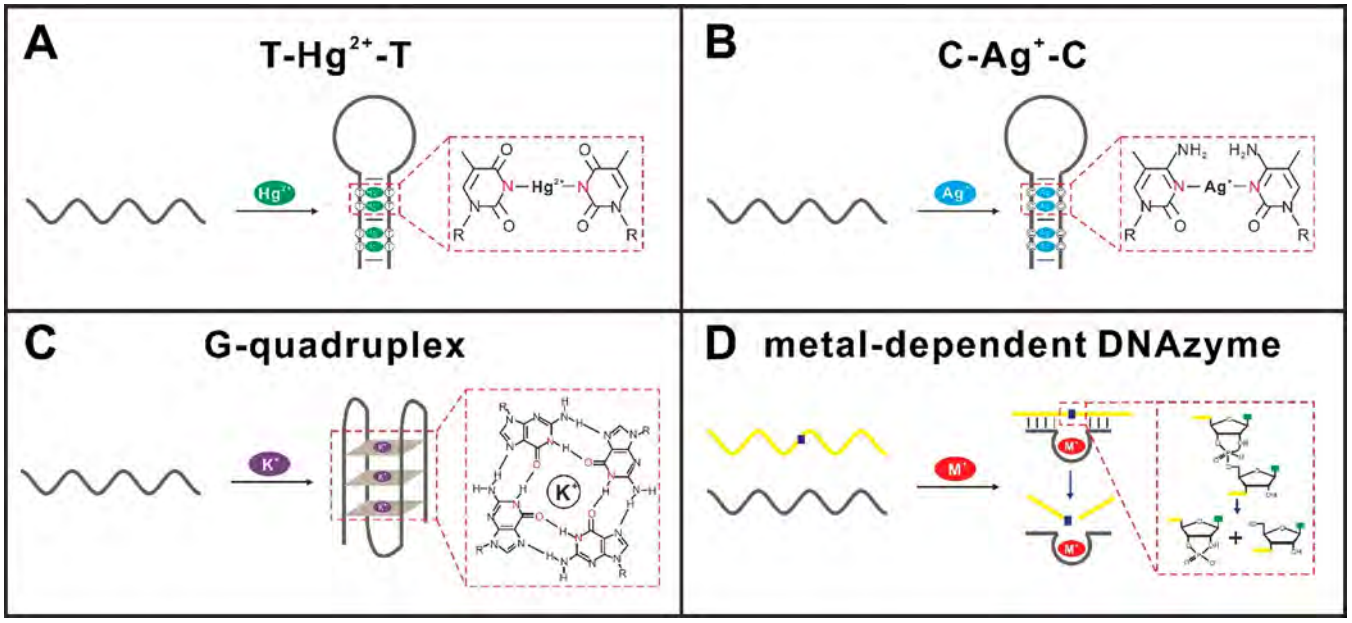

Figure 35. DNA structures used for ion sensing including (A) T-Hg^{2+}-T, (B) C-Ag^{+}-C, (C) G-quadruplex, and (D) metal-dependent DNAzymes.

4.5. Biomolecules and Metal Ion Detection

Nucleic acid components such as aptamers and DNAzymes[615,811] are used in creating biosensors for metal ions, proteins, small molecules, cells, viruses, and bacteria.[616,804−810] In addition to diagnostic applications, sensing of biomolecules also allows the study of their functions in biological processes.[812,813] Although numerous functional nucleic acid-based biosensors are used to detect different biomolecules,[814−817] their applications in complex biological samples are restricted by the fact that functional nucleic acids have difficulty in penetrating the cell membrane,[331] are susceptible to nuclease digestion,[818,819] and nonspecifically bind to nontarget protein.[820] Functional DNA nanostructures such as aptamers or DNAzyme-integrated DNA nanostructures provide a promising solution to address these issues. For example, the Tan group developed target-responsive DNA hydrogels for adenosine detection.[821,822] The same group developed DNA dendrimers assembled from Y-shaped DNA structures for drug delivery and biosensing purposes.[823,824] The DNA dendrimeric scaffold contained histidine-dependent DNAzyme or anti-ATP aptamer and retained the activity of both these cargos in the cellular milieu (Figure 34A).[825] Moreover, these dendritic nanocarriers display excellent biocompatibility, cell membrane permeability, and enhanced intracellular stability. These features make these functional nucleic acid-embedded DNA dendrimers useful in monitoring levels of histidine *in situ* and ATP levels in living cells. In another example, Zhang et al. used an aptamer-functionalized DNA hydrogel to detect thrombin detection with a LODof 67 nM (Figure 34B).[826] In this strategy, polyethyleneimine (PEI)-functionalized QDs and AuNPs served as signal indicators.

As mentioned earlier in this review, accessibility to target molecules is one of the main challenges in surface-based assays.[827,828] To enhance the recognition abilities of such heterogeneous surface probes, the Fan group constructed a series of tetrahedral DDNA nanostructures (TDN) probes for detecting biomolecules.[625,829,830] The tetrahedra are attached to the gold electrode surface via thiol groups on three of the vertices. The fourth vertex contains a probe for the detection of different biomarkers. Using this structure, they designed a sensitive cocaine sensor by introducing an anticocaine aptamer into TDN architectures, achieving a low detection limit of 33 nM.[829] In follow-up studies, they also used this strategy to detect miRNA (1 fM) and prostate specific antigen (PSA) (1 pM) (Figure 34C).[625] Moreover, Heck et al. utilized DNA origami scaffolds for assembly of silver nanolenses.[831] By selectively placing single molecules of the protein streptavidin in the gaps, they can detect SERS signals of the alkyne labels of a single streptavidin molecule.

Metal ions are known to have roles in biological processes such as cell signaling and enzyme catalysis.[832,833] Thus, detection of metal ions is an important research area in biosensing.[476] With the advent of DNA nanotechnology, several DNA structures including T-Hg^{2+}-T (Figure 35A), C-Ag^{+}-C (Figure 35B), G-quadruplex (Figure 35C), and metal-dependent DNAzymes (Figure 35D) have been used for ion sensing. Among them, DNAzyme-based sensors are the most studied because of the metal binding sites, metal-dependent activity, and catalytic mechanisms for these DNAzymes.[476,834−837] For example, a DNAzyme used for Pb^{2+} detection is about 400 000-fold more selective to Pb^{2+} compared to other competing metal ions,[838] and the DNAzyme for UO_2^{2+} is over 1 000 000-fold more selective.[839] Moreover, DNA structures containing T−T or C−C mismatches and G-quadruplex structures have been shown to selectively bind metal ions (e.g., Hg^{2+}, Ag^{+}, K^{+}) to form stable metal-mediated DNA structures.[840−842] By combining the specific properties of DNAzyme/DNA molecules and the strong signal transduction capacity of the nanostructures, novel sensing systems provide improved sensitivity, selectivity, multiplexed detection capability, and portability.[835]

Several DNAzymes have been reported to possess catalytic activities toward specific substrates since the early 1990s.[843] These DNA molecules join protein enzymes and ribozymes as catalytic biomolecules.[844] Similar to protein enzymes, most DNAzymes also require certain metal ion cofactors, but DNAzymes are more convenient due to their cost-effective properties and resistance to hydrolysis. Moreover, most

DOI: 10.1021/acs.chemrev.9b00121
Chem. Rev. XXXX, XXX, XXX−XXX

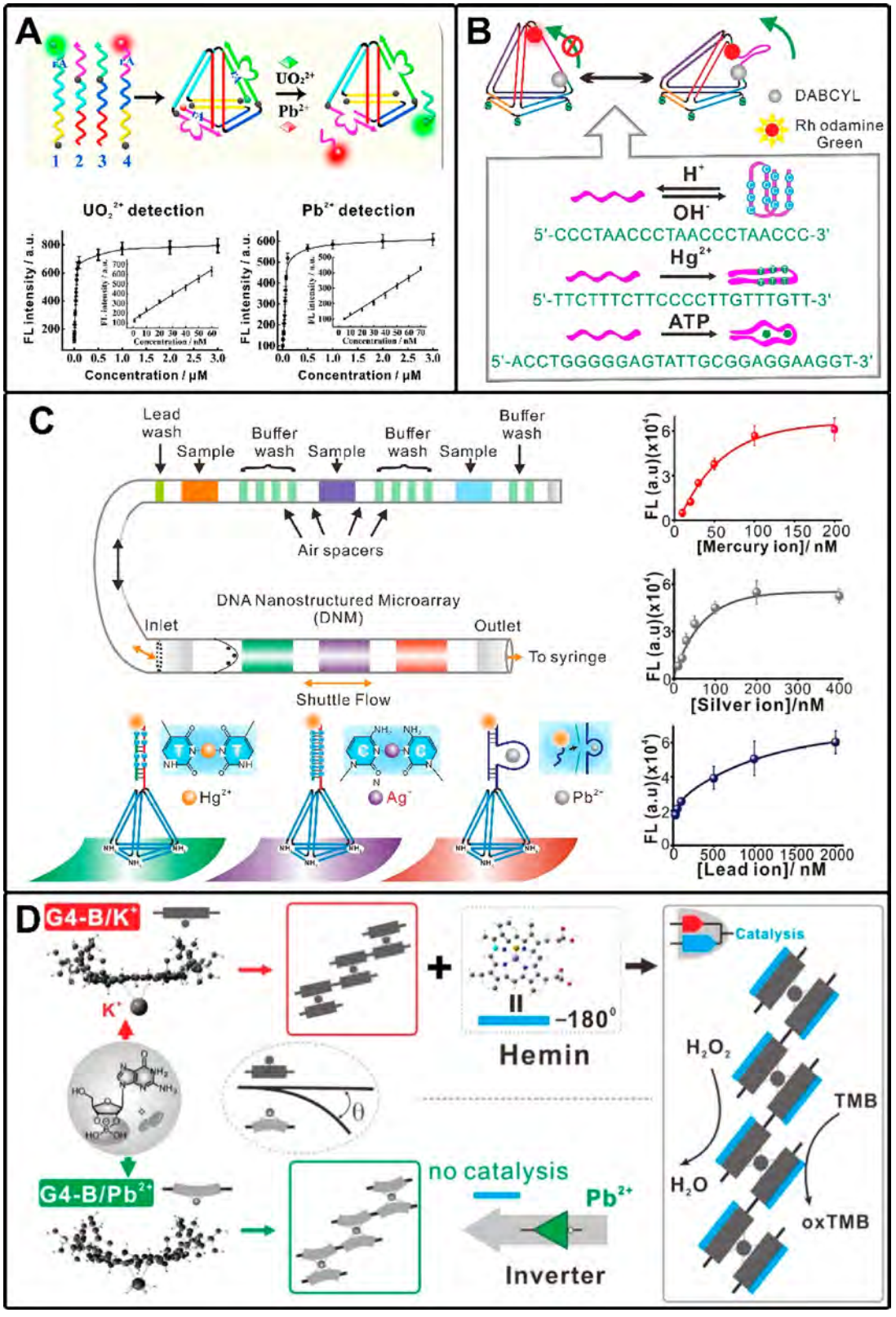

Figure 36. (A) Dual-color encoded DNAzyme nanostructures for multiplexed detection of intracellular UO_2^{2+} and Pb^{2+}. Adapted with permission from ref 856. Copyright 2016 Elsevier. (B) Reconfigurable 3D DNA nanostructures as intracellular logic sensors for pH, Hg^{2+}, and ATP. Adapted with permission from ref 859. Copyright 2012 Wiley-VCH. (C) DNA-nanostructured microarray for detection of multiple heavy-metal ions (i.e., Hg^{2+}, Ag^{+}, and Pb^{2+}). Adapted with permission from ref 855. Copyright 2017 American Chemical Society. (D) Logic catalytic interconversion of G-molecular hydrogel for Pb^{2+} detection. Reproduced with permission from ref 877. Copyright 2018 American Chemical Society.

DNAzymes still maintain their binding ability or activity toward substrates even after repeated denaturation and renaturation. Accordingly, all these features make DNAzymes ideal for constructing metal ion biosensors, and the sensing signal can be

DOI: 10.1021/acs.chemrev.9b00121
Chem. Rev. XXXX, XXX, XXX−XXX

read out using fluorescence, colorimetry, or electrochemistry. DNAzyme-based metal ion biosensors have so far been used to detect a wide range of metal ions such as Pb^{2+},[838,845] Cu^{2+},[810,846,847] Mg^{2+},[848] Ca^{2+},[849] Zn^{2+},[850,851] Co^{2+},[852] UO_2^{2+},[839,853] and Hg^{2+}.[854]

To improve the microconfined molecular recognition, Qu et al. appended Pb^{2+}-specific DNAzyme and its substrate stand on DNA TSPs .[855] In the presence of Pb^{2+}, the DNAzyme is activated to cleave the substrate strands, and the cleaved strands are subsequently substituted by the Cy3-labled reporter, generating a fluorescence signal. As such, this sensor based on DNAzyme and DNA nanostructure enables Pb^{2+} detection down to 20 nM. By self-assembling four single stranded sequences with a simple thermal annealing step, the Xiang group constructed a dual-color encoded DNAzyme tetrahedron nanoprobe (Figure 36A).[856] Target metal ions digest the substrate sequence in the nanostructures, providing a fluorescent signal for *in vitro* detection of UO_2^{2+} and Pb^{2+} at the same time with LODs of 0.6 nM and 3.9 nM, respectively. These nanoprobes can also be transfected into cells for intracellular detection of UO_2^{2+} and Pb^{2+}. Moreover, this nanoprobe also shows excellent biocompatibility and non-cytotoxicity. Given its capability of simultaneous imaging of UO_2^{2+} and Pb^{2+} in one cell, this dual-color encoded DNAzyme nanostructure provides a novel approach to indicate the distributions and concentrations of the target metal ions, revealing insights into physiological and pathological functions of the toxic metal ions.

Ono and Togashi first discovered that Hg^{2+} specifically binds to two DNA thymine (T) bases to form strong T-Hg^{2+}-T pairs in a DNA duplex.[841] In turn, such formed complexes can thermally stabilize the DNA duplex. On the basis of this phenomenon, T-Hg^{2+}-T coordination chemistry has been adopted to develop biosensors for Hg^{2+}. Liu et al. developed a DNA-functionalized hydrogel for the visual detection of Hg^{2+} based on this concept,[857,858] with a naked eye LOD of 10 nM Hg^{2+}. In addition to ease of handling, this aptamer-functionalized hydrogel, in contrast to monolithic gels, possesses much faster kinetics of signal generation. By adapting a series of DNA structures (i-motif, anti-ATP aptamer, T-rich mercury specific oligonucleotide, and hairpin structures) to one or two edges, Pei et al. built reconfigurable TDNs that can detect targets such as protons, ATP, and mercury ions (Figure 36B).[859] By taking advantage of a FRET reporter strategy, they demonstrated that a Hg^{2+}-responsive TDN with one edge containing the T-rich mercury specific oligonucleotide can sensitively detect mercury down to 20 nM with high discrimination against 11 different metal ions.

In a follow-up study, Ono and co-workers found that similar to T-Hg^{2+}-T interactions, Ag^+ can specifically bind to two cytosines (C) and can promote these C−C mismatches to form stable base pairs.[860] On the basis of this C-Ag^+-C coordination chemistry, they developed a fluorescent biosensor for Ag^+.[860] Lin and Tseng used repeats of 20 C nucleotides (C_{20}) and SYBR Green I (a double-strand-chelating dye) to create a label-free fluorescent sensor for Ag^+.[861] The C_{20} binds to Ag^+ to form C-Ag^+-C complexes, resulting in enhanced fluorescent signal. This sensor enables highly sensitive (32 nM) and selective (more than 1000-fold) detection of Ag^+. Qi et al. utilized T-Hg^{2+}-T bridges to induce the aggregation of SERS nanotags, giving rise to the drastic amplification in the SERS signals with a detection range of 0.1 to 1000 nM and good selectivity over other metal ions.[578] The Willner group took advantage of T-rich and C-rich nucleic acids-functionalized CdSe-ZnS quantum dots for multiplexed analysis of Hg^{2+} (LOD: 10 nM) and Ag^+ (LOD: 1 μM).[862] Qu et al. used DNA TSPs to engineer the sensing interface for improving microconfined molecular recognition (Figure 36C).[855] By combining T-Hg^{2+}-T interaction, C-Ag^+-C interaction, and Pb^{2+}-specific DNAzymes, all three metal ions can be simultaneously detected with LODs of 10, 10, and 20 nM for Hg^{2+}, Ag^+, and Pb^{2+}, respectively.

K^+ together with Na^+, Ca^{2+}, and other metal ions plays a vital role in biological systems. Therefore, the development of biosensors for K^+ is of great importance. Folding of G-rich strands into a G-quadruplex in the presence of K^+ is one of the main strategies to detect K^+.[863,864] Hence, the oligonucleotide with guanine-rich segments offer unique K^+-binding sites, allowing the strands to be folded to generate a G_4. Additionally, G_4 is highly specific for K^+. On the basis of the interaction of K^+ with G_4, many groups have converted G_4 into highly sensitive and selective sensors for K^+. He et al. reported a homogeneous fluorescence amplification assay for G_4 structures of DNA that interfaces DNA association with the light-harvesting properties of conjugated polymers.[865] In this assay, the FRET efficiency for cationic conjugated polymer (CCP)/G_4 pair depends on the electrostatic interactions of G_4 with CCP. Kim and co-workers rationally designed the polydiacetylene liposome conjugated with dense G-rich ssDNA probes.[866] Upon binding with K^+, the G-rich ssDNA probes form bulky quadruplexes at the liposome surface. The resulting bulky quadruplexes lead to the conformational change of the eneyne backbone of the polydiacetylene. As a result, polydiacetylene liposomes turn into the emissive red phase from the nonfluorescent blue phase. The highly selective polydiacetylene liposome-based sensory system is suitable for the detection of the physiological potassium level (3.50−5.30 mM) with a LOD of 0.1 mM. To further realize biological applications of potassium ion sensors, several efforts have been devoted to increase their selectivity. For example, the Bald group took advantage of potassium ion-selective formation of a G_4 on DNA origami structures for K^+ biosensing. This method was able to detect potassium in the range of 0.5 mM to 50 mM even in the presence of high sodium concentration (145 mM).[867] Other studies have also shown specific detection of K^+ over Na^+.[868,869] Detection of K^+ using G_4 DNA has also been achieved in serum and urine.[868−870]

Lead is one of the main metal pollutants that is highly toxic, with lead poisoning occurring from use of lead in gasoline, pipes, and paint.[871] Lead toxicity can cause developmental disorders and mental illnesses, making Pb^{2+} detection a major research focus in the past decades. Similar to K^+, Pb^{2+} is found to strongly and specifically bind G_4 structures and is also more efficient in folding G_4 DNAs compared to K^+ and Na^+ (μM levels of Pb^{2+} compared to millimolar concentrations of K^+ and Na^+).[872,873,834] As a result, Pb^{2+}-dependent, G-rich ssDNAs can be integrated into Pb^{2+} biosensors.[874−876] Li et al. found that Pb^{2+} induces a K^+-stabilized G_4 DNAzyme to change its conformation, thus inhibiting the DNAzyme's peroxidase-like activity.[876] On the basis of the greatly decreased enzyme activity, they developed a Pb^{2+}-induced, allosteric G_4 DNAzyme as a colorimetric and chemiluminescent Pb^{2+} biosensor, achieving a detection limit of 32 nM and 1 nM, respectively. Since Pb^{2+} can more effectively fold G_4 DNAs, they can substitute K^+ ions that are part of G-quadruplexes. This releases hemin molecules bound to G-quadruplexes and in turn reduction in enzymatic activity of the G_4/hemin complex. Zhong et al. used the Pb^{2+}-

DOI: 10.1021/acs.chemrev.9b00121
Chem. Rev. XXXX, XXX, XXX−XXX

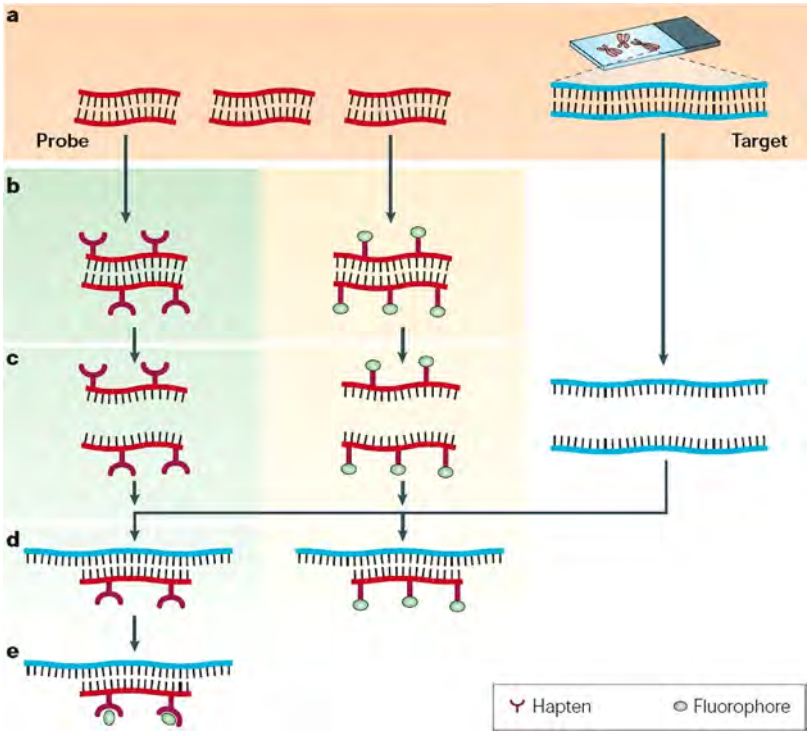

Figure 37. Principles of fluorescence in situ hybridization (FISH). (A) Basic elements of FISH are a DNA probe and a target sequence. (b) Before hybridization, the DNA probe is labeled by nick translation, random primed labeling, or PCR. Two labeling strategies are commonly used: indirect labeling (left panel) and direct labeling (right panel). For indirect labeling, probes are labeled with modified nucleotides that contain a hapten, whereas direct labeling uses nucleotides that have been directly modified to contain a fluorophore. (C) Labeled probe and the target DNA are denatured. (D) Combining the denatured probe and target allows the annealing of complementary DNA sequences. (E) If the probe has been labeled indirectly, an extra step is required for visualization of the nonfluorescent hapten that uses an enzymatic or immunological detection system. Whereas FISH is faster with directly labeled probes, indirect labeling offers the advantage of signal amplification by using several layers of antibodies, and it might therefore produce a signal that is brighter compared with background levels. Reproduced with permission from ref 890. Copyright 2005 Springer Nature.

induced catalytic interconversion for detecting Pb^{2+} with a LOD of ~0.32 pM (Figure 36D).[877]

5. *IN SITU* SENSING

Analysis of gene expression on a genomic scale in healthy and diseased cell states allows an insight into the regulation of genetic networks and their involvement in biological processes. Such measurements provide information on the expression patterns of genes[878] and their alterations in diseases such as cancer.[879−881] With the widespread use of genome-wide gene expression profiling technologies, gene expression signatures have emerged as a major class of cancer biomarkers.[881,882] However, more detailed experimental characterization of gene expression in individual cells is needed to eliminate variations in single-cell gene expression in biological systems (especially in tissues and tumors).[883] High-throughput gene expression screens can be used to obtain quantitative analysis of average expression signatures, but further development is required in quantitative *in situ* measurement techniques to analyze spatial gene expression patterns with single-cell resolution.

RT-PCR (i.e., quantitative RT-PCR, digital RT-PCR), considered the gold standard in gene expression analysis, is the current platform of choice for implementing these genomic signatures in clinical diagnostic assays.[884−886] Nevertheless, this grind-and-bind technology suffers from several serious drawbacks: (1) the process of target extraction destroys the tissue context of gene expression measurements, resulting in the complete loss of spatial information and making it impossible to map the observed signals to individual cells; (2) these assays are prone to contain interference from unintended cell types (e.g., noncancer cells) and from unwanted tissue elements (e.g., fibrosis, necrosis); and (3) the reverse transcription and the exponential amplification steps in PCR could lead to high error rates in analysis.[885] Microdissection techniques can alleviate these issues to some extent,[887] but they are too cumbersome and laborious to be useful on a routine basis. As a result, there is a need to develop methods that can quantify gene expression profiles of single cells in heterogeneous samples and intact tissues while also preserving spatial context of these expression profiles.[888,889]

5.1. *In Situ* Hybridization for Sensing

Fluorescence *in situ* hybridization (FISH) is one of the classical methods used to measure gene expression in intact tissues. The method involves the use of a fluorescently labeled oligonucleotide probe that can bind specifically to its complementary sequence present in fixed and permeabilized tissue samples (Figure 37).[891] FISH methods allow integration of molecular information with histopathology for optical clinical interpretation. Using traditional FISH, Adam Paré et al. constructed a specific probe for detection of single mRNA molecules in *Drosophila melanogaster*.[892] While some FISH studies have achieved sensing of single copies of an RNA transcript,, most traditional ISH and FISH techniques that study gene expression only provide qualitative information.[888] In these processes, hybridization of the probe with its target strand can also be affected by the distribution of dyes, which also might quench the fluorescence of adjacent dye molecules.[893] In addition, long

DOI: 10.1021/acs.chemrev.9b00121
Chem. Rev. XXXX, XXX, XXX−XXX

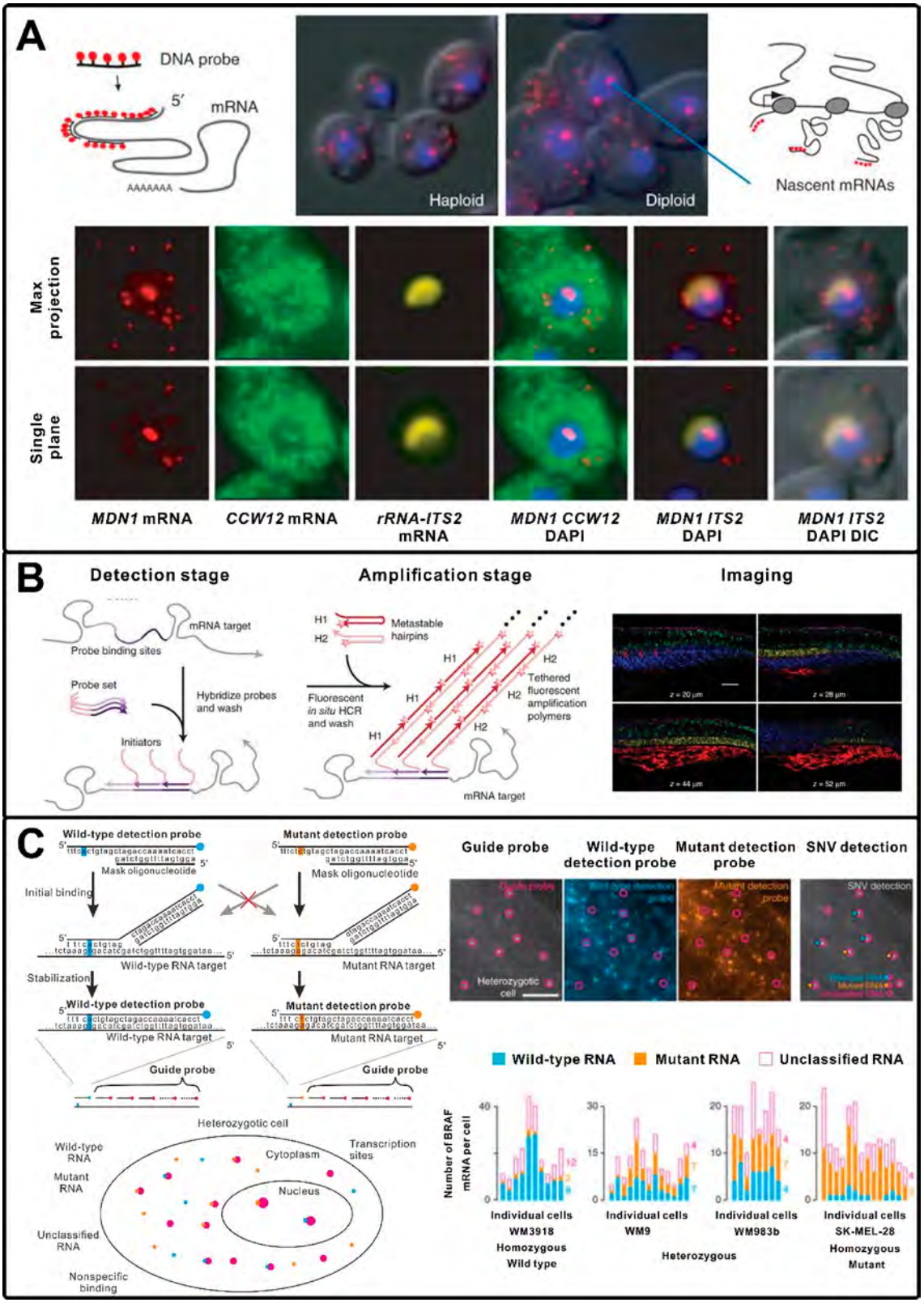

Figure 38. (A) FISH technology for single mRNA detection in cells. Reproduced with permission from ref 901. Copyright 2008 Springer Nature. (B) Multiplexed *in situ* hybridization using fluorescent HCR *in situ* amplification. Reproduced with permission from ref 909. Copyright 2010 Springer Nature. (C) SNV detection on individual RNA molecules *in situ* with toehold probes. Reproduced with permission from ref 908. Copyright 2013 Springer Nature.

probes with poor permeation have high background and low sensitivity, making them difficult to detect many low-abundance RNA biomarkers.[894]

FISH methods can be improved by designing the probes to be specific to the transcript of interest. The Singer group developed such a strategy where instead of a long fluorescently labeled

DOI: 10.1021/acs.chemrev.9b00121
Chem. Rev. XXXX, XXX, XXX−XXX

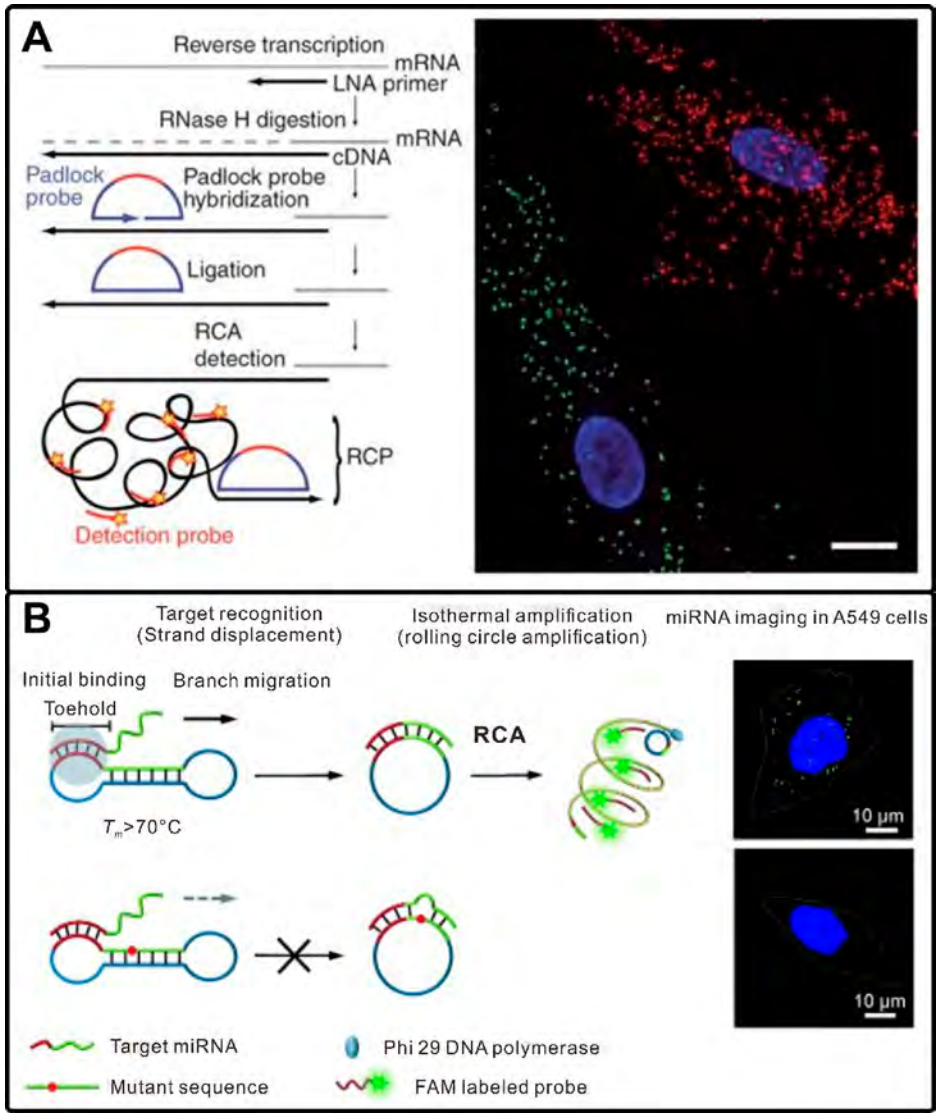

Figure 39. (A) Detection of individual transcripts *in situ* with padlock probes and target-primed RCA. Reproduced with permission from ref 933. Copyright 2010 Springer Nature. (B) Schematic representation of TIRCA for visualizing individual miRNAs *in situ* inside cells. Adapted with permission from ref 934. Copyright 2014 Wiley-VCH.

probe, they used multiple 50 nt probes (each with 3−5 fluorophores) that can hybridize to parts of the target mRNA.[895] Further, by controlling the positions of the dyes on the probes, the quenching of adjacent dyes can be minimized.[896] As a result, these short probes labeled with multiple fluorophores allow visualization of single RNA transcripts *in situ*. This strategy was then adopted by many different research groups to study distribution of mRNA transcripts in yeast and mammalian cells.[897−900] For example, Zenklusen et al. used an ISH method to measure transcriptional activity and abundance of mRNA in single *Saccharomyces cerevisiae* cells (Figure 38A).[901] This approach was used to detect transcription sites in paraffin-embedded human tumors but has not yet allowed single-transcript resolution in mammalian tissue.[902] This strategy so far is affected by the high variability in the number of probes bound to the target, making it difficult to identify specific targets from nonspecific binding.[895]

On the basis of Singer's method, Raj et al. created short probes with single fluorophores to visualize individual mRNA molecules in fixed cells.[903] In contrast to previous short probes labeled with multiple fluorophores, this method presents more efficient purification, and a reduced variability in spot intensity that is caused by inefficient binding. By using probes labeled with different fluorophores, multiple mRNA species can be identified simultaneously. In addition to its simplicity and universality, the approach benefits from easy probe design. As a result, the use of monolabeled probes to detect samples has been extended from yeast[904] and mammalian cells[903,905] to *Drosophila*[903] and *Caenorhabditis elegans* embryos.[906] Further, amplified strategies based on HCR or strand displacement reactions can be used to increase the sensitivity and specificity of this method.[907,908] For example, Choi et al. developed a multiplexed FISH method based on orthogonal amplification with HCR (Figure 38B).[909] HCR-based amplification provided high signal-to-noise ratios and sharp signal localization, and they used this method to image five target mRNAs simultaneously in fixed whole-mount and sectioned zebrafish embryos. Using a combination of strand displacement and single-molecule FISH, Raj and colleagues realized discrimination at the level of individual nucleotides (Figure 38C).[908] This method also allows

DOI: 10.1021/acs.chemrev.9b00121
Chem. Rev. XXXX, XXX, XXX−XXX

colocalization of the single-nucleotide variant (SNV) probe with the transcript to be identified since a mismatch on the toehold, and the target binding region slows down the strand displacement process. To detect short transcripts, Taniguchi et al. developed a 20-bp fluorescently labeled probe for single-mRNA detection in *Escherichia coli*.[910] These strategies need further development to be able to detect single transcripts in mammalian cells due to the larger cell volumes and the presence of off-target sequences.

One other challenge in this method is the detection of short target sequences. Optimizing probe design and increasing the sensitivity and specificity of individual probes will somewhat address this issue and help detect short targets such as miRNAs with the specificity to identify SNVs.[911] Modified nucleic acids such as peptide nucleic acids (PNA) and locked nucleic acids (LNA) can also be used to increase probe specificity and sensitivity for *in situ* detection of short transcripts.[912−917]

PNAs with an uncharged peptide-like backbone, compared with DNA probes, can hybridize more stably to RNA.[918,919] Lansdorp and co-workers developed a PNA-based FISH method to study telomere repeats at individual chromosomes.[920] The Min group proposed a PNA probe/nanosized graphene oxide (NGO)-based strategy to quantitatively monitor miRNA expression in living cells.[921] In this case, the PNA probes showed high loading efficiency on the NGO surface as well as high sequence specificity for target miRNAs. The presence of target miRNA causes the quenched dye-labeled PNA to recover fluorescence, making this strategy sensitive to ∼1 pM LOD while allowing simultaneous detection of three different miRNAs in a living cell.

LNA, 2′-*O*,4′-C-methylene-linked ribonucleotide derivative of RNA, has been shown to be more efficient in hybridizing with DNA and RNA when compared to DNA or RNA probes, and it has been used to detect short transcripts.[922,923] For instance, the Plasterk group used LNA probes to study the temporal and spatial expression patterns of multiple miRNAs in zebrafish embryos.[924] In a follow-up study, the Plasterk group used LNA-modified DNA probes for *in situ* detection of miRNAs in mouse embryos under optimal hybridization conditions.[925] Obernosterer et al. proposed an LNA probe-based FISH method for histological detection of miRNAs in mouse tissue sections.[926] To decrease the analysis time and simultaneously retain high detection sensitivity, Silahtaroglu and colleagues integrated LNA-modified probes with tyramide signal amplification technology.[927] As such, the unique miRNA recognition properties and high detection sensitivity of the method enable miRNA detection in samples such as animal tissue cryosections and human tumor biopsies.

5.2. Rolling-Circle Amplification for *in Situ* Sensing

Circularizable oligonucleotides, called padlock probes, with high sequence specificity and great potential for discriminating point mutations *in situ* have been used for the detection of single-molecule transcripts[928] since Nilsson et al. utilized padlock probes for detecting repeated alphoid sequences in metaphase chromosomes.[929] Moreover, padlock probes have been demonstrated to serve as templates for DNA polymerases.[930,931] In another strategy, the Lizardi group coupled padlock probes to RCA-based amplification to detect single copy genes in the total human genome.[449]

The Nilsson group used padlock probes as templates for rolling circle reactions.[932] The process involved recognition of specific target sequences combined with signal amplification to allow *in situ* detection of single-nucleotide variations of individual DNA molecules. In a follow-up study, the same group introduced the padlock probes to study SNV transcript at the level of single cells (Figure 39A).[933] In this work, the mRNA is first reverse-transcribed into cDNA with an LNA primer. Then the linear padlock probes are hybridized to opposite segments of the target sequence, followed by enzymatic ligation. These products are then used as templates in an RCA reaction, resulting in a DNA strand with tandem repeats of the padlock probe sequence. After hybridization to fluorescently labeled probes, this formed DNA strand yields bright diffraction-limited spots. This method can be used to detect somatic point mutations, differentiate members of a gene family, and for multiplexed detection of transcripts cells and tissues.

Other *in situ* amplification strategies have also been developed to enhance mismatch discrimination and improve fluorescent signal. The Li group developed a strategy called toehold-initiated rolling circle amplification (TIRCA) to identify miRNAs at physiological temperature and to visualize them in single cells (Figure 39B).[934] They constructed a dumbbell-shaped seal probe as the probe for toehold-mediated strand displacement and the template for the subsequent RCA. Target miRNA hybridizes to the seal probe, causing a shift from the dumbbell-shaped structure to the activated circular form, while a mismatched miRNA fails to migrate through. Through RCA for extending target miRNA with hundreds of tandem repeats, the hybridization of a FAM-labeled probe with target miRNA facilitates a fine diffraction-limited spot corresponding to single miRNA to be distinguished from the background. As a result, the TIRCA-based technique allows the visualization of individual miRNAs *in situ* in single cells.

6. CONCLUSION AND OUTLOOK

DNA-based biosensors are useful for a variety of chemical and bioanalytical purposes. Strategies that combine the functionalization of different ligands and chemical groups on DNA with specific spatial arrangement of such probes on surfaces provide efficient detection of biomarkers. These hybrid materials are versatile building blocks for sensitive molecular detection that is not achievable using conventional sensing methods. These strategies have been developed from mere proof-of-concept studies to "platform technologies" that can be modified to detect different targets and are also useful for detection in cells and *in vivo*. Systems involving DNA origami, despite the designs being more complex, have shown widespread uses in biotechnology.[9] Previously limited by the length of the scaffold strand (∼7kb M13),[79] the DNA origami strategies are now expanded to be created from scaffolds that can range from ∼700 to ∼50 000 nucleotides in length.[88,935−940] To optimize the construction (and yield) of these nanostructures, the kinetic and thermodynamic constraints involved in forming these structures have been analyzed recently as well as the folding pathways of origami.[941−944] Moreover, structures have been designed so that they can be assembled isothermally without the need for a thermal annealing process, especially in cases involving DNA−protein hybrids.[945−950] For large scale production, scientists have looked at different strategies such as enzymatic production of DNA strands[951] using a specific set of strands to fold an origami structure,[952] mass production of DNA-origami using biotechnological processes,[953] and using intact bacteriophages to assemble DNA nanostructures.[954] Moreover, chip-synthesized oligonucleotides have reduced the cost involved in building such an array of structures.[939,955−957] Once these

DOI: 10.1021/acs.chemrev.9b00121
Chem. Rev. XXXX, XXX, XXX−XXX

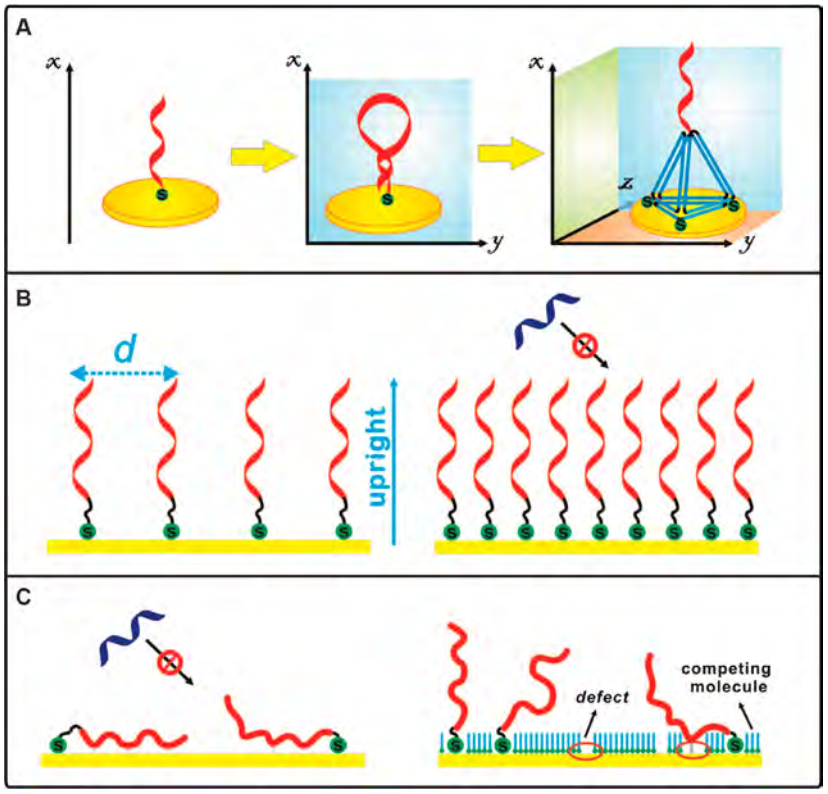

Figure 40. DNA nanotechnology concepts aiding in improvements of biosensing strategies. (A) Development of 1D, 2D, and 3D DNA nanostructures. (B) Control over interprobe spacing. (C) Configuration of probes on surface for efficient target capture. Reproduced from ref 407 (open access).

DNA nanostructures are produced in large scale, purification after assembly is another important step in using them for specific applications.[958] Purification strategies developed for this purpose include gel electrophoresis extraction,[959,960] PEG-based separation,[959,961,962] spin filters,[736] rate-zonal centrifugation,[959,963] magnetic bead capture,[959] size exclusion columns,[959,964] liquid chromatography-based techniques,[965] and free-flow electrophoresis.[966]

Compared to traditional methods of biosensing, DNA nanotechnology-based strategies have some advantages. The main among these is the signal enhancement provided by framework structures (Figure 40A). Single stranded DNA probes in surface-based assays are usually in an uncontrolled fashion, unable to control the density of such probes, resulting in nonspecific adsorption of DNA on the surface and steric hindrance to binding of target molecules. Use of DNA nanostructures addresses these issues by providing control over the density of capture probes (Figure 40B,C). The DNA tetrahedra-based electrochemical sensors described in the study are examples where the probe-to-probe spacing can be controlled (~4 nm) as well as control over density of the probes (4.8×10^{12} tetrahedral probes per cm^2).[638] This parameter is also true for any biomarker, and in fact, the steric interference has been used in DNA devices to provide a signal.[118] Adding to these features, custom-designed DNA nanostructures allow multiple capture probes to be placed in an array or incorporated as part of a device to both sense and act. The programmable nature of these structures also allows multiplexing to detect more than one biomarker (or types of biomarkers) in a single assay. Some examples include the DNA tetrahedra that can be multiplexed to detect four different microRNAs[967] and the DNA nanoswitches that was showed to detect five microRNAs in a single assay.[501] The multiplexing feature is important in moving toward clinical applications where detecting panels of biomarkers for a specific disease might be more accurate than a single biomarker, which overlaps with another disease.[968−971]

The wide use of DNA-based materials is mainly fast-tracked since DNA strands of any desired sequences can be chemically synthesized with many different functional groups. In addition, structures can also be modified using click-based functionalization[972,973] and recognize DNA sequences by functional ligands and triplexes.[974,975] Furthermore, a variety of DNA nanostructures use logic-gated responses[618] and activation by light.[976−978] By combining chemical, biological, and physical inputs, DNA devices can be made to respond to a variety of "senses" and react according to design. In the context of biosensing and *in vivo* nanostructures, other variations such as xeno nucleic acids,[979] modified nucleotides,[980] and nontraditional base pairs can also be useful.[981,982] Some developments involving DNA nanostructures, for example, DNA PAINT, have successfully been commercialized and demonstrated to be useful in sensing and super-resolution imaging.[983−985] Development of DNA nanostructure-based sensors will also help in understanding complex biological systems while providing a route to highly specific and sensitive detection. For studying biological processes, tools have been developed to probe cellular functions,[986−989] biomolecular interactions,[505,990] transport of materials within cells,[991−994] and disease mechanisms.[995,996] With regard to sensitive and specific sensing, DNA nanostructures are on par or better than current techniques. Moving forward, the field could be more oriented toward practical use of such sensors. Most biosensing strategies

DOI: 10.1021/acs.chemrev.9b00121
Chem. Rev. XXXX, XXX, XXX−XXX

are built on design parameters developed for DNA nanostructures. While it might not be feasible to sustain the high sensitivity obtained from lab-based instruments in a portable reader, DNA-based techniques should be transferable to such low-resource scenarios so that they can be used by anyone.[997−1000] In that context, a tradeoff between high sensitivity and ease-of-use is a step toward clinical usage. These strategies, some of which are in early stages of development toward point-of-care techniques, hold potential in moving from the bench to the bedside for clinical applications.

AUTHOR INFORMATION

Corresponding Authors

*E-mail: arun@albany.edu.
*E-mail: peihao@chem.ecnu.edu.cn.

ORCID

Binbin Chang: 0000-0001-6172-9952
Li Li: 0000-0001-8494-4997
Arun Richard Chandrasekaran: 0000-0001-6757-5464
Hao Pei: 0000-0002-6885-6708

Notes

The authors declare no competing financial interest.

Biographies

Mingshu Xiao completed his Bachelor's degree (2013) and Master's degree (2016) at University of Shanghai for Science and Technology. He now pursues his Ph.D. degree in analytical chemistry at East China Normal University. His research is focused on nucleic acid-based sensors for biomarker analysis and drug delivery systems for theranostics.

Wei Lai received his Bachelor's degree from Nanchang University and Master's degree from Ningbo University. He now pursues his Ph.D. degree in analytical chemistry at East China Normal University. His research interests include the use of DNA strand displacement technology to construct nonlinear chemical reaction networks for biological analysis.

Tiantian Man received her Bachelor's degree (2015) from Soochow University. She now is a Ph.D. candidate in analytical chemistry at East China Normal University. Her research interests include nucleic acid-based plasmonic nanostructures and heterostructures of semiconductor/metal for SERS analysis.

Binbin Chang received his Bachelor's degree in Chemistry at Dalian University in 2011, and obtained his Master's degree in Applied Chemistry at Zhejiang Sci-Tech University in 2014. He now pursues his Ph.D. degree in Analytical Chemistry at East China Normal University. His research interest includes the manufacture of 2D nanomaterials and their application in drug delivery systems.

Li Li graduated from University of Science and Technology of China (USTC) in 2006. She received her Master's degree (2008) from Chinese University of Hong Kong (CUHK) and her Ph.D. degree (2012) in Cavendish Laboratory from University of Cambridge, and then conducted her postdoctoral research at University of Southampton. Since 2014, she has been a professor at East China Normal University. Her current research interests focus on constructing SERS-active nanomaterials for biosensing, bioimaging, and liquid biopsy.

Arun Richard Chandrasekaran is a Research Scientist at The RNA Institute, University at Albany, State University of New York, NY, USA. He received his M. Tech in Nanoscience from the University of Madras, India in 2009 and Ph.D. in chemistry from New York University in 2015. His research focusses on developing biomolecular detection assays using DNA nanoswitches and functionalization of DNA-based nanostructures.

Hao Pei received his B.S. degree (2006) in Chemistry at Nanjing University and his Ph.D. degree (2012) from the Shanghai Institute of Applied Physics (SINAP), Chinese Academy of Sciences (CAS). After his postdoctoral research at New York University with Prof. Ned Seeman, he became a professor at East China Normal University in 2015. His current research focuses on artificial intelligent biosystems/bioelectronics and their application in therapeutics and diagnostics.

ACKNOWLEDGMENTS

This work was supported by the National Science Foundation of China (Grant No. 21722502), National Key Research and Development Program of China for International Science & Innovation Cooperation Major Project between Governments (2018YFE0113200), Shanghai Rising-Star Program (19QA1403000), and Shanghai Science and Technology Committee (STCSM) (Grant No. 18490740500).

ABBREVIATIONS

AFB1	aflatoxin B1
AFM	atomic force microscope
BA	bacillary angiomatosis
CNTs	carbon nanotubes
CP	carrier probe
CAMB	catalytic and molecular beacon
CHA	catalyzed hairpin assembly
CCP	cationic conjugated polymer
CRET	chemiluminescence resonance energy transfer
CTC	circulating tumor cell
CFU	colony-forming unit
CF-DTMB	competition-mediated FRET-switching DNA tetrahedron molecular beacon
DGGE	denaturing gradient gel electrophoresis
DIG	digoxigenin
DCP	DNA clutch probe
DTNT	DNA tetrahedron nanotweezer
DX	double-crossover
DSNSA	duplex-specific nuclease signal amplification
EV	Ebola virus
ECL	electrochemiluminescence
ET	electron transfer
EF	enhancement factors
ELISA	enzyme-linked immunosorbent assay
Exo III	exonuclease III
FISH	fluorescence in situ hybridization
FRET	Forster or fluorescence resonance energy transfer
FNA	framework nucleic acid
FB1	fumonisin B1
FO	functional oligonucleotide
GOx	glucose oxidase
AuNPs	gold nanoparticles
GN	graphite nanoparticles
GQD	graphene quantum dot
GO	graphene oxide
HP	hairpin probe
HBV	hepatitis B virus surface-antigen gene
HRP	horseradish peroxidase
anti-DIG-HRP	horseradish peroxidase-linked-anti-DIG antibody

DOI: 10.1021/acs.chemrev.9b00121
Chem. Rev. XXXX, XXX, XXX−XXX

HIV	human immunodeficiency virus
HCR	hybridization chair reaction
iMS	inverse molecular sentinel
KSHV	Kaposi's sarcoma-associated herpesvirus
LFA	lateral flow assay
LOD	limit of detection
LYS	lysozyme
MTase	methyltransferases
MB	molecular beacon
NC	nanoclusters
NP	nanoparticle
NME	nanostructured microelectrode
nano-SNEL	nanosnail-inspired nucleic acid locator
NHBu	*N*-butylamine
NMM	*N*-methyl mesoporphyrin IX
OTA	ochratoxin A
oPAD	origami paper analytical device
PX	paranemic-crossover
PNA	peptide nucleic acid
PET	photoinduced electron transfer
PDGF-BB	platelet-derived growth factor-BB
PCR	polymerase chain reaction
PSA	prostate-specific antigen
QD	quantum dot
RT-PCR	reverse transcription polymerase chain reaction
RCA	rolling circle amplification
SAM	self-assembled monolayer
SNP	single nucleotide polymorphism
SWCNT	single-walled carbon nanotube
SNA	spherical nucleic acid
SERS	surface-enhanced Raman scattering
TREAS	target-responsive electrochemical aptamer switch
TSP	tetrahedra structured probes
TIRCA	toehold-initiated rolling circle amplification
TNT	2,4,6 trinitrotoluene
UCNP	upconversion nanoparticle
VV	variola virus

REFERENCES

(1) Seeman, N. C. *Structural DNA Nanotechnology*; Cambridge University Press, 2016.

(2) Chandrasekaran, A. R. Nucleic acid nanotechnology. *Comprehensive Nanoscience and Nanotechnology*, 2nd ed.; ScienceDirect, 2019; Vol. 2, pp 13−34.

(3) Seeman, N. C. DNA in a Material World. *Nature* **2003**, *421*, 427−431.

(4) Chandrasekaran, A. R.; Levchenko, O. DNA Nanocages. *Chem. Mater.* **2016**, *28*, 5569−5581.

(5) Madhanagopal, B. R.; Zhang, S. Q.; Demirel, E.; Wady, H.; Chandrasekaran, A. R. DNA Nanocarriers: Programmed to Deliver. *Trends Biochem. Sci.* **2018**, *43*, 997−1013.

(6) Wang, X. W.; Lai, W.; Man, T. T.; Qu, X. M.; Li, L.; Chandrasekaran, A. R.; Pei, H. Bio-Surface Engineering with DNA Scaffolds for Theranostic Applications. *Nanofabrication* **2018**, *4*, 1−16.

(7) Xavier, P. L.; Chandrasekaran, A. R. DNA-Based Construction at the Nanoscale: Emerging Trends and Applications. *Nanotechnology* **2018**, *29*, 062001.

(8) Chandrasekaran, A. R.; Anderson, N.; Kizer, M.; Halvorsen, K.; Wang, X. Beyond the Fold: Emerging Biological Applications of DNA Origami. *ChemBioChem* **2016**, *17*, 1081−1089.

(9) Chandrasekaran, A. R. DNA Origami and Biotechnology Applications: A Perspective. *J. Chem. Technol. Biotechnol.* **2016**, *91*, 843−846.

(10) Qu, X. M.; Wang, S. P.; Ge, Z. L.; Wang, J. B.; Yao, G. B.; Li, J.; Zuo, X. L.; Shi, J. Y.; Song, S. P.; Wang, L. H.; Li, L.; Pei, H.; Fan, C. H. Programming Cell Adhesion for on-Chip Sequential Boolean Logic Functions. *J. Am. Chem. Soc.* **2017**, *139*, 10176−10179.

(11) Lai, W.; Ren, L.; Tang, Q.; Qu, X. M.; Li, J.; Wang, L. H.; Li, L.; Fan, C. H.; Pei, H. Programming Chemical Reaction Networks Using Intramolecular Conformational Motions of DNA. *ACS Nano* **2018**, *12*, 7093−7099.

(12) Kizer, M. E.; Linhardt, R. J.; Chandrasekaran, A. R.; Wang, X. A Molecular Hero Suit for in Vitro and in Vivo DNA Nanostructures. *Small* **2019**, *15*, 1805386.

(13) Seeman, N. C. Nucleic Acid Junctions and Lattices. *J. Theor. Biol.* **1982**, *99*, 237−247.

(14) Holliday, R. A. Mechanism for Gene Conversion in Fungi. *Genet. Res.* **1964**, *5*, 282−304.

(15) Kallenbach, N. R.; Ma, R.-I.; Seeman, N. C. An Immobile Nucleic Acid Junction Constructed from Oligonucleotides. *Nature* **1983**, *305*, 829.

(16) Wang, Y.; Mueller, J. E.; Kemper, B.; Seeman, N. C. Assembly and Characterization of Five-Arm and Six-Arm DNA Branched Junctions. *Biochemistry* **1991**, *30*, 5667−5674.

(17) Wang, X.; Seeman, N. C. Assembly and Characterization of 8-Arm and 12-Arm DNA Branched Junctions. *J. Am. Chem. Soc.* **2007**, *129*, 8169−8176.

(18) Ortiz-Lombardia, M.; Gonzalez, A.; Eritja, R.; Aymami, J.; Azorin, F.; Coll, M. Crystal Structure of a DNA Holliday Junction. *Nat. Struct. Biol.* **1999**, *6*, 913−917.

(19) Ariyoshi, M.; Nishino, T.; Iwasaki, H.; Shinagawa, H.; Morikawa, K. Crystal Structure of the Holliday Junction DNA in Complex with a Single RuvA Tetramer. *Proc. Natl. Acad. Sci. U. S. A.* **2000**, *97*, 8257−8262.

(20) Hyeon, C.; Lee, J.; Yoon, J.; Hohng, S.; Thirumalai, D. Hidden Complexity in the Isomerization Dynamics of Holliday Junctions. *Nat. Chem.* **2012**, *4*, 907−914.

(21) Chen, J.; Seeman, N. C. Synthesis from DNA of a Molecule with the Connectivity of a Cube. *Nature* **1991**, *350*, 631.

(22) Zhang, Y.; Seeman, N. C. Construction of a DNA-Truncated Octahedron. *J. Am. Chem. Soc.* **1994**, *116*, 1661−1669.

(23) Shih, W. M.; Quispe, J. D.; Joyce, G. F. A 1.7-Kilobase Single-Stranded DNA That Folds into a Nanoscale Octahedron. *Nature* **2004**, *427*, 618−621.

(24) Wang, X.; Chandrasekaran, A. R.; Shen, Z.; Ohayon, Y. P.; Wang, T.; Kizer, M. E.; Sha, R.; Mao, C.; Yan, H.; Zhang, X.; Liao, S.; Ding, B.; Chakraborty, B.; Jonoska, N.; Niu, D.; Gu, H.; Chao, J.; Gao, X.; Li, Y.; Ciengshin, T.; Seeman, N. C. Paranemic Crossover DNA: There and Back Again. *Chem. Rev.* **2018**, *119*, 6273−6289.

(25) Bhatia, D.; Mehtab, S.; Krishnan, R.; Indi, S. S.; Basu, A.; Krishnan, Y. Icosahedral DNA Nanocapsules by Modular Assembly. *Angew. Chem., Int. Ed.* **2009**, *48*, 4134−4137.

(26) Goodman, R. P.; Schaap, I. A. T.; Tardin, C. F.; Erben, C. M.; Berry, R. M.; Schmidt, C. F.; Turberfield, A. J. Rapid Chiral Assembly of Rigid DNA Building Blocks for Molecular Nanofabrication. *Science* **2005**, *310*, 1661−1665.

(27) Aldaye, F. A.; Sleiman, H. F. Modular Access to Structurally Switchable 3D Discrete DNA Assemblies. *J. Am. Chem. Soc.* **2007**, *129*, 13376−13377.

(28) He, Y.; Chen, Y.; Liu, H. P.; Ribbe, A. E.; Mao, C. D. Self-Assembly of Hexagonal DNA Two-Dimensional (2D) Arrays. *J. Am. Chem. Soc.* **2005**, *127*, 12202−12203.

(29) Zhang, C.; Wu, W. M.; Li, X.; Tian, C.; Qian, H.; Wang, G. S.; Jiang, W.; Mao, C. D. Controlling the Chirality of DNA Nanocages. *Angew. Chem., Int. Ed.* **2012**, *51*, 7999−8002.

(30) Liu, Z. Y.; Tian, C.; Yu, J. W.; Li, Y. L.; Jiang, W.; Mao, C. D. Self-Assembly of Responsive Multilayered DNA Nanocages. *J. Am. Chem. Soc.* **2015**, *137*, 1730−1733.

(31) Li, Y. L.; Tian, C.; Liu, Z. Y.; Jiang, W.; Mao, C. D. Structural Transformation: Assembly of an Otherwise Inaccessible DNA Nanocage. *Angew. Chem., Int. Ed.* **2015**, *54*, 5990−5993.

DOI: 10.1021/acs.chemrev.9b00121
Chem. Rev. XXXX, XXX, XXX−XXX

(32) He, Y.; Ye, T.; Su, M.; Zhang, C.; Ribbe, A. E.; Jiang, W.; Mao, C. D. Hierarchical Self-Assembly of DNA into Symmetric Supramolecular Polyhedra. *Nature* **2008**, *452*, 198−201.
(33) Zhang, C.; Ko, S. H.; Su, M.; Leng, Y. J.; Ribbe, A. E.; Jiang, W.; Mao, C. D. Symmetry Controls the Face Geometry of DNA Polyhedra. *J. Am. Chem. Soc.* **2009**, *131*, 1413−1415.
(34) Zhang, C.; Su, M.; He, Y.; Zhao, X.; Fang, P. A.; Ribbe, A. E.; Jiang, W.; Mao, C. D. Conformational Flexibility Facilitates Self-Assembly of Complex DNA Nanostructures. *Proc. Natl. Acad. Sci. U. S. A.* **2008**, *105*, 10665−10669.
(35) Tian, C.; Li, X.; Liu, Z. Y.; Jiang, W.; Wang, G. S.; Mao, C. D. Directed Self-Assembly of DNA Tiles into Complex Nanocages. *Angew. Chem., Int. Ed.* **2014**, *53*, 8041−8044.
(36) Ko, S. H.; Su, M.; Zhang, C. A.; Ribbe, A. E.; Jiang, W.; Mao, C. D. Synergistic Self-Assembly of RNA and DNA Molecules. *Nat. Chem.* **2010**, *2*, 1050−1055.
(37) Zuo, H.; Wu, S. Y.; Li, M.; Li, Y. L.; Jiang, W.; Mao, C. D. A Case Study of the Likes and Dislikes of DNA and RNA in Self-Assembly. *Angew. Chem., Int. Ed.* **2015**, *54*, 15118−15121.
(38) Guo, P. X. The Emerging Field of RNA Nanotechnology. *Nat. Nanotechnol.* **2010**, *5*, 833−842.
(39) Jasinski, D.; Haque, F.; Binzel, D. W.; Guo, P. X. Advancement of the Emerging Field of RNA Nanotechnology. *ACS Nano* **2017**, *11*, 1142−1164.
(40) Grabow, W. W.; Jaeger, L. RNA Self-Assembly and RNA Nanotechnology. *Acc. Chem. Res.* **2014**, *47*, 1871−1880.
(41) Yu, J. W.; Liu, Z. Y.; Jiang, W.; Wang, G. S.; Mao, C. D. De Novo Design of an RNA Tile That Self-Assembles into a Homo-Octameric Nanoprism. *Nat. Commun.* **2015**, *6*, 5724.
(42) Hao, C. H.; Li, X.; Tian, C.; Jiang, W.; Wang, G. S.; Mao, C. D. Construction of RNA Nanocages by Re-Engineering the Packaging RNA of Phi29 Bacteriophage. *Nat. Commun.* **2014**, *5*, 3890.
(43) Li, M.; Zheng, M. X.; Wu, S. Y.; Tian, C.; Liu, D.; Weizmann, Y.; Jiang, W.; Wang, G. S.; Mao, C. D. In Vivo Production of RNA Nanostructures via Programmed Folding of Single-Stranded RNAs. *Nat. Commun.* **2018**, *9*, 2196.
(44) Ohno, H.; Kobayashi, T.; Kabata, R.; Endo, K.; Iwasa, T.; Yoshimura, S. H.; Takeyasu, K.; Inoue, T.; Saito, H. Synthetic RNA-Protein Complex Shaped Like an Equilateral Triangle. *Nat. Nanotechnol.* **2011**, *6*, 115−119.
(45) Afonin, K. A.; Bindewald, E.; Yaghoubian, A. J.; Voss, N.; Jacovetty, E.; Shapiro, B. A.; Jaeger, L. Vitro Assembly of Cubic RNA-Based Scaffolds Designed in Silico. *Nat. Nanotechnol.* **2010**, *5*, 676−682.
(46) Khisamutdinov, E. F.; Jasinski, D. L.; Li, H.; Zhang, K. M.; Chiu, W.; Guo, P. X. Fabrication of RNA 3D Nanoprisms for Loading and Protection of Small RNAs and Model Drugs. *Adv. Mater.* **2016**, *28*, 10079−10087.
(47) Seeman, N. C. Macromolecular Design, Nucleic Acid Junctions, and Crystal Formation. *J. Biomol. Struct. Dyn.* **1985**, *3*, 11−34.
(48) Winfree, E.; Liu, F. R.; Wenzler, L. A.; Seeman, N. C. Design and Self-Assembly of Two-Dimensional DNA Crystals. *Nature* **1998**, *394*, 539−544.
(49) Majumder, U.; Rangnekar, A.; Gothelf, K. V.; Reif, J. H.; LaBean, T. H. Design and Construction of Double-Decker Tile as a Route to Three-Dimensional Periodic Assembly of DNA. *J. Am. Chem. Soc.* **2011**, *133*, 3843−3845.
(50) Zheng, J. W.; Constantinou, P. E.; Micheel, C.; Alivisatos, A. P.; Kiehl, R. A.; Seeman, N. C. Two-Dimensional Nanoparticle Arrays Show the Organizational Power of Robust DNA Motifs. *Nano Lett.* **2006**, *6*, 1502−1504.
(51) He, Y.; Tian, Y.; Chen, Y.; Deng, Z. X.; Ribbe, A. E.; Mao, C. D. Sequence Symmetry as a Tool for Designing DNA Nanostructures. *Angew. Chem., Int. Ed.* **2005**, *44*, 6694−6696.
(52) He, Y.; Tian, Y.; Ribbe, A. E.; Mao, C. D. Highly Connected Two-Dimensional Crystals of DNA Six-Point-Stars. *J. Am. Chem. Soc.* **2006**, *128*, 15978−15979.
(53) Fu, T. J.; Seeman, N. C. DNA Double-Crossover Molecules. *Biochemistry* **1993**, *32*, 3211−3220.
(54) LaBean, T. H.; Yan, H.; Kopatsch, J.; Liu, F.; Winfree, E.; Reif, J. H.; Seeman, N. C. Construction, Analysis, Ligation, and Self-Assembly of DNA Triple Crossover Complexes. *J. Am. Chem. Soc.* **2000**, *122*, 1848−1860.
(55) Shen, Z. Y.; Yan, H.; Wang, T.; Seeman, N. C. Paranemic Crossover DNA: A Generalized Holliday Structure with Applications in Nanotechnology. *J. Am. Chem. Soc.* **2004**, *126*, 1666−1674.
(56) Ohayon, Y. P.; Sha, R. J.; Flint, O.; Chandrasekaran, A. R.; Abdallah, H. O.; Wang, T.; Wang, X.; Zhang, X. P.; Seeman, N. C. Topological Linkage of DNA Tiles Bonded by Paranemic Cohesion. *ACS Nano* **2015**, *9*, 10296−10303.
(57) Ohayon, Y. R.; Sha, R. J.; Flint, O.; Liu, W. Y.; Chakraborty, B.; Subramanian, H. K. K.; Zheng, J. P.; Chandrasekaran, A. R.; Abdallah, H. O.; Wang, X.; Zhang, X. P.; Seeman, N. C. Covalent Linkage of One-Dimensional DNA Arrays Bonded by Paranemic Cohesion. *ACS Nano* **2015**, *9*, 10304−10312.
(58) Shen, W. L.; Liu, Q.; Ding, B. Q.; Shen, Z. Y.; Zhu, C. Q.; Mao, C. D. The Study of the Paranemic Crossover (PX) Motif in the Context of Self-Assembly of DNA 2D Crystals. *Org. Biomol. Chem.* **2016**, *14*, 7187−7190.
(59) Shen, W. L.; Liu, Q.; Ding, B. Q.; Zhu, C. Q.; Shen, Z. Y.; Seeman, N. C. Facilitation of DNA Self-Assembly by Relieving the Torsional Strains between Building Blocks. *Org. Biomol. Chem.* **2017**, *15*, 465−469.
(60) Seeman, N. C.; Wang, H.; Yang, X. P.; Liu, F. R.; Mao, C. D.; Sun, W. Q.; Wenzler, L.; Shen, Z. Y.; Sha, R. J.; Yan, H.; Wong, M. H.; Sa-Ardyen, P.; Liu, B.; Qiu, H. X.; Li, X. J.; Qi, J.; Du, S. M.; Zhang, Y. W.; Mueller, J. E.; Fu, T. J.; Wang, Y. L.; Chen, J. H. New Motifs in DNA Nanotechnology. *Nanotechnology* **1998**, *9*, 257−273.
(61) Sharma, J.; Chhabra, R.; Liu, Y.; Ke, Y. G.; Yan, H. DNA-Templated Self-Assembly of Two-Dimensional and Periodical Gold Nanoparticle Arrays. *Angew. Chem., Int. Ed.* **2006**, *45*, 730−735.
(62) Park, S. H.; Yin, P.; Liu, Y.; Reif, J. H.; LaBean, T. H.; Yan, H. Programmable DNA Self-Assemblies for Nanoscale Organization of Ligands and Proteins. *Nano Lett.* **2005**, *5*, 729−733.
(63) Chandrasekaran, A. R.; Zhuo, R. A 'Tile' Tale: Hierarchical Self-Assembly of DNA Lattices. *Appl. Mater. Today* **2016**, *2*, 7−16.
(64) Chandrasekaran, A. R. Programmable DNA Scaffolds for Spatially-Ordered Protein Assembly. *Nanoscale* **2016**, *8*, 4436−4446.
(65) Liu, D.; Wang, M.; Deng, Z.; Walulu, R.; Mao, C. Tensegrity: Construction of Rigid DNA Triangles with Flexible Four-Arm DNA Junctions. *J. Am. Chem. Soc.* **2004**, *126*, 2324−2325.
(66) Zheng, J. P.; Birktoft, J. J.; Chen, Y.; Wang, T.; Sha, R. J.; Constantinou, P. E.; Ginell, S. L.; Mao, C. D.; Seeman, N. C. From Molecular to Macroscopic via the Rational Design of a Self-Assembled 3D DNA Crystal. *Nature* **2009**, *461*, 74−77.
(67) Nguyen, N.; Birktoft, J. J.; Sha, R.; Wang, T.; Zheng, J.; Constantinou, P. E.; Ginell, S. L.; Chen, Y.; Mao, C.; Seeman, N. C. The Absence of Tertiary Interactions in a Self-Assembled DNA Crystal Structure. *J. Mol. Recognit.* **2012**, *25*, 234−237.
(68) Wang, T.; Sha, R. J.; Birktoft, J.; Zheng, J. P.; Mao, C. D.; Seeman, N. C. A DNA Crystal Designed to Contain Two Molecules Per Asymmetric Unit. *J. Am. Chem. Soc.* **2010**, *132*, 15471−15473.
(69) Sha, R. J.; Birktoft, J. J.; Nguyen, N.; Chandrasekaran, A. R.; Zheng, J. P.; Zhao, X. S.; Mao, C. D.; Seeman, N. C. Self-Assembled DNA Crystals: The Impact on Resolution of 5 '-Phosphates and the DNA Source. *Nano Lett.* **2013**, *13*, 793−797.
(70) Ohayon, Y. P.; Hernandez, C.; Chandrasekaran, A. R.; Wang, X.; Abdallah, H. O.; Jong, M. A.; Mohsen, M. G.; Sha, R.; Birktoft, J. J.; Lukeman, P. S.; Chaikin, P. M.; Ginell, S. L.; Mao, C.; Seeman, N. C. Designing Higher Resolution Self-Assembled 3D DNA Crystals via Strand Terminus Modifications. *ACS Nano* **2019**, *13*, 7957−7965.
(71) Zhao, J. M.; Chandrasekaran, A. R.; Li, Q.; Li, X.; Sha, R. J.; Seeman, N. C.; Mao, C. D. Post-Assembly Stabilization of Rationally Designed DNA Crystals. *Angew. Chem., Int. Ed.* **2015**, *54*, 9936−9939.
(72) Abdallah, H. O.; Ohayon, Y. P.; Chandrasekaran, A. R.; Sha, R. J.; Fox, K. R.; Brown, T.; Rusling, D. A.; Mao, C.; Seeman, N. C. Stabilisation of Self-Assembled DNA Crystals by Triplex-Directed Photo-Cross-Linking. *Chem. Commun.* **2016**, *52*, 8014−8017.

DOI: 10.1021/acs.chemrev.9b00121
Chem. Rev. XXXX, XXX, XXX−XXX

(73) Zhao, J.; Zhao, Y.; Li, Z.; Wang, Y.; Sha, R.; Seeman, N. C.; Mao, C. Modulating Self-Assembly of DNA Crystals with Rationally Designed Agents. *Angew. Chem., Int. Ed.* **2018**, *57*, 16529−16532.
(74) Stahl, E.; Praetorius, F.; Mann, C. C. D.; Hopfner, K. P.; Dietz, H. Impact of Heterogeneity and Lattice Bond Strength on DNA Triangle Crystal Growth. *ACS Nano* **2016**, *10*, 9156−9164.
(75) Rusling, D. A.; Chandrasekaran, A. R.; Ohayon, Y. P.; Brown, T.; Fox, K. R.; Sha, R.; Mao, C.; Seeman, N. C. Functionalizing Designer DNA Crystals with a Triple-Helical Veneer. *Angew. Chem.* **2014**, *126*, 4060−4063.
(76) Wang, X.; Sha, R. J.; Kristiansen, M.; Hernandez, C.; Hao, Y. D.; Mao, C. D.; Canary, J. W.; Seeman, N. C. An Organic Semiconductor Organized into 3D DNA Arrays by "Bottom-up" Rational Design. *Angew. Chem., Int. Ed.* **2017**, *56*, 6445−6448.
(77) Hao, Y. D.; Kristiansen, M.; Sha, R. J.; Birktoft, J. J.; Hernandez, C.; Mao, C. D.; Seeman, N. C. A Device That Operates within a Self-Assembled 3D DNA Crystal. *Nat. Chem.* **2017**, *9*, 824−827.
(78) Hernandez, C.; Birktoft, J. J.; Ohayon, Y. P.; Chandrasekaran, A. R.; Abdallah, H.; Sha, R. J.; Stojanoff, V.; Mao, C. D.; Seeman, N. C. Self-Assembly of 3D DNA Crystals Containing a Torsionally Stressed Component. *Cell Chem. Biol.* **2017**, *24*, 1401−1406.
(79) Rothemund, P. W. Folding DNA to Create Nanoscale Shapes and Patterns. *Nature* **2006**, *440*, 297−302.
(80) Hong, F.; Zhang, F.; Liu, Y.; Yan, H. DNA Origami: Scaffolds for Creating Higher Order Structures. *Chem. Rev.* **2017**, *117*, 12584−12640.
(81) Dietz, H.; Douglas, S. M.; Shih, W. M. Folding DNA into Twisted and Curved Nanoscale Shapes. *Science* **2009**, *325*, 725−730.
(82) Douglas, S. M.; Dietz, H.; Liedl, T.; Hogberg, B.; Graf, F.; Shih, W. M. Self-Assembly of DNA into Nanoscale Three-Dimensional Shapes. *Nature* **2009**, *459*, 414−418.
(83) Andersen, E. S.; Dong, M.; Nielsen, M. M.; Jahn, K.; Subramani, R.; Mamdouh, W.; Golas, M. M.; Sander, B.; Stark, H.; Oliveira, C. L. P.; Pedersen, J. S.; Birkedal, V.; Besenbacher, F.; Gothelf, K. V.; Kjems, J. Self-Assembly of a Nanoscale DNA Box with a Controllable Lid. *Nature* **2009**, *459*, 73−76.
(84) Han, D. R.; Pal, S.; Nangreave, J.; Deng, Z. T.; Liu, Y.; Yan, H. DNA Origami with Complex Curvatures in Three-Dimensional Space. *Science* **2011**, *332*, 342−346.
(85) Zhang, F.; Jiang, S. X.; Wu, S. Y.; Li, Y. L.; Mao, C. D.; Liu, Y.; Yan, H. Complex Wireframe DNA Origami Nanostructures with Multi-Arm Junction Vertices. *Nat. Nanotechnol.* **2015**, *10*, 779−784.
(86) Benson, E.; Mohammed, A.; Gardell, J.; Masich, S.; Czeizler, E.; Orponen, P.; Hogberg, B. DNA Rendering of Polyhedral Meshes at the Nanoscale. *Nature* **2015**, *523*, 441−U139.
(87) Liu, W. Y.; Zhong, H.; Wang, R. S.; Seeman, N. C. Crystalline Two-Dimensional DNA-Origami Arrays. *Angew. Chem., Int. Ed.* **2011**, *50*, 264−267.
(88) Iinuma, R.; Ke, Y. G.; Jungmann, R.; Schlichthaerle, T.; Woehrstein, J. B.; Yin, P. Polyhedra Self-Assembled from DNA Tripods and Characterized with 3D DNA-Paint. *Science* **2014**, *344*, 65−69.
(89) Wei, B.; Dai, M. J.; Yin, P. Complex Shapes Self-Assembled from Single-Stranded DNA Tiles. *Nature* **2012**, *485*, 623−626.
(90) Ke, Y. G.; Ong, L. L.; Shih, W. M.; Yin, P. Three-Dimensional Structures Self-Assembled from DNA Bricks. *Science* **2012**, *338*, 1177−1183.
(91) Yin, P.; Hariadi, R. F.; Sahu, S.; Choi, H. M. T.; Park, S. H.; LaBean, T. H.; Reif, J. H. Programming DNA Tube Circumferences. *Science* **2008**, *321*, 824−826.
(92) Seeman, N. C. De Novo Design of Sequences for Nucleic Acid Structural Engineering. *J. Biomol. Struct. Dyn.* **1990**, *8*, 573−581.
(93) Wei, B.; Wang, Z.; Mi, Y. Uniquimer: Software of De Novo DNA Sequence Generation for DNA Self-Assembly—an Introduction and the Related Applications in DNA Self-Assembly. *J. Comput. Theor. Nanos.* **2007**, *4*, 133−141.
(94) Birac, J. J.; Sherman, W. B.; Kopatsch, J.; Constantinou, P. E.; Seeman, N. C. Architecture with Gideon, a Program for Design in Structural DNA Nanotechnology. *J. Mol. Graphics Modell.* **2006**, *25*, 470−480.
(95) Williams, S.; Lund, K.; Lin, C.; Wonka, P.; Lindsay, S.; Yan, H. Tiamat: A Three-Dimensional Editing Tool for Complex DNA Structures. *International Workshop on DNA-Based Computers*; Springer, 2008; pp 90−101.
(96) Zhu, J. H.; Wei, B.; Yuan, Y.; Mi, Y. L. Uniquimer 3D, a Software System for Structural DNA Nanotechnology Design, Analysis and Evaluation. *Nucleic Acids Res.* **2009**, *37*, 2164−2175.
(97) Douglas, S. M.; Marblestone, A. H.; Teerapittayanon, S.; Vazquez, A.; Church, G. M.; Shih, W. M. Rapid Prototyping of 3D DNA-Origami Shapes with Cadnano. *Nucleic Acids Res.* **2009**, *37*, 5001−5006.
(98) Veneziano, R.; Ratanalert, S.; Zhang, K. M.; Zhang, F.; Yan, H.; Chiu, W.; Bathe, M. DNA Nanotechnology Designer Nanoscale DNA Assemblies Programmed from the Top Down. *Science* **2016**, *352*, 1534.
(99) Castro, C. E.; Kilchherr, F.; Kim, D. N.; Shiao, E. L.; Wauer, T.; Wortmann, P.; Bathe, M.; Dietz, H. A Primer to Scaffolded DNA Origami. *Nat. Methods* **2011**, *8*, 221−229.
(100) Jun, H.; Zhang, F.; Shepherd, T.; Ratanalert, S.; Qi, X. D.; Yan, H.; Bathe, M. Autonomously Designed Free-Form 2D DNA Origami. *Sci. Adv.* **2019**, *5*, No. eaav0655.
(101) Bath, J.; Turberfield, A. J. DNA Nanomachines. *Nat. Nanotechnol.* **2007**, *2*, 275−284.
(102) Elbaz, J.; Cecconello, A.; Fan, Z. Y.; Govorov, A. O.; Willner, I. Powering the Programmed Nanostructure and Function of Gold Nanoparticles with Catenated DNA Machines. *Nat. Commun.* **2013**, *4*, 2000.
(103) Liu, X. Q.; Lu, C. H.; Willner, I. Switchable Reconfiguration of Nucleic Acid Nanostructures by Stimuli-Responsive DNA Machines. *Acc. Chem. Res.* **2014**, *47*, 1673−1680.
(104) Simmel, F. C.; Dittmer, W. U. DNA Nanodevices. *Small* **2005**, *1*, 284−299.
(105) Gerling, T.; Wagenbauer, K. F.; Neuner, A. M.; Dietz, H. Dynamic DNA Devices and Assemblies Formed by Shape-Complementary, Non-Base Pairing 3D Components. *Science* **2015**, *347*, 1446−1452.
(106) Hudoba, M. W.; Luo, Y.; Zacharias, A.; Poirier, M. G.; Castro, C. E. Dynamic DNA Origami Device for Measuring Compressive Depletion Forces. *ACS Nano* **2017**, *11*, 6566−6573.
(107) Du, Y.; Dong, S. J. Nucleic Acid Biosensors: Recent Advances and Perspectives. *Anal. Chem.* **2017**, *89*, 189−215.
(108) Bell, N. A. W.; Keyser, U. F. Digitally Encoded DNA Nanostructures for Multiplexed, Single-Molecule Protein Sensing with Nanopores. *Nat. Nanotechnol.* **2016**, *11*, 645−651.
(109) Chandrasekaran, A. R.; Punnoose, J. A.; Zhou, L.; Dey, P.; Dey, B. K.; Halvorsen, K. DNA nanotechnology approaches for microRNA detection and diagnosis. *Nucleic Acids Res.* **2019**, DOI: 10.1093/nar/gkz580.
(110) Mahshid, S. S.; Camire, S.; Ricci, F.; Vallee-Belisle, A. A Highly Selective Electrochemical DNA-Based Sensor That Employs Steric Hindrance Effects to Detect Proteins Directly in Whole Blood. *J. Am. Chem. Soc.* **2015**, *137*, 15596−15599.
(111) Ban, F. F.; Shi, H.; Feng, C.; Mao, X. X.; Yin, Y. M.; Zhu, X. L. A One-Pot Strategy for the Detection of Proteins Based on Sterically and Allosterically Tunable Hybridization Chain Reaction. *Biosens. Bioelectron.* **2016**, *86*, 219−224.
(112) Hansen-Bruhn, M.; Nielsen, L. D. F.; Gothelf, K. V. Rapid Detection of Drugs in Human Plasma Using a Small-Molecule-Linked Hybridization Chain Reaction. *ACS Sensors* **2018**, *3*, 1706−1711.
(113) Shi, H.; Mao, X. X.; Chen, X. X.; Wang, Z. H.; Wang, K. M.; Zhu, X. L. The Analysis of Proteins and Small Molecules Based on Sterically Tunable Nucleic Acid Hyperbranched Rolling Circle Amplification. *Biosens. Bioelectron.* **2017**, *91*, 136−142.
(114) Ou, L. J.; Wang, H. B.; Chu, X. Terminal Protection of Small-Molecule-Linked DNA for Sensitive Fluorescence Detection of Protein Binding Based on Nucleic Acid Amplification. *Analyst* **2013**, *138*, 7218−7223.
(115) Zhang, Z.; Hejesen, C.; Kjelstrup, M. B.; Birkedal, V.; Gothelf, K. V. A DNA-Mediated Homogeneous Binding Assay for Proteins and Small Molecules. *J. Am. Chem. Soc.* **2014**, *136*, 11115−11120.

DOI: 10.1021/acs.chemrev.9b00121
Chem. Rev. XXXX, XXX, XXX−XXX

(116) Porchetta, A.; Ippodrino, R.; Marini, B.; Caruso, A.; Caccuri, F.; Ricci, F. Programmable Nucleic Acid Nanoswitches for the Rapid, Single-Step Detection of Antibodies in Bodily Fluids. *J. Am. Chem. Soc.* **2018**, *140*, 947−953.
(117) Wu, Z.; Zhen, Z.; Jiang, J. H.; Shen, G. L.; Yu, R. Q. Terminal Protection of Small-Molecule-Linked DNA for Sensitive Electrochemical Detection of Protein Binding via Selective Carbon Nanotube Assembly. *J. Am. Chem. Soc.* **2009**, *131*, 12325−12332.
(118) Ranallo, S.; Rossetti, M.; Plaxco, K. W.; Vallee-Belisle, A.; Ricci, F. A Modular, DNA-Based Beacon for Single-Step Fluorescence Detection of Antibodies and Other Proteins Ranallo, Simona; Rossetti, Marianna; Plaxco, Kevin W.; Vallee-Belisle, Alexis; Ricci, Francesco. *Angew. Chem., Int. Ed.* **2015**, *54*, 13214−13218.
(119) Idili, A.; Vallee-Belisle, A.; Ricci, F. Programmable pH-Triggered DNA Nanoswitches. *J. Am. Chem. Soc.* **2014**, *136*, 5836−5839.
(120) Modi, S.; Swetha, M. G.; Goswami, D.; Gupta, G. D.; Mayor, S.; Krishnan, Y. A DNA Nanomachine That Maps Spatial and Temporal pH Changes inside Living Cells. *Nat. Nanotechnol.* **2009**, *4*, 325−330.
(121) Chakraborty, S.; Sharma, S.; Maiti, P. K.; Krishnan, Y. The Poly dA Helix: A New Structural Motif for High Performance DNA-Based Molecular Switches. *Nucleic Acids Res.* **2009**, *37*, 2810−2817.
(122) Burge, S.; Parkinson, G. N.; Hazel, P.; Todd, A. K.; Neidle, S. Quadruplex DNA: Sequence, Topology and Structure. *Nucleic Acids Res.* **2006**, *34*, 5402−5415.
(123) Song, S.; Wang, L.; Li, J.; Fan, C.; Zhao, J. Aptamer-Based Biosensors. *TrAC, Trends Anal. Chem.* **2008**, *27*, 108−117.
(124) Tombelli, S.; Minunni, M.; Mascini, M. Analytical Applications of Aptamers. *Biosens. Bioelectron.* **2005**, *20*, 2424−2434.
(125) Yurke, B.; Turberfield, A. J.; Mills, A. P.; Simmel, F. C.; Neumann, J. L. A DNA-Fuelled Molecular Machine Made of DNA. *Nature* **2000**, *406*, 605−608.
(126) Chandrasekaran, A. R.; Halvorsen, K. Controlled Disassembly of a DNA Tetrahedron Using Strand Displacement. *Nanoscale Advances* **2019**, *1*, 969−972.
(127) Kelley, S. O.; Mirkin, C. A.; Walt, D. R.; Ismagilov, R. F.; Toner, M.; Sargent, E. H. Advancing the Speed, Sensitivity and Accuracy of Biomolecular Detection Using Multi-Length-Scale Engineering. *Nat. Nanotechnol.* **2014**, *9*, 969−980.
(128) Gosling, J. P. A Decade of Development in Immunoassay Methodology. *Clin. Chem.* **1990**, *36*, 1408−1427.
(129) Yang, S.; Rothman, R. E. PCR-Based Diagnostics for Infectious Diseases: Uses, Limitations, and Future Applications in Acute-Care Settings. *Lancet Infect. Dis.* **2004**, *4*, 337−348.
(130) Ellington, A. A.; Kullo, I. J.; Bailey, K. R.; Klee, G. G. Antibody-Based Protein Multiplex Platforms: Technical and Operational Challenges. *Clin. Chem.* **2010**, *56*, 186−193.
(131) Chen, S.; Svedendahl, M.; Van Duyne, R. P.; Kall, M. Plasmon-Enhanced Colorimetric Elisa with Single Molecule Sensitivity. *Nano Lett.* **2011**, *11*, 1826−1830.
(132) Chandrasekaran, A. R. DNA Nanobiosensors: An Outlook on Signal Readout Strategies. *J. Nanomater.* **2017**, *2017*, 2820619.
(133) Chandrasekaran, A. R.; Wady, H.; Subramanian, H. K. K. Nucleic Acid Nanostructures for Chemical and Biological Sensing. *Small* **2016**, *12*, 2689−2700.
(134) Nutiu, R.; Li, Y. F. Structure-Switching Signaling Aptamers: Transducing Molecular Recognition into Fluorescence Signaling. *Chem. - Eur. J.* **2004**, *10*, 1868−1876.
(135) Nutiu, R.; Li, Y. F. Aptamers with Fluorescence-Signaling Properties. *Methods* **2005**, *37*, 16−25.
(136) Onidas, D.; Markovitsi, D.; Marguet, S.; Sharonov, A.; Gustavsson, T. Fluorescence Properties of DNA Nucleosides and Nucleotides: A Refined Steady-State and Femtosecond Investigation. *J. Phys. Chem. B* **2002**, *106*, 11367−11374.
(137) Hall, B. D.; Spiegelman, S. Sequence Complementarity of T2-DNA and T2-Specific RNA. *Proc. Natl. Acad. Sci. U. S. A.* **1961**, *47*, 137−146.
(138) Bolton, E. T.; McCarthy, B. J. A General Method for the Isolation of RNA Complementary to DNA. *Proc. Natl. Acad. Sci. U. S. A.* **1962**, *48*, 1390−1397.
(139) Tyagi, S.; Kramer, F. R. Molecular Beacons: Probes That Fluoresce upon Hybridization. *Nat. Biotechnol.* **1996**, *14*, 303−308.
(140) Chen, A. K.; Davydenko, O.; Behlke, M. A.; Tsourkas, A. Ratiometric Bimolecular Beacons for the Sensitive Detection of RNA in Single Living Cells. *Nucleic Acids Res.* **2010**, *38*, No. e148.
(141) Tan, W. H.; Wang, K. M.; Drake, T. J. Molecular Beacons. *Curr. Opin. Chem. Biol.* **2004**, *8*, 547−553.
(142) Li, J. W. J.; Fang, X. H.; Schuster, S. M.; Tan, W. H. Molecular Beacons: A Novel Approach to Detect Protein-DNA Interactions. *Angew. Chem., Int. Ed.* **2000**, *39*, 1049−1052.
(143) Wang, K. M.; Tang, Z. W.; Yang, C. Y. J.; Kim, Y. M.; Fang, X. H.; Li, W.; Wu, Y. R.; Medley, C. D.; Cao, Z. H.; Li, J.; Colon, P.; Lin, H.; Tan, W. H. Molecular Engineering of DNA: Molecular Beacons. *Angew. Chem., Int. Ed.* **2009**, *48*, 856−870.
(144) Zhang, P.; Beck, T.; Tan, W. H. Design of a Molecular Beacon DNA Probe with Two Fluorophores. *Angew. Chem., Int. Ed.* **2001**, *40*, 402−405.
(145) Tyagi, S.; Bratu, D. P.; Kramer, F. R. Multicolor Molecular Beacons for Allele Discrimination. *Nat. Biotechnol.* **1998**, *16*, 49−53.
(146) Tyagi, S.; Marras, S. A. E.; Kramer, F. R. Wavelength-Shifting Molecular Beacons. *Nat. Biotechnol.* **2000**, *18*, 1191−1196.
(147) Zhang, M.; Guo, S. M.; Li, Y. R.; Zuo, P.; Ye, B. C. A Label-Free Fluorescent Molecular Beacon Based on DNA-Templated Silver Nanoclusters for Detection of Adenosine and Adenosine Deaminase. *Chem. Commun.* **2012**, *48*, 5488−5490.
(148) Yeh, H. C.; Sharma, J.; Han, J. J.; Martinez, J. S.; Werner, J. H. A DNA-Silver Nanocluster Probe That Fluoresces upon Hybridization. *Nano Lett.* **2010**, *10*, 3106−3110.
(149) Lee, C. C.; Liao, Y. C.; Lai, Y. H.; Chuang, M. C. Recognition of Dual Targets by a Molecular Beacon-Based Sensor: Subtyping of Influenza a Virus. *Anal. Chem.* **2015**, *87*, 5410−5416.
(150) Zhang, X. M.; Song, Y.; Shah, A. Y.; Lekova, V.; Raj, A.; Huang, L.; Behlke, M. A.; Tsourkas, A. Quantitative Assessment of Ratiometric Bimolecular Beacons as a Tool for Imaging Single Engineered RNA Transcripts and Measuring Gene Expression in Living Cells. *Nucleic Acids Res.* **2013**, *41*, No. e152.
(151) Bratu, D. P.; Cha, B. J.; Mhlanga, M. M.; Kramer, F. R.; Tyagi, S. Visualizing the Distribution and Transport of mRNAs in Living Cells. *Proc. Natl. Acad. Sci. U. S. A.* **2003**, *100*, 13308−13313.
(152) Santangelo, P. J.; Lifland, A. W.; Curt, P.; Sasaki, Y.; Bassell, G. J.; Lindquist, M. E.; Crowe, J. E. Single Molecule-Sensitive Probes for Imaging RNA in Live Cells. *Nat. Methods* **2009**, *6*, 347−349.
(153) Qiu, L. P.; Wu, C. C.; You, M. X.; Han, D.; Chen, T.; Zhu, G. Z.; Jiang, J. H.; Yu, R. Q.; Tan, W. H. A Targeted, Self-Delivered, and Photocontrolled Molecular Beacon for mRNA Detection in Living Cells. *J. Am. Chem. Soc.* **2013**, *135*, 12952−12955.
(154) Lu, C. H.; Wang, F. A.; Willner, I. Zn^{2+}-Ligation Dnazyme-Driven Enzymatic and Nonenzymatic Cascades for the Amplified Detection of DNA. *J. Am. Chem. Soc.* **2012**, *134*, 10651−10658.
(155) Zuo, X. L.; Xia, F.; Xiao, Y.; Plaxco, K. W. Sensitive and Selective Amplified Fluorescence DNA Detection Based on Exonuclease III-Aided Target Recycling. *J. Am. Chem. Soc.* **2010**, *132*, 1816−1818.
(156) Kong, R. M.; Zhang, X. B.; Zhang, L. L.; Huang, Y.; Lu, D. Q.; Tan, W. H.; Shen, G. L.; Yu, R. Q. Molecular Beacon-Based Junction Probes for Efficient Detection of Nucleic Acids via a True Target-Triggered Enzymatic Recycling Amplification. *Anal. Chem.* **2011**, *83*, 14−17.
(157) Duan, R. X.; Zuo, X. L.; Wang, S. T.; Quan, X. Y.; Chen, D. L.; Chen, Z. F.; Jiang, L.; Fan, C. H.; Xia, F. Lab in a Tube: Ultrasensitive Detection of MicroRNAs at the Single-Cell Level and in Breast Cancer Patients Using Quadratic Isothermal Amplification. *J. Am. Chem. Soc.* **2013**, *135*, 4604−4607.
(158) Lin, X. Y.; Zhang, C.; Huang, Y. S.; Zhu, Z.; Chen, X.; Yang, C. J. Backbone-Modified Molecular Beacons for Highly Sensitive and Selective Detection of MicroRNAs Based on Duplex Specific Nuclease Signal Amplification. *Chem. Commun.* **2013**, *49*, 7243−7245.

DOI: 10.1021/acs.chemrev.9b00121
Chem. Rev. XXXX, XXX, XXX−XXX

(159) Zhang, X. B.; Wang, Z. D.; Xing, H.; Xiang, Y.; Lu, Y. Catalytic and Molecular Beacons for Amplified Detection of Metal Ions and Organic Molecules with High Sensitivity. *Anal. Chem.* **2010**, *82*, 5005−5011.
(160) Huang, J.; Wu, Y. R.; Chen, Y.; Zhu, Z.; Yang, X. H.; Yang, C. J.; Wang, K. M.; Tan, W. H. Pyrene-Excimer Probes Based on the Hybridization Chain Reaction for the Detection of Nucleic Acids in Complex Biological Fluids. *Angew. Chem., Int. Ed.* **2011**, *50*, 401−404.
(161) Huang, J. H.; Gao, X.; Jia, J. J.; Kim, J. K.; Li, Z. G. Graphene Oxide-Based Amplified Fluorescent Biosensor for Hg^{2+} Detection through Hybridization Chain Reactions. *Anal. Chem.* **2014**, *86*, 3209−3215.
(162) Wu, Z.; Liu, G. Q.; Yang, X. L.; Jiang, J. H. Electrostatic Nucleic Acid Nanoassembly Enables Hybridization Chain Reaction in Living Cells for Ultrasensitive mRNA Imaging. *J. Am. Chem. Soc.* **2015**, *137*, 6829−6836.
(163) Ren, J. T.; Wang, J. H.; Han, L.; Wang, E. K.; Wang, J. Kinetically Grafting G-Quadruplexes onto DNA Nanostructures for Structure and Function Encoding via a DNA Machine. *Chem. Commun.* **2011**, *47*, 10563−10565.
(164) Wang, F.; Elbaz, J.; Orbach, R.; Magen, N.; Willner, I. Amplified Analysis of DNA by the Autonomous Assembly of Polymers Consisting of Dnazyme Wires. *J. Am. Chem. Soc.* **2011**, *133*, 17149−17151.
(165) Swierczewska, M.; Lee, S.; Chen, X. Y. The Design and Application of Fluorophore-Gold Nanoparticle Activatable Probes. *Phys. Chem. Chem. Phys.* **2011**, *13*, 9929−9941.
(166) Song, S. P.; Liang, Z. Q.; Zhang, J.; Wang, L. H.; Li, G. X.; Fan, C. H. Gold-Nanoparticle-Based Multicolor Nanobeacons for Sequence-Specific DNA Analysis. *Angew. Chem., Int. Ed.* **2009**, *48*, 8670−8674.
(167) Zheng, D.; Seferos, D. S.; Giljohann, D. A.; Patel, P. C.; Mirkin, C. A. Aptamer Nano-Flares for Molecular Detection in Living Cells. *Nano Lett.* **2009**, *9*, 3258−3261.
(168) Prigodich, A. E.; Seferos, D. S.; Massich, M. D.; Giljohann, D. A.; Lane, B. C.; Mirkin, C. A. Nano-Flares for mRNA Regulation and Detection. *ACS Nano* **2009**, *3*, 2147−2152.
(169) Prigodich, A. E.; Randeria, P. S.; Briley, W. E.; Kim, N. J.; Daniel, W. L.; Giljohann, D. A.; Mirkin, C. A. Multiplexed Nanoflares: mRNA Detection in Live Cells. *Anal. Chem.* **2012**, *84*, 2062−2066.
(170) Halo, T. L.; McMahon, K. M.; Angeloni, N. L.; Xu, Y. L.; Wang, W.; Chinen, A. B.; Malin, D.; Strekalova, E.; Cryns, V. L.; Cheng, C. H.; Mirkin, C. A.; Thaxton, C. S. Nanoflares for the Detection, Isolation, and Culture of Live Tumor Cells from Human Blood. *Proc. Natl. Acad. Sci. U. S. A.* **2014**, *111*, 17104−17109.
(171) Yang, R. H.; Jin, J. Y.; Chen, Y.; Shao, N.; Kang, H. Z.; Xiao, Z.; Tang, Z. W.; Wu, Y. R.; Zhu, Z.; Tan, W. H. Carbon Nanotube-Quenched Fluorescent Oligonucleotides: Probes That Fluoresce upon Hybridization. *J. Am. Chem. Soc.* **2008**, *130*, 8351−8358.
(172) Zhang, L. B.; Tao, L.; Li, B. L.; Jing, L.; Wang, E. K. Carbon Nanotube-DNA Hybrid Fluorescent Sensor for Sensitive and Selective Detection of Mercury(II) Ion. *Chem. Commun.* **2010**, *46*, 1476−1478.
(173) He, S. J.; Song, B.; Li, D.; Zhu, C. F.; Qi, W. P.; Wen, Y. Q.; Wang, L. H.; Song, S. P.; Fang, H. P.; Fan, C. H. A Graphene Nanoprobe for Rapid, Sensitive, and Multicolor Fluorescent DNA Analysis. *Adv. Funct. Mater.* **2010**, *20*, 453−459.
(174) Lu, C. H.; Yang, H. H.; Zhu, C. L.; Chen, X.; Chen, G. N. A Graphene Platform for Sensing Biomolecules. *Angew. Chem., Int. Ed.* **2009**, *48*, 4785−4787.
(175) Wu, W. H.; Hu, H. Y.; Li, F.; Wang, L. H.; Gao, J. M.; Lu, J. X.; Fan, C. H. A Graphene Oxide-Based Nano-Beacon for DNA Phosphorylation Analysis. *Chem. Commun.* **2011**, *47*, 1201−1203.
(176) Lu, C. H.; Li, J.; Zhang, X. L.; Zheng, A. X.; Yang, H. H.; Chen, X.; Chen, G. N. General Approach for Monitoring Peptide-Protein Interactions Based on Graphene-Peptide Complex. *Anal. Chem.* **2011**, *83*, 7276−7282.
(177) Dong, H. F.; Zhang, J.; Ju, H. X.; Lu, H. T.; Wang, S. Y.; Jin, S.; Hao, K. H.; Du, H. W.; Zhang, X. J. Highly Sensitive Multiple MicroRNA Detection Based on Fluorescence Quenching of Graphene Oxide and Isothermal Strand-Displacement Polymerase Reaction. *Anal. Chem.* **2012**, *84*, 4587−4593.
(178) Zhang, M.; Yin, B.-C.; Tan, W.; Ye, B.-C. A Versatile Graphene-Based Fluorescence "On/Off" Switch for Multiplex Detection of Various Targets. *Biosens. Bioelectron.* **2011**, *26*, 3260−3265.
(179) Piao, Y. X.; Liu, F.; Seo, T. S. A Novel Molecular Beacon Bearing a Graphite Nanoparticle as a Nanoquencher for in Situ mRNA Detection in Cancer Cells. *ACS Appl. Mater. Interfaces* **2012**, *4*, 6784−6788.
(180) Zhang, Y. W.; Liu, S.; Wang, L.; Luo, Y. L.; Tian, J. Q.; Asiri, A. M.; Al-Youbi, A. O.; Sun, X. P. Novel Use of Poly(3,4-Ethylenedioxythiophene) Nanoparticles for Fluorescent Nucleic Acid Detection. *ACS Comb. Sci.* **2012**, *14*, 191−196.
(181) Zhang, L. B.; Zhu, J. B.; Guo, S. J.; Li, T.; Li, J.; Wang, E. K. Photoinduced Electron Transfer of DNA/Ag Nanoclusters Modulated by G-Quadruplex/Hemin Complex for the Construction of Versatile Biosensors. *J. Am. Chem. Soc.* **2013**, *135*, 2403−2406.
(182) Yuan, Y. X.; Li, R. Q.; Liu, Z. H. Establishing Water-Soluble Layered WS_2 Nanosheet as a Platform for Biosensing. *Anal. Chem.* **2014**, *86*, 3610−3615.
(183) Xi, Q.; Zhou, D. M.; Kan, Y. Y.; Ge, J.; Wu, Z. K.; Yu, R. Q.; Jiang, J. H. Highly Sensitive and Selective Strategy for MicroRNA Detection Based on WS_2 Nanosheet Mediated Fluorescence Quenching and Duplex-Specific Nuclease Signal Amplification. *Anal. Chem.* **2014**, *86*, 1361−1365.
(184) Tan, C. L.; Qi, X. Y.; Huang, X.; Yang, J.; Zheng, B.; An, Z. F.; Chen, R. F.; Wei, J.; Tang, B. Z.; Huang, W.; Zhang, H. Single-Layer Transition Metal Dichalcogenide Nanosheet-Assisted Assembly of Aggregation-Induced Emission Molecules to Form Organic Nanosheets with Enhanced Fluorescence. *Adv. Mater.* **2014**, *26*, 1735−1739.
(185) Walter, H. K.; Bauer, J.; Steinmeyer, J.; Kuzuya, A.; Niemeyer, C. M.; Wagenknecht, H. A. "DNA Origami Traffic Lights" with a Split Aptamer Sensor for a Bicolor Fluorescence Readout. *Nano Lett.* **2017**, *17*, 2467−2472.
(186) Saha, S.; Prakash, V.; Halder, S.; Chakraborty, K.; Krishnan, Y. A pH-Independent DNA Nanodevice for Quantifying Chloride Transport in Organelles of Living Cells. *Nat. Nanotechnol.* **2015**, *10*, 645−651.
(187) Li, Y. G.; Cu, Y. T. H.; Luo, D. Multiplexed Detection of Pathogen DNA with DNA-Based Fluorescence Nanobarcodes. *Nat. Biotechnol.* **2005**, *23*, 885−889.
(188) Medintz, I. L.; Clapp, A. R.; Mattoussi, H.; Goldman, E. R.; Fisher, B.; Mauro, J. M. Self-Assembled Nanoscale Biosensors Based on Quantum Dot FRET Donors. *Nat. Mater.* **2003**, *2*, 630−638.
(189) Aoki, K.; Matsuda, M. Visualization of Small Gtpase Activity with Fluorescence Resonance Energy Transfer-Based Biosensors. *Nat. Protoc.* **2009**, *4*, 1623−1631.
(190) Hodgson, L.; Chan, E. W. L.; Hahn, K. M.; Yousaf, M. N. Combining Surface Chemistry with a FRET-Based Biosensor to Study the Dynamics of RhoA GTPase Activation in Cells on Patterned Substrates. *J. Am. Chem. Soc.* **2007**, *129*, 9264−9265.
(191) Tu, D. T.; Liu, L. Q.; Ju, Q.; Liu, Y. S.; Zhu, H. M.; Li, R. F.; Chen, X. Y. Time-Resolved FRET Biosensor Based on Amine-Functionalized Lanthanide-Doped $NaYF_4$ Nanocrystals. *Angew. Chem., Int. Ed.* **2011**, *50*, 6306−6310.
(192) Dennis, A. M.; Rhee, W. J.; Sotto, D.; Dublin, S. N.; Bao, G. Quantum Dot-Fluorescent Protein FRET Probes for Sensing Intracellular pH. *ACS Nano* **2012**, *6*, 2917−2924.
(193) Clegg, R. M. Fluorescence Resonance Energy Transfer. *Curr. Opin. Biotechnol.* **1995**, *6*, 103−110.
(194) Sahoo, H. Förster Resonance Energy Transfer−A Spectroscopic Nanoruler: Principle and Applications. *J. Photochem. Photobiol., C* **2011**, *12*, 20−30.
(195) Forster, T. Energiewanderung und Fluoreszenz. *Naturwissenschaften* **1946**, *33*, 166−175.
(196) Förster, T. Zwischenmolekulare Energiewanderung und Fluoreszenz. *Ann. Phys.* **1948**, *437*, 55−75.
(197) Ha, T.; Enderle, T.; Ogletree, D.; Chemla, D. S.; Selvin, P. R.; Weiss, S. Probing the Interaction between Two Single Molecules:

DOI: 10.1021/acs.chemrev.9b00121
Chem. Rev. XXXX, XXX, XXX−XXX

Fluorescence Resonance Energy Transfer between a Single Donor and a Single Acceptor. *Proc. Natl. Acad. Sci. U. S. A.* **1996**, *93*, 6264−6268.
(198) Heim, R.; Tsien, R. Y. Engineering Green Fluorescent Protein for Improved Brightness, Longer Wavelengths and Fluorescence Resonance Energy Transfer. *Curr. Biol.* **1996**, *6*, 178−182.
(199) Selvin, P. R. The Renaissance of Fluorescence Resonance Energy Transfer. *Nat. Struct. Biol.* **2000**, *7*, 730.
(200) Margittai, M.; Widengren, J.; Schweinberger, E.; Schroder, G. F.; Felekyan, S.; Haustein, E.; Konig, M.; Fasshauer, D.; Grubmuller, H.; Jahn, R.; Seidel, C. A. M. Single-Molecule Fluorescence Resonance Energy Transfer Reveals a Dynamic Equilibrium between Closed and Open Conformations of Syntaxin 1. *Proc. Natl. Acad. Sci. U. S. A.* **2003**, *100*, 15516−15521.
(201) Schuler, B.; Eaton, W. A. Protein Folding Studied by Single-Molecule FRET. *Curr. Opin. Struct. Biol.* **2008**, *18*, 16−26.
(202) Santoso, Y.; Joyce, C. M.; Potapova, O.; Le Reste, L.; Hohlbein, J.; Torella, J. P.; Grindley, N. D. F.; Kapanidis, A. N. Conformational Transitions in DNA Polymerase I Revealed by Single-Molecule FRET. *Proc. Natl. Acad. Sci. U. S. A.* **2010**, *107*, 715−720.
(203) Qiu, X.; Guo, J.; Jin, Z.; Petreto, A.; Medintz, I. L.; Hildebrandt, N. Multiplexed Nucleic Acid Hybridization Assays Using Single-FRET-Pair Distance-Tuning. *Small* **2017**, *13*, 1700332.
(204) Fritz, R. D.; Letzelter, M.; Reimann, A.; Martin, K.; Fusco, L.; Ritsma, L.; Ponsioen, B.; Fluri, E.; Schulte-Merker, S.; van Rheenen, J.; Pertz, O. A Versatile Toolkit to Produce Sensitive FRET Biosensors to Visualize Signaling in Time and Space. *Sci. Signaling* **2013**, *6*, rs12.
(205) Hildebrandt, N.; Wegner, K. D.; Algar, W. R. Luminescent Terbium Complexes: Superior Forster Resonance Energy Transfer Donors for Flexible and Sensitive Multiplexed Biosensing. *Coord. Chem. Rev.* **2014**, *273*, 125−138.
(206) Resch-Genger, U.; Grabolle, M.; Cavaliere-Jaricot, S.; Nitschke, R.; Nann, T. Quantum Dots Versus Organic Dyes as Fluorescent Labels. *Nat. Methods* **2008**, *5*, 763−775.
(207) Sapsford, K. E.; Berti, L.; Medintz, I. L. Materials for Fluorescence Resonance Energy Transfer Analysis: Beyond Traditional Donor-Acceptor Combinations. *Angew. Chem., Int. Ed.* **2006**, *45*, 4562−4588.
(208) Nguyen, A. W.; Daugherty, P. S. Evolutionary Optimization of Fluorescent Proteins for Intracellular FRET. *Nat. Biotechnol.* **2005**, *23*, 355−360.
(209) Lam, A. J.; St-Pierre, F.; Gong, Y. Y.; Marshall, J. D.; Cranfill, P. J.; Baird, M. A.; McKeown, M. R.; Wiedenmann, J.; Davidson, M. W.; Schnitzer, M. J.; Tsien, R. Y.; Lin, M. Z. Improving FRET Dynamic Range with Bright Green and Red Fluorescent Proteins. *Nat. Methods* **2012**, *9*, 1005−1012.
(210) Piston, D. W.; Kremers, G. J. Fluorescent Protein FRET: The Good, the Bad and the Ugly. *Trends Biochem. Sci.* **2007**, *32*, 407−414.
(211) Shi, J. Y.; Tian, F.; Lyu, J.; Yang, M. Nanoparticle Based Fluorescence Resonance Energy Transfer (FRET) for Biosensing Applications. *J. Mater. Chem. B* **2015**, *3*, 6989−7005.
(212) Stanisavljevic, M.; Krizkova, S.; Vaculovicova, M.; Kizek, R.; Adam, V. Quantum Dots-Fluorescence Resonance Energy Transfer-Based Nanosensors and Their Application. *Biosens. Bioelectron.* **2015**, *74*, 562−574.
(213) Li, L. L.; Zhang, R. B.; Yin, L. L.; Zheng, K. Z.; Qin, W. P.; Selvin, P. R.; Lu, Y. Biomimetic Surface Engineering of Lanthanide-Doped Upconversion Nanoparticles as Versatile Bioprobes. *Angew. Chem., Int. Ed.* **2012**, *51*, 6121−6125.
(214) Wang, F.; Deng, R. R.; Wang, J.; Wang, Q. X.; Han, Y.; Zhu, H. M.; Chen, X. Y.; Liu, X. G. Tuning Upconversion through Energy Migration in Core-Shell Nanoparticles. *Nat. Mater.* **2011**, *10*, 968−973.
(215) Wang, Y.; Liu, K.; Liu, X. M.; Dohnalova, K.; Gregorkiewicz, T.; Kong, X. G.; Aalders, M. C. G.; Buma, W. J.; Zhang, H. Critical Shell Thickness of Core/Shell Upconversion Luminescence Nanoplatform for FRET Application. *J. Phys. Chem. Lett.* **2011**, *2*, 2083−2088.
(216) Tian, F.; Lyu, J.; Shi, J. Y.; Yang, M. Graphene and Graphene-Like Two-Denominational Materials Based Fluorescence Resonance Energy Transfer (FRET) Assays for Biological Applications. *Biosens. Bioelectron.* **2017**, *89*, 123−135.
(217) Wang, Y.; Li, Z. H.; Wang, J.; Li, J. H.; Lin, Y. H. Graphene and Graphene Oxide: Biofunctionalization and Applications in Biotechnology. *Trends Biotechnol.* **2011**, *29*, 205−212.
(218) Glazer, A. N.; Mathies, R. A. Energy-Transfer Fluorescent Reagents for DNA Analyses. *Curr. Opin. Biotechnol.* **1997**, *8*, 94−102.
(219) Fang, X. H.; Liu, X. J.; Schuster, S.; Tan, W. H. Designing a Novel Molecular Beacon for Surface-Immobilized DNA Hybridization Studies. *J. Am. Chem. Soc.* **1999**, *121*, 2921−2922.
(220) Stein, I. H.; Steinhauer, C.; Tinnefeld, P. Single-Molecule Four-Color FRET Visualizes Energy-Transfer Paths on DNA Origami. *J. Am. Chem. Soc.* **2011**, *133*, 4193−4195.
(221) You, M. X.; Lyu, Y. F.; Han, D.; Qiu, L. P.; Liu, Q. L.; Chen, T.; Wu, C. S.; Peng, L.; Zhang, L. Q.; Bao, G.; Tan, W. H. DNA Probes for Monitoring Dynamic and Transient Molecular Encounters on Live Cell Membranes. *Nat. Nanotechnol.* **2017**, *12*, 453−459.
(222) Jin, Z. W.; Geissler, D.; Qiu, X.; Wegner, K. D.; Hildebrandt, N. A Rapid, Amplification-Free, and Sensitive Diagnostic Assay for Single-Step Multiplexed Fluorescence Detection of MicroRNA. *Angew. Chem., Int. Ed.* **2015**, *54*, 10024−10029.
(223) Chalfie, M. Gfp: Lighting up Life. *Proc. Natl. Acad. Sci. U. S. A.* **2009**, *106*, 10073−10080.
(224) Patterson, G. H.; Piston, D. W.; Barisas, B. G. Forster Distances between Green Fluorescent Protein Pairs. *Anal. Biochem.* **2000**, *284*, 438−440.
(225) Han, X. G.; Zhou, Z. H.; Yang, F.; Deng, Z. X. Catch and Release: DNA Tweezers That Can Capture, Hold, and Release an Object under Control. *J. Am. Chem. Soc.* **2008**, *130*, 14414−14415.
(226) Dittmer, W. U.; Reuter, A.; Simmel, F. C. A DNA-Based Machine That Can Cyclically Bind and Release Thrombin. *Angew. Chem., Int. Ed.* **2004**, *43*, 3550−3553.
(227) Quan, K.; Huang, J.; Yang, X. H.; Yang, Y. J.; Ying, L.; Wang, H.; Xie, N. L.; Ou, M.; Wang, K. M. Powerful Amplification Cascades of FRET-Based Two-Layer Nonenzymatic Nucleic Acid Circuits. *Anal. Chem.* **2016**, *88*, 5857−5864.
(228) Wang, H. M.; Li, C. X.; Liu, X. Q.; Zhou, X.; Wang, F. Construction of an Enzyme-Free Concatenated DNA Circuit for Signal Amplification and Intracellular Imaging. *Chem. Sci.* **2018**, *9*, 5842−5849.
(229) Pan, W.; Li, Y. L.; Wang, M. M.; Yang, H. J.; Li, N.; Tang, B. FRET-Based Nanoprobes for Simultaneous Monitoring of Multiple mRNAs in Living Cells Using Single Wavelength Excitation. *Chem. Commun.* **2016**, *52*, 4569−4572.
(230) Yang, Y. J.; Huang, J.; Yang, X. H.; Quan, K.; Wang, H.; Ying, L.; Xie, N. L.; Ou, M.; Wang, K. M. FRET Nanoflares for Intracellular mRNA Detection: Avoiding False Positive Signals and Minimizing Effects of System Fluctuations. *J. Am. Chem. Soc.* **2015**, *137*, 8340−8343.
(231) Xie, N. L.; Huang, J.; Yang, X. H.; Yang, Y. J.; Quan, K.; Ou, M.; Fang, H. M.; Wang, K. M. Competition-Mediated FRET-Switching DNA Tetrahedron Molecular Beacon for Intracellular Molecular Detection. *ACS Sensors* **2016**, *1*, 1445−1452.
(232) Zheng, X. F.; Peng, R. Z.; Jiang, X.; Wang, Y. Y.; Xu, S.; Ke, G. L.; Fu, T.; Liu, Q. L.; Huan, S. Y.; Zhang, X. B. Fluorescence Resonance Energy Transfer-Based DNA Nanoprism with a Split Aptamer for Adenosine Triphosphate Sensing in Living Cells. *Anal. Chem.* **2017**, *89*, 10941−10947.
(233) Ye, W. W.; Tsang, M. K.; Liu, X.; Yang, M.; Hao, J. H. Upconversion Luminescence Resonance Energy Transfer (LRET)-Based Biosensor for Rapid and Ultrasensitive Detection of Avian Influenza Virus H7 Subtype. *Small* **2014**, *10*, 2390−2397.
(234) Dong, H. F.; Gao, W. C.; Yan, F.; Ji, H. X.; Ju, H. X. Fluorescence Resonance Energy Transfer between Quantum Dots and Graphene Oxide for Sensing Biomolecules. *Anal. Chem.* **2010**, *82*, 5511−5517.
(235) Shi, J. Y.; Chan, C. Y.; Pang, Y. T.; Ye, W. W.; Tian, F.; Lyu, J.; Zhang, Y.; Yang, M. A Fluorescence Resonance Energy Transfer (FRET) Biosensor Based on Graphene Quantum Dots (GQDs) and Gold Nanoparticles (AuNPs) for the Detection of mecA Gene

DOI: 10.1021/acs.chemrev.9b00121
Chem. Rev. XXXX, XXX, XXX−XXX

Sequence of *Staphylococcus Aureus*. *Biosens. Bioelectron.* **2015**, *67*, 595−600.
(236) Wang, Y.; Li, Z. H.; Hu, D. H.; Lin, C. T.; Li, J. H.; Lin, Y. H. Aptamer/Graphene Oxide Nanocomplex for in Situ Molecular Probing in Living Cells. *J. Am. Chem. Soc.* **2010**, *132*, 9274−9276.
(237) Lee, J.; Kim, J.; Kim, S.; Min, D. H. Biosensors Based on Graphene Oxide and Its Biomedical Application. *Adv. Drug Delivery Rev.* **2016**, *105*, 275−287.
(238) Zhang, X. L.; Zheng, C.; Guo, S. S.; Li, J.; Yang, H. H.; Chen, G. N. Turn-on Fluorescence Sensor for Intracellular Imaging of Glutathione Using g-C_3N_4 Nanosheet-MnO_2 Sandwich Nanocomposite. *Anal. Chem.* **2014**, *86*, 3426−3434.
(239) Chimene, D.; Alge, D. L.; Gaharwar, A. K. Two-Dimensional Nanomaterials for Biomedical Applications: Emerging Trends and Future Prospects. *Adv. Mater.* **2015**, *27*, 7261−7284.
(240) Zrazhevskiy, P.; Sena, M.; Gao, X. H. Designing Multifunctional Quantum Dots for Bioimaging, Detection, and Drug Delivery. *Chem. Soc. Rev.* **2010**, *39*, 4326−4354.
(241) Michalet, X.; Pinaud, F. F.; Bentolila, L. A.; Tsay, J. M.; Doose, S.; Li, J. J.; Sundaresan, G.; Wu, A. M.; Gambhir, S. S.; Weiss, S. Quantum Dots for Live Cells, in Vivo Imaging, and Diagnostics. *Science* **2005**, *307*, 538−544.
(242) Medintz, I. L.; Mattoussi, H. Quantum Dot-Based Resonance Energy Transfer and Its Growing Application in Biology. *Phys. Chem. Chem. Phys.* **2009**, *11*, 17−45.
(243) Hines, M. A.; Guyot-Sionnest, P. Synthesis and Characterization of Strongly Luminescing ZnS-Capped CdSe Nanocrystals. *J. Phys. Chem.* **1996**, *100*, 468−471.
(244) Nirmal, M.; Brus, L. Luminescence Photophysics in Semiconductor Nanocrystals. *Acc. Chem. Res.* **1999**, *32*, 407−414.
(245) Zhang, Y.; Wang, T. H. Quantum Dot Enabled Molecular Sensing and Diagnostics. *Theranostics* **2012**, *2*, 631−654.
(246) Algar, W. R.; Krull, U. J. Quantum Dots as Donors in Fluorescence Resonance Energy Transfer for the Bioanalysis of Nucleic Acids, Proteins, and Other Biological Molecules. *Anal. Bioanal. Chem.* **2008**, *391*, 1609−1618.
(247) Alivisatos, A. P.; Gu, W. W.; Larabell, C. Quantum Dots as Cellular Probes. *Annu. Rev. Biomed. Eng.* **2005**, *7*, 55−76.
(248) Probst, C. E.; Zrazhevskiy, P.; Bagalkot, V.; Gao, X. H. Quantum Dots as a Platform for Nanoparticle Drug Delivery Vehicle Design. *Adv. Drug Delivery Rev.* **2013**, *65*, 703−718.
(249) Yu, W. W.; Qu, L. H.; Guo, W. Z.; Peng, X. G. Experimental Determination of the Extinction Coefficient of CdTe, CdSe, and CdS Nanocrystals. *Chem. Mater.* **2003**, *15*, 2854−2860.
(250) Sun, J. J.; Goldys, E. M. Linear Absorption and Molar Extinction Coefficients in Direct Semiconductor Quantum Dots. *J. Phys. Chem. C* **2008**, *112*, 9261−9266.
(251) Kim, J. H.; Morikis, D.; Ozkan, M. Adaptation of Inorganic Quantum Dots for Stable Molecular Beacons. *Sens. Actuators, B* **2004**, *102*, 315−319.
(252) Kudr, J.; Richtera, L.; Xhaxhiu, K.; Hynek, D.; Heger, Z.; Zitka, O.; Adam, V. Carbon Dots Based FRET for the Detection of DNA Damage. *Biosens. Bioelectron.* **2017**, *92*, 133−139.
(253) Zhang, C. Y.; Yeh, H. C.; Kuroki, M. T.; Wang, T. H. Single-Quantum-Dot-Based DNA Nanosensor. *Nat. Mater.* **2005**, *4*, 826−831.
(254) Peng, H.; Zhang, L. J.; Kjallman, T. H. M.; Soeller, C.; Travas-Sejdic, J. DNA Hybridization Detection with Blue Luminescent Quantum Dots and Dye-Labeled Single-Stranded DNA. *J. Am. Chem. Soc.* **2007**, *129*, 3048−3049.
(255) Jiang, G. X.; Susha, A. S.; Lutich, A. A.; Stefani, F. D.; Feldmann, J.; Rogach, A. L. Cascaded FRET in Conjugated Polymer/Quantum Dot/Dye-Labeled DNA Complexes for DNA Hybridization Detection. *ACS Nano* **2009**, *3*, 4127−4131.
(256) Algar, W. R.; Krull, U. J. Toward a Multiplexed Solid-Phase Nucleic Acid Hybridization Assay Using Quantum Dots as Donors in Fluorescence Resonance Energy Transfer. *Anal. Chem.* **2009**, *81*, 4113−4120.
(257) Algar, W. R.; Krull, U. J. Interfacial Transduction of Nucleic Acid Hybridization Using Immobilized Quantum Dots as Donors in Fluorescence Resonance Energy Transfer. *Langmuir* **2009**, *25*, 633−638.
(258) Algar, W. R.; Krull, U. J. Developing Mixed Films of Immobilized Oligonucleotides and Quantum Dots for the Multiplexed Detection of Nucleic Acid Hybridization Using a Combination of Fluorescence Resonance Energy Transfer and Direct Excitation of Fluorescence. *Langmuir* **2010**, *26*, 6041−6047.
(259) Qiu, X.; Hildebrandt, N. Rapid and Multiplexed Microrna Diagnostic Assay Using Quantum Dot-Based Forster Resonance Energy Transfer. *ACS Nano* **2015**, *9*, 8449−8457.
(260) Chi, C. W.; Lao, Y. H.; Li, Y. S.; Chen, L. C. A Quantum Dot-Aptamer Beacon Using a DNA Intercalating Dye as the FRET Reporter: Application to Label-Free Thrombin Detection. *Biosens. Bioelectron.* **2011**, *26*, 3346−3352.
(261) Wagner, M. K.; Li, F.; Li, J. J.; Li, X. F.; Le, X. C. Use of Quantum Dots in the Development of Assays for Cancer Biomarkers. *Anal. Bioanal. Chem.* **2010**, *397*, 3213−3224.
(262) Cheng, A. K. H.; Su, H. P.; Wang, A.; Yu, H. Z. Aptamer-Based Detection of Epithelial Tumor Marker Mucin 1 with Quantum Dot-Based Fluorescence Readout. *Anal. Chem.* **2009**, *81*, 6130−6139.
(263) Li, L.; Tian, G. J.; Luo, Y.; Brismar, H.; Fu, Y. Blinking, Flickering, and Correlation in Fluorescence of Single Colloidal CdSe Quantum Dots with Different Shells under Different Excitations. *J. Phys. Chem. C* **2013**, *117*, 4844−4851.
(264) Boeneman, K.; Deschamps, J. R.; Buckhout-White, S.; Prasuhn, D. E.; Blanco-Canosa, J. B.; Dawson, P. E.; Stewart, M. H.; Susumu, K.; Goldman, E. R.; Ancona, M.; Medintz, I. L. Quantum Dot DNA Bioconjugates: Attachment Chemistry Strongly Influences the Resulting Composite Architecture. *ACS Nano* **2010**, *4*, 7253−7266.
(265) Wu, W. T.; Shen, J.; Banerjee, P.; Zhou, S. Q. Core-Shell Hybrid Nanogels for Integration of Optical Temperature-Sensing, Targeted Tumor Cell Imaging, and Combined Chemo-Photothermal Treatment. *Biomaterials* **2010**, *31*, 7555−7566.
(266) Gao, J. H.; Chen, K.; Miao, Z.; Ren, G.; Chen, X. Y.; Gambhir, S. S.; Cheng, Z. Affibody-Based Nanoprobes for HER2-Expressing Cell and Tumor Imaging. *Biomaterials* **2011**, *32*, 2141−2148.
(267) Li, J. M.; Zhao, M. X.; Su, H.; Wang, Y. Y.; Tan, C. P.; Ji, L. N.; Mao, Z. W. Multifunctional Quantum-Dot-Based siRNA Delivery for HPV18 E6 Gene Silence and Intracellular Imaging. *Biomaterials* **2011**, *32*, 7978−7987.
(268) Haase, M.; Schäfer, H. Upconverting Nanoparticles. *Angew. Chem., Int. Ed.* **2011**, *50*, 5808−5829.
(269) Auzel, F. Upconversion and Anti-Stokes Processes with F and D Ions in Solids. *Chem. Rev.* **2004**, *104*, 139−173.
(270) Chen, G. Y.; Qju, H. L.; Prasad, P. N.; Chen, X. Y. Upconversion Nanoparticles: Design, Nanochemistry, and Applications in Theranostics. *Chem. Rev.* **2014**, *114*, 5161−5214.
(271) Zhang, P.; Rogelj, S.; Nguyen, K.; Wheeler, D. Design of a Highly Sensitive and Specific Nucleotide Sensor Based on Photon Upconverting Particles. *J. Am. Chem. Soc.* **2006**, *128*, 12410−12411.
(272) Chen, Z. G.; Chen, H. L.; Hu, H.; Yu, M. X.; Li, F. Y.; Zhang, Q.; Zhou, Z. G.; Yi, T.; Huang, C. H. Versatile Synthesis Strategy for Carboxylic Acid-Functionalized Upconverting Nanophosphors as Biological Labels. *J. Am. Chem. Soc.* **2008**, *130*, 3023−3029.
(273) Hwang, S. H.; Im, S. G.; Sung, H.; Hah, S. S.; Cong, V. T.; Lee, D. H.; Son, S. J.; Oh, H. B. Upconversion Nanoparticle-Based Forster Resonance Energy Transfer for Detecting the IS6110 Sequence of Mycobacterium Tuberculosis Complex in Sputum. *Biosens. Bioelectron.* **2014**, *53*, 112−116.
(274) Wu, B.; Cao, Z. Q.; Zhang, Q.; Wang, G. J. NIR-Responsive DNA Hybridization Detection by High Efficient FRET from 10-nm Upconversion Nanoparticles to SYBR Green I. *Sens. Actuators, B* **2018**, *255*, 2853−2860.
(275) Chen, H. Q.; Yuan, F.; Wang, S. Z.; Xu, J.; Zhang, Y. Y.; Wang, L. Aptamer-Based Sensing for Thrombin in Red Region via Fluorescence Resonant Energy Transfer between $NaYF_4$: Yb, Er Upconversion Nanoparticles and Gold Nanorods. *Biosens. Bioelectron.* **2013**, *48*, 19−25.

DOI: 10.1021/acs.chemrev.9b00121
Chem. Rev. XXXX, XXX, XXX−XXX

(276) Ye, W. W.; Tsang, M. K.; Liu, X.; Yang, M.; Hao, J. Upconversion Luminescence Resonance Energy Transfer (LRET)-Based Biosensor for Rapid and Ultrasensitive Detection of Avian Influenza Virus H7 Subtype. *Small* **2014**, *10*, 2390−2397.
(277) Tsang, M. K.; Ye, W. W.; Wang, G. J.; Li, J. M.; Yang, M.; Hao, J. H. Ultrasensitive Detection of Ebola Virus Oligonucleotide Based on Upconversion Nanoprobe/Nanoporous Membrane System. *ACS Nano* **2016**, *10*, 598−605.
(278) Li, S.; Xu, L. G.; Ma, W.; Wu, X. L.; Sun, M. Z.; Kuang, H.; Wang, L. B.; Kotov, N. A.; Xu, C. L. Dual-Mode Ultrasensitive Quantification of MicroRNA in Living Cells by Chiroplasmonic Nanopyramids Self-Assembled from Gold and Upconversion Nanoparticles. *J. Am. Chem. Soc.* **2016**, *138*, 306−312.
(279) Wu, S. J.; Duan, N.; Ma, X. Y.; Xia, Y.; Wang, H. G.; Wang, Z. P.; Zhang, Q. Multiplexed Fluorescence Resonance Energy Transfer Aptasensor between Upconversion Nanoparticles and Graphene Oxide for the Simultaneous Determination of Mycotoxins. *Anal. Chem.* **2012**, *84*, 6263−6270.
(280) Liu, C. H.; Wang, Z.; Jia, H. X.; Li, Z. P. Efficient Fluorescence Resonance Energy Transfer between Upconversion Nanophosphors and Graphene Oxide: A Highly Sensitive Biosensing Platform. *Chem. Commun.* **2011**, *47*, 4661−4663.
(281) Alonso-Cristobal, P.; Vilela, P.; El-Sagheer, A.; Lopez-Cabarcos, E.; Brown, T.; Muskens, O. L.; Rubio-Retama, J.; Kanaras, A. G. Highly Sensitive DNA Sensor Based on Upconversion Nanoparticles and Graphene Oxide. *ACS Appl. Mater. Interfaces* **2015**, *7*, 12422−12429.
(282) Li, H.; Sun, D. E.; Liu, Y. J.; Liu, Z. H. An Ultrasensitive Homogeneous Aptasensor for Kanamycin Based on Upconversion Fluorescence Resonance Energy Transfer. *Biosens. Bioelectron.* **2014**, *55*, 149−156.
(283) Resch-Genger, U.; Gorris, H. H. Perspectives and Challenges of Photon-Upconversion Nanoparticles-Part I: Routes to Brighter Particles and Quantitative Spectroscopic Studies. *Anal. Bioanal. Chem.* **2017**, *409*, 5855−5874.
(284) Gorris, H. H.; Resch-Genger, U. Perspectives and Challenges of Photon-Upconversion Nanoparticles-Part II: Bioanalytical Applications. *Anal. Bioanal. Chem.* **2017**, *409*, 5875−5890.
(285) Lin, M.; Zhao, Y.; Wang, S. Q.; Liu, M.; Duan, Z. F.; Chen, Y. M.; Li, F.; Xu, F.; Lu, T. J. Recent Advances in Synthesis and Surface Modification of Lanthanide-Doped Upconversion Nanoparticles for Biomedical Applications. *Biotechnol. Adv.* **2012**, *30*, 1551−1561.
(286) Sedlmeier, A.; Gorris, H. H. Surface Modification and Characterization of Photon-Upconverting Nanoparticles for Bioanalytical Applications. *Chem. Soc. Rev.* **2015**, *44*, 1526−1560.
(287) Gu, Z. J.; Yan, L.; Tian, G.; Li, S. J.; Chai, Z. F.; Zhao, Y. L. Recent Advances in Design and Fabrication of Upconversion Nanoparticles and Their Safe Theranostic Applications. *Adv. Mater.* **2013**, *25*, 3758−3779.
(288) Wang, F.; Han, Y.; Lim, C. S.; Lu, Y. H.; Wang, J.; Xu, J.; Chen, H. Y.; Zhang, C.; Hong, M. H.; Liu, X. G. Simultaneous Phase and Size Control of Upconversion Nanocrystals through Lanthanide Doping. *Nature* **2010**, *463*, 1061−1065.
(289) Zhang, H.; Li, Y. J.; Ivanov, I. A.; Qu, Y. Q.; Huang, Y.; Duan, X. F. Plasmonic Modulation of the Upconversion Fluorescence in $NaYF_4$:Yb/Tm Hexaplate Nanocrystals Using Gold Nanoparticles or Nanoshells. *Angew. Chem., Int. Ed.* **2010**, *49*, 2865−2868.
(290) Novoselov, K. S.; Geim, A. K.; Morozov, S. V.; Jiang, D.; Zhang, Y.; Dubonos, S. V.; Grigorieva, I. V.; Firsov, A. A. Electric Field Effect in Atomically Thin Carbon Films. *Science* **2004**, *306*, 666−669.
(291) Novoselov, K. S.; Jiang, D.; Schedin, F.; Booth, T. J.; Khotkevich, V. V.; Morozov, S. V.; Geim, A. K. Two-Dimensional Atomic Crystals. *Proc. Natl. Acad. Sci. U. S. A.* **2005**, *102*, 10451−10453.
(292) Schedin, F.; Geim, A. K.; Morozov, S. V.; Hill, E. W.; Blake, P.; Katsnelson, M. I.; Novoselov, K. S. Detection of Individual Gas Molecules Adsorbed on Graphene. *Nat. Mater.* **2007**, *6*, 652−655.
(293) Li, L. S.; Yan, X. Colloidal Graphene Quantum Dots. *J. Phys. Chem. Lett.* **2010**, *1*, 2572−2576.
(294) Eda, G.; Lin, Y. Y.; Mattevi, C.; Yamaguchi, H.; Chen, H. A.; Chen, I. S.; Chen, C. W.; Chhowalla, M. Blue Photoluminescence from Chemically Derived Graphene Oxide. *Adv. Mater.* **2010**, *22*, 505−509.
(295) Gokus, T.; Nair, R. R.; Bonetti, A.; Bohmler, M.; Lombardo, A.; Novoselov, K. S.; Geim, A. K.; Ferrari, A. C.; Hartschuh, A. Making Graphene Luminescent by Oxygen Plasma Treatment. *ACS Nano* **2009**, *3*, 3963−3968.
(296) Luo, Z. T.; Vora, P. M.; Mele, E. J.; Johnson, A. T. C.; Kikkawa, J. M. Photoluminescence and Band Gap Modulation in Graphene Oxide. *Appl. Phys. Lett.* **2009**, *94*, 111909.
(297) Mei, Q. S.; Zhang, K.; Guan, G. J.; Liu, B. H.; Wang, S. H.; Zhang, Z. P. Highly Efficient Photoluminescent Graphene Oxide with Tunable Surface Properties. *Chem. Commun.* **2010**, *46*, 7319−7321.
(298) Galande, C.; Mohite, A. D.; Naumov, A. V.; Gao, W.; Ci, L. J.; Ajayan, A.; Gao, H.; Srivastava, A.; Weisman, R. B.; Ajayan, P. M. Quasi-Molecular Fluorescence from Graphene Oxide. *Sci. Rep.* **2011**, *1*, 85.
(299) Liu, F.; Choi, J. Y.; Seo, T. S. Graphene Oxide Arrays for Detecting Specific DNA Hybridization by Fluorescence Resonance Energy Transfer. *Biosens. Bioelectron.* **2010**, *25*, 2361−2365.
(300) Jung, J. H.; Cheon, D. S.; Liu, F.; Lee, K. B.; Seo, T. S. A Graphene Oxide Based Immuno-Biosensor for Pathogen Detection. *Angew. Chem., Int. Ed.* **2010**, *49*, 5708−5711.
(301) Mei, Q. S.; Zhang, Z. P. Photoluminescent Graphene Oxide Ink to Print Sensors onto Microporous Membranes for Versatile Visualization Bioassays. *Angew. Chem., Int. Ed.* **2012**, *51*, 5602−5606.
(302) Zhu, S. J.; Zhang, J. H.; Tang, S. J.; Qiao, C. Y.; Wang, L.; Wang, H. Y.; Liu, X.; Li, B.; Li, Y. F.; Yu, W. L.; Wang, X. F.; Sun, H. C.; Yang, B. Surface Chemistry Routes to Modulate the Photoluminescence of Graphene Quantum Dots: From Fluorescence Mechanism to Up-Conversion Bioimaging Applications. *Adv. Funct. Mater.* **2012**, *22*, 4732−4740.
(303) Shen, J. H.; Zhu, Y. H.; Chen, C.; Yang, X. L.; Li, C. Z. Facile Preparation and Upconversion Luminescence of Graphene Quantum Dots. *Chem. Commun.* **2011**, *47*, 2580−2582.
(304) Pan, D. Y.; Zhang, J. C.; Li, Z.; Wu, M. H. Hydrothermal Route for Cutting Graphene Sheets into Blue-Luminescent Graphene Quantum Dots. *Adv. Mater.* **2010**, *22*, 734−738.
(305) Li, Y.; Hu, Y.; Zhao, Y.; Shi, G. Q.; Deng, L. E.; Hou, Y. B.; Qu, L. T. An Electrochemical Avenue to Green-Luminescent Graphene Quantum Dots as Potential Electron-Acceptors for Photovoltaics. *Adv. Mater.* **2011**, *23*, 776−780.
(306) Zhou, X. J.; Zhang, Y.; Wang, C.; Wu, X. C.; Yang, Y. Q.; Zheng, B.; Wu, H. X.; Guo, S. W.; Zhang, J. Y. Photo-Fenton Reaction of Graphene Oxide: A New Strategy to Prepare Graphene Quantum Dots for DNA Cleavage. *ACS Nano* **2012**, *6*, 6592−6599.
(307) Tetsuka, H.; Asahi, R.; Nagoya, A.; Okamoto, K.; Tajima, I.; Ohta, R.; Okamoto, A. Optically Tunable Amino-Functionalized Graphene Quantum Dots. *Adv. Mater.* **2012**, *24*, 5333−5338.
(308) Zhu, S. J.; Zhang, J. H.; Qiao, C. Y.; Tang, S. J.; Li, Y. F.; Yuan, W. J.; Li, B.; Tian, L.; Liu, F.; Hu, R.; Gao, H. N.; Wei, H. T.; Zhang, H.; Sun, H. C.; Yang, B. Strongly Green-Photoluminescent Graphene Quantum Dots for Bioimaging Applications. *Chem. Commun.* **2011**, *47*, 6858−6860.
(309) Yan, X.; Cui, X.; Li, B. S.; Li, L. S. Large, Solution-Processable Graphene Quantum Dots as Light Absorbers for Photovoltaics. *Nano Lett.* **2010**, *10*, 1869−1873.
(310) Liu, F.; Jang, M. H.; Ha, H. D.; Kim, J. H.; Cho, Y. H.; Seo, T. S. Facile Synthetic Method for Pristine Graphene Quantum Dots and Graphene Oxide Quantum Dots: Origin of Blue and Green Luminescence. *Adv. Mater.* **2013**, *25*, 3657−3662.
(311) Yang, F.; Zhao, M. L.; Zheng, B. Z.; Xiao, D.; Wu, L.; Guo, Y. Influence of pH on the Fluorescence Properties of Graphene Quantum Dots Using Ozonation Pre-Oxide Hydrothermal Synthesis. *J. Mater. Chem.* **2012**, *22*, 25471−25479.
(312) Zhuo, S. J.; Shao, M. W.; Lee, S. T. Upconversion and Downconversion Fluorescent Graphene Quantum Dots: Ultrasonic Preparation and Photocatalysis. *ACS Nano* **2012**, *6*, 1059−1064.
(313) Pal, S. K. Versatile Photoluminescence from Graphene and Its Derivatives. *Carbon* **2015**, *88*, 86−112.

DOI: 10.1021/acs.chemrev.9b00121
Chem. Rev. XXXX, XXX, XXX−XXX

(314) Qian, Z. S.; Shan, X. Y.; Chai, L. J.; Ma, J. J.; Chen, J. R.; Feng, H. DNA Nanosensor Based on Biocompatible Graphene Quantum Dots and Carbon Nanotubes. *Biosens. Bioelectron.* **2014**, *60*, 64−70.
(315) Qian, Z. S.; Shan, X. Y.; Chai, L. J.; Chen, J. R.; Feng, H. Simultaneous Detection of Multiple DNA Targets by Integrating Dual-Color Graphene Quantum Dot Nanoprobes and Carbon Nanotubes. *Chem. - Eur. J.* **2014**, *20*, 16065−16069.
(316) Qian, Z. S.; Shan, X. Y.; Chai, L. J.; Ma, J. J.; Chen, J. R.; Feng, H. A Universal Fluorescence Sensing Strategy Based on Biocompatible Graphene Quantum Dots and Graphene Oxide for the Detection of DNA. *Nanoscale* **2014**, *6*, 5671−5674.
(317) He, Y. H.; Wen, X. Y.; Zhang, B. Y.; Fan, Z. F. Novel Aptasensor for the Ultrasensitive Detection of Kanamycin Based on Grapheneoxide Quantum-Dot-Linked Single-Stranded DNA-Binding Protein. *Sens. Actuators, B* **2018**, *265*, 20−26.
(318) Niu, X.; Zhong, Y.; Chen, R.; Wang, F.; Liu, Y.; Luo, D. A "Turn-on" Fluorescence Sensor for Pb^{2+} Detection Based on Graphene Quantum Dots and Gold Nanoparticles. *Sens. Actuators, B* **2018**, *255*, 1577−1581.
(319) Ping, J. F.; Zhou, Y. B.; Wu, Y. Y.; Papper, V.; Boujday, S.; Marks, R. S.; Steele, T. W. J. Recent Advances in Aptasensors Based on Graphene and Graphene-Like Nanomaterials. *Biosens. Bioelectron.* **2015**, *64*, 373−385.
(320) Gan, Z. X.; Xu, H.; Hao, Y. L. Mechanism for Excitation-Dependent Photoluminescence from Graphene Quantum Dots and Other Graphene Oxide Derivates: Consensus, Debates and Challenges. *Nanoscale* **2016**, *8*, 7794−7807.
(321) Valencia, P. M.; Farokhzad, O. C.; Karnik, R.; Langer, R. Microfluidic Technologies for Accelerating the Clinical Translation of Nanoparticles. *Nat. Nanotechnol.* **2012**, *7*, 623−629.
(322) Ray, P. C.; Khan, S. A.; Singh, A. K.; Senapati, D.; Fan, Z. Nanomaterials for Targeted Detection and Photothermal Killing of Bacteria. *Chem. Soc. Rev.* **2012**, *41*, 3193−3209.
(323) Konvalina, G.; Haick, H. Sensors for Breath Testing: From Nanomaterials to Comprehensive Disease Detection. *Acc. Chem. Res.* **2014**, *47*, 66−76.
(324) Zhou, W.; Gao, X.; Liu, D. B.; Chen, X. Y. Gold Nanoparticles for in Vitro Diagnostics. *Chem. Rev.* **2015**, *115*, 10575−10636.
(325) Lu, C. H.; Willner, B.; Willner, I. DNA Nanotechnology: From Sensing and DNA Machines to Drug-Delivery Systems. *ACS Nano* **2013**, *7*, 8320−8332.
(326) Liang, H.; Zhang, X. B.; Lv, Y. F.; Gong, L.; Wang, R. W.; Zhu, X. Y.; Yang, R. H.; Tan, W. H. Functional DNA-Containing Nanomaterials: Cellular Applications in Biosensing, Imaging, and Targeted Therapy. *Acc. Chem. Res.* **2014**, *47*, 1891−1901.
(327) Jin, Y.; Li, H. Y.; Bai, J. Y. Homogeneous Selecting of a Quadruplex-Binding Ligand-Based Gold Nanoparticle Fluorescence Resonance Energy Transfer Assay. *Anal. Chem.* **2009**, *81*, 5709−5715.
(328) Chandrasekaran, A. R. DNA-Nanoparticle Tinkertoys. *ChemBioChem* **2016**, *17*, 1090−1092.
(329) Fan, C. H.; Wang, S.; Hong, J. W.; Bazan, G. C.; Plaxco, K. W.; Heeger, A. J. Beyond Superquenching: Hyper-Efficient Energy Transfer from Conjugated Polymers to Gold Nanoparticles. *Proc. Natl. Acad. Sci. U. S. A.* **2003**, *100*, 6297−6301.
(330) Chen, L. Z.; Chao, J.; Qu, X. M.; Zhang, H. B.; Zhu, D.; Su, S.; Aldalbahi, A.; Wang, L. H.; Pei, H. Probing Cellular Molecules with PolyA-Based Engineered Aptamer Nanobeacon. *ACS Appl. Mater. Interfaces* **2017**, *9*, 8014−8020.
(331) Seferos, D. S.; Giljohann, D. A.; Hill, H. D.; Prigodich, A. E.; Mirkin, C. A. Nano-Flares: Probes for Transfection and mRNA Detection in Living Cells. *J. Am. Chem. Soc.* **2007**, *129*, 15477−15479.
(332) Wu, P. W.; Hwang, K. V.; Lan, T.; Lu, Y. A DNAzyme-Gold Nanoparticle Probe for Uranyl Ion in Living Cells. *J. Am. Chem. Soc.* **2013**, *135*, 5254−5257.
(333) Qu, X. M.; Zhu, D.; Yao, G. B.; Su, S.; Chao, J.; Liu, H. J.; Zuo, X. L.; Wang, L. H.; Shi, J. Y.; Wang, L. H.; Huang, W.; Pei, H.; Fan, C. H. An Exonuclease III-Powered, on-Particle Stochastic DNA Walker. *Angew. Chem., Int. Ed.* **2017**, *56*, 1855−1858.
(334) Srivastava, S.; Frankamp, B. L.; Rotello, V. M. Controlled Plasmon Resonance of Gold Nanoparticles Self-Assembled with Pamam Dendrimers. *Chem. Mater.* **2005**, *17*, 487−490.
(335) Lee, J. S.; Han, M. S.; Mirkin, C. A. Colorimetric Detection of Mercuric Ion (Hg^{2+}) in Aqueous Media Using DNA-Functionalized Gold Nanoparticles. *Angew. Chem., Int. Ed.* **2007**, *46*, 4093−4096.
(336) Xue, X. J.; Wang, F.; Liu, X. G. One-Step, Room Temperature, Colorimetric Detection of Mercury (Hg^{2+}) Using DNA/Nanoparticle Conjugates. *J. Am. Chem. Soc.* **2008**, *130*, 3244−3245.
(337) Wang, J.; Wang, L. H.; Liu, X. F.; Liang, Z. Q.; Song, S. P.; Li, W. X.; Li, G. X.; Fan, C. H. A Gold Nanoparticle-Based Aptamer Target Binding Readout for ATP Assay. *Adv. Mater.* **2007**, *19*, 3943−3946.
(338) Medley, C. D.; Smith, J. E.; Tang, Z.; Wu, Y.; Bamrungsap, S.; Tan, W. H. Gold Nanoparticle-Based Colorimetric Assay for the Direct Detection of Cancerous Cells. *Anal. Chem.* **2008**, *80*, 1067−1072.
(339) Schofield, C. L.; Field, R. A.; Russell, D. A. Glyconanoparticles for the Colorimetric Detection of Cholera Toxin. *Anal. Chem.* **2007**, *79*, 1356−1361.
(340) Stoeva, S. I.; Lee, J. S.; Thaxton, C. S.; Mirkin, C. A. Multiplexed DNA Detection with Biobarcoded Nanoparticle Probes. *Angew. Chem., Int. Ed.* **2006**, *45*, 3303−3306.
(341) Yang, R. H.; Tang, Z. W.; Yan, J. L.; Kang, H. Z.; Kim, Y. M.; Zhu, Z.; Tan, W. H. Noncovalent Assembly of Carbon Nanotubes and Single-Stranded DNA: An Effective Sensing Platform for Probing Biomolecular Interactions. *Anal. Chem.* **2008**, *80*, 7408−7413.
(342) Ouyang, X. Y.; Yu, R. Q.; Jin, J. Y.; Li, J. S.; Yang, R. H.; Tan, W. H.; Yuan, J. L. New Strategy for Label-Free and Time-Resolved Luminescent Assay of Protein: Conjugate Eu^{3+} Complex and Aptamer-Wrapped Carbon Nanotubes. *Anal. Chem.* **2011**, *83*, 782−789.
(343) Robinson, J. T.; Perkins, F. K.; Snow, E. S.; Wei, Z. Q.; Sheehan, P. E. Reduced Graphene Oxide Molecular Sensors. *Nano Lett.* **2008**, *8*, 3137−3140.
(344) Loh, K. P.; Bao, Q. L.; Eda, G.; Chhowalla, M. Graphene Oxide as a Chemically Tunable Platform for Optical Applications. *Nat. Chem.* **2010**, *2*, 1015−1024.
(345) Gao, L.; Lian, C. Q.; Zhou, Y.; Yan, L. R.; Li, Q.; Zhang, C. X.; Chen, L.; Chen, K. P. Graphene Oxide-DNA Based Sensors. *Biosens. Bioelectron.* **2014**, *60*, 22−29.
(346) Liu, B. W.; Sun, Z. Y.; Zhang, X.; Liu, J. W. Mechanisms of DNA Sensing on Graphene Oxide. *Anal. Chem.* **2013**, *85*, 7987−7993.
(347) Balapanuru, J.; Yang, J. X.; Xiao, S.; Bao, Q. L.; Jahan, M.; Polavarapu, L.; Wei, J.; Xu, Q. H.; Loh, K. P. A Graphene Oxide-Organic Dye Ionic Complex with DNA-Sensing and Optical-Limiting Properties. *Angew. Chem., Int. Ed.* **2010**, *49*, 6549−6553.
(348) Wang, L.; Zhu, J. B.; Han, L.; Jin, L. H.; Zhu, C. Z.; Wang, E. K.; Dong, S. J. Graphene-Based Aptamer Logic Gates and Their Application to Multiplex Detection. *ACS Nano* **2012**, *6*, 6659−6666.
(349) Chhowalla, M.; Shin, H. S.; Eda, G.; Li, L. J.; Loh, K. P.; Zhang, H. The Chemistry of Two-Dimensional Layered Transition Metal Dichalcogenide Nanosheets. *Nat. Chem.* **2013**, *5*, 263−275.
(350) Huang, X.; Zeng, Z. Y.; Zhang, H. Metal Dichalcogenide Nanosheets: Preparation, Properties and Applications. *Chem. Soc. Rev.* **2013**, *42*, 1934−1946.
(351) Tan, C. L.; Zhang, H. Two-Dimensional Transition Metal Dichalcogenide Nanosheet-Based Composites. *Chem. Soc. Rev.* **2015**, *44*, 2713−2731.
(352) Ge, J.; Ou, E. C.; Yu, R. Q.; Chu, X. A Novel Aptameric Nanobiosensor Based on the Self-Assembled DNA-MoS_2 Nanosheet Architecture for Biomolecule Detection. *J. Mater. Chem. B* **2014**, *2*, 625−628.
(353) Zhu, C. F.; Zeng, Z. Y.; Li, H.; Li, F.; Fan, C. H.; Zhang, H. Single-Layer MoS_2-Based Nanoprobes for Homogeneous Detection of Biomolecules. *J. Am. Chem. Soc.* **2013**, *135*, 5998−6001.
(354) Lu, C.; Liu, Y. B.; Ying, Y. B.; Liu, J. W. Comparison of MoS_2, WS_2, and Graphene Oxide for DNA Adsorption and Sensing. *Langmuir* **2017**, *33*, 630−637.
(355) Xiao, M. S.; Man, T. T.; Zhu, C. F.; Pei, H.; Shi, J. Y.; Li, L.; Qu, X. M.; Shen, X. Z.; Li, J. MoS_2 Nanoprobe for MicroRNA

DOI: 10.1021/acs.chemrev.9b00121
Chem. Rev. XXXX, XXX, XXX−XXX

Quantification Based on Duplex-Specific Nuclease Signal Amplification. *ACS Appl. Mater. Interfaces* **2018**, *10*, 7852−7858.
(356) Lu, C.; Huang, Z. C.; Liu, B. W.; Liu, Y. B.; Ying, Y. B.; Liu, J. W. Poly-Cytosine DNA as a High-Affinity Ligand for Inorganic Nanomaterials. *Angew. Chem., Int. Ed.* **2017**, *56*, 6208−6212.
(357) Huang, Z. C.; Liu, J. W. Length-Dependent Diblock DNA with Poly-Cytosine (Poly-C) as High-Affinity Anchors on Graphene Oxide. *Langmuir* **2018**, *34*, 1171−1177.
(358) Xiao, M. S.; Chandrasekaran, A. R.; Ji, W.; Li, F.; Man, T. T.; Zhu, C. F.; Shen, X. Z.; Pei, H.; Li, Q.; Li, L. Affinity-Modulated Molecular Beacons on MoS_2 Nanosheets for MicroRNA Detection. *ACS Appl. Mater. Interfaces* **2018**, *10*, 35794−35800.
(359) Gill, R.; Zayats, M.; Willner, I. Semiconductor Quantum Dots for Bioanalysis. *Angew. Chem., Int. Ed.* **2008**, *47*, 7602−7625.
(360) Freeman, R.; Girsh, J.; Willner, I. Nucleic Acid/Quantum Dots (QDs) Hybrid Systems for Optical and Photoelectrochemical Sensing. *ACS Appl. Mater. Interfaces* **2013**, *5*, 2815−2834.
(361) Freeman, R.; Liu, X. Q.; Willner, I. Chemiluminescent and Chemiluminescence Resonance Energy Transfer (CRET) Detection of DNA, Metal Ions, and Aptamer-Substrate Complexes Using Hemin/G-Quadruplexes and CdSe/ZnS Quantum Dots. *J. Am. Chem. Soc.* **2011**, *133*, 11597−11604.
(362) Liu, X. Q.; Freeman, R.; Golub, E.; Willner, I. Chemiluminescence and Chemiluminescence Resonance Energy Transfer (CRET) Aptamer Sensors Using Catalytic Hemin/G-Quadruplexes. *ACS Nano* **2011**, *5*, 7648−7655.
(363) Freeman, R.; Liu, X. Q.; Willner, I. Amplified Multiplexed Analysis of DNA by the Exonuclease III-Catalyzed Regeneration of the Target DNA in the Presence of Functionalized Semiconductor Quantum Dots. *Nano Lett.* **2011**, *11*, 4456−4461.
(364) Freeman, R.; Girsh, J.; Jou, A. F. J.; Ho, J. A. A.; Hug, T.; Dernedde, J.; Willner, I. Optical Aptasensors for the Analysis of the Vascular Endothelial Growth Factor (VEGF). *Anal. Chem.* **2012**, *84*, 6192−6198.
(365) Choi, S.; Dickson, R. M.; Yu, J. H. Developing Luminescent Silver Nanodots for Biological Applications. *Chem. Soc. Rev.* **2012**, *41*, 1867−1891.
(366) Liu, X. Q.; Wang, F.; Aizen, R.; Yehezkeli, O.; Willner, I. Graphene Oxide/Nucleic-Acid-Stabilized Silver Nanoclusters: Functional Hybrid Materials for Optical Aptamer Sensing and Multiplexed Analysis of Pathogenic DNAs. *J. Am. Chem. Soc.* **2013**, *135*, 11832−11839.
(367) Drummond, T. G.; Hill, M. G.; Barton, J. K. Electrochemical DNA Sensors. *Nat. Biotechnol.* **2003**, *21*, 1192−1199.
(368) Zuo, X. L.; Xiao, Y.; Plaxco, K. W. High Specificity, Electrochemical Sandwich Assays Based on Single Aptamer Sequences and Suitable for the Direct Detection of Small-Molecule Targets in Blood and Other Complex Matrices. *J. Am. Chem. Soc.* **2009**, *131*, 6944−6945.
(369) Li, H.; Sun, Z. Y.; Zhong, W. Y.; Hao, N.; Xu, D. K.; Chen, H. Y. Ultrasensitive Electrochemical Detection for DNA Arrays Based on Silver Nanoparticle Aggregates. *Anal. Chem.* **2010**, *82*, 5477−5483.
(370) Zhang, S. S.; Xia, J. P.; Li, X. M. Electrochemical Biosensor for Detection of Adenosine Based on Structure-Switching Aptamer and Amplification with Reporter Probe DNA Modified Au Nanoparticles. *Anal. Chem.* **2008**, *80*, 8382−8388.
(371) Schoukroun-Barnes, L. R.; Glaser, E. P.; White, R. J. Heterogeneous Electrochemical Aptamer-Based Sensor Surfaces for Controlled Sensor Response. *Langmuir* **2015**, *31*, 6563−6569.
(372) Schoukroun-Barnes, L. R.; Macazo, F. C.; Gutierrez, B.; Lottermoser, J.; Liu, J.; White, R. J. Reagentless, Structure-Switching, Electrochemical Aptamer-Based Sensors. *Annu. Rev. Anal. Chem.* **2016**, *9*, 163−181.
(373) Vasilyeva, E.; Lam, B.; Fang, Z. C.; Minden, M. D.; Sargent, E. H.; Kelley, S. O. Direct Genetic Analysis of Ten Cancer Cells: Tuning Sensor Structure and Molecular Probe Design for Efficient mRNA Capture. *Angew. Chem., Int. Ed.* **2011**, *50*, 4137−4141.
(374) Das, J.; Ivanov, I.; Safaei, T. S.; Sargent, E. H.; Kelley, S. O. Combinatorial Probes for High-Throughput Electrochemical Analysis of Circulating Nucleic Acids in Clinical Samples. *Angew. Chem., Int. Ed.* **2018**, *57*, 3711−3716.
(375) Xiong, E. H.; Yan, X. X.; Zhang, X. H.; Liu, Y. Q.; Zhou, J. W.; Chen, J. H. Exonuclease III-Assisted Cascade Signal Amplification Strategy for Label-Free and Ultrasensitive Electrochemical Detection of Nucleic Acids. *Biosens. Bioelectron.* **2017**, *87*, 732−736.
(376) Jie, G. F.; Tan, L.; Zhao, Y.; Wang, X. C. A Novel Silver Nanocluster in Situ Synthesized as Versatile Probe for Electrochemiluminescence and Electrochemical Detection of Thrombin by Multiple Signal Amplification Strategy. *Biosens. Bioelectron.* **2017**, *94*, 243−249.
(377) Ji, Y. H.; Zhang, L.; Zhu, L. Y.; Lei, J. P.; Wu, J.; Ju, H. X. Binding-Induced DNA Walker for Signal Amplification in Highly Selective Electrochemical Detection of Protein. *Biosens. Bioelectron.* **2017**, *96*, 201−205.
(378) Wang, Y. H.; Jiang, L.; Leng, Q. G.; Wu, Y. H.; He, X. X.; Wang, K. M. Electrochemical Sensor for Glutathione Detection Based on Mercury Ion Triggered Hybridization Chain Reaction Signal Amplification. *Biosens. Bioelectron.* **2016**, *77*, 914−920.
(379) Sheng, Q. L.; Liu, R. X.; Zhang, S.; Zheng, J. B. Ultrasensitive Electrochemical Cocaine Biosensor Based on Reversible DNA Nanostructure. *Biosens. Bioelectron.* **2014**, *51*, 191−194.
(380) Zhu, C. Z.; Yang, G. H.; Li, H.; Du, D.; Lin, Y. H. Electrochemical Sensors and Biosensors Based on Nanomaterials and Nanostructures. *Anal. Chem.* **2015**, *87*, 230−249.
(381) Zhang, Y. X.; Xia, J. F.; Zhang, F. F.; Wang, Z. H.; Liu, Q. Y. Ultrasensitive Label-Free Homogeneous Electrochemical Aptasensor Based on Sandwich Structure for Thrombin Detection. *Sens. Actuators, B* **2018**, *267*, 412−418.
(382) Torrente-Rodriguez, R. M.; Campuzano, S.; Montiel, V. R. V.; Montoya, J. J.; Pingarron, J. M. Sensitive Electrochemical Determination of miRNAs Based on a Sandwich Assay onto Magnetic Microcarriers and Hybridization Chain Reaction Amplification. *Biosens. Bioelectron.* **2016**, *86*, 516−521.
(383) Ho, M. Y.; D'Souza, N.; Migliorato, P. Electrochemical Aptamer-Based Sandwich Assays for the Detection of Explosives. *Anal. Chem.* **2012**, *84*, 4245−4247.
(384) Xia, F.; White, R. J.; Zuo, X. L.; Patterson, A.; Xiao, Y.; Kang, D.; Gong, X.; Plaxco, K. W.; Heeger, A. J. An Electrochemical Supersandwich Assay for Sensitive and Selective DNA Detection in Complex Matrices. *J. Am. Chem. Soc.* **2010**, *132*, 14346−14348.
(385) Fapyane, D.; Nielsen, J. S.; Ferapontova, E. E. Electrochemical Enzyme-Linked Sandwich Assay with a Cellulase Label for Ultrasensitive Analysis of Synthetic DNA and Cell-Isolated RNA. *ACS Sensors* **2018**, *3*, 2104−2111.
(386) Yang, Y. H.; Fu, Y. Y.; Su, H. L.; Mao, L.; Chen, M. Sensitive Detection of MCF-7 Human Breast Cancer Cells by Using a Novel DNA-Labeled Sandwich Electrochemical Biosensor. *Biosens. Bioelectron.* **2018**, *122*, 175−182.
(387) Park, S. J.; Taton, T. A.; Mirkin, C. A. Array-Based Electrical Detection of DNA with Nanoparticle Probes. *Science* **2002**, *295*, 1503−1506.
(388) Zhang, Y.; Zeng, G. M.; Tang, L.; Chen, J.; Zhu, Y.; He, X. X.; He, Y. Electrochemical Sensor Based on Electrodeposited Graphene-Au Modified Electrode and NanoAu Carrier Amplified Signal Strategy for Attomolar Mercury Detection. *Anal. Chem.* **2015**, *87*, 989−996.
(389) Zhu, Y.; Wang, H. J.; Wang, L.; Zhu, J.; Jiang, W. Cascade Signal Amplification Based on Copper Nanoparticle-Reported Rolling Circle Amplification for Ultrasensitive Electrochemical Detection of the Prostate Cancer Biomarker. *ACS Appl. Mater. Interfaces* **2016**, *8*, 2573−2581.
(390) Zhang, J.; Song, S. P.; Zhang, L. Y.; Wang, L. H.; Wu, H. P.; Pan, D.; Fan, C. H. Sequence-Specific Detection of Femtomolar DNA via a Chronocoulometric DNA Sensor (CdS): Effects of Nanoparticle-Mediated Amplification and Nanoscale Control of DNA Assembly at Electrodes. *J. Am. Chem. Soc.* **2006**, *128*, 8575−8580.
(391) Zhao, T.; Liu, R.; Ding, X. F.; Zhao, J. C.; Yu, H. X.; Wang, L.; Xu, Q.; Wang, X.; Lou, X. H.; He, M.; Xiao, Y. Nanoprobe-Enhanced, Split Aptamer-Based Electrochemical Sandwich Assay for Ultra-

DOI: 10.1021/acs.chemrev.9b00121
Chem. Rev. XXXX, XXX, XXX−XXX

sensitive Detection of Small Molecules. *Anal. Chem.* **2015**, *87*, 7712−7719.
(392) Hu, K. C.; Lan, D. X.; Li, X. M.; Zhang, S. S. Electrochemical DNA Biosensor Based on Nanoporous Gold Electrode and Multifunctional Encoded DNA-Au Bio Bar Codes. *Anal. Chem.* **2008**, *80*, 9124−9130.
(393) Gao, F. L.; Du, L. L.; Zhang, Y.; Zhou, F. Y.; Tang, D. Q. A Sensitive Sandwich-Type Electrochemical Aptasensor for Thrombin Detection Based on Platinum Nanoparticles Decorated Carbon Nanocages as Signal Labels. *Biosens. Bioelectron.* **2016**, *86*, 185−193.
(394) Zhu, G. B.; Lee, H. J. Electrochemical Sandwich-Type Biosensors for Alpha-1 Antitrypsin with Carbon Nanotubes and Alkaline Phosphatase Labeled Antibody-Silver Nanoparticles. *Biosens. Bioelectron.* **2017**, *89*, 959−963.
(395) Wang, J.; Liu, G.; Merkoçi, A. Electrochemical Coding Technology for Simultaneous Detection of Multiple DNA Targets. *J. Am. Chem. Soc.* **2003**, *125*, 3214−3215.
(396) Hermann, T.; Patel, D. J. Biochemistry-Adaptive Recognition by Nucleic Acid Aptamers. *Science* **2000**, *287*, 820−825.
(397) Fan, C. H.; Plaxco, K. W.; Heeger, A. J. Electrochemical Interrogation of Conformational Changes as a Reagentless Method for the Sequence-Specific Detection of DNA. *Proc. Natl. Acad. Sci. U. S. A.* **2003**, *100*, 9134−9137.
(398) Li, D.; Song, S. P.; Fan, C. H. Target-Responsive Structural Switching for Nucleic Acid-Based Sensors. *Acc. Chem. Res.* **2010**, *43*, 631−641.
(399) Bang, G. S.; Cho, S.; Kim, B. G. A Novel Electrochemical Detection Method for Aptamer Biosensors. *Biosens. Bioelectron.* **2005**, *21*, 863−870.
(400) Zuo, X. L.; Song, S. P.; Zhang, J.; Pan, D.; Wang, L. H.; Fan, C. H. A Target-Responsive Electrochemical Aptamer Switch (TREAS) for Reagentless Detection of Nanomolar ATP. *J. Am. Chem. Soc.* **2007**, *129*, 1042−1043.
(401) Liu, G.; Wan, Y.; Gau, V.; Zhang, J.; Wang, L. H.; Song, S. P.; Fan, C. H. An Enzyme-Based E-DNA Sensor for Sequence-Specific Detection of Femtomolar DNA Targets. *J. Am. Chem. Soc.* **2008**, *130*, 6820−6825.
(402) Xiang, Y.; Lu, Y. Using Personal Glucose Meters and Functional DNA Sensors to Quantify a Variety of Analytical Targets. *Nat. Chem.* **2011**, *3*, 697−703.
(403) Pavlov, V.; Xiao, Y.; Shlyahovsky, B.; Willner, I. Aptamer-Functionalized Au Nanoparticles for the Amplified Optical Detection of Thrombin. *J. Am. Chem. Soc.* **2004**, *126*, 11768−11769.
(404) Deng, C. Y.; Chen, J. H.; Nie, L. H.; Nie, Z.; Yao, S. Z. Sensitive Bifunctional Aptamer-Based Electrochemical Biosensor for Small Molecules and Protein. *Anal. Chem.* **2009**, *81*, 9972−9978.
(405) Su, S.; Sun, H. F.; Cao, W. F.; Chao, J.; Peng, H. Z.; Zuo, X. L.; Yuwen, L. H.; Fan, C. H.; Wang, L. H. Dual-Target Electrochemical Biosensing Based on DNA Structural Switching on Gold Nanoparticle-Decorated MoS_2 Nanosheets. *ACS Appl. Mater. Interfaces* **2016**, *8*, 6826−6833.
(406) Liu, H.; Xiang, Y.; Lu, Y.; Crooks, R. M. Aptamer-Based Origami Paper Analytical Device for Electrochemical Detection of Adenosine. *Angew. Chem., Int. Ed.* **2012**, *51*, 6925−6928.
(407) Pei, H.; Zuo, X. L.; Pan, D.; Shi, J. Y.; Huang, Q.; Fan, C. H. Scaffolded Biosensors with Designed DNA Nanostructures. *NPG Asia Mater.* **2013**, *5*, No. e51.
(408) Pei, H.; Zuo, X. L.; Zhu, D.; Huang, Q.; Fan, C. H. Functional DNA Nanostructures for Theranostic Applications. *Acc. Chem. Res.* **2014**, *47*, 550−559.
(409) Lu, N.; Pei, H.; Ge, Z. L.; Simmons, C. R.; Yan, H.; Fan, C. H. Charge Transport within a Three-Dimensional DNA Nanostructure Framework. *J. Am. Chem. Soc.* **2012**, *134*, 13148−13151.
(410) Mitchell, N.; Schlapak, R.; Kastner, M.; Armitage, D.; Chrzanowski, W.; Riener, J.; Hinterdorfer, P.; Ebner, A.; Howorka, S. A DNA Nanostructure for the Functional Assembly of Chemical Groups with Tunable Stoichiometry and Defined Nanoscale Geometry. *Angew. Chem., Int. Ed.* **2009**, *48*, 525−527.
(411) Schlapak, R.; Danzberger, J.; Armitage, D.; Morgan, D.; Ebner, A.; Hinterdorfer, P.; Pollheimer, P.; Gruber, H. J.; Schaffler, F.; Howorka, S. Nanoscale DNA Tetrahedra Improve Biomolecular Recognition on Patterned Surfaces. *Small* **2012**, *8*, 89−97.
(412) Wen, Y. L.; Pei, H.; Shen, Y.; Xi, J. J.; Lin, M. H.; Lu, N.; Shen, X. Z.; Li, J.; Fan, C. H. DNA Nanostructure-Based Interfacial Engineering for PCR-Free Ultrasensitive Electrochemical Analysis of MicroRNA. *Sci. Rep.* **2012**, *2*, 867.
(413) Lin, M.; Wen, Y.; Li, L.; Pei, H.; Liu, G.; Song, H.; Zuo, X.; Fan, C.; Huang, Q. Target-Responsive, DNA Nanostructure-Based E-DNA Sensor for MicroRNA Analysis. *Anal. Chem.* **2014**, *86*, 2285−2288.
(414) Bu, N.-N.; Tang, C.-X.; He, X.-W.; Yin, X.-B. Tetrahedron-Structured DNA and Functional Oligonucleotide for Construction of an Electrochemical DNA-Based Biosensor. *Chem. Commun.* **2011**, *47*, 7689−7691.
(415) Wen, Y.; Pei, H.; Wan, Y.; Su, Y.; Huang, Q.; Song, S.; Fan, C. DNA Nanostructure-Decorated Surfaces for Enhanced Aptamer-Target Binding and Electrochemical Cocaine Sensors. *Anal. Chem.* **2011**, *83*, 7418−7423.
(416) Ge, Z. L.; Pei, H.; Wang, L. H.; Song, S. P.; Fan, C. H. Electrochemical Single Nucleotide Polymorphisms Genotyping on Surface Immobilized Three-Dimensional Branched DNA Nanostructure. *Sci. China: Chem.* **2011**, *54*, 1273−1276.
(417) Bu, N. N.; Gao, A.; He, X. W.; Yin, X. B. Electrochemiluminescent Biosensor of ATP Using Tetrahedron Structured DNA and a Functional Oligonucleotide for $Ru(Phen)_3^{2+}$ Intercalation and Target Identification. *Biosens. Bioelectron.* **2013**, *43*, 200−204.
(418) Pei, H.; Wan, Y.; Li, J.; Hu, H. Y.; Su, Y.; Huang, Q.; Fan, C. H. Regenerable Electrochemical Immunological Sensing at DNA Nanostructure-Decorated Gold Surfaces. *Chem. Commun.* **2011**, *47*, 6254−6256.
(419) Soleymani, L.; Fang, Z. C.; Sargent, E. H.; Kelley, S. O. Programming the Detection Limits of Biosensors through Controlled Nanostructuring. *Nat. Nanotechnol.* **2009**, *4*, 844−848.
(420) Smith, S. J.; Nemr, C. R.; Kelley, S. O. Chemistry-Driven Approaches for Ultrasensitive Nucleic Acid Detection. *J. Am. Chem. Soc.* **2017**, *139*, 1020−1028.
(421) Hill, H. D.; Millstone, J. E.; Banholzer, M. J.; Mirkin, C. A. The Role Radius of Curvature Plays in Thiolated Oligonucleotide Loading on Gold Nanoparticles. *ACS Nano* **2009**, *3*, 418−424.
(422) Bin, X. M.; Sargent, E. H.; Kelley, S. O. Nanostructuring of Sensors Determines the Efficiency of Biomolecular Capture. *Anal. Chem.* **2010**, *82*, 5928−5931.
(423) De Luna, P.; Mahshid, S. S.; Das, J.; Luan, B. Q.; Sargent, E. H.; Kelley, S. O.; Zhou, R. H. High-Curvature Nanostructuring Enhances Probe Display for Biomolecular Detection. *Nano Lett.* **2017**, *17*, 1289−1295.
(424) Mahshid, S. S.; Vallee-Belisle, A.; Kelley, S. O. Biomolecular Steric Hindrance Effects Are Enhanced on Nanostructured Microelectrodes. *Anal. Chem.* **2017**, *89*, 9751−9757.
(425) Lam, B.; Fang, Z. C.; Sargent, E. H.; Kelley, S. O. Polymerase Chain Reaction-Free, Sample-to-Answer Bacterial Detection in 30 minutes with Integrated Cell Lysis. *Anal. Chem.* **2012**, *84*, 21−25.
(426) Das, J.; Ivanov, I.; Montermini, L.; Rak, J.; Sargent, E. H.; Kelley, S. O. An Electrochemical Clamp Assay for Direct, Rapid Analysis of Circulating Nucleic Acids in Serum. *Nat. Chem.* **2015**, *7*, 569−575.
(427) Liu, J.; Wagan, S.; Dávila Morris, M.; Taylor, J.; White, R. J. Achieving Reproducible Performance of Electrochemical, Folding Aptamer-Based Sensors on Microelectrodes: Challenges and Prospects. *Anal. Chem.* **2014**, *86*, 11417−11424.
(428) Li, F.; Han, X.; Liu, S. Development of an Electrochemical DNA Biosensor with a High Sensitivity of fM by Dendritic Gold Nanostructure Modified Electrode. *Biosens. Bioelectron.* **2011**, *26*, 2619−2625.
(429) Das, J.; Ivanov, I.; Sargent, E. H.; Kelley, S. O. DNA Clutch Probes for Circulating Tumor DNA Analysis. *J. Am. Chem. Soc.* **2016**, *138*, 11009−11016.

DOI: 10.1021/acs.chemrev.9b00121
Chem. Rev. XXXX, XXX, XXX−XXX

(430) Das, J.; Cederquist, K. B.; Zaragoza, A. A.; Lee, P. E.; Sargent, E. H.; Kelley, S. O. An Ultrasensitive Universal Detector Based on Neutralizer Displacement. *Nat. Chem.* **2012**, *4*, 642−648.
(431) Mohamadi, R. M.; Ivanov, I.; Stojcic, J.; Nam, R. K.; Sargent, E. H.; Kelley, S. O. Sample-to-Answer Isolation and mRNA Profiling of Circulating Tumor Cells. *Anal. Chem.* **2015**, *87*, 6258−6264.
(432) Yang, H.; Hui, A.; Pampalakis, G.; Soleymani, L.; Liu, F. F.; Sargent, E. H.; Kelley, S. O. Direct, Electronic MicroRNA Detection for the Rapid Determination of Differential Expression Profiles. *Angew. Chem., Int. Ed.* **2009**, *48*, 8461−8464.
(433) Lam, B.; Das, J.; Holmes, R. D.; Live, L.; Sage, A.; Sargent, E. H.; Kelley, S. O. Solution-Based Circuits Enable Rapid and Multiplexed Pathogen Detection. *Nat. Commun.* **2013**, *4*, 2001.
(434) Soleymani, L.; Fang, Z. C.; Lam, B.; Bin, X. M.; Vasilyeva, E.; Ross, A. J.; Sargent, E. H.; Kelley, S. O. Hierarchical Nanotextured Microelectrodes Overcome the Molecular Transport Barrier to Achieve Rapid, Direct Bacterial Detection. *ACS Nano* **2011**, *5*, 3360−3366.
(435) Ivanov, I.; Stojcic, J.; Stanimirovic, A.; Sargent, E.; Nam, R. K.; Kelley, S. O. Chip-Based Nanostructured Sensors Enable Accurate Identification and Classification of Circulating Tumor Cells in Prostate Cancer Patient Blood Samples. *Anal. Chem.* **2013**, *85*, 398−403.
(436) Liu, R. H.; Yang, J. N.; Lenigk, R.; Bonanno, J.; Grodzinski, P. Self-Contained, Fully Integrated Biochip for Sample Preparation, Polymerase Chain Reaction Amplification, and DNA Microarray Detection. *Anal. Chem.* **2004**, *76*, 1824−1831.
(437) Cho, E. J.; Yang, L. T.; Levy, M.; Ellington, A. D. Using a Deoxyribozyme Ligase and Rolling Circle Amplification to Detect a Non-Nucleic Acid Analyte, Atp. *J. Am. Chem. Soc.* **2005**, *127*, 2022−2023.
(438) Sheng, Q. L.; Cheng, N.; Bai, W. S.; Zheng, J. B. Ultrasensitive Electrochemical Detection of Breast Cancer Cells Based on DNA-Rolling-Circle-Amplification-Directed Enzyme-Catalyzed Polymerization. *Chem. Commun.* **2015**, *51*, 2114−2117.
(439) Liu, Z. Y.; Zhang, W.; Zhu, S. Y.; Zhang, L.; Hu, L. Z.; Parveen, S.; Xu, G. B. Ultrasensitive Signal-on DNA Biosensor Based on Nicking Endonuclease Assisted Electrochemistry Signal Amplification. *Biosens. Bioelectron.* **2011**, *29*, 215−218.
(440) Liu, S. F.; Wei, W. J.; Wang, Y. Q.; Fang, L.; Wang, L.; Li, F. Ultrasensitive Electrochemical Detection of Nucleic Acid by Coupling an Autonomous Cascade Target Replication and Enzyme/Gold Nanoparticle-Based Post-Amplification. *Biosens. Bioelectron.* **2016**, *80*, 208−214.
(441) Yang, H. Enzyme-Based Ultrasensitive Electrochemical Biosensors. *Curr. Opin. Chem. Biol.* **2012**, *16*, 422−428.
(442) Yeung, S. S. W.; Lee, T. M. H.; Hsing, I. M. Electrochemical Real-Time Polymerase Chain Reaction. *J. Am. Chem. Soc.* **2006**, *128*, 13374−13375.
(443) Yan, M.; Bai, W.; Zhu, C.; Huang, Y.; Yan, J.; Chen, A. Design of Nuclease-Based Target Recycling Signal Amplification in Aptasensors. *Biosens. Bioelectron.* **2016**, *77*, 613−623.
(444) Huang, L.; Wang, D. B.; Singh, N.; Yang, F.; Gu, N.; Zhang, X. E. A Dual-Signal Amplification Platform for Sensitive Fluorescence Biosensing of Leukemia-Derived Exosomes. *Nanoscale* **2018**, *10*, 20289−20295.
(445) Qing, T. P.; He, D. G.; He, X. X.; Wang, K. M.; Xu, F. Z.; Wen, L.; Shangguan, J. F.; Mao, Z. G.; Lei, Y. L. Nucleic Acid Tool Enzymes-Aided Signal Amplification Strategy for Biochemical Analysis: Status and Challenges. *Anal. Bioanal. Chem.* **2016**, *408*, 2793−2811.
(446) Liu, L.; Xia, N.; Liu, H. P.; Kang, X. J.; Liu, X. S.; Xue, C.; He, X. L. Highly Sensitive and Label-Free Electrochemical Detection of MicroRNAs Based on Triple Signal Amplification of Multifunctional Gold Nanoparticles, Enzymes and Redox-Cycling Reaction. *Biosens. Bioelectron.* **2014**, *53*, 399−405.
(447) Mohsen, M. G.; Kool, E. T. The Discovery of Rolling Circle Amplification and Rolling Circle Transcription. *Acc. Chem. Res.* **2016**, *49*, 2540−2550.
(448) Deng, R.; Zhang, K.; Sun, Y.; Ren, X.; Li, J. Highly Specific Imaging of mRNA in Single Cells by Target RNA-Initiated Rolling Circle Amplification. *Chem. Sci.* **2017**, *8*, 3668−3675.
(449) Lizardi, P. M.; Huang, X. H.; Zhu, Z. R.; Bray-Ward, P.; Thomas, D. C.; Ward, D. C. Mutation Detection and Single-Molecule Counting Using Isothermal Rolling-Circle Amplification. *Nat. Genet.* **1998**, *19*, 225−232.
(450) Wang, Q.; Yang, C. Y.; Xiang, Y.; Yuan, R.; Chai, Y. Q. Dual Amplified and Ultrasensitive Electrochemical Detection of Mutant DNA Biomarkers Based on Nuclease-Assisted Target Recycling and Rolling Circle Amplifications. *Biosens. Bioelectron.* **2014**, *55*, 266−271.
(451) Yan, M. M.; Bai, W. H.; Zhu, C.; Huang, Y. F.; Yan, J.; Chen, A. L. Design of Nuclease-Based Target Recycling Signal Amplification in Aptasensors. *Biosens. Bioelectron.* **2016**, *77*, 613−623.
(452) Tan, Y.; Wei, X. F.; Zhang, Y.; Wang, P. L.; Qiu, B.; Guo, L. H.; Lin, Z. Y.; Yang, H. H. Exonuclease-Catalyzed Target Recycling Amplification and Immobilization-Free Electrochemical Aptasensor. *Anal. Chem.* **2015**, *87*, 11826−11831.
(453) Ji, H. X.; Yan, F.; Lei, J. P.; Ju, H. X. Ultrasensitive Electrochemical Detection of Nucleic Acids by Template Enhanced Hybridization Followed with Rolling Circle Amplification. *Anal. Chem.* **2012**, *84*, 7166−7171.
(454) Li, J. W. J.; Chu, Y. Z.; Lee, B. Y. H.; Xie, X. L. S. Enzymatic Signal Amplification of Molecular Beacons for Sensitive DNA Detection. *Nucleic Acids Res.* **2008**, *36*, e36.
(455) Kiesling, T.; Cox, K.; Davidson, E. A.; Dretchen, K.; Grater, G.; Hibbard, S.; Lasken, R. S.; Leshin, J.; Skowronski, E.; Danielsen, M. Sequence Specific Detection of DNA Using Nicking Endonuclease Signal Amplification (NESA). *Nucleic Acids Res.* **2007**, *35*, No. e117.
(456) Xuan, F.; Luo, X. T.; Hsing, I. M. Ultrasensitive Solution-Phase Electrochemical Molecular Beacon-Based DNA Detection with Signal Amplification by Exonuclease III-Assisted Target Recycling. *Anal. Chem.* **2012**, *84*, 5216−5220.
(457) Wu, D.; Yin, B. C.; Ye, B. C. A Label-Free Electrochemical DNA Sensor Based on Exonuclease III-Aided Target Recycling Strategy for Sequence-Specific Detection of Femtomolar DNA. *Biosens. Bioelectron.* **2011**, *28*, 232−238.
(458) Liu, S. F.; Wang, Y.; Zhang, C. X.; Lin, Y.; Li, F. Homogeneous Electrochemical Aptamer-Based ATP Assay with Signal Amplification by Exonuclease III Assisted Target Recycling. *Chem. Commun.* **2013**, *49*, 2335−2337.
(459) Liu, S. F.; Wang, C. F.; Zhang, C. X.; Wang, Y.; Tang, B. Label-Free and Ultrasensitive Electrochemical Detection of Nucleic Acids Based on Autocatalytic and Exonuclease III-Assisted Target Recycling Strategy. *Anal. Chem.* **2013**, *85*, 2282−2288.
(460) Liu, Z. J.; Mei, S. H. J.; Brennan, J. D.; Li, Y. F. Assemblage of Signaling DNA Enzymes with Intriguing Metal-Ion Specificities and pH Dependences. *J. Am. Chem. Soc.* **2003**, *125*, 7539−7545.
(461) Roth, A.; Breaker, R. R. An Amino Acid as a Cofactor for a Catalytic Polynucleotide. *Proc. Natl. Acad. Sci. U. S. A.* **1998**, *95*, 6027−6031.
(462) Golub, E.; Freeman, R.; Willner, I. A Hemin/G-Quadruplex Acts as an NADH Oxidase and NADH Peroxidase Mimicking Dnazyme. *Angew. Chem., Int. Ed.* **2011**, *50*, 11710−11714.
(463) Deng, M. G.; Zhang, D.; Zhou, Y. Y.; Zhou, X. Highly Effective Colorimetric and Visual Detection of Nucleic Acids Using an Asymmetrically Split Peroxidase DNAzyme. *J. Am. Chem. Soc.* **2008**, *130*, 13095−13102.
(464) Agresti, J. J.; Kelly, B. T.; Jaschke, A.; Griffiths, A. D. Selection of Ribozymes That Catalyse Multiple-Turnover Diels-Alder Cycloadditions by Using in Vitro Compartmentalization. *Proc. Natl. Acad. Sci. U. S. A.* **2005**, *102*, 16170−16175.
(465) Pelossof, G.; Tel-Vered, R.; Elbaz, J.; Willner, I. Amplified Biosensing Using the Horseradish Peroxidase-Mimicking DNAzyme as an Electrocatalyst. *Anal. Chem.* **2010**, *82*, 4396−4402.
(466) Chen, J. H.; Zhang, J.; Guo, Y.; Li, J.; Fu, F. F.; Yang, H. H.; Chen, G. N. An Ultrasensitive Electrochemical Biosensor for Detection of DNA Species Related to Oral Cancer Based on Nuclease-Assisted Target Recycling and Amplification of Dnazyme. *Chem. Commun.* **2011**, *47*, 8004−8006.
(467) Hu, R.; Fu, T.; Zhang, X. B.; Kong, R. M.; Qiu, L. P.; Liu, Y. R.; Liang, X. T.; Tan, W. H.; Shen, G. L.; Yu, R. Q. A Proximity-Dependent

DOI: 10.1021/acs.chemrev.9b00121
Chem. Rev. XXXX, XXX, XXX−XXX

Surface Hybridization Strategy for Constructing an Efficient Signal-on Electrochemical Dnazyme Sensing System. *Chem. Commun.* **2012**, *48*, 9507−9509.
(468) Xia, H.; Li, L. L.; Yin, Z. Y.; Hou, X. D.; Zhu, J. J. Biobar-Coded Gold Nanoparticles and DNAzyme-Based Dual Signal Amplification Strategy for Ultrasensitive Detection of Protein by Electrochemiluminescence. *ACS Appl. Mater. Interfaces* **2015**, *7*, 696−703.
(469) Yang, X. R.; Xu, J.; Tang, X. M.; Liu, H. X.; Tian, D. B. A Novel Electrochemical DNAzyme Sensor for the Amplified Detection of Pb^{2+} Ions. *Chem. Commun.* **2010**, *46*, 3107−3109.
(470) Dong, X. Y.; Mi, X. N.; Zhang, L.; Liang, T. M.; Xu, J. J.; Chen, H. Y. DNAzyme-Functionalized Pt Nanoparticles/Carbon Nanotubes for Amplified Sandwich Electrochemical DNA Analysis. *Biosens. Bioelectron.* **2012**, *38*, 337−341.
(471) Liang, J. F.; Chen, Z. B.; Guo, L.; Li, L. D. Electrochemical Sensing of L-Histidine Based on Structure-Switching DNAzymes and Gold Nanoparticle-Graphene Nanosheet Composites. *Chem. Commun.* **2011**, *47*, 5476−5478.
(472) Yuan, Y. L.; Yuan, R.; Chai, Y. Q.; Zhuo, Y.; Ye, X. Y.; Gan, X. X.; Bai, L. J. Hemin/G-Quadruplex Simultaneously Acts as NADH Oxidase and HRP-Mimicking DNAzyme for Simple, Sensitive Pseudobienzyme Electrochemical Detection of Thrombin. *Chem. Commun.* **2012**, *48*, 4621−4623.
(473) Lu, L.; Si, J. C.; Gao, Z. F.; Zhang, Y.; Lei, J. L.; Luo, H. Q.; Li, N. B. Highly Selective and Sensitive Electrochemical Biosensor for ATP Based on the Dual Strategy Integrating the Cofactor-Dependent Enzymatic Ligation Reaction with Self-Cleaving DNAzyme-Amplified Electrochemical Detection. *Biosens. Bioelectron.* **2015**, *63*, 14−20.
(474) Xiao, Y.; Rowe, A. A.; Plaxco, K. W. Electrochemical Detection of Parts-Per-Billion Lead via an Electrode-Bound DNAzyme Assembly. *J. Am. Chem. Soc.* **2007**, *129*, 262−263.
(475) Wang, F.; Lu, C. H.; Willner, I. From Cascaded Catalytic Nucleic Acids to Enzyme-DNA Nanostructures: Controlling Reactivity, Sensing, Logic Operations, and Assembly of Complex Structures. *Chem. Rev.* **2014**, *114*, 2881−2941.
(476) Zhang, X. B.; Kong, R. M.; Lu, Y. Metal Ion Sensors Based on DNAzymes and Related DNA Molecules. *Annu. Rev. Anal. Chem.* **2011**, *4*, 105−128.
(477) Gong, L.; Zhao, Z. L.; Lv, Y. F.; Huan, S. Y.; Fu, T.; Zhang, X. B.; Shen, G. L.; Yu, R. Q. DNAzyme-Based Biosensors and Nanodevices. *Chem. Commun.* **2015**, *51*, 979−995.
(478) Pelossof, G.; Tel-Vered, R.; Willner, I. Amplified Surface Plasmon Resonance and Electrochemical Detection of Pb^{2+} Ions Using the Pb^{2+}-Dependent DNAzyme and Hemin/G-Quadruplex as a Label. *Anal. Chem.* **2012**, *84*, 3703−3709.
(479) Li, B. L.; Jiang, Y.; Chen, X.; Ellington, A. D. Probing Spatial Organization of DNA Strands Using Enzyme-Free Hairpin Assembly Circuits. *J. Am. Chem. Soc.* **2012**, *134*, 13918−13921.
(480) Zhuang, J. Y.; Lai, W. Q.; Chen, G. N.; Tang, D. P. A Rolling Circle Amplification-Based DNA Machine for miRNA Screening Coupling Catalytic Hairpin Assembly with DNAzyme Formation. *Chem. Commun.* **2014**, *50*, 2935−2938.
(481) Jiang, Y.; Li, B. L.; Milligan, J. N.; Bhadra, S.; Ellington, A. D. Real-Time Detection of Isothermal Amplification Reactions with Thermostable Catalytic Hairpin Assembly. *J. Am. Chem. Soc.* **2013**, *135*, 7430−7433.
(482) Zhang, B.; Liu, B. Q.; Tang, D. P.; Niessner, R.; Chen, G. N.; Knopp, D. DNA-Based Hybridization Chain Reaction for Amplified Bioelectronic Signal and Ultrasensitive Detection of Proteins. *Anal. Chem.* **2012**, *84*, 5392−5399.
(483) Chen, X.; Lin, Y. H.; Li, J.; Lin, L. S.; Chen, G. N.; Yang, H. H. A Simple and Ultrasensitive Electrochemical DNA Biosensor Based on DNA Concatamers. *Chem. Commun.* **2011**, *47*, 12116−12118.
(484) Liu, S. F.; Wang, Y.; Ming, J. J.; Lin, Y.; Cheng, C. B.; Li, F. Enzyme-Free and Ultrasensitive Electrochemical Detection of Nucleic Acids by Target Catalyzed Hairpin Assembly Followed with Hybridization Chain Reaction. *Biosens. Bioelectron.* **2013**, *49*, 472−477.
(485) Chen, Y.; Xu, J.; Su, J.; Xiang, Y.; Yuan, R.; Chai, Y. Q. In Situ Hybridization Chain Reaction Amplification for Universal and Highly Sensitive Electrochemiluminescent Detection of DNA. *Anal. Chem.* **2012**, *84*, 7750−7755.
(486) Chen, X.; Hong, C. Y.; Lin, Y. H.; Chen, J. H.; Chen, G. N.; Yang, H. H. Enzyme-Free and Label-Free Ultrasensitive Electrochemical Detection of Human Immunodeficiency Virus DNA in Biological Samples Based on Long-Range Self-Assembled DNA Nanostructures. *Anal. Chem.* **2012**, *84*, 8277−8283.
(487) Green, S. J.; Lubrich, D.; Turberfield, A. J. DNA Hairpins: Fuel for Autonomous DNA Devices. *Biophys. J.* **2006**, *91*, 2966−2975.
(488) Turberfield, A. J.; Mitchell, J. C.; Yurke, B.; Mills, A. P.; Blakey, M. I.; Simmel, F. C. DNA Fuel for Free-Running Nanomachines. *Phys. Rev. Lett.* **2003**, *90*, 118102.
(489) Li, B. L.; Ellington, A. D.; Chen, X. Rational, Modular Adaptation of Enzyme-Free DNA Circuits to Multiple Detection Methods. *Nucleic Acids Res.* **2011**, *39*, e110.
(490) Zang, Y.; Lei, J. P.; Ling, P. H.; Ju, H. X. Catalytic Hairpin Assembly-Programmed Porphyrin-DNA Complex as Photoelectrochemical Initiator for DNA Biosensing. *Anal. Chem.* **2015**, *87*, 5430−5436.
(491) Bishop, D.; Claybrook, J. R.; Spiegelman, S. Electrophoretic Separation of Viral Nucleic Acids on Polyacrylamide Gels. *J. Mol. Biol.* **1967**, *26*, 373−387.
(492) Serwer, P. Agarose Gels: Properties and Use for Electrophoresis. *Electrophoresis* **1983**, *4*, 375−382.
(493) Viovy, J. L. Electrophoresis of DNA and Other Polyelectrolytes: Physical Mechanisms. *Rev. Mod. Phys.* **2000**, *72*, 813−872.
(494) Hanauer, M.; Pierrat, S.; Zins, I.; Lotz, A.; Sonnichsen, C. Separation of Nanoparticles by Gel Electrophoresis According to Size and Shape. *Nano Lett.* **2007**, *7*, 2881−2885.
(495) Sperling, R. A.; Pellegrino, T.; Li, J. K.; Chang, W. H.; Parak, W. J. Electrophoretic Separation of Nanoparticles with a Discrete Number of Functional Groups. *Adv. Funct. Mater.* **2006**, *16*, 943−948.
(496) Claridge, S. A.; Goh, S. L.; Frechet, J. M. J.; Williams, S. C.; Micheel, C. M.; Alivisatos, A. P. Directed Assembly of Discrete Gold Nanoparticle Groupings Using Branched DNA Scaffolds. *Chem. Mater.* **2005**, *17*, 1628−1635.
(497) Wang, D.; Shi, J.; Carlson, S. R.; Cregan, P. B.; Ward, R. W.; Diers, B. W. A Low-Cost, High-Throughput Polyacrylamide Gel Electrophoresis System for Genotyping with Microsatellite DNA Markers. *Crop Sci.* **2003**, *43*, 1828−1832.
(498) Gibson, D. G.; Young, L.; Chuang, R. Y.; Venter, J. C.; Hutchison, C. A.; Smith, H. O. Enzymatic Assembly of DNA Molecules up to Several Hundred Kilobases. *Nat. Methods* **2009**, *6*, 343−345.
(499) Chandrasekaran, A. R.; Zavala, J.; Halvorsen, K. Programmable DNA Nanoswitches for Detection of Nucleic Acid Sequences. *ACS Sensors* **2016**, *1*, 120−123.
(500) Chandrasekaran, A. R. Detecting miRNAs Using DNA Nanoswitches. *Trends Biochem. Sci.* **2019**, *44*, 819−820.
(501) Chandrasekaran, A. R.; MacIsaac, M.; Dey, P.; Levchenko, O.; Zhou, L.; Andres, M.; Dey, B. K.; Halvorsen, K. Cellular MicroRNA Detection with Miracles: MicroRNA-Activated Conditional Looping of Engineered Switches. *Sci. Adv.* **2019**, *5*, No. eaau9443.
(502) Chandrasekaran, A. R.; Levchenko, O.; Patel, D. S.; MacIsaac, M.; Halvorsen, K. Addressable Configurations of DNA Nanostructures for Rewritable Memory. *Nucleic Acids Res.* **2017**, *45*, 11459−11465.
(503) Chandrasekaran, A. R. Reconfigurable DNA Nanoswitches for Graphical Readout of Molecular Signals. *ChemBioChem* **2018**, *19*, 1018−1021.
(504) Hansen, C. H.; Yang, D. R.; Koussa, M. A.; Wong, W. P. Nanoswitch-Linked Immunosorbent Assay (NLISA) for Fast, Sensitive, and Specific Protein Detection. *Proc. Natl. Acad. Sci. U. S. A.* **2017**, *114*, 10367−10372.
(505) Koussa, M. A.; Halvorsen, K.; Ward, A.; Wong, W. P. DNA Nanoswitches: A Quantitative Platform for Gel-Based Biomolecular Interaction Analysis. *Nat. Methods* **2015**, *12*, 123−126.
(506) Dirks, R. M.; Pierce, N. A. Triggered Amplification by Hybridization Chain Reaction. *Proc. Natl. Acad. Sci. U. S. A.* **2004**, *101*, 15275−15278.

DOI: 10.1021/acs.chemrev.9b00121
Chem. Rev. XXXX, XXX, XXX−XXX

(507) Noll, W. W.; Collins, M. Detection of Human DNA Polymorphisms with a Simplified Denaturing Gradient Gel Electrophoresis Technique. *Proc. Natl. Acad. Sci. U. S. A.* **1987**, *84*, 3339−3343.
(508) Sheffield, V. C.; Cox, D. R.; Lerman, L. S.; Myers, R. M. Attachment of a 40-Base-Pair G+C-Rich Sequence (GC-Clamp) to Genomic DNA Fragments by the Polymerase Chain Reaction Results in Improved Detection of Single-Base Changes. *Proc. Natl. Acad. Sci. U. S. A.* **1989**, *86*, 232−236.
(509) Weinstein, L. S.; Gejman, P. V.; Friedman, E.; Kadowaki, T.; Collins, R. M.; Gershon, E. S.; Spiegel, A. M. Mutations of the Gs Alpha-Subunit Gene in Albright Hereditary Osteodystrophy Detected by Denaturing Gradient Gel Electrophoresis. *Proc. Natl. Acad. Sci. U. S. A.* **1990**, *87*, 8287−8290.
(510) Abrams, E. S.; Murdaugh, S. E.; Lerman, L. S. Comprehensive Detection of Single Base Changes in Human Genomic DNA Using Denaturing Gradient Gel Electrophoresis and a GC Clamp. *Genomics* **1990**, *7*, 463−475.
(511) Orita, M.; Iwahana, H.; Kanazawa, H.; Hayashi, K.; Sekiya, T. Detection of Polymorphisms of Human DNA by Gel Electrophoresis as Single-Strand Conformation Polymorphisms. *Proc. Natl. Acad. Sci. U. S. A.* **1989**, *86*, 2766−2770.
(512) O'Farrell, P. H. High Resolution Two-Dimensional Electrophoresis of Proteins. *J. Biol. Chem.* **1975**, *250*, 4007−4021.
(513) MacBeath, G. Protein Microarrays and Proteomics. *Nat. Genet.* **2002**, *32*, 526.
(514) Xie, S. N.; Walton, S. P. Development of a Dual-Aptamer-Based Multiplex Protein Biosensor. *Biosens. Bioelectron.* **2010**, *25*, 2663−2668.
(515) Welsher, K.; McManus, S. A.; Hsia, C.-H.; Yin, S.; Yang, H. Discovery of Protein-and DNA-Imperceptible Nanoparticle Hard Coating Using Gel-Based Reaction Tuning. *J. Am. Chem. Soc.* **2015**, *137*, 580−583.
(516) Binnig, G.; Quate, C. F.; Gerber, C. Atomic Force Microscope. *Phys. Rev. Lett.* **1986**, *56*, 930.
(517) Neuman, K. C.; Nagy, A. Single-Molecule Force Spectroscopy: Optical Tweezers, Magnetic Tweezers and Atomic Force Microscopy. *Nat. Methods* **2008**, *5*, 491−505.
(518) Endo, M.; Sugiyama, H. Single-Molecule Imaging of Dynamic Motions of Biomolecules in DNA Origami Nanostructures Using High-Speed Atomic Force Microscopy. *Acc. Chem. Res.* **2014**, *47*, 1645−1653.
(519) Drake, B.; Prater, C.; Weisenhorn, A.; Gould, S.; Albrecht, T.; Quate, C.; Cannell, D.; Hansma, H.; Hansma, P. Imaging Crystals, Polymers, and Processes in Water with the Atomic Force Microscope. *Science* **1989**, *243*, 1586−1589.
(520) Bustamante, C.; Rivetti, C.; Keller, D. J. Scanning Force Microscopy under Aqueous Solutions. *Curr. Opin. Struct. Biol.* **1997**, *7*, 709−716.
(521) Dufrene, Y. F.; Ando, T.; Garcia, R.; Alsteens, D.; Martinez-Martin, D.; Engel, A.; Gerber, C.; Muller, D. J. Imaging Modes of Atomic Force Microscopy for Application in Molecular and Cell Biology. *Nat. Nanotechnol.* **2017**, *12*, 295−307.
(522) Benoit, M.; Gabriel, D.; Gerisch, G.; Gaub, H. E. Discrete Interactions in Cell Adhesion Measured by Single-Molecule Force Spectroscopy. *Nat. Cell Biol.* **2000**, *2*, 313−317.
(523) Engel, A.; Muller, D. J. Observing Single Biomolecules at Work with the Atomic Force Microscope. *Nat. Struct. Biol.* **2000**, *7*, 715−718.
(524) Clausen-Schaumann, H.; Seitz, M.; Krautbauer, R.; Gaub, H. E. Force Spectroscopy with Single Bio-Molecules. *Curr. Opin. Chem. Biol.* **2000**, *4*, 524−530.
(525) Fisher, T. E.; Marszalek, P. E.; Fernandez, J. M. Stretching Single Molecules into Novel Conformations Using the Atomic Force Microscope. *Nat. Struct. Biol.* **2000**, *7*, 719−724.
(526) Florin, E.-L.; Moy, V. T.; Gaub, H. E. Adhesion Forces between Individual Ligand-Receptor Pairs. *Science* **1994**, *264*, 415−417.
(527) Lee, G. U.; Chrisey, L. A.; Colton, R. J. Direct Measurement of the Forces between Complementary Strands of DNA. *Science* **1994**, *266*, 771−773.
(528) Hinterdorfer, P.; Baumgartner, W.; Gruber, H. J.; Schilcher, K.; Schindler, H. Detection and Localization of Individual Antibody-Antigen Recognition Events by Atomic Force Microscopy. *Proc. Natl. Acad. Sci. U. S. A.* **1996**, *93*, 3477−3481.
(529) Rief, M.; Gautel, M.; Oesterhelt, F.; Fernandez, J. M.; Gaub, H. E. Reversible Unfolding of Individual Titin Immunoglobulin Domains by AFM. *Science* **1997**, *276*, 1109−1112.
(530) Hinterdorfer, P.; Dufrene, Y. F. Detection and Localization of Single Molecular Recognition Events Using Atomic Force Microscopy. *Nat. Methods* **2006**, *3*, 347−355.
(531) Shirude, P. S.; Okumus, B.; Ying, L. M.; Ha, T.; Balasubramanian, S. Single-Molecule Conformational Analysis of G-Quadruplex Formation in the Promoter DNA Duplex of the Proto-Oncogene C-Kit. *J. Am. Chem. Soc.* **2007**, *129*, 7484−7485.
(532) Sannohe, Y.; Endo, M.; Katsuda, Y.; Hidaka, K.; Sugiyama, H. Visualization of Dynamic Conformational Switching of the G-Quadruplex in a DNA Nanostructure. *J. Am. Chem. Soc.* **2010**, *132*, 16311−16313.
(533) Ricci, F.; Lai, R. Y.; Heeger, A. J.; Plaxco, K. W.; Sumner, J. J. Effect of Molecular Crowding on the Response of an Electrochemical DNA Sensor. *Langmuir* **2007**, *23*, 6827−6834.
(534) Wong, E. L.; Chow, E.; Gooding, J. J. DNA Recognition Interfaces: The Influence of Interfacial Design on the Efficiency and Kinetics of Hybridization. *Langmuir* **2005**, *21*, 6957−6965.
(535) Josephs, E. A.; Ye, T. Electric-Field Dependent Conformations of Single DNA Molecules on a Model Biosensor Surface. *Nano Lett.* **2012**, *12*, 5255−5261.
(536) Abel, G. R.; Josephs, E. A.; Luong, N.; Ye, T. A Switchable Surface Enables Visualization of Single DNA Hybridization Events with Atomic Force Microscopy. *J. Am. Chem. Soc.* **2013**, *135*, 6399−6402.
(537) Lu, Z. S.; Wang, Y.; Xu, D.; Pang, L. Aptamer-Tagged DNA Origami for Spatially Addressable Detection of Aflatoxin B1. *Chem. Commun.* **2017**, *53*, 941−944.
(538) Han, W. H.; Liao, J. M.; Chen, K. L.; Wu, S. M.; Chiang, Y. W.; Lo, S. T.; Chen, C. L.; Chiang, C. M. Enhanced Recognition of Single-Base Mismatch Using Locked Nucleic Acid-Integrated Hairpin DNA Probes Revealed by Atomic Force Microscopy Nanolithography. *Anal. Chem.* **2010**, *82*, 2395−2400.
(539) Subramanian, H. K. K.; Chakraborty, B.; Sha, R.; Seeman, N. C. The Label-Free Unambiguous Detection and Symbolic Display of Single Nucleotide Polymorphisms on DNA Origami. *Nano Lett.* **2011**, *11*, 910−913.
(540) Zhang, H.; Chao, J.; Pan, D.; Liu, H.; Qiang, Y.; Liu, K.; Cui, C.; Chen, J.; Huang, Q.; Hu, J.; et al. DNA Origami-Based Shape IDs for Single-Molecule Nanomechanical Genotyping. *Nat. Commun.* **2017**, *8*, 14738.
(541) Rief, M.; Clausen-Schaumann, H.; Gaub, H. E. Sequence-Dependent Mechanics of Single DNA Molecules. *Nat. Struct. Biol.* **1999**, *6*, 346−349.
(542) Leitner, M.; Mitchell, N.; Kastner, M.; Schlapak, R.; Gruber, H. J.; Hinterdorfer, P.; Howorka, S.; Ebner, A. Single-Molecule Afm Characterization of Individual Chemically Tagged DNA Tetrahedra. *ACS Nano* **2011**, *5*, 7048−7054.
(543) Kuzuya, A.; Sakai, Y.; Yamazaki, T.; Xu, Y.; Komiyama, M. Nanomechanical DNA Origami 'Single-Molecule Beacons' Directly Imaged by Atomic Force Microscopy. *Nat. Commun.* **2011**, *2*, 449.
(544) Garcia-Rico, E.; Alvarez-Puebla, R. A.; Guerrini, L. Direct Surface-Enhanced Raman Scattering (SERS) Spectroscopy of Nucleic Acids: From Fundamental Studies to Real-Life Applications. *Chem. Soc. Rev.* **2018**, *47*, 4909−4923.
(545) Cialla-May, D.; Zheng, X.-S.; Weber, K.; Popp, J. Recent Progress in Surface-Enhanced Raman Spectroscopy for Biological and Biomedical Applications: From Cells to Clinics. *Chem. Soc. Rev.* **2017**, *46*, 3945−3961.
(546) Li, L.; Steiner, U.; Mahajan, S. Single Nanoparticle SERS Probes of Ion Intercalation in Metal-Oxide Electrodes. *Nano Lett.* **2014**, *14*, 495−498.
(547) Li, L.; Hutter, T.; Finnemore, A. S.; Huang, F. M.; Baumberg, J. J.; Elliott, S. R.; Steiner, U.; Mahajan, S. Metal Oxide Nanoparticle Mediated Enhanced Raman Scattering and Its Use in Direct

DOI: 10.1021/acs.chemrev.9b00121
Chem. Rev. XXXX, XXX, XXX−XXX

Monitoring of Interfacial Chemical Reactions. *Nano Lett.* **2012**, *12*, 4242−4246.
(548) Nie, S. M.; Emery, S. R. Probing Single Molecules and Single Nanoparticles by Surface-Enhanced Raman Scattering. *Science* **1997**, *275*, 1102−1106.
(549) Wang, Y. Q.; Yan, B.; Chen, L. X. SERS Tags: Novel Optical Nanoprobes for Bioanalysis. *Chem. Rev.* **2013**, *113*, 1391−1428.
(550) Song, S. P.; Qin, Y.; He, Y.; Huang, Q.; Fan, C. H.; Chen, H. Y. Functional Nanoprobes for Ultrasensitive Detection of Biomolecules. *Chem. Soc. Rev.* **2010**, *39*, 4234−4243.
(551) Xu, J. J.; Zhao, W. W.; Song, S. P.; Fan, C. H.; Chen, H. Y. Functional Nanoprobes for Ultrasensitive Detection of Biomolecules: An Update. *Chem. Soc. Rev.* **2014**, *43*, 1601−1611.
(552) Lim, D. K.; Jeon, K. S.; Hwang, J. H.; Kim, H.; Kwon, S.; Suh, Y. D.; Nam, J. M. Highly Uniform and Reproducible Surface-Enhanced Raman Scattering from DNA-Tailorable Nanoparticles with 1-nm Interior Gap. *Nat. Nanotechnol.* **2011**, *6*, 452−460.
(553) Graham, D.; Thompson, D. G.; Smith, W. E.; Faulds, K. Control of Enhanced Raman Scattering Using a DNA-Based Assembly Process of Dye-Coded Nanoparticles. *Nat. Nanotechnol.* **2008**, *3*, 548−551.
(554) Pal, S.; Deng, Z. T.; Ding, B. Q.; Yan, H.; Liu, Y. DNA-Origami-Directed Self-Assembly of Discrete Silver-Nanoparticle Architectures. *Angew. Chem., Int. Ed.* **2010**, *49*, 2700−2704.
(555) Shi, M. L.; Zheng, J.; Liu, C. H.; Tan, G. X.; Qing, Z. H.; Yang, S.; Yang, J. F.; Tan, Y. J.; Yang, R. H. SERS Assay of Telomerase Activity at Single-Cell Level and Colon Cancer Tissues via Quadratic Signal Amplification. *Biosens. Bioelectron.* **2016**, *77*, 673−680.
(556) Zong, S. F.; Wang, Z. Y.; Chen, H.; Hu, G. H.; Liu, M.; Chen, P.; Cui, Y. P. Colorimetry and SERS Dual-Mode Detection of Telomerase Activity: Combining Rapid Screening with High Sensitivity. *Nanoscale* **2014**, *6*, 1808−1816.
(557) Fu, X.; Cheng, Z.; Yu, J.; Choo, P.; Chen, L.; Choo, J. A SERS-Based Lateral Flow Assay Biosensor for Highly Sensitive Detection of HIV-1 DNA. *Biosens. Bioelectron.* **2016**, *78*, 530−537.
(558) Cao, Y. W. C.; Jin, R. C.; Mirkin, C. A. Nanoparticles with Raman Spectroscopic Fingerprints for DNA and RNA Detection. *Science* **2002**, *297*, 1536−1540.
(559) Braun, G.; Lee, S. J.; Dante, M.; Nguyen, T. Q.; Moskovits, M.; Reich, N. Surface-Enhanced Raman Spectroscopy for DNA Detection by Nanoparticle Assembly onto Smooth Metal Films. *J. Am. Chem. Soc.* **2007**, *129*, 6378−6379.
(560) Wang, Z.; Zong, S.; Wu, L.; Zhu, D.; Cui, Y. SERS-Activated Platforms for Immunoassay: Probes, Encoding Methods, and Applications. *Chem. Rev.* **2017**, *117*, 7910−7963.
(561) Li, M.; Zhang, J. M.; Suri, S.; Sooter, L. J.; Ma, D. L.; Wu, N. Q. Detection of Adenosine Triphosphate with an Aptamer Biosensor Based on Surface-Enhanced Raman Scattering. *Anal. Chem.* **2012**, *84*, 2837−2842.
(562) Cottat, M.; D'Andrea, C.; Yasukuni, R.; Malashikhina, N.; Grinyte, R.; Lidgi-Guigui, N.; Fazio, B.; Sutton, A.; Oudar, O.; Charnaux, N.; Pavlov, V.; Toma, A.; Di Fabnzio, E.; Gucciardi, P. G.; de la Chapelle, M. L. High Sensitivity, High Selectivity SERS Detection of Mnsod Using Optical Nanoantennas Functionalized with Aptamers. *J. Phys. Chem. C* **2015**, *119*, 15532−15540.
(563) Rodriguez-Lorenzo, L.; Fabris, L.; Alvarez-Puebla, R. A. Multiplex Optical Sensing with Surface-Enhanced Raman Scattering: A Critical Review. *Anal. Chim. Acta* **2012**, *745*, 10−23.
(564) Zavaleta, C. L.; Smith, B. R.; Walton, I.; Doering, W.; Davis, G.; Shojaei, B.; Natan, M. J.; Gambhir, S. S. Multiplexed Imaging of Surface Enhanced Raman Scattering Nanotags in Living Mice Using Noninvasive Raman Spectroscopy. *Proc. Natl. Acad. Sci. U. S. A.* **2009**, *106*, 13511−13516.
(565) He, S. J.; Liu, K. K.; Su, S.; Yan, J.; Mao, X. H.; Wang, D. F.; He, Y.; Li, L. J.; Song, S. P.; Fan, C. H. Graphene-Based High-Efficiency Surface-Enhanced Raman Scattering-Active Platform for Sensitive and Multiplex DNA Detection. *Anal. Chem.* **2012**, *84*, 4622−4627.
(566) Sun, L.; Yu, C. X.; Irudayaraj, J. Surface-Enhanced Raman Scattering Based Nonfluorescent Probe for Multiplex DNA Detection. *Anal. Chem.* **2007**, *79*, 3981−3988.
(567) Zhang, Z. L.; Wen, Y. Q.; Ma, Y.; Luo, J.; Jiang, L.; Song, Y. L. Mixed DNA-Functionalized Nanoparticle Probes for Surface-Enhanced Raman Scattering-Based Multiplex DNA Detection. *Chem. Commun.* **2011**, *47*, 7407−7409.
(568) Wang, H. N.; Crawford, B. M.; Fales, A. M.; Bowie, M. L.; Seewaldt, V. L.; Vo-Dinh, T. Multiplexed Detection of MicroRNA Biomarkers Using SERS-Based Inverse Molecular Sentinel (IMS) Nanoprobes. *J. Phys. Chem. C* **2016**, *120*, 21047−21055.
(569) Wang, X.; Choi, N.; Cheng, Z.; Ko, J.; Chen, L. X.; Choo, J. Simultaneous Detection of Dual Nucleic Acids Using a SERS-Based Lateral Flow Assay Biosensor. *Anal. Chem.* **2017**, *89*, 1163−1169.
(570) Ye, S. J.; Wang, M. L.; Wang, Z. X.; Zhang, N.; Luo, X. L. A DNA-Linker-DNA Bifunctional Probe for Simultaneous SERS Detection of MiRNAs via Symmetric Signal Amplification. *Chem. Commun.* **2018**, *54*, 7786−7789.
(571) Gao, F. L.; Du, L. L.; Tang, D. Q.; Lu, Y.; Zhang, Y. Z.; Zhang, L. X. A Cascade Signal Amplification Strategy for Surface Enhanced Raman Spectroscopy Detection of Thrombin Based on Dnazyme Assistant DNA Recycling and Rolling Circle Amplification. *Biosens. Bioelectron.* **2015**, *66*, 423−430.
(572) Ye, S. J.; Guo, Y. Y.; Xiao, J.; Zhang, S. S. A Sensitive SERS Assay of L-Histidine via a DNAzyme-Activated Target Recycling Cascade Amplification Strategy. *Chem. Commun.* **2013**, *49*, 3643−3645.
(573) Ye, S.; Yang, Y.; Xiao, J.; Zhang, S. Surface-Enhanced Raman Scattering Assay Combined with Autonomous DNA Machine for Detection of Specific DNA and Cancer Cells. *Chem. Commun.* **2012**, *48*, 8535−8537.
(574) Zhang, H.; Liu, Y.; Gao, J.; Zhen, J. H. A Sensitive SERS Detection of MiRNA Using a Label-Free Multifunctional Probe. *Chem. Commun.* **2015**, *51*, 16836−16839.
(575) Zhang, H.; Harpster, M. H.; Park, H. J.; Johnson, P. A.; et al. Surface-Enhanced Raman Scattering Detection of DNA Derived from the West Nile Virus Genome Using Magnetic Capture of Raman-Active Gold Nanoparticles. *Anal. Chem.* **2011**, *83*, 254−260.
(576) Pang, Y. F.; Wang, C. W.; Wang, J.; Sun, Z. W.; Xiao, R.; Wang, S. Q. Fe_3O_4@Ag Magnetic Nanoparticles for MicroRNA Capture and Duplex-Specific Nuclease Signal Amplification Based SERS Detection in Cancer Cells. *Biosens. Bioelectron.* **2016**, *79*, 574−580.
(577) Qi, L.; Xiao, M. S.; Wang, X. W.; Wang, C.; Wang, L. H.; Song, S. P.; Qu, X. M.; Li, L.; Shi, J. Y.; Pei, H. DNA-Encoded Raman-Active Anisotropic Nanoparticles for MicroRNA Detection. *Anal. Chem.* **2017**, *89*, 9850−9856.
(578) Qi, L.; Xiao, M. S.; Wang, F.; Wang, L. H.; Ji, W.; Man, T. T.; Aldalbahi, A.; Khan, M. N.; Periyasami, G.; Rahaman, M.; Alrohaili, A.; Qu, X. M.; Pei, H.; Wang, C.; Li, L. Poly-Cytosine-Mediated Nanotags for SERS Detection of Hg^{2+}. *Nanoscale* **2017**, *9*, 14184−14191.
(579) Xu, L. G.; Yin, H. H.; Ma, W.; Kuang, H.; Wang, L. B.; Xu, C. L. Ultrasensitive SERS Detection of Mercury Based on the Assembled Gold Nanochains. *Biosens. Bioelectron.* **2015**, *67*, 472−476.
(580) Li, W. Y.; Camargo, P. H. C.; Lu, X. M.; Xia, Y. N. Dimers of Silver Nanospheres: Facile Synthesis and Their Use as Hot Spots for Surface-Enhanced Raman Scattering. *Nano Lett.* **2009**, *9*, 485−490.
(581) Kang, T.; Yoo, S. M.; Yoon, I.; Lee, S. Y.; Kim, B. Patterned Multiplex Pathogen DNA Detection by Au Particle-on-Wire SERS Sensor. *Nano Lett.* **2010**, *10*, 1189−1193.
(582) Li, M.; Cushing, S. K.; Liang, H. Y.; Suri, S.; Ma, D. L.; Wu, N. Q. Plasmonic Nanorice Antenna on Triangle Nanoarray for Surface-Enhanced Raman Scattering Detection of Hepatitis B Virus DNA. *Anal. Chem.* **2013**, *85*, 2072−2078.
(583) Gandra, N.; Abbas, A.; Tian, L. M.; Singamaneni, S. Plasmonic Planet-Satellite Analogues: Hierarchical Self-Assembly of Gold Nanostructures. *Nano Lett.* **2012**, *12*, 2645−2651.
(584) Yan, J.; Su, S.; He, S. J.; He, Y.; Zhao, B.; Wang, D. F.; Zhang, H. L.; Huang, Q.; Song, S. P.; Fan, C. Nano Rolling-Circle Amplification for Enhanced SERS Hot Spots in Protein Microarray Analysis. *Anal. Chem.* **2012**, *84*, 9139−9145.
(585) Ma, M.; Yin, H. H.; Xu, L. G.; Wu, X. L.; Kuang, H.; Wang, L. B.; Xu, C. L. Ultrasensitive Aptamer-Based SERS Detection of PSAs by

DOI: 10.1021/acs.chemrev.9b00121
Chem. Rev. XXXX, XXX, XXX−XXX

Heterogeneous Satellite Nanoassemblies. *Chem. Commun.* **2014**, *50*, 9737−9740.
(586) Feng, J. J.; Wu, X. L.; Ma, W.; Kuang, H.; Xu, L. G.; Xu, C. L. A SERS Active Bimetallic Core-Satellite Nanostructure for the Ultrasensitive Detection of Mucin-1. *Chem. Commun.* **2015**, *51*, 14761−14763.
(587) Lim, D. K.; Jeon, K. S.; Kim, H. M.; Nam, J. M.; Suh, Y. D. Nanogap-Engineerable Raman-Active Nanodumbbells for Single-Molecule Detection. *Nat. Mater.* **2010**, *9*, 60−67.
(588) Lee, J. H.; Nam, J. M.; Jeon, K. S.; Lim, D. K.; Kim, H.; Kwon, S.; Lee, H.; Suh, Y. D. Tuning and Maximizing the Single-Molecule Surface-Enhanced Raman Scattering from DNA-Tethered Nanodumbbells. *ACS Nano* **2012**, *6*, 9574−9584.
(589) Xu, L. G.; Yan, W. J.; Ma, W.; Kuang, H.; Wu, X. L.; Liu, L. Q.; Zhao, Y.; Wang, L. B.; Xu, C. L. SERS Encoded Silver Pyramids for Attomolar Detection of Multiplexed Disease Biomarkers. *Adv. Mater.* **2015**, *27*, 1706−1711.
(590) Xu, L. G.; Zhao, S.; Ma, W.; Wu, X. L.; Li, S.; Kuang, H.; Wang, L. B.; Xu, C. L. Multigaps Embedded Nanoassemblies Enhance in Situ Raman Spectroscopy for Intracellular Telomerase Activity Sensing. *Adv. Funct. Mater.* **2016**, *26*, 1602−1608.
(591) Shen, J. L.; Su, J.; Yan, J.; Zhao, B.; Wang, D. F.; Wang, S. Y.; Li, K.; Liu, M. M.; He, Y.; Mathur, S.; Fan, C. H.; Song, S. P. Bimetallic Nano-Mushrooms with DNA-Mediated Interior Nanogaps for High-Efficiency SERS Signal Amplification. *Nano Res.* **2015**, *8*, 731−742.
(592) Su, J.; Wang, D. F.; Norbel, L.; Shen, J. L.; Zhao, Z. H.; Dou, Y. Z.; Peng, T. H.; Shi, J. Y.; Mathur, S.; Fan, C. H.; Song, S. P. Multicolor Gold Silver Nano-Mushrooms as Ready-to-Use SERS Probes for Ultrasensitive and Multiplex DNA/miRNA Detection. *Anal. Chem.* **2017**, *89*, 2531−2538.
(593) Acuna, G. P.; Moller, F. M.; Holzmeister, P.; Beater, S.; Lalkens, B.; Tinnefeld, P. Fluorescence Enhancement at Docking Sites of DNA-Directed Self-Assembled Nanoantennas. *Science* **2012**, *338*, 506−510.
(594) Chikkaraddy, R.; Turek, V. A.; Kongsuwan, N.; Benz, F.; Carnegie, C.; van de Goor, T.; de Nijs, B.; Demetriadou, A.; Hess, O.; Keyser, U. F.; Baumberg, J. J. Mapping Nanoscale Hotspots with Single-Molecule Emitters Assembled into Plasmonic Nanocavities Using DNA Origami. *Nano Lett.* **2018**, *18*, 405−411.
(595) Tan, S. J.; Campolongo, M. J.; Luo, D.; Cheng, W. L. Building Plasmonic Nanostructures with DNA. *Nat. Nanotechnol.* **2011**, *6*, 268−276.
(596) Kuzyk, A.; Schreiber, R.; Fan, Z. Y.; Pardatscher, G.; Roller, E. M.; Hogele, A.; Simmel, F. C.; Govorov, A. O.; Liedl, T. DNA-Based Self-Assembly of Chiral Plasmonic Nanostructures with Tailored Optical Response. *Nature* **2012**, *483*, 311−314.
(597) Kuzyk, A.; Schreiber, R.; Zhang, H.; Govorov, A. O.; Liedl, T.; Liu, N. Reconfigurable 3D Plasmonic Metamolecules. *Nat. Mater.* **2014**, *13*, 862−866.
(598) Man, T.; Ji, W.; Liu, X.; Zhang, C.; Li, L.; Pei, H.; Fan, C. Chiral Metamolecules with Active Plasmonic Transition. *ACS Nano* **2019**, *13*, 4826−4833.
(599) Puchkova, A.; Vietz, C.; Pibiri, E.; Wunsch, B.; Paz, M. S.; Acuna, G. P.; Tinnefeld, P. DNA Origami Nanoantennas with over 5000-Fold Fluorescence Enhancement and Single-Molecule Detection at 25 μM. *Nano Lett.* **2015**, *15*, 8354−8359.
(600) Tanwar, S.; Haldar, K. K.; Sen, T. DNA Origami Directed Au Nanostar Dimers for Single-Molecule Surface-Enhanced Raman Scattering. *J. Am. Chem. Soc.* **2017**, *139*, 17639−17648.
(601) Zhan, P. F.; Wen, T.; Wang, Z. G.; He, Y. B.; Shi, J.; Wang, T.; Liu, X. F.; Lu, G. W.; Ding, B. Q. DNA Origami Directed Assembly of Gold Bowtie Nanoantennas for Single-Molecule Surface-Enhanced Raman Scattering. *Angew. Chem., Int. Ed.* **2018**, *57*, 2846−2850.
(602) Thacker, V. V.; Herrmann, L. O.; Sigle, D. O.; Zhang, T.; Liedl, T.; Baumberg, J. J.; Keyser, U. F. DNA Origami Based Assembly of Gold Nanoparticle Dimers for Surface-Enhanced Raman Scattering. *Nat. Commun.* **2014**, *5*, 3448.
(603) Simoncelli, S.; Roller, E. M.; Urban, P.; Schreiber, R.; Turberfield, A. J.; Liedl, T.; Lohmuller, T. Quantitative Single-Molecule Surface Enhanced Raman Scattering by Optothermal Tuning of DNA Origami-Assembled Plasmonic Nanoantennas. *ACS Nano* **2016**, *10*, 9809−9815.
(604) Yan, H.; Zhang, X. P.; Shen, Z. Y.; Seeman, N. C. A Robust DNA Mechanical Device Controlled by Hybridization Topology. *Nature* **2002**, *415*, 62−65.
(605) Pei, H.; Zuo, X. L.; Pan, D.; Shi, J. Y.; Huang, Q.; Fan, C. H. Scaffolded Biosensors with Designed DNA Nanostructures. *NPG Asia Mater.* **2013**, *5*, No. e51.
(606) Rothemund, P. W. K. Folding DNA to Create Nanoscale Shapes and Patterns. *Nature* **2006**, *440*, 297−302.
(607) Pinheiro, A. V.; Han, D. R.; Shih, W. M.; Yan, H. Challenges and Opportunities for Structural DNA Nanotechnology. *Nat. Nanotechnol.* **2011**, *6*, 763−772.
(608) Su, Y.; Li, D.; Liu, B.; Xiao, M.; Wang, F.; Li, L.; Zhang, X.; Pei, H. Rational Design of Framework Nucleic Acids for Bioanalytical Applications. *ChemPlusChem* **2019**, *84*, 512−523.
(609) Chao, J.; Zhu, D.; Zhang, Y. N.; Wang, L. H.; Fan, C. H. DNA Nanotechnology-Enabled Biosensors. *Biosens. Bioelectron.* **2016**, *76*, 68−79.
(610) Yang, F.; Li, Q.; Wang, L. H.; Zhang, G. J.; Fan, C. H. Framework-Nucleic-Acid-Enabled Biosensor Development. *ACS Sensors* **2018**, *3*, 903−919.
(611) Ge, Z. L.; Gu, H. Z.; Li, Q.; Fan, C. H. Concept and Development of Framework Nucleic Acids. *J. Am. Chem. Soc.* **2018**, *140*, 17808−17819.
(612) So, H. M.; Won, K.; Kim, Y. H.; Kim, B. K.; Ryu, B. H.; Na, P. S.; Kim, H.; Lee, J. O. Single-Walled Carbon Nanotube Biosensors Using Aptamers as Molecular Recognition Elements. *J. Am. Chem. Soc.* **2005**, *127*, 11906−11907.
(613) Madsen, M.; Gothelf, K. V. Chemistries for DNA Nanotechnology. *Chem. Rev.* **2019**, *119*, 6384−6458.
(614) Voigt, N. V.; Torring, T.; Rotaru, A.; Jacobsen, M. F.; Ravnsbaek, J. B.; Subramani, R.; Mamdouh, W.; Kjems, J.; Mokhir, A.; Besenbacher, F.; Gothelf, K. V. Single-Molecule Chemical Reactions on DNA Origami. *Nat. Nanotechnol.* **2010**, *5*, 200−203.
(615) Meng, H. M.; Liu, H.; Kuai, H. L.; Peng, R. Z.; Mo, L. T.; Zhang, X. B. Aptamer-Integrated DNA Nanostructures for Biosensing, Bioimaging and Cancer Therapy. *Chem. Soc. Rev.* **2016**, *45*, 2583−2602.
(616) Liu, J. W.; Cao, Z. H.; Lu, Y. Functional Nucleic Acid Sensors. *Chem. Rev.* **2009**, *109*, 1948−1998.
(617) Chen, Y. J.; Groves, B.; Muscat, R. A.; Seelig, G. DNA Nanotechnology from the Test Tube to the Cell. *Nat. Nanotechnol.* **2015**, *10*, 748−760.
(618) Wang, D. F.; Fu, Y. M.; Yan, J.; Zhao, B.; Dai, B.; Chao, J.; Liu, H. J.; He, D. N.; Zhang, Y.; Fan, C. H.; Song, S. P. Molecular Logic Gates on DNA Origami Nanostructures for MicroRNA Diagnostics. *Anal. Chem.* **2014**, *86*, 1932−1936.
(619) Ye, D.; Zuo, X.; Fan, C. DNA Nanotechnology-Enabled Interfacial Engineering for Biosensor Development. *Annu. Rev. Anal. Chem.* **2018**, *11*, 171−195.
(620) Rosi, N. L.; Mirkin, C. A. Nanostructures in Biodiagnostics. *Chem. Rev.* **2005**, *105*, 1547−1562.
(621) Ke, Y.; Castro, C.; Choi, J. H. Structural DNA Nanotechnology: Artificial Nanostructures for Biomedical Research. *Annu. Rev. Biomed. Eng.* **2018**, *20*, 375−401.
(622) Li, S.; Tian, T.; Zhang, T.; Cai, X.; Lin, Y. Advances in Biological Applications of Self-Assembled DNA Tetrahedral Nanostructures. *Mater. Today* **2019**, *24*, 57−68.
(623) Xie, N.; Liu, S.; Yang, X.; He, X.; Huang, J.; Wang, K. DNA Tetrahedron Nanostructures for Biological Applications: Biosensors and Drug Delivery. *Analyst* **2017**, *142*, 3322−3332.
(624) Gradisar, H.; Bozic, S.; Doles, T.; Vengust, D.; Hafner-Bratkovic, I.; Mertelj, A.; Webb, B.; Sali, A.; Klavzar, S.; Jerala, R. Design of a Single-Chain Polypeptide Tetrahedron Assembled from Coiled-Coil Segments. *Nat. Chem. Biol.* **2013**, *9*, 362−366.
(625) Lin, M. H.; Song, P.; Zhou, G. B.; Zuo, X. L.; Aldalbahi, A.; Lou, X. D.; Shi, J. Y.; Fan, C. H. Electrochemical Detection of Nucleic Acids, Proteins, Small Molecules and Cells Using a DNA-Nanostructure-

DOI: 10.1021/acs.chemrev.9b00121
Chem. Rev. XXXX, XXX, XXX−XXX

Based Universal Biosensing Platform. *Nat. Protoc.* **2016**, *11*, 1244−1263.
(626) Wang, J. P.; Leong, M. C.; Leong, E. Z. W.; Sen Kuan, W.; Leong, D. T. Clinically Relevant Detection of Streptococcus Pneumoniae with DNA-Antibody Nanostructures. *Anal. Chem.* **2017**, *89*, 6900−6906.
(627) Dong, S. B.; Zhao, R. T.; Zhu, J. G.; Lu, X.; Li, Y.; Qiu, S. F.; Jia, L. L.; Jiao, X.; Song, S. P.; Fan, C. H.; Hao, R. Z.; Song, H. B. Electrochemical DNA Biosensor Based on a Tetrahedral Nanostructure Probe for the Detection of Avian Influenza a (H7N9) Virus. *ACS Appl. Mater. Interfaces* **2015**, *7*, 8834−8842.
(628) Qu, X.; Xiao, M.; Li, F.; Lai, W.; Li, L.; Zhou, Y.; Lin, C.; Li, Q.; Ge, Z.; Wen, Y.; et al. Framework Nucleic Acid-Mediated Pull-Down MicroRNA Detection with Hybridization Chain Reaction Amplification. *ACS Appl. Bio Mater.* **2018**, *1*, 859−864.
(629) Qu, X.; Zhang, H.; Chen, H.; Aldalbahi, A.; Li, L.; Tian, Y.; Weitz, D. A.; Pei, H. Convection-Driven Pull-Down Assays in Nanoliter Droplets Using Scaffolded Aptamers. *Anal. Chem.* **2017**, *89*, 3468−3473.
(630) Qu, X.; Xiao, M.; Li, F.; Lai, W.; Li, L.; Zhou, Y.; Lin, C.; Li, Q.; Ge, Z.; Wen, Y.; Pei, H.; Liu, G. Framework Nucleic Acid-Mediated Pull-Down MicroRNA Detection with Hybridization Chain Reaction Amplification. *ACS Appl. Bio Mater.* **2018**, *1*, 859−864.
(631) Xiao, M.; Qu, X.; Li, L.; Pei, H. *DNA Nanotechnology*; Springer, 2018.
(632) Lionnet, T.; Czaplinski, K.; Darzacq, X.; Shav-Tal, Y.; Wells, A. L.; Chao, J. A.; Park, H. Y.; de Turris, V.; Lopez-Jones, M.; Singer, R. H. A Transgenic Mouse for in Vivo Detection of Endogenous Labeled mRNA. *Nat. Methods* **2011**, *8*, 165−170.
(633) Heller, M. J. DNA Microarray Technology: Devices, Systems, and Applications. *Annu. Rev. Biomed. Eng.* **2002**, *4*, 129−153.
(634) Ochmann, S. E.; Vietz, C.; Trofymchuk, K.; Acuna, G. P.; Lalkens, B.; Tinnefeld, P. Optical Nanoantenna for Single Molecule-Based Detection of Zika Virus Nucleic Acids without Molecular Multiplication. *Anal. Chem.* **2017**, *89*, 13000−13007.
(635) Gong, P.; Levicky, R. DNA Surface Hybridization Regimes. *Proc. Natl. Acad. Sci. U. S. A.* **2008**, *105*, 5301−5306.
(636) Liu, G.; Sun, C. F.; Li, D.; Song, S. P.; Mao, B. W.; Fan, C. H.; Tian, Z. Q. Gating of Redox Currents at Gold Nanoelectrodes via DNA Hybridization. *Adv. Mater.* **2010**, *22*, 2148−2150.
(637) Wong, E. L. S.; Chow, E.; Gooding, J. J. DNA Recognition Interfaces: The Influence of Interfacial Design on the Efficiency and Kinetics of Hybridization. *Langmuir* **2005**, *21*, 6957−6965.
(638) Pei, H.; Lu, N.; Wen, Y. L.; Song, S. P.; Liu, Y.; Yan, H.; Fan, C. H. A DNA Nanostructure-Based Biomolecular Probe Carrier Platform for Electrochemical Biosensing. *Adv. Mater.* **2010**, *22*, 4754−4758.
(639) Choi, Y.; Schmidt, C.; Tinnefeld, P.; Bald, I.; Rodiger, S. A New Reporter Design Based on DNA Origami Nanostructures for Quantification of Short Oligonucleotides Using Microbeads. *Sci. Rep.* **2019**, *9*, 4769.
(640) Selnihhin, D.; Sparvath, S. M.; Preus, S.; Birkedal, V.; Andersen, E. S. Multifluorophore DNA Origami Beacon as a Biosensing Platform. *ACS Nano* **2018**, *12*, 5699−5708.
(641) Squires, T. M.; Messinger, R. J.; Manalis, S. R. Making It Stick: Convection, Reaction and Diffusion in Surface-Based Biosensors. *Nat. Biotechnol.* **2008**, *26*, 417−426.
(642) Sheehan, P. E.; Whitman, L. J. Detection Limits for Nanoscale Biosensors. *Nano Lett.* **2005**, *5*, 803−807.
(643) Lin, M. H.; Wang, J. J.; Zhou, G. B.; Wang, J. B.; Wu, N.; Lu, J. X.; Gao, J. M.; Chen, X. Q.; Shi, J. Y.; Zuo, X. L.; Fan, C. H. Programmable Engineering of a Biosensing Interface with Tetrahedral DNA Nanostructures for Ultrasensitive DNA Detection. *Angew. Chem., Int. Ed.* **2015**, *54*, 2151−2155.
(644) Lee, J.; Bisso, P. W.; Srinivas, R. L.; Kim, J. J.; Swiston, A. J.; Doyle, P. S. Universal Process-Inert Encoding Architecture for Polymer Microparticles. *Nat. Mater.* **2014**, *13*, 524−529.
(645) Allen, F.; Pon, A.; Wilson, M.; Greiner, R.; Wishart, D. CFM-ID: A Web Server for Annotation, Spectrum Prediction and Metabolite Identification from Tandem Mass Spectra. *Nucleic Acids Res.* **2014**, *42*, W94−W99.
(646) Pregibon, D. C.; Toner, M.; Doyle, P. S. Multifunctional Encoded Particles for High-Throughput Biomolecule Analysis. *Science* **2007**, *315*, 1393−1396.
(647) Sun, S.; Yao, H. X.; Zhang, F. F.; Zhu, J. Multiplexed DNA Detection Based on Positional Encoding/Decoding with Self-Assembled DNA Nanostructures. *Chem. Sci.* **2015**, *6*, 930−934.
(648) Jin, L. Y.; Dong, Y. M.; Wu, X. M.; Cao, G. X.; Wang, G. L. Versatile and Amplified Biosensing through Enzymatic Cascade Reaction by Coupling Alkaline Phosphatase in Situ Generation of Photoresponsive Nanozyme. *Anal. Chem.* **2015**, *87*, 10429−10436.
(649) Zhang, Y. F.; Hess, H. Toward Rational Design of High-Efficiency Enzyme Cascades. *ACS Catal.* **2017**, *7*, 6018−6027.
(650) Fu, J. L.; Yang, Y. R.; Johnson-Buck, A.; Liu, M. H.; Liu, Y.; Walter, N. G.; Woodbury, N. W.; Yan, H. Multi-Enzyme Complexes on DNA Scaffolds Capable of Substrate Channelling with an Artificial Swinging Arm. *Nat. Nanotechnol.* **2014**, *9*, 531−536.
(651) Fu, J. L.; Yang, Y. R.; Dhakal, S.; Zhao, Z.; Liu, M. H.; Zhang, T.; Walter, N. G.; Yan, H. Assembly of Multienzyme Complexes on DNA Nanostructures. *Nat. Protoc.* **2016**, *11*, 2243−2273.
(652) Kou, B. B.; Chai, Y. Q.; Yuan, Y.; Yuan, R. Dynamical Regulation of Enzyme Cascade Amplification by a Regenerated DNA Nanotweezer for Ultrasensitive Electrochemical DNA Detection. *Anal. Chem.* **2018**, *90*, 10701−10706.
(653) Funck, T.; Nicoli, F.; Kuzyk, A.; Liedl, T. Sensing Picomolar Concentrations of RNA Using Switchable Plasmonic Chirality. *Angew. Chem.* **2018**, *130*, 13683−13686.
(654) Schwarzenbach, H.; Hoon, D. S. B.; Pantel, K. Cell-Free Nucleic Acids as Biomarkers in Cancer Patients. *Nat. Rev. Cancer* **2011**, *11*, 426−437.
(655) Pall, G. S.; Codony-Servat, C.; Byrne, J.; Ritchie, L.; Hamilton, A. Carbodiimide-Mediated Cross-Linking of RNA to Nylon Membranes Improves the Detection of siRNA, miRNA and piRNA by Northern Blot. *Nucleic Acids Res.* **2007**, *35*, No. e60.
(656) Couzin, J. Genomics-Microarray Data Reproduced, but Some Concerns Remain. *Science* **2006**, *313*, 1559−1559.
(657) Nolan, T.; Hands, R. E.; Bustin, S. A. Quantification of mRNA Using Real-Time RT-PCR. *Nat. Protoc.* **2006**, *1*, 1559−1582.
(658) He, L.; Lu, D. Q.; Liang, H.; Xie, S. T.; Luo, C.; Hu, M. M.; Xu, L. J.; Zhang, X. B.; Tan, W. H. Fluorescence Resonance Energy Transfer-Based DNA Tetrahedron Nanotweezer for Highly Reliable Detection of Tumor-Related mRNA in Living Cells. *ACS Nano* **2017**, *11*, 4060−4066.
(659) Tay, C. Y.; Yuan, L.; Leong, D. T. Nature-Inspired DNA Nanosensor for Real-Time in Situ Detection of mRNA in Living Cells. *ACS Nano* **2015**, *9*, 5609−5617.
(660) Lu, J.; Getz, G.; Miska, E. A.; Alvarez-Saavedra, E.; Lamb, J.; Peck, D.; Sweet-Cordero, A.; Ebet, B. L.; Mak, R. H.; Ferrando, A. A.; Downing, J. R.; Jacks, T.; Horvitz, H. R.; Golub, T. R. MicroRNA Expression Profiles Classify Human Cancers. *Nature* **2005**, *435*, 834−838.
(661) Pritchard, C. C.; Cheng, H. H.; Tewari, M. MicroRNA Profiling: Approaches and Considerations. *Nat. Rev. Genet.* **2012**, *13*, 358−369.
(662) Lin, M. H.; Wen, Y. L.; Li, L. Y.; Pei, H.; Liu, G.; Song, H. Y.; Zuo, X. L.; Fan, C. H.; Huang, Q. Target-Responsive, DNA Nanostructure-Based E-DNA Sensor for MicroRNA Analysis. *Anal. Chem.* **2014**, *86*, 2285−2288.
(663) Ge, Z. L.; Lin, M. H.; Wang, P.; Pei, H.; Yan, J.; Sho, J. Y.; Huang, Q.; He, D. N.; Fan, C. H.; Zuo, X. L. Hybridization Chain Reaction Amplification of MicroRNA Detection with a Tetrahedral DNA Nanostructure-Based Electrochemical Biosensor. *Anal. Chem.* **2014**, *86*, 2124−2130.
(664) Zhang, P.; Jiang, J.; Yuan, R.; Zhuo, Y.; Chai, Y. Q. Highly Ordered and Field-Free 3D DNA Nanostructure: The Next Generation of DNA Nanomachine for Rapid Single-Step Sensing. *J. Am. Chem. Soc.* **2018**, *140*, 9361−9364.

DOI: 10.1021/acs.chemrev.9b00121
Chem. Rev. XXXX, XXX, XXX−XXX

(665) Liu, D. B.; Xie, Y. Y.; Shao, H. W.; Jiang, X. Y. Using Azobenzene-Embedded Self-Assembled Monolayers to Photochemically Control Cell Adhesion Reversibly. *Angew. Chem., Int. Ed.* **2009**, *48*, 4406−4408.
(666) You, M. X.; Chen, Y.; Zhang, X. B.; Liu, H. P.; Wang, R. W.; Wang, K. L.; Williams, K. R.; Tan, W. H. An Autonomous and Controllable Light-Driven DNA Walking Device. *Angew. Chem., Int. Ed.* **2012**, *51*, 2457−2460.
(667) Nishi, T.; Forgac, M. The Vacuolar (H^+)-ATPases—Nature's Most Versatile Proton Pumps. *Nat. Rev. Mol. Cell Biol.* **2002**, *3*, 94−103.
(668) Paroutis, P.; Touret, N.; Grinstein, S. The pH of the Secretory Pathway: Measurement, Determinants, and Regulation. *Physiology* **2004**, *19*, 207−215.
(669) Tews, I.; Findeisen, F.; Sinning, I.; Schultz, A.; Schultz, J. E.; Linder, J. U. The Structure of a pH-Sensing Mycobacterial Adenylyl Cyclase Holoenzyme. *Science* **2005**, *308*, 1020−1023.
(670) Matsuyama, S.; Llopis, J.; Deveraux, Q. L.; Tsien, R. Y.; Reed, J. C. Changes in Intramitochondrial and Cytosolic pH: Early Events That Modulate Caspase Activation During Apoptosis. *Nat. Cell Biol.* **2000**, *2*, 318−325.
(671) Zhou, K. J.; Liu, H. M.; Zhang, S. R.; Huang, X. N.; Wang, Y. G.; Huang, G.; Sumer, B. D.; Gao, J. M. Multicolored pH-Tunable and Activatable Fluorescence Nanoplatform Responsive to Physiologic pH Stimuli. *J. Am. Chem. Soc.* **2012**, *134*, 7803−7811.
(672) Gallagher, F. A.; Kettunen, M. I.; Day, S. E.; Hu, D. E.; Ardenkjaer-Larsen, J. H.; in't Zandt, R.; Jensen, P. R.; Karlsson, M.; Golman, K.; Lerche, M. H.; Brindle, K. M. Magnetic Resonance Imaging of pH in Vivo Using Hyperpolarized ^{13}C-Labelled Bicarbonate. *Nature* **2008**, *453*, 940−943.
(673) Mura, S.; Nicolas, J.; Couvreur, P. Stimuli-Responsive Nanocarriers for Drug Delivery. *Nat. Mater.* **2013**, *12*, 991−1003.
(674) Chandrasekaran, A. R. Designer DNA Architectures: Applications in Nanomedicine. *Nanobiomedicine* **2016**, *3*, 6.
(675) McLaughlin, C. K.; Hamblin, G. D.; Sleiman, H. F. Supramolecular DNA Assembly. *Chem. Soc. Rev.* **2011**, *40*, 5647−5656.
(676) Seeman, N. C. Nanomaterials Based on DNA. *Annu. Rev. Biochem.* **2010**, *79*, 65−87.
(677) Greschner, A. A.; Bujold, K. E.; Sleiman, H. F. Intercalators as Molecular Chaperones in DNA Self-Assembly. *J. Am. Chem. Soc.* **2013**, *135*, 11283−11288.
(678) Krishnan, Y.; Simmel, F. C. Nucleic Acid Based Molecular Devices. *Angew. Chem., Int. Ed.* **2011**, *50*, 3124−3156.
(679) Li, T.; Famulok, M. I-Motif-Programmed Functionalization of DNA Nanocircles. *J. Am. Chem. Soc.* **2013**, *135*, 1593−1599.
(680) Liu, D. S.; Bruckbauer, A.; Abell, C.; Balasubramanian, S.; Kang, D. J.; Klenerman, D.; Zhou, D. J. A Reversible pH-Driven DNA Nanoswitch Array. *J. Am. Chem. Soc.* **2006**, *128*, 2067−2071.
(681) Zhou, J.; Amrane, S.; Korkut, D. N.; Bourdoncle, A.; He, H. Z.; Ma, D. L.; Mergny, J. L. Combination of I-Motif and G-Quadruplex Structures within the Same Strand: Formation and Application. *Angew. Chem., Int. Ed.* **2013**, *52*, 7742−7746.
(682) Chen, Y.; Lee, S. H.; Mao, C. A DNA Nanomachine Based on a Duplex-Triplex Transition. *Angew. Chem., Int. Ed.* **2004**, *43*, 5335−5338.
(683) Yatsunyk, L. A.; Mendoza, O.; Mergny, J. L. "Nano-Oddities": Unusual Nucleic Acid Assemblies for DNA-Based Nanostructures and Nanodevices. *Acc. Chem. Res.* **2014**, *47*, 1836−1844.
(684) Chandrasekaran, A. R.; Rusling, D. A. Triplex-Forming Oligonucleotides: A Third Strand for DNA Nanotechnology. *Nucleic Acids Res.* **2018**, *46*, 1021−1037.
(685) Abou Assi, H.; Garavís, M.; González, C.; Damha, M. J. I-Motif DNA: Structural Features and Significance to Cell Biology. *Nucleic Acids Res.* **2018**, *46*, 8038−8056.
(686) Elbaz, J.; Wang, Z. G.; Orbach, R.; Willner, I. pH-Stimulated Concurrent Mechanical Activation of Two DNA "Tweezers". A "Set-Reset" Logic Gate System. *Nano Lett.* **2009**, *9*, 4510−4514.
(687) Liu, D. S.; Balasubramanian, S. A Proton-Fuelled DNA Nanomachine. *Angew. Chem., Int. Ed.* **2003**, *42*, 5734−5736.
(688) Narayanaswamy, N.; Nair, R. R.; Suseela, Y. V.; Saini, D. K.; Govindaraju, T. A Molecular Beacon-Based DNA Switch for Reversible pH Sensing in Vesicles and Live Cells. *Chem. Commun.* **2016**, *52*, 8741−8744.
(689) Gehring, K.; Leroy, J.-L.; Guéron, M. A Tetrameric DNA Structure with Protonated Cytosine-Cytosine Base Pairs. *Nature* **1993**, *363*, 561−565.
(690) Dong, Y. C.; Yang, Z. Q.; Liu, D. S. DNA Nanotechnology Based on I-Motif Structures. *Acc. Chem. Res.* **2014**, *47*, 1853−1860.
(691) Pugh, G. C.; Burns, J. R.; Howorka, S. Comparing Proteins and Nucleic Acids for Next-Generation Biomolecular Engineering. *Nat. Rev. Chem.* **2018**, *2*, 113−130.
(692) Cheng, E. J.; Xing, Y. Z.; Chen, P.; Yang, Y.; Sun, Y. W.; Zhou, D. J.; Xu, L. J.; Fan, Q. H.; Liu, D. S. A pH-Triggered, Fast-Responding DNA Hydrogel. *Angew. Chem., Int. Ed.* **2009**, *48*, 7660−7663.
(693) Shu, W. M.; Liu, D. S.; Watari, M.; Riener, C. K.; Strunz, T.; Welland, M. E.; Balasubramanian, S.; McKendry, R. A. DNA Molecular Motor Driven Micromechanical Cantilever Arrays. *J. Am. Chem. Soc.* **2005**, *127*, 17054−17060.
(694) Chen, C.; Li, M.; Xing, Y. Z.; Li, Y. M.; Joedecke, C. C.; Jin, J.; Yang, Z. Q.; Liu, D. S. Study of pH-Induced Folding and Unfolding Kinetics of the DNA I-Motif by Stopped-Flow Circular Dichroism. *Langmuir* **2012**, *28*, 17743−17748.
(695) Nesterova, I. V.; Nesterov, E. E. Rational Design of Highly Responsive pH Sensors Based on DNA I-Motif. *J. Am. Chem. Soc.* **2014**, *136*, 8843−8846.
(696) Kuzuya, A.; Watanabe, R.; Yamanaka, Y.; Tamaki, T.; Kaino, M.; Ohya, Y. Nanomechanical DNA Origami pH Sensors. *Sensors* **2014**, *14*, 19329−19335.
(697) Surana, S.; Bhat, J. M.; Koushika, S. P.; Krishnan, Y. An Autonomous DNA Nanomachine Maps Spatiotemporal pH Changes in a Multicellular Living Organism. *Nat. Commun.* **2011**, *2*, 340.
(698) Modi, S.; Nizak, C.; Surana, S.; Halder, S.; Krishnan, Y. Two DNA Nanomachines Map pH Changes Along Intersecting Endocytic Pathways inside the Same Cell. *Nat. Nanotechnol.* **2013**, *8*, 459−467.
(699) Modi, S.; Halder, S.; Nizak, C.; Krishnan, Y. Recombinant Antibody Mediated Delivery of Organelle-Specific DNA pH Sensors along Endocytic Pathways. *Nanoscale* **2014**, *6*, 1144−1152.
(700) Sugimoto, N.; Wu, P.; Hara, H.; Kawamoto, Y. pH and Cation Effects on the Properties of Parallel Pyrimidine Motif DNA Triplexes. *Biochemistry* **2001**, *40*, 9396−9405.
(701) Leitner, D.; Schroder, W.; Weisz, K. Influence of Sequence-Dependent Cytosine Protonation and Methylation on DNA Triplex Stability. *Biochemistry* **2000**, *39*, 5886−5892.
(702) Vasquez, K. M.; Glazer, P. M. Triplex-Forming Oligonucleotides: Principles and Applications. *Q. Rev. Biophys.* **2002**, *35*, 89−107.
(703) Yang, M. Q.; Zhang, X. L.; Liu, H. P.; Kang, H. Z.; Zhu, Z.; Yang, W.; Tan, W. H. Stable DNA Nanomachine Based on Duplex-Triplex Transition for Ratiometric Imaging Instantaneous pH Changes in Living Cells. *Anal. Chem.* **2015**, *87*, 5854−5859.
(704) Bettinger, T.; Remy, J. S.; Erbacher, P. Size Reduction of Galactosylated PEI/DNA Complexes Improves Lectin-Mediated Gene Transfer into Hepatocytes. *Bioconjugate Chem.* **1999**, *10*, 558−561.
(705) Blessing, T.; Kursa, M.; Holzhauser, R.; Kircheis, R.; Wagner, E. Different Strategies for Formation of Pegylated EGF-Conjugated PEI/DNA Complexes for Targeted Gene Delivery. *Bioconjugate Chem.* **2001**, *12*, 529−537.
(706) Ji, W.; Li, D.; Lai, W.; Yao, X.; Alam, M. F.; Zhang, W.; Pei, H.; Li, L.; Chandrasekaran, A. R. A pH-Operated Triplex DNA Device on MoS_2 Nanosheets. *Langmuir* **2019**, *35*, 5050−5053.
(707) Soto, A. M.; Loo, J.; Marky, L. A. Energetic Contributions for the Formation of TAT/TAT, TAT/CGC^+, and CGC^+/CGC^+ Base Triplet Stacks. *J. Am. Chem. Soc.* **2002**, *124*, 14355−14363.
(708) Saenger, W. *Principles of Nucleic Acid Structure*; Springer Science & Business Media: New York, 2013.
(709) Saha, S.; Bhatia, D.; Krishnan, Y. pH-Toggled DNA Architectures: Reversible Assembly of Three-Way Junctions into Extended 1D Architectures through A-Motif Formation. *Small* **2010**, *6*, 1288−1292.

DOI: 10.1021/acs.chemrev.9b00121
Chem. Rev. XXXX, XXX, XXX−XXX

(710) Bhatia, D.; Sharma, S.; Krishnan, Y. Synthetic, Biofunctional Nucleic Acid-Based Molecular Devices. *Curr. Opin. Biotechnol.* **2011**, *22*, 475−484.
(711) Srivastava, S.; Fukuto, M.; Gang, O. Liquid Interfaces with pH-Switchable Nanoparticle Arrays. *Soft Matter* **2018**, *14*, 3929−3934.
(712) Huang, Z. C.; Liu, B. W.; Liu, J. W. Parallel Polyadenine Duplex Formation at Low pH Facilitates DNA Conjugation onto Gold Nanoparticles. *Langmuir* **2016**, *32*, 11986−11992.
(713) Saha, S.; Chakraborty, K.; Krishnan, Y. Tunable, Colorimetric DNA-Based pH Sensors Mediated by A-Motif Formation. *Chem. Commun.* **2012**, *48*, 2513−2515.
(714) Mathur, V.; Verma, A.; Maiti, S.; Chowdhury, S. Thermodynamics of I-Tetraplex Formation in the Nuclease Hypersensitive Element of Human c-myc Promoter. *Biochem. Biophys. Res. Commun.* **2004**, *320*, 1220−1227.
(715) Choi, Y.; Kotthoff, L.; Olejko, L.; Resch-Genger, U.; Bald, I. DNA Origami-Based FöRster Resonance Energy-Transfer Nanoarrays and Their Application as Ratiometric Sensors. *ACS Appl. Mater. Interfaces* **2018**, *10*, 23295−23302.
(716) Bairoch, A. The Enzyme Database in 2000. *Nucleic Acids Rev* **2000**, *28*, 304−305.
(717) Drews, J. Drug Discovery: A Historical Perspective. *Science* **2000**, *287*, 1960−1964.
(718) Atkinson, D. E. Regulation of Enzyme Activity. *Annu. Rev. Biochem.* **1966**, *35*, 85−124.
(719) Coussens, L. M.; Fingleton, B.; Matrisian, L. M. Matrix Metalloproteinase Inhibitors and Cancer: Trials and Tribulations. *Science* **2002**, *295*, 2387−2392.
(720) Puente, X. S.; Sanchez, L. M.; Overall, C. M.; Lopez-Otin, C. Human and Mouse Proteases: A Comparative Genomic Approach. *Nat. Rev. Genet.* **2003**, *4*, 544−558.
(721) Esler, W. P.; Wolfe, M. S. A Portrait of Alzheimer Secretases-New Features and Familiar Faces. *Science* **2001**, *293*, 1449−1454.
(722) Vassar, R.; Bennett, B. D.; Babu-Khan, S.; Kahn, S.; Mendiaz, E. A.; Denis, P.; Teplow, D. B.; Ross, S.; Amarante, P.; Loeloff, R.; Luo, Y.; Fisher, S.; Fuller, L.; Edenson, S.; Lile, J.; Jarosinski, M. A.; Biere, A. L.; Curran, E.; Burgess, T.; Louis, J. C.; Collins, F.; Treanor, J.; Rogers, G.; Citron, M. Beta-Secretase Cleavage of Alzheimer's Amyloid Precursor Protein by the Transmembrane Aspartic Protease Bace. *Science* **1999**, *286*, 735−741.
(723) Orosco, M. M.; Pacholski, C.; Sailor, M. J. Real-Time Monitoring of Enzyme Activity in a Mesoporous Silicon Double Layer. *Nat. Nanotechnol.* **2009**, *4*, 255−258.
(724) Liu, Q.; Wang, H.; Shi, X. H.; Wang, Z. G.; Ding, B. Q. Self-Assembled DNA/Peptide-Based Nanoparticle Exhibiting Synergistic Enzymatic Activity. *ACS Nano* **2017**, *11*, 7251−7258.
(725) Golub, E.; Niazov, A.; Freeman, R.; Zatsepin, M.; Willner, I. Photoelectrochemical Biosensors without External Irradiation: Probing Enzyme Activities and DNA Sensing Using Hemin/G-Quadruplex-Stimulated Chemiluminescence Resonance Energy Transfer (CRET) Generation of Photocurrents. *J. Phys. Chem. C* **2012**, *116*, 13827−13834.
(726) Khosla, C.; Harbury, P. B. Modular Enzymes. *Nature* **2001**, *409*, 247−252.
(727) Ostermeier, M. Designing Switchable Enzymes. *Curr. Opin. Struct. Biol.* **2009**, *19*, 442−448.
(728) Angelin, A.; Weigel, S.; Garrecht, R.; Meyer, R.; Bauer, J.; Kumar, R. K.; Hirtz, M.; Niemeyer, C. M. Multiscale Origami Structures as Interface for Cells. *Angew. Chem., Int. Ed.* **2015**, *54*, 15813−15817.
(729) Fu, J. L.; Liu, M. H.; Liu, Y.; Yan, H. Spatially-Interactive Biomolecular Networks Organized by Nucleic Acid Nanostructures. *Acc. Chem. Res.* **2012**, *45*, 1215−1226.
(730) Liu, D. S.; Cheng, E. J.; Yang, Z. Q. DNA-Based Switchable Devices and Materials. *NPG Asia Mater.* **2011**, *3*, 109−114.
(731) Gu, H. Z.; Chao, J.; Xiao, S. J.; Seeman, N. C. A Proximity-Based Programmable DNA Nanoscale Assembly Line. *Nature* **2010**, *465*, 202−205.
(732) Lund, K.; Manzo, A. J.; Dabby, N.; Michelotti, N.; Johnson-Buck, A.; Nangreave, J.; Taylor, S.; Pei, R. J.; Stojanovic, M. N.; Walter, N. G.; Winfree, E.; Yan, H. Molecular Robots Guided by Prescriptive Landscapes. *Nature* **2010**, *465*, 206−210.
(733) Liedl, T.; Hogberg, B.; Tytell, J.; Ingber, D. E.; Shih, W. M. Self-Assembly of Three-Dimensional Prestressed Tensegrity Structures from DNA. *Nat. Nanotechnol.* **2010**, *5*, 520−524.
(734) Zhou, C.; Yang, Z. Q.; Liu, D. S. Reversible Regulation of Protein Binding Affinity by a DNA Machine. *J. Am. Chem. Soc.* **2012**, *134*, 1416−1418.
(735) Andersen, E. S.; Dong, M.; Nielsen, M. M.; Jahn, K.; Subramani, R.; Mamdouh, W.; Golas, M. M.; Sander, B.; Stark, H.; Oliveira, C. L. P.; Pedersen, J. S.; Birkedal, V.; Besenbacher, F.; Gothelf, K. V.; Kjems, J. Self-Assembly of a Nanoscale DNA Box with a Controllable Lid. *Nature* **2009**, *459*, 73−U75.
(736) Douglas, S. M.; Bachelet, I.; Church, G. M. A Logic-Gated Nanorobot for Targeted Transport of Molecular Payloads. *Science* **2012**, *335*, 831−834.
(737) Niemeyer, C. M. Semisynthetic DNA-Protein Conjugates for Biosensing and Nanofabrication. *Angew. Chem., Int. Ed.* **2010**, *49*, 1200−1216.
(738) Liu, M. H.; Fu, J. L.; Hejesen, C.; Yang, Y. H.; Woodbury, N. W.; Gothelf, K.; Liu, Y.; Yan, H. A DNA Tweezer-Actuated Enzyme Nanoreactor. *Nat. Commun.* **2013**, *4*, 2127.
(739) Grossi, G.; Jepsen, M. D. E.; Kjems, J.; Andersen, E. S. Control of Enzyme Reactions by a Reconfigurable DNA Nanovault. *Nat. Commun.* **2017**, *8*, 992.
(740) Zhao, Z.; Fu, J.; Dhakal, S.; Johnson-Buck, A.; Liu, M.; Zhang, T.; Woodbury, N. W.; Liu, Y.; Walter, N. G.; Yan, H. Nanocaged Enzymes with Enhanced Catalytic Activity and Increased Stability against Protease Digestion. *Nat. Commun.* **2016**, *7*, 10619.
(741) Baur, J. A.; Zou, Y.; Shay, J. W.; Wright, W. E. Telomere Position Effect in Human Cells. *Science* **2001**, *292*, 2075−2077.
(742) Blackburn, E. H. Telomere States and Cell Fates. *Nature* **2000**, *408*, 53−56.
(743) Shay, J. W.; Wright, W. E. Senescence and Immortalization: Role of Telomeres and Telomerase. *Carcinogenesis* **2005**, *26*, 867−874.
(744) Rodier, F.; Campisi, J. Four Faces of Cellular Senescence. *J. Cell Biol.* **2011**, *192*, 547−556.
(745) Masutomi, K.; Yu, E. Y.; Khurts, S.; Ben-Porath, I.; Currier, J. L.; Metz, G. B.; Brooks, M. W.; Kaneko, S.; Murakami, S.; DeCaprio, J. A.; Weinberg, R. A.; Stewart, S. A.; Hahn, W. C. Telomerase Maintains Telomere Structure in Normal Human Cells. *Cell* **2003**, *114*, 241−253.
(746) Blasco, M. A. Telomeres and Human Disease: Ageing, Cancer and Beyond. *Nat. Rev. Genet.* **2005**, *6*, 611−622.
(747) Hahn, W. C.; Stewart, S. A.; Brooks, M. W.; York, S. G.; Eaton, E.; Kurachi, A.; Beijersbergen, R. L.; Knoll, J. H. M.; Meyerson, M.; Weinberg, R. A. Inhibition of Telomerase Limits the Growth of Human Cancer Cells. *Nat. Med.* **1999**, *5*, 1164−1170.
(748) Harley, C. B. Telomerase and Cancer Therapeutics. *Nat. Rev. Cancer* **2008**, *8*, 167−179.
(749) Shay, J. W.; Wright, W. E. Role of Telomeres and Telomerase in Cancer. *Semin. Cancer Biol.* **2011**, *21*, 349−353.
(750) Williams, S. C. P. No End in Sight for Telomerase-Targeted Cancer Drugs. *Nat. Med.* **2013**, *19*, 6−6.
(751) Zhou, Y.; Xu, Z.; Yoon, J. Fluorescent and Colorimetric Chemosensors for Detection of Nucleotides, FAD and NADH: Highlighted Research During 2004−2010. *Chem. Soc. Rev.* **2011**, *40*, 2222−2235.
(752) Qian, R. C.; Ding, L.; Yan, L. W.; Lin, M. F.; Ju, H. X. Smart Vesicle Kit for in Situ Monitoring of Intracellular Telomerase Activity Using a Telomerase-Responsive Probe. *Anal. Chem.* **2014**, *86*, 8642−8648.
(753) Yun, C. S.; Javier, A.; Jennings, T.; Fisher, M.; Hira, S.; Peterson, S.; Hopkins, B.; Reich, N. O.; Strouse, G. F. Nanometal Surface Energy Transfer in Optical Rulers, Breaking the FRET Barrier. *J. Am. Chem. Soc.* **2005**, *127*, 3115−3119.
(754) Freeman, R.; Sharon, E.; Teller, C.; Henning, A.; Tzfati, Y.; Willner, I. DNAzyme-Like Activity of Hemin-Telomeric G-Quad-

DOI: 10.1021/acs.chemrev.9b00121
Chem. Rev. XXXX, XXX, XXX−XXX

ruplexes for the Optical Analysis of Telomerase and Its Inhibitors. *ChemBioChem* **2010**, *11*, 2362−2367.
(755) Pavlov, V.; Xiao, Y.; Gill, R.; Dishon, A.; Kotler, M.; Willner, I. Amplified Chemiluminescence Surface Detection of DNA and Telomerase Activity Using Catalytic Nucleic Acid Labels. *Anal. Chem.* **2004**, *76*, 2152−2156.
(756) Egger, G.; Liang, G. N.; Aparicio, A.; Jones, P. A. Epigenetics in Human Disease and Prospects for Epigenetic Therapy. *Nature* **2004**, *429*, 457−463.
(757) Probst, A. V.; Dunleavy, E.; Almouzni, G. Epigenetic Inheritance During the Cell Cycle. *Nat. Rev. Mol. Cell Biol.* **2009**, *10*, 192−206.
(758) Smith, Z. D.; Meissner, A. DNA Methylation: Roles in Mammalian Development. *Nat. Rev. Genet.* **2013**, *14*, 204−220.
(759) Nishikawa, K.; Iwamoto, Y.; Kobayashi, Y.; Katsuoka, F.; Kawaguchi, S.; Tsujita, T.; Nakamura, T.; Kato, S.; Yamamoto, M.; Takayanagi, H.; Ishii, M. DNA Methyltransferase 3A Regulates Osteoclast Differentiation by Coupling to an S-Adenosylmethionine-Producing Metabolic Pathway. *Nat. Med.* **2015**, *21*, 281−287.
(760) Pathania, R.; Ramachandran, S.; Elangovan, S.; Padia, R.; Yang, P. Y.; Cinghu, S.; Veeranan-Karmegam, R.; Arjunan, P.; Gnana-Prakasam, J. P.; Sadanand, F.; Pei, L. R.; Chang, C. S.; Choi, J. H.; Shi, H. D.; Manicassamy, S.; Prasad, P. D.; Sharma, S.; Ganapathy, V.; Jothi, R.; Thangaraju, M. DNMT1 Is Essential for Mammary and Cancer Stem Cell Maintenance and Tumorigenesis. *Nat. Commun.* **2015**, *6*, 6910.
(761) Spencer, D. H.; Russler-Germain, D. A.; Ketkar, S.; Helton, N. M.; Lamprecht, T. L.; Fulton, R. S.; Fronick, C. C.; O'Laughlin, M.; Heath, S. E.; Shinawi, M.; Westervelt, P.; Payton, J. E.; Wartman, L. D.; Welch, J. S.; Wilson, R. K.; Walter, M. J.; Link, D. C.; DiPersio, J. F.; Ley, T. J. CpG Island Hypermethylation Mediated by DNMT3A Is a Consequence of AML Progression. *Cell* **2017**, *168*, 801−816.
(762) Robertson, K. D. DNA Methylation and Human Disease. *Nat. Rev. Genet.* **2005**, *6*, 597−610.
(763) Heithoff, D. M.; Sinsheimer, R. L.; Low, D. A.; Mahan, M. J. An Essential Role for DNA Adenine Methylation in Bacterial Virulence. *Science* **1999**, *284*, 967−970.
(764) Appleton, K.; Mackay, H. J.; Judson, I.; Plumb, J. A.; McCormick, C.; Strathdee, G.; Lee, C.; Barrett, S.; Reade, S.; Jadayel, D.; Tang, A.; Bellenger, K.; Mackay, L.; Setanoians, A.; Schatzlein, A.; Twelves, C.; Kaye, S. B.; Brown, R. Phase I and Pharmacodynamic Trial of the DNA Methyltransferase Inhibitor Decitabine and Carboplatin in Solid Tumors. *J. Clin. Oncol.* **2007**, *25*, 4603−4609.
(765) Fang, G.; Munera, D.; Friedman, D. I.; Mandlik, A.; Chao, M. C.; Banerjee, O.; Feng, Z. X.; Losic, B.; Mahajan, M. C.; Jabado, O. J.; Deikus, G.; Clark, T. A.; Luong, K.; Murray, I. A.; Davis, B. M.; Keren-Paz, A.; Chess, A.; Roberts, R. J.; Korlach, J.; Turner, S. W.; Kumar, V.; Waldor, M. K.; Schadt, E. E. Genome-Wide Mapping of Methylated Adenine Residues in Pathogenic Escherichia Coli Using Single-Molecule Real-Time Sequencing. *Nat. Biotechnol.* **2012**, *30*, 1232−1239.
(766) He, X. X.; Su, J.; Wang, Y. H.; Wang, K. M.; Ni, X. Q.; Chen, Z. F. A Sensitive Signal-on Electrochemical Assay for MTase Activity Using AuNPs Amplification. *Biosens. Bioelectron.* **2011**, *28*, 298−303.
(767) Liu, T.; Zhao, J.; Zhang, D. M.; Li, G. X. Novel Method to Detect DNA Methylation Using Gold Nanoparticles Coupled with Enzyme-Linkage Reactions. *Anal. Chem.* **2010**, *82*, 229−233.
(768) Xing, X. W.; Tang, F.; Wu, J.; Chu, J. M.; Feng, Y. Q.; Zhou, X.; Yuan, B. F. Sensitive Detection of DNA Methyltransferase Activity Based on Exonuclease-Mediated Target Recycling. *Anal. Chem.* **2014**, *86*, 11269−11274.
(769) Zhou, X. Y.; Zhao, M.; Duan, X. L.; Guo, B.; Cheng, W.; Ding, S. J.; Ju, H. X. Collapse of DNA Tetrahedron Nanostructure for "Off-On" Fluorescence Detection of DNA Methyltransferase Activity. *ACS Appl. Mater. Interfaces* **2017**, *9*, 40087−40093.
(770) Parkin, D. M.; Pisani, P.; Ferlay, J. Global Cancer Statistics. *Ca-Cancer J. Clin.* **1999**, *49*, 33−64.
(771) Wu, L.; Qu, X. G. Cancer Biomarker Detection: Recent Achievements and Challenges. *Chem. Soc. Rev.* **2015**, *44*, 2963−2997.
(772) Huang, R. R.; He, N. Y.; Li, Z. Y. Recent Progresses in DNA Nanostructure-Based Biosensors for Detection of Tumor Markers. *Biosens. Bioelectron.* **2018**, *109*, 27−34.
(773) Nagrath, S.; Sequist, L. V.; Maheswaran, S.; Bell, D. W.; Irimia, D.; Ulkus, L.; Smith, M. R.; Kwak, E. L.; Digumarthy, S.; Muzikansky, A.; Ryan, P.; Balis, U. J.; Tompkins, R. G.; Haber, D. A.; Toner, M. Isolation of Rare Circulating Tumour Cells in Cancer Patients by Microchip Technology. *Nature* **2007**, *450*, 1235−1239.
(774) Huang, R. R.; Chen, Z. S.; He, L.; He, N. Y.; Xi, Z. J.; Li, Z. Y.; Deng, Y.; Zeng, X. Mass Spectrometry-Assisted Gel-Based Proteomics in Cancer Biomarker Discovery: Approaches and Application. *Theranostics* **2017**, *7*, 3559−3572.
(775) Yu, M.; Bardia, A.; Wittner, B.; Stott, S. L.; Smas, M. E.; Ting, D. T.; Isakoff, S. J.; Ciciliano, J. C.; Wells, M. N.; Shah, A. M.; Concannon, K. F.; Donaldson, M. C.; Sequist, L. V.; Brachtel, E.; Sgroi, D.; Baselga, J.; Ramaswamy, S.; Toner, M.; Haber, D. A.; Maheswaran, S. Circulating Breast Tumor Cells Exhibit Dynamic Changes in Epithelial and Mesenchymal Composition. *Science* **2013**, *339*, 580−584.
(776) Yoon, H. J.; Kim, T. H.; Zhang, Z.; Azizi, E.; Pham, T. M.; Paoletti, C.; Lin, J.; Ramnath, N.; Wicha, M. S.; Hayes, D. F.; Simeone, D. M.; Nagrath, S. Sensitive Capture of Circulating Tumour Cells by Functionalized Graphene Oxide Nanosheets. *Nat. Nanotechnol.* **2013**, *8*, 735−741.
(777) Song, P.; Ye, D. K.; Zuo, X. L.; Li, J.; Wang, J. B.; Liu, H. J.; Hwang, M. T.; Chao, J.; Su, S.; Wang, L. H.; Shi, J. Y.; Wang, L. H.; Huang, W.; La, R.; Fan, C. H. DNA Hydrogel with Aptamer-Toehold-Based Recognition, Cloaking, and Decloaking of Circulating Tumor Cells for Live Cell Analysis. *Nano Lett.* **2017**, *17*, 5193−5198.
(778) Zhang, F.; Nangreave, J.; Liu, Y.; Yan, H. Structural DNA Nanotechnology: State of the Art and Future Perspective. *J. Am. Chem. Soc.* **2014**, *136*, 11198−11211.
(779) Zhang, Q.; Jiang, Q.; Li, N.; Dai, L. R.; Liu, Q.; Song, L. L.; Wang, J. Y.; Li, Y. Q.; Tian, J.; Ding, B. Q.; Du, Y. DNA Origami as an in Vivo Drug Delivery Vehicle for Cancer Therapy. *ACS Nano* **2014**, *8*, 6633−6643.
(780) Kumar, V.; Palazzolo, S.; Bayda, S.; Corona, G.; Toffoli, G.; Rizzolio, F. DNA Nanotechnology for Cancer Therapy. *Theranostics* **2016**, *6*, 710−725.
(781) Li, N.; Wang, M. M.; Gao, X. N.; Yu, Z. Z.; Pan, W.; Wang, H. Y.; Tang, B. A DNA Tetrahedron Nanoprobe with Controlled Distance of Dyes for Multiple Detection in Living Cells and in Vivo. *Anal. Chem.* **2017**, *89*, 6670−6677.
(782) Schreiber, R.; Do, J.; Roller, E. M.; Zhang, T.; Schuller, V. J.; Nickels, P. C.; Feldmann, J.; Liedl, T. Hierarchical Assembly of Metal Nanoparticles, Quantum Dots and Organic Dyes Using DNA Origami Scaffolds. *Nat. Nanotechnol.* **2014**, *9*, 74−78.
(783) Sharma, J.; Ke, Y. G.; Lin, C. X.; Chhabra, R.; Wang, Q. B.; Nangreave, J.; Liu, Y.; Yan, H. DNA-Tile-Directed Self-Assembly of Quantum Dots into Two-Dimensional Nanopatterns. *Angew. Chem., Int. Ed.* **2008**, *47*, 5157−5159.
(784) Wu, C. C.; Han, D.; Chen, T.; Peng, L.; Zhu, G. Z.; You, M. X.; Qiu, L. P.; Sefah, K.; Zhang, X. B.; Tan, W. H. Building a Multifunctional Aptamer-Based DNA Nanoassembly for Targeted Cancer Therapy. *J. Am. Chem. Soc.* **2013**, *135*, 18644−18650.
(785) Li, J.; Fan, C. H.; Pei, H.; Shi, J. Y.; Huang, Q. Smart Drug Delivery Nanocarriers with Self-Assembled DNA Nanostructures. *Adv. Mater.* **2013**, *25*, 4386−4396.
(786) Zhao, W. A.; Cui, C. H.; Bose, S.; Guo, D. G.; Shen, C.; Wong, W. P.; Halvorsen, K.; Farokhzad, O. C.; Teo, G. S. L.; Phillips, J. A.; Dorfman, D. M.; Karnik, R.; Karp, J. M. Bioinspired Multivalent DNA Network for Capture and Release of Cells. *Proc. Natl. Acad. Sci. U. S. A.* **2012**, *109*, 19626−19631.
(787) Marcotte, E. M.; Pellegrini, M.; Ng, H.-L.; Rice, D. W.; Yeates, T. O.; Eisenberg, D. Detecting Protein Function and Protein-Protein Interactions from Genome Sequences. *Science* **1999**, *285*, 751−753.
(788) Dalle-Donne, I.; Scaloni, A.; Giustarini, D.; Cavarra, E.; Tell, G.; Lungarella, G.; Colombo, R.; Rossi, R.; Milzani, A. Proteins as Biomarkers of Oxidative/Nitrosative Stress in Diseases: The Contribution of Redox Proteomics. *Mass Spectrom. Rev.* **2005**, *24*, 55−99.

DOI: 10.1021/acs.chemrev.9b00121
Chem. Rev. XXXX, XXX, XXX−XXX

(789) Wulfkuhle, J. D.; Liotta, L. A.; Petricoin, E. F. Proteomic Applications for the Early Detection of Cancer. *Nat. Rev. Cancer* **2003**, *3*, 267−275.
(790) Morin, P. J. Claudin Proteins in Human Cancer: Promising New Targets for Diagnosis and Therapy. *Cancer Res.* **2005**, *65*, 9603−9606.
(791) Qu, X. M.; Li, M.; Zhang, H. B.; Lin, C. L.; Wang, F.; Xiao, M. S.; Zhou, Y.; Shi, J.; Aldalbahi, A.; Pei, H.; Chen, H.; Li, L. Real-Time Continuous Identification of Greenhouse Plant Pathogens Based on Recyclable Microfluidic Bioassay System. *ACS Appl. Mater. Interfaces* **2017**, *9*, 31568−31575.
(792) Chen, X. Q.; Zhou, G. B.; Song, P.; Wang, J. J.; Gao, J. M.; Lu, J. X.; Fan, C. H.; Zuo, X. L. Ultrasensitive Electrochemical Detection of Prostate-Specific Antigen by Using Antibodies Anchored on a DNA Nanostructural Scaffold. *Anal. Chem.* **2014**, *86*, 7337−7342.
(793) Lin, C. X.; Katilius, E.; Liu, Y.; Zhang, J. P.; Yan, H. Self-Assembled Signaling Aptamer DNA Arrays for Protein Detection. *Angew. Chem., Int. Ed.* **2006**, *45*, 5296−5301.
(794) Daems, D.; Pfeifer, W.; Rutten, I.; Sacca, B.; Spasic, D.; Lammertyn, J. Three-Dimensional DNA Origami as Programmable Anchoring Points for Bioreceptors in Fiber Optic Surface Plasmon Resonance Biosensing. *ACS Appl. Mater. Interfaces* **2018**, *10*, 23539−23547.
(795) Plaks, V.; Koopman, C. D.; Werb, Z. Circulating Tumor Cells. *Science* **2013**, *341*, 1186−1188.
(796) Zhou, G. B.; Lin, M. H.; Song, P.; Chen, X. Q.; Chao, J.; Wang, L. H.; Huang, Q.; Huang, W.; Fan, C. H.; Zuo, X. L. Multivalent Capture and Detection of Cancer Cells with DNA Nanostructured Biosensors and Multibranched Hybridization Chain Reaction Amplification. *Anal. Chem.* **2014**, *86*, 7843−7848.
(797) Li, S. H.; Chen, N. C.; Zhang, Z. Y.; Wang, Y. Endonuclease-Responsive Aptamer-Functionalized Hydrogel Coating for Sequential Catch and Release of Cancer Cells. *Biomaterials* **2013**, *34*, 460−469.
(798) Thery, C.; Zitvogel, L.; Amigorena, S. Exosomes: Composition, Biogenesis and Function. *Nat. Rev. Immunol.* **2002**, *2*, 569−579.
(799) Raposo, G.; Stoorvogel, W. Extracellular Vesicles: Exosomes, Microvesicles, and Friends. *J. Cell Biol.* **2013**, *200*, 373−383.
(800) Li, Y.; Zheng, Q. P.; Bao, C. Y.; Li, S. Y.; Guo, W. J.; Zhao, J.; Chen, D.; Gu, J. R.; He, X. H.; Huang, S. L. Circular RNA Is Enriched and Stable in Exosomes: A Promising Biomarker for Cancer Diagnosis. *Cell Res.* **2015**, *25*, 981−984.
(801) Thakur, B. K.; Zhang, H.; Becker, A.; Matei, I.; Huang, Y.; Costa-Silva, B.; Zheng, Y.; Hoshino, A.; Brazier, H.; Xiang, J.; Williams, C.; Rodriguez-Barrueco, R.; Silva, J. M; Zhang, W.; Hearn, S.; Elemento, O.; Paknejad, N.; Manova-Todorova, K.; Welte, K.; Bromberg, J.; Peinado, H.; Lyden, D. Double-Stranded DNA in Exosomes: A Novel Biomarker in Cancer Detection. *Cell Res.* **2014**, *24*, 766−769.
(802) Nilsson, J.; Skog, J.; Nordstrand, A.; Baranov, V.; Mincheva-Nilsson, L.; Breakefield, X. O.; Widmark, A. Prostate Cancer-Derived Urine Exosomes: A Novel Approach to Biomarkers for Prostate Cancer. *Br. J. Cancer* **2009**, *100*, 1603−1607.
(803) Wang, S.; Zhang, L. Q.; Wan, S.; Cansiz, S.; Cui, C.; Liu, Y.; Cai, R.; Hong, C. Y.; Teng, I. T.; Shi, M. L.; Wu, Y.; Dong, Y. Y.; Tan, W. H. Aptasensor with Expanded Nucleotide Using DNA Nanotetrahedra for Electrochemical Detection of Cancerous Exosomes. *ACS Nano* **2017**, *11*, 3943−3949.
(804) Fang, X. H.; Tan, W. H. Aptamers Generated from Cell-Selex for Molecular Medicine: A Chemical Biology Approach. *Acc. Chem. Res.* **2010**, *43*, 48−57.
(805) Song, S. P.; Wang, L. H.; Li, J.; Zhao, J. L.; Fan, C. H. Aptamer-Based Biosensors. *TrAC, Trends Anal. Chem.* **2008**, *27*, 108−117.
(806) Jayasena, S. D. Aptamers: An Emerging Class of Molecules That Rival Antibodies in Diagnostics. *Clin. Chem.* **1999**, *45*, 1628−1650.
(807) Tombelli, S.; Minunni, M.; Mascini, A. Analytical Applications of Aptamers. *Biosens. Bioelectron.* **2005**, *20*, 2424−2434.
(808) Zuo, X. L.; Xiao, Y.; Plaxco, K. W. High Specificity, Electrochemical Sandwich Assays Based on Single Aptamer Sequences and Suitable for the Direct Detection of Small-Molecule Targets in Blood and Other Complex Matrices. *J. Am. Chem. Soc.* **2009**, *131*, 6944−6945.
(809) Tang, Z. W.; Mallikaratchy, P.; Yang, R. H.; Kim, Y. M.; Zhu, Z.; Wang, H.; Tan, W. H. Aptamer Switch Probe Based on Intramolecular Displacement. *J. Am. Chem. Soc.* **2008**, *130*, 11268−11269.
(810) Yin, B. C.; Ye, B. C.; Tan, W. H.; Wang, H.; Xie, C. C. An Allosteric Dual-DNAzyme Unimolecular Probe for Colorimetric Detection of Copper(II). *J. Am. Chem. Soc.* **2009**, *131*, 14624−14625.
(811) Lv, Y. F.; Hu, R.; Zhu, G. Z.; Zhang, X. B.; Mei, L.; Liu, Q. L.; Qiu, L. P.; Wu, C. C.; Tan, W. H. Preparation and Biomedical Applications of Programmable and Multifunctional DNA Nanoflowers. *Nat. Protoc.* **2015**, *10*, 1508−1524.
(812) Cotrina, M. L.; Lin, J. H. C.; Alves-Rodrigues, A.; Liu, S.; Li, J.; Azmi-Ghadimi, H.; Kang, J.; Naus, C. C. G.; Nedergaard, M. Connexins Regulate Calcium Signaling by Controlling ATP Release. *Proc. Natl. Acad. Sci. U. S. A.* **1998**, *95*, 15735−15740.
(813) Chen, L.; Chao, J.; Qu, X.; Zhang, H.; Zhu, D.; Su, S.; Aldalbahi, A.; Wang, L.; Pei, H. Probing Cellular Molecules with PolyA-Based Engineered Aptamer Nanobeacon. *ACS Appl. Mater. Interfaces* **2017**, *9*, 8014−8020.
(814) Nutiu, R.; Li, Y. F. Structure-Switching Signaling Aptamers. *J. Am. Chem. Soc.* **2003**, *125*, 4771−4778.
(815) Xiao, Y.; Lai, R. Y.; Plaxco, K. W. Preparation of Electrode-Immobilized, Redox-Modified Oligonucleotides for Electrochemical DNA and Aptamer-Based Sensing. *Nat. Protoc.* **2007**, *2*, 2875−2880.
(816) Xiao, Y.; Piorek, B. D.; Plaxco, K. W.; Heeger, A. J. A Reagentless Signal-on Architecture for Electronic, Aptamer-Based Sensors via Target-Induced Strand Displacement. *J. Am. Chem. Soc.* **2005**, *127*, 17990−17991.
(817) Lubin, A. A.; Plaxco, K. W. Folding-Based Electrochemical Biosensors: The Case for Responsive Nucleic Acid Architectures. *Acc. Chem. Res.* **2010**, *43*, 496−505.
(818) Biggins, J. B.; Prudent, J. R.; Marshall, D. J.; Ruppen, M.; Thorson, J. S. A Continuous Assay for DNA Cleavage: The Application of "Break Lights" to Enediynes, Iron-Dependent Agents, and Nucleases. *Proc. Natl. Acad. Sci. U. S. A.* **2000**, *97*, 13537−13542.
(819) Connelly, J. C.; de Leau, E. S.; Leach, D. R. F. DNA Cleavage and Degradation by the SbcCD Protein Complex from *Escherichia Coli*. *Nucleic Acids Rev* **1999**, *27*, 1039−1046.
(820) Tan, X. H.; Chen, T.; Xiong, X. L.; Mao, Y.; Zhu, G. Z.; Yasun, E.; Li, C. M.; Zhu, Z.; Tan, W. H. Semiquantification of ATP in Live Cells Using Nonspecific Desorption of DNA from Graphene Oxide as the Internal Reference. *Anal. Chem.* **2012**, *84*, 8622−8627.
(821) Yang, H. H.; Liu, H. P.; Kang, H. Z.; Tan, W. H. Engineering Target-Responsive Hydrogels Based on Aptamer-Target Interactions. *J. Am. Chem. Soc.* **2008**, *130*, 6320−6321.
(822) Zhu, Z.; Wu, C. C.; Liu, H. P.; Zou, Y.; Zhang, X. L.; Kang, H. Z.; Yang, C. J.; Tan, W. H. An Aptamer Cross-Linked Hydrogel as a Colorimetric Platform for Visual Detection. *Angew. Chem., Int. Ed.* **2010**, *49*, 1052−1056.
(823) Astruc, D.; Boisselier, E.; Ornelas, C. Dendrimers Designed for Functions: From Physical, Photophysical, and Supramolecular Properties to Applications in Sensing, Catalysis, Molecular Electronics, Photonics, and Nanomedicine. *Chem. Rev.* **2010**, *110*, 1857−1959.
(824) Mintzer, M. A.; Grinstaff, M. W. Biomedical Applications of Dendrimers: A Tutorial. *Chem. Soc. Rev.* **2011**, *40*, 173−190.
(825) Meng, H. M.; Zhang, X. B.; Lv, Y. F.; Zhao, Z. L.; Wang, N. N.; Fu, T.; Fan, H. H.; Liang, H.; Qiu, L. P.; Zhu, G. Z.; Tan, W. H. DNA Dendrimer: An Efficient Nanocarrier of Functional Nucleic Acids for Intracellular Molecular Sensing. *ACS Nano* **2014**, *8*, 6171−6181.
(826) Zhang, L.; Lei, J. P.; Liu, L.; Li, C. F.; Ju, H. X. Self-Assembled DNA Hydrogel as Switchable Material for Aptamer-Based Fluorescent Detection of Protein. *Anal. Chem.* **2013**, *85*, 11077−11082.
(827) Heller, M. J. DNA Microarray Technology: Devices, Systems, and Applications. *Annu. Rev. Biomed. Eng.* **2002**, *4*, 129−153.
(828) Levicky, R.; Herne, T. M.; Tarlov, M. J.; Satija, S. K. Using Self-Assembly to Control the Structure of DNA Monolayers on Gold: A Neutron Reflectivity Study. *J. Am. Chem. Soc.* **1998**, *120*, 9787−9792.

DOI: 10.1021/acs.chemrev.9b00121
Chem. Rev. XXXX, XXX, XXX−XXX

(829) Wen, Y. L.; Pei, H.; Wan, Y.; Su, Y.; Huang, Q.; Song, S. P.; Fan, C. H. DNA Nanostructure-Decorated Surfaces for Enhanced Aptamer-Target Binding and Electrochemical Cocaine Sensors. *Anal. Chem.* **2011**, *83*, 7418−7423.
(830) Li, Z. H.; Zhao, B.; Wang, D. F.; Wen, Y. L.; Liu, G.; Dong, H. Q.; Song, S. P.; Fan, C. H. DNA Nanostructure-Based Universal Microarray Platform for High-Efficiency Multiplex Bioanalysis in Biofluids. *ACS Appl. Mater. Interfaces* **2014**, *6*, 17944−17953.
(831) Heck, C.; Kanehira, Y.; Kneipp, J.; Bald, I. Placement of Single Proteins within the SERS Hot Spots of Self-Assembled Silver Nanolenses. *Angew. Chem., Int. Ed.* **2018**, *57*, 7444−7447.
(832) Hare, D. J.; New, E. J.; de Jonge, M. D.; McColl, G. Imaging Metals in Biology: Balancing Sensitivity, Selectivity and Spatial Resolution. *Chem. Soc. Rev.* **2015**, *44*, 5941−5958.
(833) Yannone, S. M.; Hartung, S.; Menon, A. L.; Adams, M. W. W.; Tainer, J. A. Metals in Biology: Defining Metalloproteomes. *Curr. Opin. Biotechnol.* **2012**, *23*, 89−95.
(834) Zhou, W. H.; Saran, R.; Liu, J. W. Metal Sensing by DNA. *Chem. Rev.* **2017**, *117*, 8272−8325.
(835) Zhou, Y. Y.; Tang, L.; Zeng, G. M.; Zhang, C.; Zhang, Y.; Xie, X. Current Progress in Biosensors for Heavy Metal Ions Based on DNAzymes/DNA Molecules Functionalized Nanostructures: A Review. *Sens. Actuators, B* **2016**, *223*, 280−294.
(836) Willner, I.; Shlyahovsky, B.; Zayats, M.; Willner, B. DNAzymes for Sensing, Nanobiotechnology and Logic Gate Applications. *Chem. Soc. Rev.* **2008**, *37*, 1153−1165.
(837) Lu, Y.; Liu, J. W. Functional DNA Nanotechnology: Emerging Applications of DNAzymes and Aptamers. *Curr. Opin. Biotechnol.* **2006**, *17*, 580−588.
(838) Lan, T.; Furuya, K.; Lu, Y. A Highly Selective Lead Sensor Based on a Classic Lead DNAzyme. *Chem. Commun.* **2010**, *46*, 3896−3898.
(839) Liu, J. W.; Brown, A. K.; Meng, X. L.; Cropek, D. M.; Istok, J. D.; Watson, D. B.; Lu, Y. A Catalytic Beacon Sensor for Uranium with Parts-Per-Trillion Sensitivity and Millionfold Selectivity. *Proc. Natl. Acad. Sci. U. S. A.* **2007**, *104*, 2056−2061.
(840) Clever, G. H.; Kaul, C.; Carell, T. DNA-Metal Base Pairs. *Angew. Chem., Int. Ed.* **2007**, *46*, 6226−6236.
(841) Ono, A.; Togashi, H. Highly Selective Oligonucleotide-Based Sensor for Mercury(II) in Aqueous Solutions. *Angew. Chem., Int. Ed.* **2004**, *43*, 4300−4302.
(842) Chandrasekaran, A. R. DNA Arrays with a Silver Lining. *ChemBioChem* **2017**, *18*, 1886−1887.
(843) Breaker, R. R.; Joyce, G. F. A DNA Enzyme That Cleaves RNA. *Chem. Biol.* **1994**, *1*, 223−229.
(844) Breaker, R. R. DNA Enzymes. *Nat. Biotechnol.* **1997**, *15*, 427−431.
(845) Li, J.; Lu, Y. A Highly Sensitive and Selective Catalytic DNA Biosensor for Lead Ions. *J. Am. Chem. Soc.* **2000**, *122*, 10466−10467.
(846) He, Y. L.; Tian, J. N.; Zhang, J. N.; Chen, S.; Jiang, Y. X.; Hu, K.; Zhao, Y. C.; Zhao, S. L. DNAzyme Self-Assembled Gold Nanorods-Based FRET or Polarization Assay for Ultrasensitive and Selective Detection of Copper(II) Ion. *Biosens. Bioelectron.* **2014**, *55*, 285−288.
(847) Liu, M.; Zhao, H. M.; Chen, S.; Yu, H. T.; Zhang, Y. B.; Quan, X. A "Turn-on" Fluorescent Copper Biosensor Based on DNA Cleavage-Dependent Graphene-Quenched DNAzyme. *Biosens. Bioelectron.* **2011**, *26*, 4111−4116.
(848) Breaker, R. R.; Joyce, G. F. A DNA Enzyme with Mg^{2+}-Dependent RNA Phosphoesterase Activity. *Chem. Biol.* **1995**, *2*, 655−660.
(849) Faulhammer, D.; Famulok, M. The Ca^{2+} Ion as a Cofactor for a Novel RNA-Cleaving Deoxyribozyme. *Angew. Chem., Int. Ed. Engl.* **1996**, *35*, 2837−2841.
(850) Li, L.; Feng, J.; Fan, Y. Y.; Tang, B. Simultaneous Imaging of Zn^{2+} and Cu^{2+} in Living Cells Based on DNAzyme Modified Gold Nanoparticle. *Anal. Chem.* **2015**, *87*, 4829−4835.
(851) Kong, R. M.; Fu, T.; Sun, N. N.; Qu, F. L.; Zhang, S. F.; Zhang, X. B. Pyrophosphate-Regulated Zn^{2+}-Dependent DNAzyme Activity: An Amplified Fluorescence Sensing Strategy for Alkaline Phosphatase. *Biosens. Bioelectron.* **2013**, *50*, 351−355.
(852) Mei, S. H. J.; Liu, Z. J.; Brennan, J. D.; Li, Y. F. An Efficient RNA-Cleaving DNA Enzyme That Synchronizes Catalysis with Fluorescence Signaling. *J. Am. Chem. Soc.* **2003**, *125*, 412−420.
(853) Lee, J. H.; Wang, Z. D.; Liu, J. W.; Lu, Y. Highly Sensitive and Selective Colorimetric Sensors for Uranyl (UO_2^{2+}): Development and Comparison of Labeled and Label-Free DNAzyme-Gold Nanoparticle Systems. *J. Am. Chem. Soc.* **2008**, *130*, 14217−14226.
(854) Hollenstein, M.; Hipolito, C.; Lam, C.; Dietrich, D.; Perrin, D. M. A Highly Selective DNAzyme Sensor for Mercuric Ions. *Angew. Chem., Int. Ed.* **2008**, *47*, 4346−4350.
(855) Qu, X. M.; Yang, F.; Chen, H.; Li, J.; Zhang, H. B.; Zhang, G. J.; Li, L.; Wang, L. H.; Song, S. P.; Tian, Y.; Pei, H. Bubble-Mediated Ultrasensitive Multiplex Detection of Metal Ions in Three-Dimensional DNA Nanostructure-Encoded Microchannels. *ACS Appl. Mater. Interfaces* **2017**, *9*, 16026−16034.
(856) Zhou, W. J.; Liang, W. B.; Li, D. X.; Yuan, R.; Xiang, Y. Dual-Color Encoded DNAzyme Nanostructures for Multiplexed Detection of Intracellular Metal Ions in Living Cells. *Biosens. Bioelectron.* **2016**, *85*, 573−579.
(857) Dave, N.; Chan, M. Y.; Huang, P. J. J.; Smith, B. D.; Liu, J. W. Regenerable DNA-Functionalized Hydrogels for Ultrasensitive, Instrument-Free Mercury(II) Detection and Removal in Water. *J. Am. Chem. Soc.* **2010**, *132*, 12668−12673.
(858) Helwa, Y.; Dave, N.; Froidevaux, R.; Samadi, A.; Liu, J. W. Aptamer-Functionalized Hydrogel Microparticles for Fast Visual Detection of Mercury(II) and Adenosine. *ACS Appl. Mater. Interfaces* **2012**, *4*, 2228−2233.
(859) Pei, H.; Liang, L.; Yao, G. B.; Li, J.; Huang, Q.; Fan, C. H. Reconfigurable Three-Dimensional DNA Nanostructures for the Construction of Intracellular Logic Sensors. *Angew. Chem., Int. Ed.* **2012**, *51*, 9020−9024.
(860) Ono, A.; Cao, S.; Togashi, H.; Tashiro, M.; Fujimoto, T.; Machinami, T.; Oda, S.; Miyake, Y.; Okamoto, I.; Tanaka, Y. Specific Interactions between Silver(I) Ions and Cytosine-Cytosine Pairs in DNA Duplexes. *Chem. Commun.* **2008**, 4825−4827.
(861) Lin, Y. H.; Tseng, W. L. Highly Sensitive and Selective Detection of Silver Ions and Silver Nanoparticles in Aqueous Solution Using an Oligonucleotide-Based Fluorogenic Probe. *Chem. Commun.* **2009**, 6619−6621.
(862) Freeman, R.; Finder, T.; Willner, I. Multiplexed Analysis of Hg^{2+} and Ag^{+} Ions by Nucleic Acid Functionalized CdSe/ZnS Quantum Dots and Their Use for Logic Gate Operations. *Angew. Chem., Int. Ed.* **2009**, *48*, 7818−7821.
(863) Mekmaysy, C. S.; Petraccone, L.; Garbett, N. C.; Ragazzon, P. A.; Gray, R.; Trent, J. O.; Chaires, J. B. Effect of O^6-Methylguanine on the Stability of G-Quadruplex DNA. *J. Am. Chem. Soc.* **2008**, *130*, 6710−6711.
(864) Zhong, R. B.; Tang, Q.; Wang, S. P.; Zhang, H. B.; Zhang, F.; Xiao, M. S.; Man, T. T.; Qu, X. M.; Li, L.; Zhang, W. J.; Pei, H. Self-Assembly of Enzyme-Like Nanofibrous G-Molecular Hydrogel for Printed Flexible Electrochemical Sensors. *Adv. Mater.* **2018**, *30*, 1706887.
(865) He, F.; Tang, Y.; Wang, S.; Li, Y.; Zhu, D. Fluorescent Amplifying Recognition for DNA G-Quadruplex Folding with a Cationic Conjugated Polymer: A Platform for Homogeneous Potassium Detection. *J. Am. Chem. Soc.* **2005**, *127*, 12343−12346.
(866) Lee, J.; Kim, H. J.; Kim, J. Polydiacetylene Liposome Arrays for Selective Potassium Detection. *J. Am. Chem. Soc.* **2008**, *130*, 5010−5011.
(867) Olejko, L.; Cywinski, P. J.; Bald, I. Ion-Selective Formation of a Guanine Quadruplex on DNA Origami Structures. *Angew. Chem., Int. Ed.* **2014**, *54*, 673−677.
(868) Huang, C. C.; Chang, H. T. Aptamer-Based Fluorescence Sensor for Rapid Detection of Potassium Ions in Urine. *Chem. Commun.* **2008**, 1461−1463.
(869) Qin, H. X.; Ren, J. T.; Wang, J. H.; Luedtke, N. W.; Wang, E. K. G-Quadruplex-Modulated Fluorescence Detection of Potassium in the Presence of a 3500-Fold Excess of Sodium Ions. *Anal. Chem.* **2010**, *82*, 8356−8360.

DOI: 10.1021/acs.chemrev.9b00121
Chem. Rev. XXXX, XXX, XXX−XXX

(870) Yang, L.; Qing, Z. H.; Liu, C. H.; Tang, Q.; Li, J. S.; Yang, S.; Zheng, J.; Yang, R. H.; Tan, W. H. Direct Fluorescent Detection of Blood Potassium by Ion-Selective Formation of Intermolecular G-Quadruplex and Ligand Binding. *Anal. Chem.* **2016**, *88*, 9285−9292.
(871) Goldstein, G. W. Developmental Neurobiology of Lead Toxicity. *Human lead exposure* **1992**, 125−135.
(872) Smirnov, I.; Shafer, R. H. Lead Is Unusually Effective in Sequence-Specific Folding of DNA. *J. Mol. Biol.* **2000**, *296*, 1−5.
(873) Li, T.; Wang, E. K.; Dong, S. J. Potassium-Lead-Switched G-Quadruplexes: A New Class of DNA Logic Gates. *J. Am. Chem. Soc.* **2009**, *131*, 15082−15083.
(874) Liu, C. W.; Huang, C. C.; Chang, H. T. Highly Selective DNA-Based Sensor for Lead(II) and Mercury(II) Ions. *Anal. Chem.* **2009**, *81*, 2383−2387.
(875) Liu, W.; Zhu, H.; Zheng, B.; Cheng, S.; Fu, Y.; Li, W.; Lau, T. C.; Liang, H. J. Kinetics and Mechanism of G-Quadruplex Formation and Conformational Switch in a G-Quadruplex of PS2.M Induced by Pb^{2+}. *Nucleic Acids Res.* **2012**, *40*, 4229−4236.
(876) Li, T.; Wang, E.; Dong, S. Lead(II)-Induced Allosteric G-Quadruplex DNAzyme as a Colorimetric and Chemiluminescence Sensor for Highly Sensitive and Selective Pb^{2+} Detection. *Anal. Chem.* **2010**, *82*, 1515−1520.
(877) Zhong, R. B.; Xiao, M. S.; Zhu, C. F.; Shen, X. Z.; Tang, Q.; Zhang, W. J.; Wang, L. H.; Song, S. P.; Qu, X. M.; Pei, H.; Wang, C.; Li, L. Logic Catalytic Interconversion of G-Molecular Hydrogel. *ACS Appl. Mater. Interfaces* **2018**, *10*, 4512−4518.
(878) Eisen, M. B.; Spellman, P. T.; Brown, P. O.; Botstein, D. Cluster Analysis and Display of Genome-Wide Expression Patterns. *Proc. Natl. Acad. Sci. U. S. A.* **1998**, *95*, 14863−14868.
(879) Heller, R. A.; Schena, M.; Chai, A.; Shalon, D.; Bedilion, T.; Gilmore, J.; Woolley, D. E.; Davis, R. W. Discovery and Analysis of Inflammatory Disease-Related Genes Using cDNA Microarrays. *Proc. Natl. Acad. Sci. U. S. A.* **1997**, *94*, 2150−2155.
(880) Sorlie, T.; Perou, C. M.; Tibshirani, R.; Aas, T.; Geisler, S.; Johnsen, H.; Hastie, T.; Eisen, M. B.; van de Rijn, M.; Jeffrey, S. S.; Thorsen, T.; Quist, H.; Matese, J. C.; Brown, P. O.; Botstein, D.; Lonning, P. E.; Borresen-Dale, A. L. Gene Expression Patterns of Breast Carcinomas Distinguish Tumor Subclasses with Clinical Implications. *Proc. Natl. Acad. Sci. U. S. A.* **2001**, *98*, 10869−10874.
(881) van't Veer, L. J.; Dai, H. Y.; van de Vijver, M. J.; He, Y. D. D.; Hart, A. A. M.; Mao, M.; Peterse, H. L.; van der Kooy, K.; Marton, M. J.; Witteveen, A. T.; Schreiber, G. J.; Kerkhoven, R. M.; Roberts, C.; Linsley, P. S.; Bernards, R.; Friend, S. H. Gene Expression Profiling Predicts Clinical Outcome of Breast Cancer. *Nature* **2002**, *415*, 530−536.
(882) Sotiriou, C.; Piccart, M. J. Opinion-Taking Gene-Expression Profiling to the Clinic: When Will Molecular Signatures Become Relevant to Patient Care? *Nat. Rev. Cancer* **2007**, *7*, 545−553.
(883) Levsky, J. M.; Singer, R. H. Gene Expression and the Myth of the Average Cell. *Trends Cell Biol.* **2003**, *13*, 4−6.
(884) Wong, M. L.; Medrano, J. F. Real-Time PCR for mRNA Quantitation. *BioTechniques* **2005**, *39*, 75−85.
(885) Freeman, W. M.; Walker, S. J.; Vrana, K. E. Quantitative RT-PCR: Pitfalls and Potential. *BioTechniques* **1999**, *26*, 112−125.
(886) Warren, L.; Bryder, D.; Weissman, I. L.; Quake, S. R. Transcription Factor Profiling in Individual Hematopoietic Progenitors by Digital RT-PCR. *Proc. Natl. Acad. Sci. U. S. A.* **2006**, *103*, 17807−17812.
(887) Bonner, R. F.; EmmertBuck, M.; Cole, K.; Pohida, T.; Chuaqui, R.; Goldstein, S.; Liotta, L. A. Cell Sampling-Laser Capture Microdissection: Molecular Analysis of Tissue. *Science* **1997**, *278*, 1481−1483.
(888) Itzkovitz, S.; van Oudenaarden, A. Validating Transcripts with Probes and Imaging Technology. *Nat. Methods* **2011**, *8*, S12−S19.
(889) Wang, F.; Flanagan, J.; Su, N.; Wang, L. C.; Bui, S.; Nielson, A.; Wu, X. Y.; Vo, H. T.; Ma, X. J.; Luo, Y. L. Rnascope a Novel in Situ RNA Analysis Platform for Formalin-Fixed, Paraffin-Embedded Tissues. *J. Mol. Diagn.* **2012**, *14*, 22−29.
(890) Speicher, M. R.; Carter, N. P. The New Cytogenetics: Blurring the Boundaries with Molecular Biology. *Nat. Rev. Genet.* **2005**, *6*, 782−792.
(891) Levsky, J. M.; Singer, R. H. Fluorescence in Situ Hybridization: Past, Present and Future. *J. Cell Sci.* **2003**, *116*, 2833−2838.
(892) Pare, A.; Lemons, D.; Kosman, D.; Beaver, W.; Freund, Y.; McGinnis, W. Visualization of Individual Scr mRNAs During Drosophila Embryogenesis Yields Evidence for Transcriptional Bursting. *Curr. Biol.* **2009**, *19*, 2037−2042.
(893) Randolph, J. B.; Waggoner, A. S. Stability, Specificity and Fluorescence Brightness of Multiply-Labeled Fluorescent DNA Probes. *Nucleic Acids Rev* **1997**, *25*, 2923−2929.
(894) Larson, D. R.; Singer, R. H.; Zenklusen, D. A Single Molecule View of Gene Expression. *Trends Cell Biol.* **2009**, *19*, 630−637.
(895) Femino, A. M.; Fay, F. S.; Fogarty, K.; Singer, R. H. Visualization of Single RNA Transcripts in Situ. *Science* **1998**, *280*, 585−590.
(896) Femino, A. M.; Fogarty, K.; Lifshitz, L. M.; Carrington, W.; Singer, R. H. Visualization of Single Molecules of mRNA in Situ. *Methods Enzymol.* **2003**, *361*, 245−304.
(897) Maamar, H.; Raj, A.; Dubnau, D. Noise in Gene Expression Determines Cell Fate in Bacillus Subtilis. *Science* **2007**, *317*, 526−529.
(898) Tan, R. Z.; van Oudenaarden, A. Transcript Counting in Single Cells Reveals Dynamics of rDNA Transcription. *Mol. Syst. Biol.* **2010**, *6*, 358.
(899) Raj, A.; Peskin, C. S.; Tranchina, D.; Vargas, D. Y.; Tyagi, S. Stochastic mRNA Synthesis in Mammalian Cells. *PLoS Biol.* **2006**, *4*, 1707−1719.
(900) Levsky, J. M.; Shenoy, S. M.; Pezo, R. C.; Singer, R. H. Single-Cell Gene Expression Profiling. *Science* **2002**, *297*, 836−840.
(901) Zenklusen, D.; Larson, D. R.; Singer, R. H. Single-RNA Counting Reveals Alternative Modes of Gene Expression in Yeast. *Nat. Struct. Mol. Biol.* **2008**, *15*, 1263−1271.
(902) Capodieci, P.; Donovan, M.; Buchinsky, H.; Jeffers, Y.; Cordon-Cardo, C.; Gerald, W.; Edelson, J.; Shenoy, S. M.; Singer, R. H. Gene Expression Profiling in Single Cells within Tissue. *Nat. Methods* **2005**, *2*, 663−665.
(903) Raj, A.; van den Bogaard, P.; Rifkin, S. A.; van Oudenaarden, A.; Tyagi, S. Imaging Individual mRNA Molecules Using Multiple Singly Labeled Probes. *Nat. Methods* **2008**, *5*, 877−879.
(904) To, T. L.; Maheshri, N. Noise Can Induce Bimodality in Positive Transcriptional Feedback Loops without Bistability. *Science* **2010**, *327*, 1142−1145.
(905) Khalil, A. M.; Guttman, M.; Huarte, M.; Garber, M.; Raj, A.; Morales, D. R.; Thomas, K.; Presser, A.; Bernstein, B. E.; van Oudenaarden, A.; Regev, A.; Lander, E. S.; Rinn, J. L. Many Human Large Intergenic Noncoding RNAs Associate with Chromatin-Modifying Complexes and Affect Gene Expression. *Proc. Natl. Acad. Sci. U. S. A.* **2009**, *106*, 11667−11672.
(906) Raj, A.; Rifkin, S. A.; Andersen, E.; van Oudenaarden, A. Variability in Gene Expression Underlies Incomplete Penetrance. *Nature* **2010**, *463*, 913−U984.
(907) Choi, H. M. T.; Beck, V. A.; Pierce, N. A. Next-Generation in Situ Hybridization Chain Reaction: Higher Gain, Lower Cost, Greater Durability. *ACS Nano* **2014**, *8*, 4284−4294.
(908) Levesque, M. J.; Ginart, P.; Wei, Y.; Raj, A. Visualizing SNVs to Quantify Allele-Specific Expression in Single Cells. *Nat. Methods* **2013**, *10*, 865−867.
(909) Choi, H. M. T.; Chang, J. Y.; Trinh, L. A.; Padilla, J. E.; Fraser, S. E.; Pierce, N. A. Programmable in Situ Amplification for Multiplexed Imaging of mRNA Expression. *Nat. Biotechnol.* **2010**, *28*, 1208−1212.
(910) Taniguchi, Y.; Choi, P. J.; Li, G.-W.; Chen, H.; Babu, M.; Hearn, J.; Emili, A.; Xie, X. S. Quantifying E. Coli Proteome and Transcriptome with Single-Molecule Sensitivity in Single Cells. *Science* **2010**, *329*, 533−538.
(911) Lu, J.; Tsourkas, A. Imaging Individual MicroRNAs in Single Mammalian Cells in Situ. *Nucleic Acids Res.* **2009**, *37*, No. e100.
(912) Egholm, M.; Nielsen, P. E.; Buchardt, O.; Berg, R. H. Recognition of Guanine and Adenine in DNA by Cytosine and

DOI: 10.1021/acs.chemrev.9b00121
Chem. Rev. XXXX, XXX, XXX−XXX

Thymine Containing Peptide Nucleic Acids (PNA). *J. Am. Chem. Soc.* **1992**, *114*, 9677−9678.
(913) Gaylord, B. S.; Heeger, A. J.; Bazan, G. C. DNA Detection Using Water-Soluble Conjugated Polymers and Peptide Nucleic Acid Probes. *Proc. Natl. Acad. Sci. U. S. A.* **2002**, *99*, 10954−10957.
(914) Várallyay, É.; Burgyán, J.; Havelda, Z. MicroRNA Detection by Northern Blotting Using Locked Nucleic Acid Probes. *Nat. Protoc.* **2008**, *3*, 190−196.
(915) Castoldi, M.; Schmidt, S.; Benes, V.; Hentze, M. W.; Muckenthaler, M. U. Michip: An Array-Based Method for MicroRNA Expression Profiling Using Locked Nucleic Acid Capture Probes. *Nat. Protoc.* **2008**, *3*, 321−329.
(916) Briones, C.; Moreno, M. Applications of Peptide Nucleic Acids (PNAs) and Locked Nucleic Acids (LNAs) in Biosensor Development. *Anal. Bioanal. Chem.* **2012**, *402*, 3071−3089.
(917) Østergaard, M. E.; Hrdlicka, P. J. Pyrene-Functionalized Oligonucleotides and Locked Nucleic Acids (LNAs): Tools for Fundamental Research, Diagnostics, and Nanotechnology. *Chem. Soc. Rev.* **2011**, *40*, 5771−5788.
(918) Wittung, P.; Nielsen, P. E.; Buchardt, O.; Egholm, M.; Norde, B. DNA-Like Double Helix Formed by Peptide Nucleic Acid. *Nature* **1994**, *368*, 561.
(919) Nielsen, P. E.; Haaima, G. Peptide Nucleic Acid (PNA): A DNA Mimic with a Pseudopeptide Backbone. *Chem. Soc. Rev.* **1997**, *26*, 73−78.
(920) Lansdorp, P. M.; Verwoerd, N. P.; vandeRijke, F. M.; Dragowska, V.; Little, M. T.; Dirks, R. W.; Raap, A. L.; Tanke, H. J. Heterogeneity in Telomere Length of Human Chromosomes. *Hum. Mol. Genet.* **1996**, *5*, 685−691.
(921) Ryoo, S. R.; Lee, J.; Yeo, J.; Na, H. K.; Kim, Y. K.; Jang, H.; Lee, J. H.; Han, S. W.; Lee, Y.; Kim, V. N.; Min, D. H. Quantitative and Multiplexed Microrna Sensing in Living Cells Based on Peptide Nucleic Acid and Nano Graphene Oxide (PANGO). *ACS Nano* **2013**, *7*, 5882−5891.
(922) Pena, J. T. G.; Sohn-Lee, C.; Rouhanifard, S. H.; Ludwig, J.; Hafner, M.; Mihailovic, A.; Lim, C.; Holoch, D.; Berninger, P.; Zavolan, M.; Tuschl, T. MiRNA in Situ Hybridization in Formaldehyde and EDC-Fixed Tissues. *Nat. Methods* **2009**, *6*, 139−141.
(923) Lu, J.; Tsourkas, A. Imaging Individual MicroRNAs in Single Mammalian Cells in Situ. *Nucleic Acids Res.* **2009**, *37*, e100.
(924) Wienholds, E.; Kloosterman, W. P.; Miska, E.; Alvarez-Saavedra, E.; Berezikov, E.; de Bruijn, E.; Horvitz, H. R.; Kauppinen, S.; Plasterk, R. H. A. MicroRNA Expression in Zebrafish Embryonic Development. *Science* **2005**, *309*, 310−311.
(925) Kloosterman, W. P.; Wienholds, E.; de Bruijn, E.; Kauppinen, S.; Plasterk, R. H. A. In Situ Detection of MiRNAs in Animal Embryos Using LNA-Modified Oligonucteotide Probes. *Nat. Methods* **2006**, *3*, 27−29.
(926) Obernosterer, G.; Martinez, J.; Alenius, M. Locked Nucleic Acid-Based in Situ Detection of MicroRNAs in Mouse Tissue Sections. *Nat. Protoc.* **2007**, *2*, 1508−1514.
(927) Silahtaroglu, A. N.; Nolting, D.; Dyrskjot, L.; Berezikov, E.; Moller, M.; Tommerup, N.; Kauppinen, S. Detection of MicroRNAs in Frozen Tissue Sections by Fluorescence in Situ Hybridization Using Locked Nucleic Acid Probes and Tyramide Signal Amplification. *Nat. Protoc.* **2007**, *2*, 2520−2528.
(928) Nilsson, M.; Krejci, K.; Koch, J.; Kwiatkowski, M.; Gustavsson, P.; Landegren, U. Padlock Probes Reveal Single-Nucleotide Differences, Parent of Origin and in Situ Distribution of Centromeric Sequences in Human Chromosomes 13 and 21. *Nat. Genet.* **1997**, *16*, 252.
(929) Nilsson, M.; Malmgren, H.; Samiotaki, M.; Kwiatkowski, M.; Chowdhary, B. P.; Landegren, U. Padlock Probes: Circularizing Oligonucleotides for Localized DNA Detection. *Science* **1994**, *265*, 2085−2088.
(930) Fire, A.; Xu, S.-Q. Rolling Replication of Short DNA Circles. *Proc. Natl. Acad. Sci. U. S. A.* **1995**, *92*, 4641−4645.
(931) Liu, D.; Daubendiek, S. L.; Zillman, M. A.; Ryan, K.; Kool, E. T. Rolling Circle DNA Synthesis: Small Circular Oligonucleotides as Efficient Templates for DNA Polymerases. *J. Am. Chem. Soc.* **1996**, *118*, 1587−1594.
(932) Larsson, C.; Koch, J.; Nygren, A.; Janssen, G.; Raap, A. K.; Landegren, U.; Nilsson, M. In Situ Genotyping Individual DNA Molecules by Target-Primed Rolling-Circle Amplification of Padlock Probes. *Nat. Methods* **2004**, *1*, 227−232.
(933) Larsson, C.; Grundberg, I.; Soderberg, O.; Nilsson, M. In Situ Detection and Genotyping of Individual mRNA Molecules. *Nat. Methods* **2010**, *7*, 395−397.
(934) Deng, R. J.; Tang, L. H.; Tian, Q. Q.; Wang, Y.; Lin, L.; Li, J. H. Toehold-Initiated Rolling Circle Amplification for Visualizing Individual MicroRNAs in Situ in Single Cells. *Angew. Chem., Int. Ed.* **2014**, *53*, 2389−2393.
(935) Pound, E.; Ashton, J. R.; Becerril, H. A.; Woolley, A. T. Polymerase Chain Reaction Based Scaffold Preparation for the Production of Thin, Branched DNA Origami Nanostructures of Arbitrary Sizes. *Nano Lett.* **2009**, *9*, 4302−4305.
(936) Zhang, H. L.; Chao, J.; Pan, D.; Liu, H. J.; Huang, Q.; Fan, C. H. Folding Super-Sized DNA Origami with Scaffold Strands from Long-Range PCR. *Chem. Commun.* **2012**, *48*, 6405−6407.
(937) Said, H.; Schuller, V. J.; Eber, F. J.; Wege, C.; Liedl, T.; Richert, C. M1.3-A Small Scaffold for DNA Origami. *Nanoscale* **2013**, *5*, 284−290.
(938) Erkelenz, M.; Bauer, D. M.; Meyer, R.; Gatsogiannis, C.; Raunser, S.; Sacca, B.; Niemeyer, C. M. A Facile Method for Preparation of Tailored Scaffolds for DNA-Origami. *Small* **2014**, *10*, 73−77.
(939) Marchi, A. N.; Saaem, I.; Vogen, B. N.; Brown, S.; LaBean, T. H. Toward Larger DNA Origami. *Nano Lett.* **2014**, *14*, 5740−5747.
(940) Chandrasekaran, A. R.; Pushpanathan, M.; Halvorsen, K. Evolution of DNA Origami Scaffolds. *Mater. Lett.* **2016**, *170*, 221−224.
(941) Wei, X. X.; Nangreave, J.; Liu, Y. Uncovering the Self-Assembly of DNA Nanostructures by Thermodynamics and Kinetics. *Acc. Chem. Res.* **2014**, *47*, 1861−1870.
(942) Dunn, K. E.; Dannenberg, F.; Ouldridge, T. E.; Kwiatkowska, M.; Turberfield, A. J.; Bath, J. Guiding the Folding Pathway of DNA Origami. *Nature* **2015**, *525*, 82−86.
(943) Marras, A. E.; Zhou, L.; Kolliopoulos, V.; Su, H. J.; Castro, C. E. Directing Folding Pathways for Multi-Component DNA Origami Nanostructures with Complex Topology. *New J. Phys.* **2016**, *18*, 055005.
(944) Li, W.; Yang, Y.; Jiang, S. X.; Yan, H.; Liu, Y. Controlled Nucleation and Growth of DNA Tile Arrays within Prescribed DNA Origami Frames and Their Dynamics. *J. Am. Chem. Soc.* **2014**, *136*, 3724−3727.
(945) Sobczak, J. P. J.; Martin, T. G.; Gerling, T.; Dietz, H. Rapid Folding of DNA into Nanoscale Shapes at Constant Temperature. *Science* **2012**, *338*, 1458−1461.
(946) Jungmann, R.; Liedl, T.; Sobey, T. L.; Shih, W.; Simmel, F. C. Isothermal Assembly of DNA Origami Structures Using Denaturing Agents. *J. Am. Chem. Soc.* **2008**, *130*, 10062−10063.
(947) Song, J.; Zhang, Z.; Zhang, S.; Liu, L.; Li, Q.; Xie, E. Q.; Gothelf, K. V.; Besenbacher, F.; Dong, M. D. Isothermal Hybridization Kinetics of DNA Assembly of Two-Dimensional DNA Origami. *Small* **2013**, *9*, 2954−2959.
(948) Myhrvold, C.; Dai, M. J.; Silver, P. A.; Yin, P. Isothermal Self-Assembly of Complex DNA Structures under Diverse and Biocompatible Conditions. *Nano Lett.* **2013**, *13*, 4242−4248.
(949) Zhang, Z.; Song, J.; Besenbacher, F.; Dong, M. D.; Gothelf, K. V. Self-Assembly of DNA Origami and Single-Stranded Tile Structures at Room Temperature. *Angew. Chem., Int. Ed.* **2013**, *52*, 9219−9223.
(950) Kopielski, A.; Schneider, A.; Csaki, A.; Fritzsche, W. Isothermal DNA Origami Folding: Avoiding Denaturing Conditions for One-Pot, Hybrid-Component Annealing. *Nanoscale* **2015**, *7*, 2102−2106.
(951) Ducani, C.; Kaul, C.; Moche, M.; Shih, W. M.; Hogberg, B. Enzymatic Production of 'Monoclonal Stoichiometric' Single-Stranded DNA Oligonucleotides. *Nat. Methods* **2013**, *10*, 647−652.

DOI: 10.1021/acs.chemrev.9b00121
Chem. Rev. XXXX, XXX, XXX−XXX

(952) Niekamp, S.; Blumer, K.; Nafisi, P. M.; Tsui, K.; Garbutt, J.; Douglas, S. M. Folding Complex DNA Nanostructures from Limited Sets of Reusable Sequences. *Nucleic Acids Res.* **2016**, *44*, No. e102.
(953) Praetorius, F.; Kick, B.; Behler, K. L.; Honemann, M. N.; Weuster-Botz, D.; Dietz, H. Biotechnological Mass Production of DNA Origami. *Nature* **2017**, *552*, 84−87.
(954) Nickels, P. C.; Ke, Y. G.; Jungmann, R.; Smith, D. M.; Leichsenring, M.; Shih, W. M.; Liedl, T.; Hogberg, B. DNA Origami Structures Directly Assembled from Intact Bacteriophages. *Small* **2014**, *10*, 1765−1769.
(955) Saaem, I.; Ma, K. S.; Marchi, A. N.; LaBean, T. H.; Tian, J. D. In Situ Synthesis of DNA Microarray on Functionalized Cyclic Olefin Copolymer Substrate. *ACS Appl. Mater. Interfaces* **2010**, *2*, 491−497.
(956) Marchi, A. N.; Saaem, I.; Tian, J. D.; LaBean, T. H. One-Pot Assembly of a Hetero-Dimeric DNA Origami from Chip-Derived Staples and Double-Stranded Scaffold. *ACS Nano* **2013**, *7*, 903−910.
(957) Schmidt, T. L.; Beliveau, B. J.; Uca, Y. O.; Theilmann, M.; Da Cruz, F.; Wu, C. T.; Shih, W. M. Scalable Amplification of Strand Subsets from Chip-Synthesized Oligonucleotide Libraries. *Nat. Commun.* **2015**, *6*, 8634.
(958) Mathur, D.; Medintz, I. L. Analyzing DNA Nanotechnology: A Call to Arms for the Analytical Chemistry Community. *Anal. Chem.* **2017**, *89*, 2646−2663.
(959) Shaw, A.; Benson, E.; Hogberg, B. Purification of Functionalized DNA Origami Nanostructures. *ACS Nano* **2015**, *9*, 4968−4975.
(960) Bellot, G.; McClintock, M. A.; Lin, C. X.; Shih, W. M. Recovery of Intact DNA Nanostructures after Agarose Gel-Based Separation. *Nat. Methods* **2011**, *8*, 192−194.
(961) Douglas, S. M.; Chou, J. J.; Shih, W. M. DNA-Nanotube-Induced Alignment of Membrane Proteins for NMR Structure Determination. *Proc. Natl. Acad. Sci. U. S. A.* **2007**, *104*, 6644−6648.
(962) Stahl, E.; Martin, T. G.; Praetorius, F.; Dietz, H. Facile and Scalable Preparation of Pure and Dense DNA Origami Solutions. *Angew. Chem., Int. Ed.* **2014**, *53*, 12735−12740.
(963) Lin, C. X.; Perrault, S. D.; Kwak, M.; Graf, F.; Shih, W. M. Purification of DNA-Origami Nanostructures by Rate-Zonal Centrifugation. *Nucleic Acids Res.* **2013**, *41*, No. e40.
(964) Wickham, S. F. J.; Endo, M.; Katsuda, Y.; Hidaka, K.; Bath, J.; Sugiyama, H.; Turberfield, A. J. Direct Observation of Stepwise Movement of a Synthetic Molecular Transporter. *Nat. Nanotechnol.* **2011**, *6*, 166−169.
(965) Halvorsen, K.; Kizer, M. E.; Wang, X.; Chandrasekaran, A. R.; Basanta-Sanchez, M. Shear Dependent LC Purification of an Engineered DNA Nanoswitch and Implications for DNA Origami. *Anal. Chem.* **2017**, *89*, 5674−5678.
(966) Timm, C.; Niemeyer, C. M. Assembly and Purification of Enzyme-Functionalized DNA Origami Structures. *Angew. Chem., Int. Ed.* **2015**, *54*, 6745−6750.
(967) Zeng, D.; Wang, Z.; Meng, Z.; Wang, P.; San, L.; Wang, W.; Aldalbahi, A.; Li, L.; Shen, J.; Mi, X. DNA Tetrahedral Nanostructure-Based Electrochemical miRNA Biosensor for Simultaneous Detection of Multiple miRNAs in Pancreatic Carcinoma. *ACS Appl. Mater. Interfaces* **2017**, *9*, 24118−24125.
(968) Liu, J.; Gao, J.; Du, Y.; Li, Z.; Ren, Y.; Gu, J.; Wang, X.; Gong, Y.; Wang, W.; Kong, X. Combination of Plasma MicroRNAs with Serum CA19−9 for Early Detection of Pancreatic Cancer. *Int. J. Cancer* **2012**, *131*, 683−691.
(969) Gonzales, J. C.; Fink, L. M.; Goodman, O. B., Jr; Symanowski, J. T.; Vogelzang, N. J.; Ward, D. C. Comparison of Circulating MicroRNA 141 to Circulating Tumor Cells, Lactate Dehydrogenase, and Prostate-Specific Antigen for Determining Treatment Response in Patients with Metastatic Prostate Cancer. *Clin. Genitourin. Cancer* **2011**, *9*, 39−45.
(970) Mor, G.; Visintin, I.; Lai, Y.; Zhao, H.; Schwartz, P.; Rutherford, T.; Yue, L.; Bray-Ward, P.; Ward, D. C. Serum Protein Markers for Early Detection of Ovarian Cancer. *Proc. Natl. Acad. Sci. U. S. A.* **2005**, *102*, 7677−7682.
(971) Karam, J. A.; Lotan, Y.; Karakiewicz, P. I.; Ashfaq, R.; Sagalowsky, A. I.; Roehrborn, C. G.; Shariat, S. F. Use of Combined Apoptosis Biomarkers for Prediction of Bladder Cancer Recurrence and Mortality after Radical Cystectomy. *Lancet Oncol.* **2007**, *8*, 128−136.
(972) Marth, G.; Hartley, A. M.; Reddington, S. C.; Sargisson, L. L.; Parcollet, M.; Dunn, K. E.; Jones, D. D.; Stulz, E. Precision Templated Bottom-up Multiprotein Nanoassembly through Defined Click Chemistry Linkage to DNA. *ACS Nano* **2017**, *11*, 5003−5010.
(973) Valsangkar, V.; Chandrasekaran, A. R.; Wang, R.; Haruehanroengra, P.; Levchenko, O.; Halvorsen, K.; Sheng, J. Click-Based Functionalization of a 2 '-O-Propargyl-Modified Branched DNA Nanostructure. *J. Mater. Chem. B* **2017**, *5*, 2074−2077.
(974) Rusling, D. A.; Fox, K. R. Sequence-Specific Recognition of DNA Nanostructures. *Methods* **2014**, *67*, 123−133.
(975) Hu, Y. W.; Cecconello, A.; Idili, A.; Ricci, F.; Willner, I. Triplex DNA Nanostructures: From Basic Properties to Applications. *Angew. Chem., Int. Ed.* **2017**, *56*, 15210−15233.
(976) Chandrasekaran, A. R.; Abraham Punnoose, J.; Valsangkar, V.; Sheng, J.; Halvorsen, K. Integration of a Photocleavable Element into DNA Nanoswitches. *Chem. Commun.* **2019**, *55*, 6587−6590.
(977) Kohman, R. E.; Han, X. Light Sensitization of DNA Nanostructures via Incorporation of Photo-Cleavable Spacers. *Chem. Commun.* **2015**, *51*, 5747−5750.
(978) Valsangkar, V.; Chandrasekaran, A. R.; Zhou, L.; Mao, S.; Lee, G. W.; Kizer, M.; Wang, X.; Halvorsen, K.; Sheng, J. Click and Photo-Release Dual-Functional Nucleic Acid Nanostructures. *Chem. Commun.* **2019**, *55*, 9709−9712.
(979) Taylor, A. I.; Beuron, F.; Peak-Chew, S. Y.; Morris, E. P.; Herdewijn, P.; Holliger, P. Nanostructures from Synthetic Genetic Polymers. *ChemBioChem* **2016**, *17*, 1107−1110.
(980) Georgiadis, M. M.; Singh, I.; Kellett, W. F.; Hoshika, S.; Benner, S. A.; Richards, N. G. J. Structural Basis for a Six Nucleotide Genetic Alphabet. *J. Am. Chem. Soc.* **2015**, *137*, 6947−6955.
(981) Malyshev, D. A.; Dhami, K.; Lavergne, T.; Chen, T. J.; Dai, N.; Foster, J. M.; Correa, I. R.; Romesberg, F. E. A Semi-Synthetic Organism with an Expanded Genetic Alphabet. *Nature* **2014**, *509*, 385−388.
(982) Liu, Q.; Liu, G. C.; Wang, T.; Fu, J.; Li, R. J.; Song, L. L.; Wang, Z. G.; Ding, B. Q.; Chen, F. Enhanced Stability of DNA Nanostructures by Incorporation of Unnatural Base Pairs. *ChemPhysChem* **2017**, *18*, 2977−2980.
(983) Nieves, D.; Gaus, K.; Baker, M. DNA-Based Super-Resolution Microscopy: DNA-Paint. *Genes* **2018**, *9*, 621.
(984) Jungmann, R.; Avendaño, M. S.; Woehrstein, J. B.; Dai, M.; Shih, W. M.; Yin, P. Multiplexed 3D Cellular Super-Resolution Imaging with DNA-Paint and Exchange-Paint. *Nat. Methods* **2014**, *11*, 313−318.
(985) Yang, F.; Zuo, X.; Fan, C.; Zhang, X.-E. Biomacromolecular Nanostructures-Based Interfacial Engineering: From Precise Assembly to Precision Biosensing. *Natl. Sci. Rev.* **2018**, *5*, 740−755.
(986) Bujold, K. E.; Lacroix, A.; Sleiman, H. F. DNA Nanostructures at the Interface with Biology. *Chem* **2018**, *4*, 495−521.
(987) DNA Nanostructures Fingerprint Cellular Organelles. *Nat. Nanotechnol.* **2019**, *14*, 99−99.
(988) Narayanaswamy, N.; Chakraborty, K.; Saminathan, A.; Zeichner, E.; Leung, K.; Devany, J.; Krishnan, Y. A pH-Correctable, DNA-Based Fluorescent Reporter for Organellar Calcium. *Nat. Methods* **2019**, *16*, 95−102.
(989) Thekkan, S.; Jani, M. S.; Cui, C.; Dan, K.; Zhou, G.; Becker, L.; Krishnan, Y. A DNA-Based Fluorescent Reporter Maps HOCl Production in the Maturing Phagosome. *Nat. Chem. Biol.* **2018**, DOI: 10.1038/s41589-018-0176-3.
(990) Rajendran, A.; Endo, M.; Sugiyama, H. Single-Molecule Analysis Using DNA Origami. *Angew. Chem., Int. Ed.* **2012**, *51*, 874−890.
(991) Zhang, H.; Demirer, G. S.; Zhang, H.; Ye, T.; Goh, N. S.; Aditham, A. J.; Cunningham, F. J.; Fan, C.; Landry, M. P. DNA Nanostructures Coordinate Gene Silencing in Mature Plants. *Proc. Natl. Acad. Sci. U. S. A.* **2019**, *116*, 7543−7548.
(992) Liang, L.; Li, J.; Li, Q.; Huang, Q.; Shi, J. Y.; Yan, H.; Fan, C. H. Single-Particle Tracking and Modulation of Cell Entry Pathways of a

DOI: 10.1021/acs.chemrev.9b00121
Chem. Rev. XXXX, XXX, XXX−XXX

Tetrahedral DNA Nanostructure in Live Cells. *Angew. Chem., Int. Ed.* **2014**, *53*, 7745−7750.
(993) Lacroix, A.; Vengut-Climent, E.; de Rochambeau, D.; Sleiman, H. F. Uptake and Fate of Fluorescently Labeled DNA Nanostructures in Cellular Environments: A Cautionary Tale. *ACS Cent. Sci.* **2019**, *5*, 882−891.
(994) Lee, D. S.; Qian, H.; Tay, C. Y.; Leong, D. T. Cellular Processing and Destinies of Artificial DNA Nanostructures. *Chem. Soc. Rev.* **2016**, *45*, 4199−4225.
(995) Xiao, M.; Gao, L.; Chandrasekaran, A. R.; Zhao, J.; Tang, Q.; Qu, Z.; Wang, F.; Li, L.; Yang, Y.; Zhang, X.; Wan, Y.; Pei, H. Bio-functional G-molecular hydrogels for accelerated wound healing. *Mater. Sci. Eng., C* **2019**, *105*, 110067.
(996) Shao, X.; Ma, W.; Xie, X.; Li, Q.; Lin, S.; Zhang, T.; Lin, Y. Neuroprotective Effect of Tetrahedral DNA Nanostructures in a Cell Model of Alzheimer's Disease. *ACS Appl. Mater. Interfaces* **2018**, *10*, 23682−23692.
(997) Mahato, K.; Srivastava, A.; Chandra, P. Paper Based Diagnostics for Personalized Health Care: Emerging Technologies and Commercial Aspects. *Biosens. Bioelectron.* **2017**, *96*, 246−259.
(998) Ansari, M. H.; Hassan, S.; Qurashi, A.; Khanday, F. A. Microfluidic-Integrated DNA Nanobiosensors. *Biosens. Bioelectron.* **2016**, *85*, 247−260.
(999) Srinivasan, B.; Tung, S. Development and Applications of Portable Biosensors. *J. Lab. Autom.* **2015**, *20*, 365−389.
(1000) Kinnamon, D.; Ghanta, R.; Lin, K.-C.; Muthukumar, S.; Prasad, S. Portable Biosensor for Monitoring Cortisol in Low-Volume Perspired Human Sweat. *Sci. Rep.* **2017**, *7*, 13312.

DOI: 10.1021/acs.chemrev.9b00121
Chem. Rev. XXXX, XXX, XXX−XXX